Catalytic Glycerol Hydrogenolysis to Produce 1,2-propanediol with Molecular Hydrogen and *in situ* Hydrogen Produced from Steam Reforming

by

Yuanqing Liu

A thesis

presented to the University of Waterloo

in fulfillment of the

thesis requirement for the degree of

Doctor of Philosophy

in

Chemical Engineering

Waterloo, Ontario, Canada, 2014

AUTHOR'S DECLARATION

I hereby declare that I am the sole author of this thesis. This is a true copy of the thesis, including any required final revisions, as accepted by my examiners.

I understand that my thesis may be made electronically available to the public.

Abstract

Biodiesel has shown great promise to supplement the fossil diesel since it is a renewable energy resource and is environmentally friendly. However, the major obstacle to biodiesel large scale commercialization is the high production cost; so converting glycerol, the by-product of a biodiesel process, into value-added products is an efficient way to promote biodiesel production. 1,2-propanediol (1,2PD), also known as propylene glycol, is an important commodity chemical used for many applications such as polyester resins, liquid detergents and anti-freeze. It can be produced via dehydration of glycerol into acetol followed by hydrogenation of acetol into 1,2PD using a bi-functional catalyst. Currently high pressure gaseous hydrogen added for hydrogenation causes safety issues as well as additional costs of hydrogen purchasing, transportation and storage. Therefore, the utilization of the *in situ* hydrogen produced by steam reforming of a hydrogen carrier could be a novel route for this process. In this work, processes of glycerol hydrogenolysis to produce 1,2PD have been developed using different hydrogen sources, i.e. molecular hydrogen and *in situ* hydrogen produced by steam reforming.

Three different preparation methods were attempted to prepare a $Cu/ZnO/Al_2O_3$ catalyst in a glycerol hydrogenolysis process, which were oxalate gel-coprecipitation, Na_2CO_3 coprecipitation and impregnation. The catalyst prepared by oxalate gel-coprecipitation showed the highest activity for production of 1,2PD. It was also found that the addition of alumina did not only improve the activity but also enhanced the stability of the Cu/ZnO catalyst as shown by the catalyst recycling experiments. The morphological and chemical properties of the catalysts were characterized via XRD, NH_3 TPD, TGA and TEM. Compared with other preparation methods, the $Cu/ZnO/Al_2O_3$ catalyst prepared by oxalate

gel-coprecipitation exhibited a well-mixed form for all the metals as suggested by the XRD and TGA results; the particle size of the $Cu/ZnO/Al_2O_3$ catalyst was smaller as shown in the XRD and TEM results, and also based on NH_3 TPD analysis the $Cu/ZnO/Al_2O_3$ catalyst showed stronger acidic sites. When Ni was loaded onto the $Cu/ZnO/Al_2O_3$ catalyst by oxalate gel-coprecipitation, it was found that the activity for acetol hydrogenation was improved but the overall glycerol hydrogenolysis reaction was slower. This was mainly due to the reduced amount of strong acidic sites caused by the addition of Ni as observed from the NH_3 TPD results. 2wt% Pd supported on a $Cu/MgO/Al_2O_3$ catalyst was used in this process. Higher reaction rate and higher 1,2PD selectivity could be obtained compared with a $Cu/ZnO/Al_2O_3$ catalyst. However, a significant deactivation was observed when the spent catalyst was used. The catalyst deactivation was mainly due to catalyst sintering during the reaction resulting in a larger particle size as suggested by XRD results. The activation energies for the glycerol hydrogenolysis reaction using $Cu/ZnO/Al_2O_3$ and Pd supported on $Cu/MgO/Al_2O_3$ catalysts have been calculated. The activation energy was calculated to be 69.39kJ/mole using a $Cu/ZnO/Al_2O_3$ catalyst and 113.62kJ/mol using a Pd supported on $Cu/MgO/Al_2O_3$ catalyst. It is suggested that the reaction was chemically kinetically controlled using both catalysts and the reaction using the Pd supported on $Cu/MgO/Al_2O_3$ catalyst was more temperature dependent.

It was found that the 1,2PD selectivity was strongly dependent on hydrogen pressure. The low 1,2PD selectivity at lower hydrogen pressure was due to the formation of by-products caused by side reactions with acetol. The kinetic data of acetol hydrogenation suggested that the acetol hydrogenation step was significantly faster than the overall reaction and hence the glycerol dehydration step was the rate-determining-step.

In the glycerol hydrogenolysis process using *in situ* hydrogen, the activities of the $Cu/ZnO/Al_2O_3$ catalysts prepared by different methods were determined and the experimental results show that the catalyst prepared by oxalate gel-coprecipitation has the best catalytic activity for glycerol conversion and 1,2PD selectivity. With Ni loaded onto a

$Cu/ZnO/Al_2O_3$ catalyst, the 1,2PD selectivity was improved and the glycerol conversion was lower. It might be because Ni could improve the steam reforming activity to produce more hydrogen, but due to the reduced strong acidic sites based on the NH_3 TPD results glycerol conversion was decreased. $Cu/MgO/Al_2O_3$ catalysts prepared by oxalate gel-coprecipitation were used in this process and the activity was found to be higher, i.e. higher glycerol conversion and 1,2PD selectivity, compared with the $Cu/ZnO/Al_2O_3$ catalyst due to a higher amount of acidic sites based on the NH_3 TPD results; the Cu/Mg/Al composition was optimized. When Ni was added into a $Cu/MgO/Al_2O_3$ catalyst, it was found that with only 1mole% Ni loaded, the glycerol conversion was lower than that without Ni loaded and the 1,2PD selectivity was slightly improved; when the Ni loading was increased to 5mole%, the catalyst was almost completely inactive, since when 5mole% Ni was loaded, the acidic sites were almost completely eliminated as observed from the NH_3 TPD results. When Pd was added onto a $Cu/MgO/Al_2O_3$ catalyst the 1,2PD selectivity was significantly improved. When Pd was loaded, more surface hydrogen atoms were provided as observed from the H_2 TPD results. $Cu/ZnO/Al_2O_3$ and $Cu/MgO/Al_2O_3$ catalysts have been recycled and reused to investigate the stability of the catalysts. All the catalysts were deactivated after they were recycled and reused, since it was apparent that catalyst sintering occurred during the reaction resulting in a larger particle size based on the XRD results. The deactivation of the spent catalyst was also possibly due to the formation of carbonate when the metals were contacted with CO_2 which was formed via steam reforming.

Acknowledgements

I would like to express my sincerest appreciation to my supervisors Professor Flora T.T. Ng and Professor Garry L. Rempel for their research guidance, financial support, continuous patience and inspiration through the course of this research project. They are always available whenever I need help even from far away. My research skills have been improved to a higher level learning from their professional experiences and encouraging research attitude.

I would like to thank all the members of Professor Ng's research group during my study. Special thanks to Dr. Kamalakar Gunda for helping me start the experiments and teaching me the autoclave, GC and catalyst preparation techniques and giving me many valuable suggestions at the beginning of my research. Thanks to Lei (Justin) Jia for helping me with the electron microscopy techniques and FTIR techniques. Thanks to Dr. Nagaraju Pasupulety for helping me with the TPD and XRD experiments. Thanks to all other members for their help with my experiments and their friendship: Dr. Dr. Amir Arivani, Donghua Zuo, Dr. Tina Liu, Dr. Tony Rao, Dr. Yinmei Ye, Dr. Aijazi Baig, Chau Mai, Ashish Gaurav, Lu Dong, Saurabh Patankar, Manish Tiwari. Thanks to the undergraduate students who helped to get the excellent data: Michael Wu, Barry Hsi, Peter Wu and Beatrize Vieira. Thanks to the visiting scholars from China for sharing their experience and their hospitality when I was in China: Dr. Weiguo Cheng and Dr. Weiguo Huang. Thanks to the members in Professor Rempel's group for their helping with the equipments: Dr. Allen Liu, Dr. Jialong Wu, Yan Liu, Ray Zou, Karl Liu and Ting Li.

I would like to thank the members of my thesis advisory committee for their time and effort in reading the PhD proposal and this thesis and giving the advice in my comprehensive

examination as well as the PhD oral defence: Professor Robert Farrauto, Professor Eric Prouzet, Professor Ali Elkamel and Professor Aiping Yu.

I would like to express my special thanks to all my friends in Waterloo and shared the good time with me during the past six years: Cici Chen, Vivian Xu, Vivian Zhu, Lu Hong, Danny Kou, Melinda Meng, Zhou Ye, Miok Park, Yutian Qie, Peng Liu (and Yingying), Yong Ding, Sheng Lu, Xuejia Liu, He Chen, Kun Feng, Gaopeng Jiang, Jian Shi, Saad Zaman, Jerry Li, Hanwen Liu, Seungwoo Park, Suhyuk Jang, Hyunki Bae, Kihun Kim, Baejung Kim, Dongun Lee, Heywoong Park, Steve Hu, Kathi Smith and Ray Smith. I would like to thank all my Korean friends who shared very good times when I visited Korea: Hoonsub Song, Sungho Park, Moongyu Park, Jacob Ahn, Taejoon Kwon and Kwangbok Yi.

To all my best brothers in China: Xiaowei Liu, Yanxiang Qu, Yanpeng Wang, Chao Wang, Lun Yang and Sizu Jiang, and in Vancouver: Xiaohu Liu, Yi Zhou, Yi Lu, Mengdan Wang, Shu Shang, Sen Yang, Iris Leung, Qingfeng Jiang, Fankun Meng, Dixon Fu and Henry Tseng, I am appreciated to have all of you as my friends.

Finally I would like to express my deepest thank to my mother Guiying Yu and my father Junlin Liu for their endless sacrifices to raise me up and support me studying in Canada, for all your love.

The financial support from Natural Science and Engineer Research Council of Canada (NSERC) Strategic Program is gratefully acknowledged.

Table of Contents

List of Figures

List of Tables

Nomenclature

1,2PD = 1,2-propanediol
1,3PD = 1,3-propanediol
BET = Brunauer–Emmett–Teller
CD = Catalytic Distillation
DMI = 1,3-dimethyl-2-imidazolidinone
DTA = Differential Thermal Analysis
EG = Ethylene Glycol
FID = Flame Ionization Detector
FTIR = Fourier Transform Infrared Spectroscopy
GC = Gas Chromatography
GHG = Greenhouse Gas
LD50 = Lethal Dose 50%
LDLO = Lethal Dose Low
MWCNT = Multi-wall Carbon Nanotube
PrOH = 1-propanol
PTFE = Polytetrafluoroethylene
RGA = Residual Gas Analyzer
RPM = Round per Minute
TCD = Thermal Conductive Detector
TEM = Transmission Electron Microscopy
TGA = Thermal Gravimetric Analysis
TPD = Temperature Programmed Desorption
TPR = Temperature Programmed Reduction
WHSV = Weight Hourly Space Velocity
wt% = weight percent
XRD = X-Ray Diffraction
Mmly = Metric Million Liters per Year

Na = Catalyst Prepared Using Sodium Carbonate Coprecipitation Method
OA = Catalyst Prepared Using Oxalic Acid Coprecipitation Method
IMP = Catalyst Prepared Using Impregnation Method

Chapter One
Introduction

1.1 Biodiesel Industry

Fossil fuel is an important feedstock used for the development of modern society. However, fossil fuel is a non-renewable resource and its global stocks are depleting very fast. The finite supply of fossil fuel and the increasing demand for energy have caused the price of energy to increase rapidly; so that it has motivated many researchers to find alternative sources of energy. Biodiesel has shown great promise to supplement fossil diesel. Biodiesel is composed of fatty acid methyl esters derived from triglyceride or free fatty acid via transesterification and esterification reactions with alcohols as shown in Scheme 1-1. The production of biodiesel utilizes some renewable oil resources such as surplus vegetable oils, waste animal fats and restaurant yellow grease; therefore, it can reduce the dependence on fossil fuel. Biodiesel has several advantages over petroleum diesel beside renewability; such as having no sulfur content, being biodegradable and producing less greenhouse gas (GHG) emissions. Furthermore it is miscible in all portions with petroleum diesel and thus no engine modification is required [1-3].

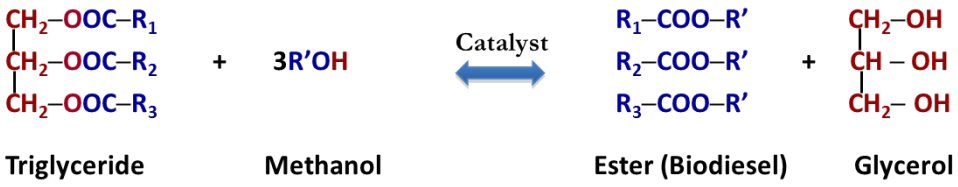

Scheme 1-1 Transesterification Reaction to Produce Biodiesel.

Biodiesel production has rapidly increased to meet the increasing demand of energy. Currently the production capacity of biodiesel in Canada is about 348 million liters (Mmly) per year (Table 1-1) [4]. In order to promote biodiesel production, the Canadian federal government has mandated that diesel fuel sold in Canada must contain a minimum of 2% biodiesel (known as B2). It was reported by the Canada Energy Board that the total diesel demand is expected to be 22400 million liters in 2013, thus the total biodiesel demand is calculated to be 448 million liters; if a 2% blend is still maintained by 2035 the total demand of biodiesel will increase to 670 million liters as shown in Table 1-2 [5]. Therefore, biodiesel production in Canada is expected to grow very fast during the next decade.

Table 1-1 Canadian Biodiesel Plants Locations and Capacities [4].

Plant	Location	Province	Feedstock	Capacity	
Archer Daniels Midland	Lloydminster	Alberta	Canola	265 Mmly	Under Construction
BIOX Corporation	Hamilton	Ontario	Multi-feedstock	66 Mmly	Operational
City-Farm Biofuel Ltd.	Delta	British Columbia	Recycled oil tallow	10 Mmly	Operational
Consolidated Biofuels Ltd.	Delta	British Columbia	Yellow grease	11 Mmly	Operational
FAME Biorefinery	Airdire	Alberta	Canola, camelina, mustard	1 Mmly	Demonstration Facility
Great Lakes Biodiesel	Welland	Ontario	Multi-feedstock	170 Mmly	Operational
Kyoto Fuels Corp	Lethbridge	Alberta	Multi-feedstock	66 Mmly	Under Construction
Methes Energies Canada Inc.	Mississauga	Ontario	Yellow grease	5 Mmly	Operational
Methes Energies Canada Inc.	Sombra	Ontario	Multi-feedstock	50 Mmly	Under Construction
Milligan Bio-Tech Inc.	Foam Lake	Saskatchewan	Canola	20 Mmly	Operational
Noroxel Energy Ltd.	Springfield	Ontario	Yellow grease	5 Mmly	Operational
QFI Biodiesel Inc.	St-Jean-d'Iberville	Quebec	Multi-feedstock	5 Mmly	Operational
Rothsay Biodiesel	Montreal	Quebec	Multi-feedstock	55 Mmly	Operational

Table 1-2 Canada Annual Diesel Consumption and Biodiesel Demand [5].

	2010	2011	2012	**2013**	2014	2015	**2035**
Diesel Demand (peta joules)	839.1	850.9	855.3	**866.4**	880.4	894.8	**1294.1**
Diesel Demand (million L)	21693.4	21998.5	22112.2	**22399.2**	22761.1	23133.4	**33456.6**
Biodiesel Demand (million L)	433.9	440.0	442.2	**448.0**	455.2	462.7	**669.1**
Glycerol Produced (ton)	39771.2	40330.5	40539.0	**41065.1**	41728.8	42411.2	**61337.0**

However, the high production cost of biodiesel is the major obstacle for the expansion of the biodiesel industry. Zhang *et al.* in 2003 proposed an economic assessment on biodiesel production from waste cooking oil by different processes with a crude glycerol credit and none of the processes provided a positive after-tax rate of return without governmental subsidies [6]. Safaei Mohamadabadi *et al.* in 2009 proposed a multi-criteria assessment comparing the use of gasoline, diesel and biodiesel with both environmental and economical considerations (Table 1-3) [7]. It was concluded that biodiesel gave the lowest greenhouse gas emissions, but it had a lower economic ranking compared with that of fossil diesel. Therefore, people have made a great effort on lowering the production cost of biodiesel including the use of different feedstocks such as yellow grease [1, 8, 9] and jatropha oil [10-12] instead of virgin vegetable oil, as well as, improving the activity of catalysts [13], using different processes and adding value from the by-products.

Table 1-3 Economic Assessment Comparison between Biodiesel & Fossil Fuels [7].

Fuel Type	Fuel cost before tax	GHG Emission	CO_2 Tax	Fuel cost after tax
	($/100km)	kg CO_2 eq/100km	$/100km	$/100km
Gasoline	4.80	23.08	2.31	7.11
Diesel	4.09	18.39	1.84	5.93
Biodiesel	5.38	9.21	0.92	6.30

1.2 Glycerol Market

Glycerol is the principle by-product obtained from biodiesel production. For every 10kg of biodiesel produced, about 1kg of glycerol is formed. Glycerol ($C_3H_8O_3$) is a colorless, odorless and viscous liquid under atmospheric conditions. It is soluble in water in all proportions due to the presence of three hydrophilic hydroxyl groups. It is sweet-tasting and of low toxicity. The main applications of glycerol are in the food industry, pharmaceuticals, personal care products, plasticizers, tobacco, emulsifiers, antifreeze and so on. It is also a very important raw material for the production of many other chemicals.

Since biodiesel production has increased dramatically in recent years, the production of glycerol has also increased accordingly. Since a large amount of crude glycerol is formed in biodiesel plants, the lowest price of crude glycerol has fallen to only 4 ¢/lb, so that the cost of storage, handling and transportation has exceeded its market value as reported by BIOX in 2011 [14]. The dramatic increase in glycerol production will not only upset the traditional glycerol production industry, but also cause many environmental problems dealing with the excess crude glycerol which contains contaminants due to the use of liquid sodium hydroxide (or potassium hydroxide) or sulfuric acid in current biodiesel plants. Some biodiesel plants burn the crude glycerol for energy. The BTU value of glycerol is very low, which is only 10% of the calorific value obtained from coal. Based on the price of crude glycerol (8 cents / pound), it costs approximately $4.5 to $5 per million BTU, which is much less economical compared to coal, whose value is reported to be only $2.8 to $3 per million BTU [15]. It has been witnessed that some biodiesel producers added glycerol to animal feed or sprayed it on roads to keep the dust down which can cause both economical waste and environmental problems due to the residue contaminants in the crude glycerol such as sulfuric acid [16]. Many biodiesel plants even pay for the disposal of glycerol as a waste.

Some plants build glycerol refinery plants to improve the crude glycerol quality to technical grade (97%), which can increase the market value to about 30 to 40¢/lb [14]. However, as the

amount of surplus crude glycerol increases, the market value of higher grade glycerol also drops very fast. Figure 1-1 lists the historical price of pharmaceutical grade glycerol (99.7%); the price of which has dropped from 100¢/lb in 1995 to 50¢/lb in 2010, when considering economical inflation over the past 15 years and the expected amount of crude glycerol will still increase over the next decade.Thus, it is becoming less profitable to refine crude glycerol into a higher grade glycerol.

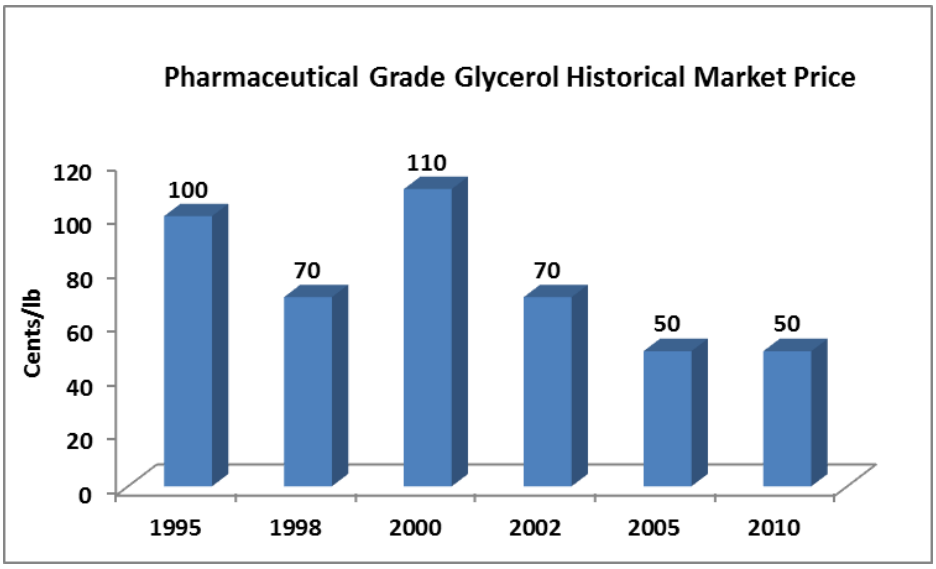

Figure 1-1 Pharmaceutical Grade Glycerol Historical Market Price [17, 18].

1.3 Converting Glycerol into Value-added Products

In order to lower the production cost of biodiesel and to avoid the environmental hazard caused by a large surplus of glycerol, many researchers have been trying to open up a number of practical ways for converting glycerol into value added products. Pagliaro and Rossi in 2008 comprehensively summarized 22 different possible ways to convert glycerol into different value added products having industrial applications in their book [19]. Some others have reported review papers which also summarize many possible ways of converting glycerol into value-added products [20-23], such as converting glycerol into 1,2-propanediol

and 1,3-propanediol, dehydration of glycerol into acrolein, halogenation of glycerol into 1,3-dichloro-2-propanol and steam reforming of glycerol to produce hydrogen. Hydrogenolysis of glycerol into lower alcohols has frequently been reported as promising processes which can produce higher value products such as 1,2-propanediol (1,2PD), 1,3-propanediol (1,3PD), ethylene glycol (EG) and 1-propanol (PrOH). It was reported by ICIS (Chemical Industry News & Chemical Market Intelligence) in 2012 Feburary that 1,2-propanediol is worth about 88 cents per pound, which is more than 10 times the price of crude glycerol and double the price of pharmaceutical grade glycerol. The price of 1,3-propanediol is reported to be about 213 cents per pound, which is the highest among all the lower alcohols; it is usually used in the production of polymethylene terephthalates (PTT) and polyurethanes [19, 24]. Recently, producing 1,3-propanediol from glycerol by bacterial strain fermentation has been reported [25, 26]; however, the process has a low metabolic efficiency, and its compatibility with existing chemical plants is poor. Many researchers are trying to develop a chemical way to produce 1,3-propanediol via glycerol hydrogenolysis using heterogeneous catalysts; however, the process is much more challenging compared with the production of 1,2-propanediol and the reported yield of 1,3-propanediol is very low so far. Ethylene glycol is also an important chemical mostly used as antifreeze in aircraft; it is commercially produced via hydration of ethylene oxide. It was reported that the price of ethylene glycol is not very high, which is about 50 cents per pound. This value is reported by the United States Security and Exchange (U.S.S.A.E) Commission in 2012 and the value is similar to the value reported by Nakagawa and Tomishige in 2011 [27]. Therefore, it is not economical to produce ethylene glycol from glycerol compared with the production of 1,2 propanediol and 1,3 propanediol; hence the selectivity to ethylene glycol should be minimized during glycerol hydrogenolysis processes. There are numerous reports on the production of 1,2-propanediol since the glycerol conversion and 1,2-propanediol selectivity are relatively high at mild reaction conditions [28].

Table 1-4 The Market Value of Different Value-added Products from Glycerol.

	Cents/pound	Year
1,2PD	87.7	2012 [29]
EG	49.7	2011 [30]
1-PrOH	54.6	2011 [27]
13PD	212.7	2012 [31]
Crude Glycerol	7.0	2011 [32]
Pharmaceutical Grade Glycerol	43.0	2011 [32]

1.4 Application of 1,2-propanediol

1,2-propanediol is a clear, colorless, practically odorless and tasteless liquid under atmospheric conditions. It is an important commodity chemical which is used for many applications such as anti-freeze, polyester resins, liquid detergents, pharmaceuticals, cosmetics, paints and animal feed. The physical properties of propylene glycol as well as glycerol are listed in Table 1-4. More detailed properties of C3 alcohols (including 1-propanol and 1,3-propanediol) and their aqueous solutions were reported by Romero *et al.* in 2008 [32].

The addition of water to glycol can generate a solution having a freezing point lower than that of water. Therefore, glycols are mostly used as antifreeze. The freezing point of different alcohol-water solutions are illustrated in Figure 1-2. 1,2-propanediol aqueous solution exhibits the lowest freezing point (e.g. -51°C at 60% propylene glycol) compared with other alcohols. The application of using glycerol as antifreeze and deicing agents has been claimed, but the high freezing point of its aqueous solutions (lowest freezing point is -33.6°C at 60% glycerol) makes this application very limited especially in some cold areas and in aircraft. Ethylene glycol is traditionally used in aircraft as a deicer since it is cheaper and the freezing point of its aqueous solution is fairly low compared with other alcohols. However, ethylene glycol is very poisonous and hence environmentally unfriendly for some applications such as the deicing of aircraft as listed in Table 1-4. Therefore, there is a potential to replace ethylene

glycol as a deicer for aircraft with 1,2-propanediol which is less toxic, environmentally friendly and renewable. The demand for 1,2-propanediol as a deicer is expected to increase.

Table 1-5 Comparison of the Physical Properties between 1,2-propanediol and Glycerol.

Properties	1,2-propanediol	Glycerol
Boiling Point (ºC)	187.3	290
Flash Point (Open cup) (ºC)	107	176
Freezing Point (ºC)	-60	17.8
$V_{Evaporation}$ at 1 atm (kJ/kg)	914	974
Specific Heat at 25 ºC (kJ/kg.K)	2.47	2.40
Viscosity at 20 ºC (Pa.s)	0.04	1.20
Surface Tension at 20 ºC (mN/m)	43.5	64.0
Specific Gravity at 20 ºC	1.036	1.261
Vapor Pressure at 20 ºC (mmHg)	0.0025 (@50 ºC)	0.05

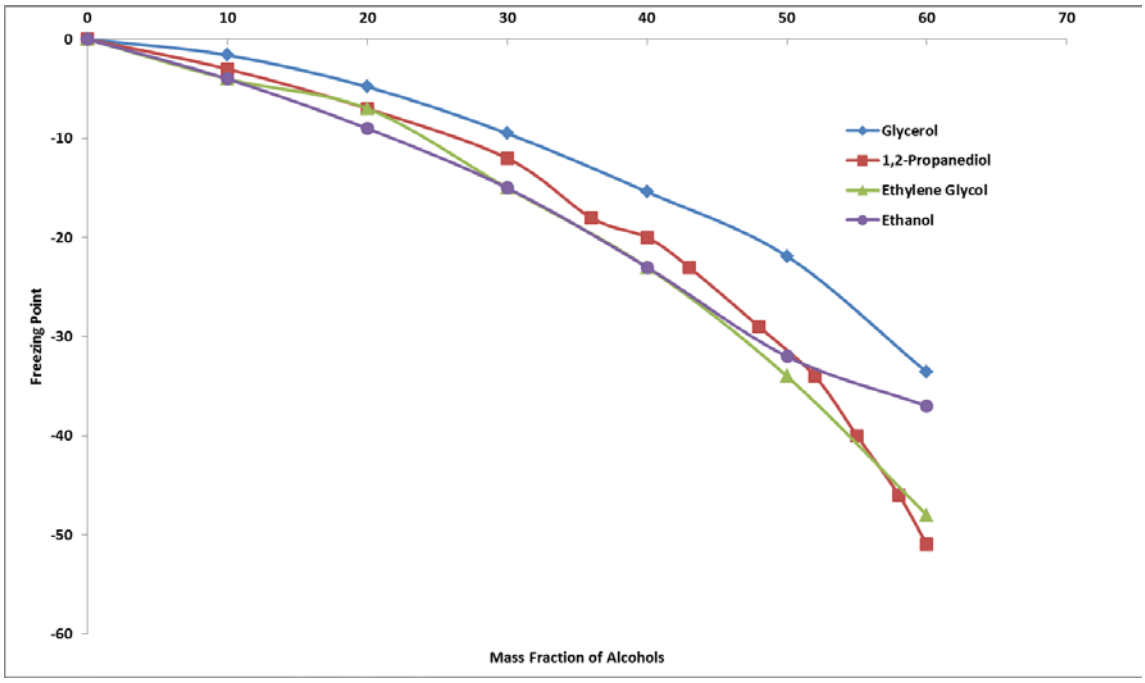

Figure 1-2 Comparison of Freezing Point of Different Aqueous Alcohol Solutions.

Table 1-6 Toxicity of Ethylene Glycol and 1,2-propanediol.

	Oral LDLO Human	Oral LD50 Rat
EG	786mg/kg	4700mg/kg
1,2PD	N/A	20g/kg

1.5 Process of Glycerol Hydrogenolysis Using *in situ* Hydrogen via Methanol Steam Reforming

There are a number of proposed pathways for the production of 1,2-propanediol. One frequently reported pathway is shown in Scheme 1-2 [19, 28]. However, the high hydrogen pressure causes a significant cost issue related to the purchase, transportation and storage of gaseous hydrogen. In most biodiesel plants hydrogen is not used, hence new hydrogen production and storage facilities will be required.

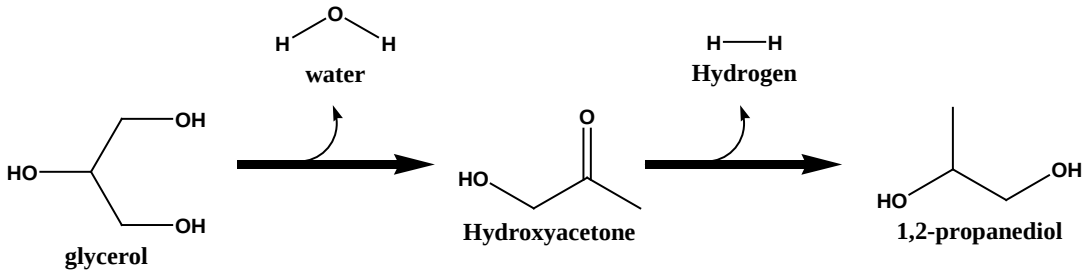

Scheme 1-2 Reaction Pathway of Glycerol Hydrogenolysis to Produce 1,2-propanediol [19, 28].

Many researchers have spent great effort on hydrogen storage and transportation due to the low energy density of gaseous hydrogen [33, 34]. Currently, hydrogen is stored either in high pressure tanks or in liquid form in cryogenic tanks. These forms of storage are not economical and also cause safety problems due to the high pressure since hydrogen poses unique challenges due to its ease of leaking, explosion on contact with air and its ability to embrittle metals. Another popular way of storing hydrogen is to use solid materials. In this way, hydrogen is adsorbed on high surface area materials physically, i.e. nano-tubes, activated carbon and graphene; alternatively, hydrogen can be adsorbed chemically on some metals to form complex hydrides, i.e. MgH_2, $NaBH_4$ and $LiAlH_4$. Solid materials may cause high cost of transportation and it requires additional processes for adsorption and desorption. Using liquid hydrogen carriers, i.e. methanol, ethanol, iso-propanol and formic acid, in hydrogenation processes have also been frequently reported for *in situ* hydrogen which is produced via steam reforming processes and used for the hydrogenation processes [35-39]; this process is called hydrogen transfer.

1.6 Research Objective

Since the glycerol is produced from biodiesel production process with methanol as a feedstock, the methanol can be used to produce hydrogen *in situ* for the hydrogenolysis of glycerol. The objective of the present work is to develop a glycerol hydrogenolysis process to produce 1,2-propanediol using *in situ* hydrogen produced from methanol steam reforming. Methanol is considered to be the most suitable hydrogen donor with several advantages over other hydrogen carriers as summarized by Palo *et al.* in their review paper on methanol steam reforming in 2007 [40].

a. Methanol is considered as a superior hydrogen carrier since it has a high H/C ratio (4:1) compare to other hydrocarbons, and it is equal to that of methane.

b. Methanol is in a liquid form at atmospheric pressure and ambient temperature, so it is easier to handle unlike methane or liquefied petroleum gas. It has a low boiling point (65℃), which can facilitate its vaporization if the gas phase is needed.

c. Methanol steam reforming process can give low CO production compared to direct methanol decomposition and methanol partial oxidation. CO is reported to be poisonous for some catalysts and causes the occurrence of side reactions.

d. Compared with other long chain hydrocarbons as hydrogen carriers (i.e. glycerol), methanol steam reforming does not transform methanol to other species since it does not involve C-C bond cleavage.

e. Supported Cu, Zn, Ni etc. can be used as the catalysts which are not very expensive; in addition, the reaction can be carried out at lower temperature (150ºC to 300ºC) than most other long chain fuels, and hence the steam reforming process is more economical.

f. The CO_2 produced from methanol steam reforming can increase the acidity of the solution caused by dissolution of CO_2 into water to form carbonic acid promoting the dehydration of glycerol to increase glycerol conversion [41-43].

g. In addition, alcohol is one of the reactants for transesterification and esterification reactions, and methanol is most frequently used. An excess of methanol is usually used to shift the reaction equilibrium to the products, which normally varies from 6:1 to 30:1 [44]. Therefore, in most of the biodiesel production plants the availability of excess methanol would not be a major concern.

The overall reaction pathway is shown in Scheme 1-3 that glycerol is dehydrated into acetol followed by a hydrogenation reaction; the hydrogen is produced *in situ* via a methanol steam reforming reaction.

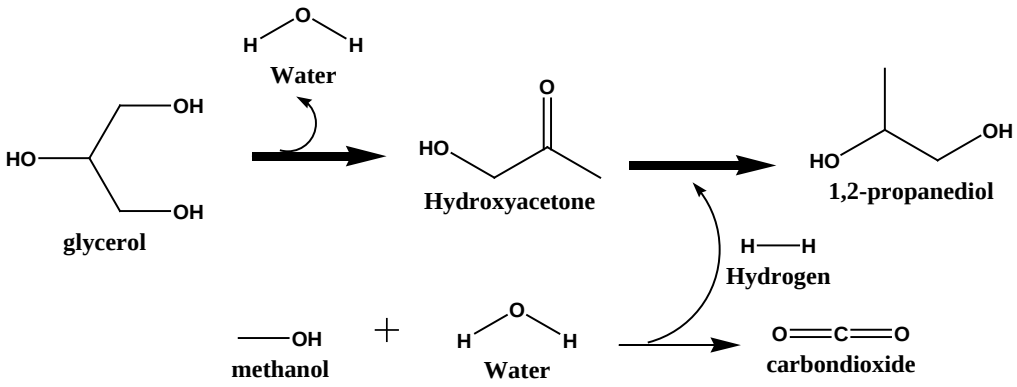

Scheme 1-3 Pathway of Glycerol Hydrogenolysis Process Using In Situ Hydrogen Produced by Methanol Steam Reforming.

Chapter Two
Literature Review

2.0 Introduction

The principle forcus of this research is to develop a glycerol hydrogenolysis process to produce 1,2-propanediol using *in situ* hydrogen produced via methanol steam reforming. The hydrogenolysis process with molecular hydrogen added has also been carried out for comparison. A comprehensive review of the scientific literature is presented in this chapter including the catalyst development and the application of the hydrogenolysis process with molecular hydrogen and with other hydrogen sources.

2.1 Reaction Mechanism

The reaction mechanism for the production of 1,2-propanediol (1,2PD) has been investigated by many researchers. Among these studies, a two-step mechanism, in which glycerol is dehydrated to acetol (1-hydroxyacetone) followed by hydrogenation of acetol to 1,2PD, has been most frequently reported and widely proposed as shown in Scheme 2-1. This mechanism is proposed for most of the copper based catalysts [19, 28, 45-51]. Some literature has reported this reaction mechanism using a Ni based catalyst [52-55], Ru based catalysts [56-58] and Pt based catalysts [59-61]. All these catalysts possess certain acidity for the glycerol dehydration step. Therefore a bi-functional catalyst is needed to obtain a high

yield of 1,2PD, the catalyst needs to be active for both the dehydration and hydrogenation reactions.

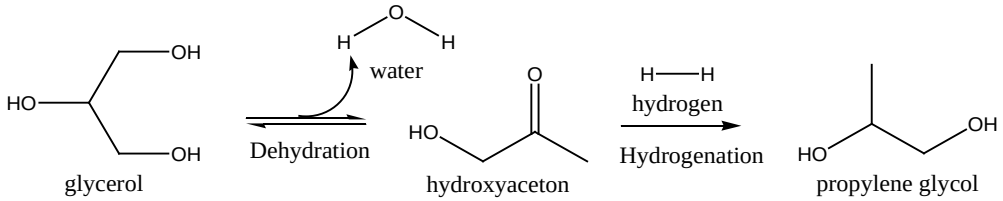

Scheme 2-1 Reaction Pathway of Catalytic Conversion of Glycerol to 1,2PD via Acetol as an Intermediate.

Recently, another reaction mechanism has also been frequently reported involving dehydrogenation of glycerol to glyceraldehyde followed by a dehydration step to form 2-hydroxyacrolein which is then hydrogenated to produce 1,2PD as shown in Scheme 2-2. Normally to observe this mechanism, alkali catalysts are usually used to catalyze the glycerol dehydrogenation reaction such as when Cu/Mg based catalysts are used [62-64]. This step has also been reported when some metals having dehydrogenation activity such as Pt [65] and Pd [66] were used.

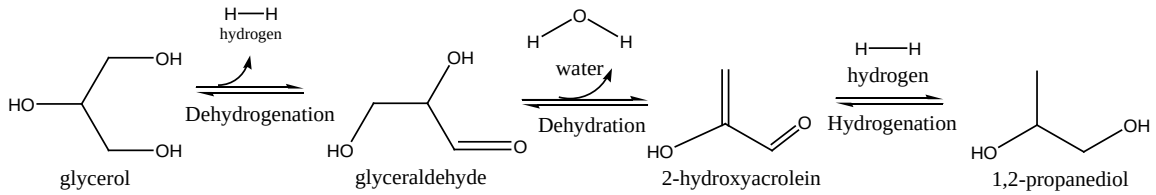

Scheme 2-2 Reaction Pathway of Catalytic Conversion of Glycerol to 1,2PD via Glyceraldehyde as an Intermediate.

In addition, some researchers also reported that, besides acetol and glyceraldehyde, glycerol can also be dehydrated into glycidol (3-hydroxy-1,2-epoxypropane) as an intermediate

simultaneously [67, 68], and then the glycidol can be hydrogenated to form 1,2-propanediol as shown in Scheme 2-3**.**

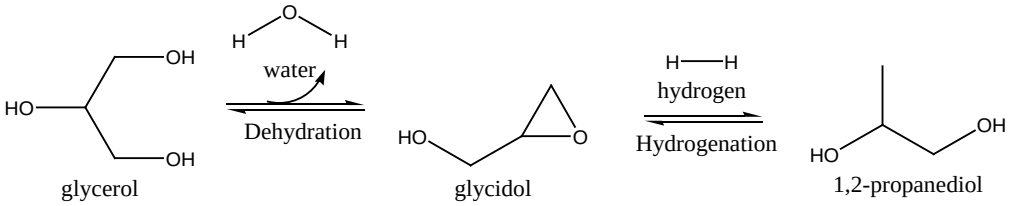

Scheme 2-3 Reaction Pathway of Catalytic Conversion of Glycerol to 1,2PD via Glycidol as an Intermediate.

Ethylene glycol (EG) is one of the main by-products in a glycerol hydrogenolysis process. It was reported that the potential route of EG formation is the direct hydrogenolysis of a C-C bond in glycerol, which would form EG and methanol [45, 52, 56, 58, 69] as shown in Scheme 2-4. Therefore, in order to obtain a high selectivity of 1,2PD, the catalyst should have a low activity for C-C bond cleavage but a high efficiency for C-O bond cleavage.

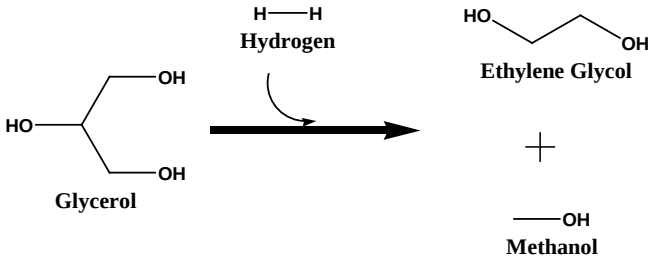

Scheme 2-4 Formation of Ethylene Glycol from Glycerol.

2.2 Reported Catalysts for Glycerol Hydrogenolysis to Produce 1,2-propanediol in an Autoclave Batch Reactor

The catalyst development experiments are usually carried out in a batch reactor. In this section, the literature reported on different types of catalyst in a batch autoclave reactor are reviewed. The reported experimental results are listed in Table A-1 shown in Appendix A.

2.2.1 Cu Based Catalysts

A copper (Cu) based catalyst has been reported to exhibit good selectivity towards 1,2PD under mild conditions. This high selectivity can be explained by the low activity of Cu for C-C bond cleavage and high efficiency for C-O bond cleavage [28, 70, 71].

2.2.1.1 Cu-Cr Catalysts

Cu-Cr catalysts have been firstly reported for glycerol hydrogenolysis. In 2005, a low-pressure process to produce 1,2PD catalyzed by a commercial copper-chromite catalyst was reported by Dasari *et al.* providing 85% selectivity to 1,2PD and 55% glycerol conversion (after 24 hours) at 473K and 200psi H_2 [28].

Liang *et al.* in 2009 proposed a route to prepare a high surface area Cu-Cr catalyst via a facile carbon template route (BET = 88m^2/g; cf. BET = 30m^2/g reported by Dasari) [72]. The effect of the Cu to Cr ratio was also investigated; an optimum Cu/Cr molar ratio was reported to be 1/5 and a selectivity of 97.1% was achieved with 51% glycerol conversion at 200ºC and 200psi H_2 after 10 hours.

Kim *et al*. in 2010 reported a Cu-Cr catalyst prepared by a NaOH coprecipitation method [73] to investigate the promoting effect of Cr on Cu based catalyst; the Cu only catalyst gave a glycerol conversion of 28% while the addition of Cr (Cu/Cr = 1/3) gave a glycerol conversion of 80.3% with 83.9% selectivity to 1,2PD after 12 hours. The conditions were 90% aqueous glycerol, 220˚C, 1160psi H_2, 2% catalyst by weight. It was shown that Cr has a significant promoting effect on the Cu catalyst.

In 2011 Mane *et al.* reported a Cu/Cr catalyst prepared by NH_4OH coprecipitation, at 220ºC and 750psi H_2 after 5 hours; the glycerol conversion was reported to be 16% and the selectivity was 82%, when Ba was added as a promoter, the catalytic activity was

significantly improved, under the same conditions and the glycerol conversion was doubled compared to that without Ba and the selectivity to 1,2PD was also increased to 85% [74]. In this report, the promoting effects of Al and Zn on the Cu/Cr catalyst were not as significant compared with those of Ba.

In 2013 Xiao *et al.* developed a novel catalyst preparation method which involves non-alkoxide sol–gel coprecipitation. The $Cu(NO_3)_2$ and $Cr(NO_3)_3$ precursor were precipitated by propylene oxide to produce nano size particles. It was reported that the catalyst can promote the reaction under a very mild reaction conditions, i.e. at only 130ºC and 290psi H_2 after 5 hours, the glycerol conversion was 52.4% and the selectivity was reported to be 99.6%, with essentially no by-products being found after the reaction except for a trace amount of acetol and glyceraldehyde detected by GC [75].

2.2.1.2 Cu/ZnO Catalysts

The toxicity associated with chromium [67, 76, 77] has led many researchers to focus on the modification of copper based catalysts and to replace chromium as the promoter. Currently Cu/ZnO catalysts have attracted many researchers' attention for this process due to its superior selectivity to 1,2PD and its nontoxicity. Cu/ZnO catalysts have been widely applied in different industrial processes such as methanol synthesis, water gas shift reaction and methanol steam reforming since it is less costly and easy to handle.

Wang & Liu in 2007 and Balaraju *et al.* in 2008 reported a Cu-ZnO catalyst prepared by a co-precipitation method [67, 70]. Both of them reported that at a 1/1 Cu/Zn molar ratio, the catalyst gave the highest activity for the production of 1,2PD. The conversion of glycerol was only 33.9% with 77.5% selectivity to 1,2PD at 200 ºC and 600psi H_2 after 12 hours; at a lower hydrogen pressure (290 psi) after 16 hours, the conversion reached 37% and the selectivity was 92% to 1,2PD. Meher *et al.* in 2009 reported that among the different

combinations of mixed metal oxides (Mg/Al, Zn/Al, Ni/Mg/Al, Co/Ni/Mg/Al, Cu/Zn/Al), $Cu/ZnO/Al_2O_3$ prepared by co-precipitation exhibited the best activity [47]. With a Cu/Zn/Al feed molar ratio of 1/1/4, the glycerol conversion was improved to 47.9% with 93.8% selectivity to 1,2PD at 200ºC and 200psi H_2.

Catalyst preparation methods have been reported to have a significant effect on Cu/ZnO catalysts activity for a glycerol hydrogenolysis process to produce 1,2PD. Bienholz *et al.* in 2010 published a report comparing two different catalyst preparation methods: NaOH coprecipitation and oxalate gel-coprecipitation [68]. The oxalate gel-coprecipitation was first reported by Deng *et al.* in 1996 for a methanol synthesis process [78]. It was reported that by this preparation method, the Cu/ZnO catalyst exhibited a better metal dispersion and a smaller particle size; therefore, the activity was high [78, 79]. In Bienholze's report, it was found that under the same experimental conditions the glycerol conversion was improved from 17% using the catalyst prepared by NaOH coprecipitation to 46% when the catalyst was prepared via the gel-oxalate copreicpitation method. However, it was reported that this catalyst deactivated when water was used as a solvent; when 50% aqueous glycerol was used as the feedstock, and the glycerol conversion was only 5%.

For a Cu/ZnO catalyst, a third metal is usually added such as Al, Zr and Ga. In 2011 Bienholz *et al.* reported that by adding Ga to a Cu/ZnO catalyst, the catalyst activity was significantly improved [80]. In their report, compared to using the Cu/ZnO catalyst prepared by NaOH coprecipitation, when Ga was added on a Cu/ZnO catalyst, the glycerol conversion was increased from 84% to 96%; the experimental conditions were 220ºC and 725psi H_2, and 80% aqueous glycerol was loaded and the reaction time was 7 hours. However, Ga is an expensive metal, which will result in a higher production cost.

Recently Tan *et al*. in 2013 reported a novel preparation method for a $Cu/ZnO/Al_2O_3$ catalyst, which was called evaporation-induced self-assembly (EISA) in which Pluronic P123 wass

used as a structure directing agent, copper-acetate as the precursor of Cu, zinc nitrate as the precursor of Zn and aluminum isopropoxide as the precursor of Al. The experimental conditions were reported to be 180ºC and 580psi H_2; 80% glycerol was loaded and 3wt% of catalyst was used, and within 10 hours the glycerol conversion was 85.8% and the 1,2PD selectivity was 92.1%.

2.2.1.3 Cu/MgO Catalyst

Recently, Cu/MgO based catalysts have been frequently reported and it was found that the basicity of the catalyst also played an important role with respect to its performance. Yuan *et al*. in 2011 first reported a $Cu/MgO/Al_2O_3$ catalyst for a glycerol hydrogenolysis process to produce 1,2PD [81]. A $Cu_{0.4}/Mg_{5.6}/Al_2/O_{8.6}$ catalyst prepared via a NaOH and Na_2CO_3 coprecipitation method was reported to be the optimum metal molar ratio. Under experimental conditions of 180ºC and 435psi H_2, 75% aqueous glycerol was loaded and the reaction time was 10 hours; the glycerol conversion was 80% and the 1,2PD selectivity was 98.2% which was very high; however, 10wt% of catalyst was loaded which was very high. It was also reported that when 5% to 10% NaOH was added in the reaction mixture, the glycerol conversion was higher and the 1,2PD selectivity was decreased due to more ethylene glycol being produced.

To improve the $Cu/MgO/Al_2O_3$ catalyst activity, another metal was added to promote the catalyst activity. Xia *et al*. in 2011 reported that when Pd was added, the catalyst was active under milder conditions compared with a $Cu/MgO/Al_2O_3$ catalyst [82]. In this report, the reaction conditions were: 180ºC and 290psi H_2, 75% aqueous glycerol was loaded with 10 hours reaction time; a glycerol conversion of 56.7% and a 1,2PD selectivity of 97.1% were obtained using the $Cu/MgO/Al_2O_3$ catalyst, and the addition of 4wt% Pd increased the

glycerol conversion and 1,2PD selectivity to 76.9% and 97.2% respectively. The promotion effect of Pd was proposed to be due to H_2 spillover from Pd to Cu.

The effect of Rh on a $Cu/MgO/Al_2O_3$ catalyst has been investigated and reported by Xia *et al*. in 2012 [83]. In this report, 2% of Rh was added to a $Cu_{0.4}/Mg_{5.6}/Al_{1.98}/O_{8.6}$ catalyst, the catalytic activity was significantly improved when 75wt% aqueous glycerol was used as the feedstock. It was also reported that the solvent played an important role on the experimental results. Under the condition of 180ºC and 290psi H_2, and 10 hours reaction time, the glycerol conversion was 95.2% when 25wt% methanol was used as the solvent but the glycerol conversion was only 56.7% when 25wt% water was used as the solvent.

Since $Cu/ZnO/Al_2O_3$ and $Cu/MgO/Al_2O_3$ have been reported to be active for glycerol hydrogenolysis to produce 1,2PD, a catalyst of $Cu/ZnO/MgO/Al_2O_3$ prepared via a Na_2CO_3 and NaOH coprecipitation has been investigated and reported by Xia *et al*. in 2012 [64]. In this work, the molar ratio of Zn:Mg was manipulated to find the optimum composition. It was reported that the $Cu_{0.4}Zn_{0.6}Mg_{5.0}Al_{2.0}$ catalyst gave the highest activity and the catalytic activity was increased with increasing basicity. When the experimental conditions were 180ºC and 290psi H_2, 75wt% aqueous glycerol and 10 hours reaction time, the glycerol conversion was reported to be 78.2% and the 1,2PD selectivity was 99.3%, which was noticeably higher than any recently reported 1,2PD selectivity.

2.2.1.4 Other Cu Based Catalysts

Some supported catalysts prepared via an impregnation method have also been reported; however, the activities of supported Cu catalysts were not as high as the activity of Cu catalysts prepared by a coprecipitation method. The most frequently reported catalysts were Cu supported on γAl_2O_3 [84-86], Cu supported on SiO_2 [50, 71, 87-89] and Cu supported on other supports [90-92]. In 2013 Xia *et al.* reported a $Cu/MgO/Al_2O_3$ supported on multi-wall

carbon nanotubes, which showed a high activity for glycerol hydrogenolysis to produce 1,2PD. When the experimental conditions were 200ºC and 435psi H_2, 33wt% aqueous glycerol with 10 hours reaction time, the glycerol conversion was reported to be 86.5% and the 1,2PD selectivity was 92.5%.

2.2.1.5 Catalyst Deactivation of Cu Based Catalysts

Catalyst deactivation is one of the major problems in most of industries using heterogeneous catalysts and has been reported frequently for Cu based catalysts. It was reported that catalyst deactivation is mainly due to (1) catalyst sintering [80]; (2) catalyst fouling by polymeric or oligomeric species (polymerization and/or oligomerization of acetol) [43], and (3) leaching of metal species. For instance, it was reported that metal leaching is due to the presence of water by a disproportionation reaction [93] as shown in Equation 2-1.

$2Cu^{1+}aq \Rightarrow Cu^{0} + Cu^{2+}aq$ **Equation 2-1**

Cu^{+2} would be drawn into water forming copper hydroxide (Equation 2-2)

$2Cu^{2+}aq + 2H_2O \Rightarrow 2Cu(OH)_2 + 2H^{+}$ **Equation 2-2**

In 2011, Vasiliadou and Lemonidou reported the deactivation of a Cu supported on silica catalyst [89]. The experimental results showed that the catalyst was significantly deactivated after the second run, i.e. the glycerol conversion was 43% and 1,2PD selectivity was 91% when a fresh catalyst was used, after the catalyst was recycled and reused the glycerol conversion was decreased to only 18%.

Bienholz *et al*. in 2009 reported a significant deactivation for a Cu/ZnO catalyst (Cu/Zn=1/2) prepared by an oxalic acid co-precipitation method [68]. The reaction conditions reported were: 1.7wt% of catalyst, 100% glycerol, 200 ºC, 725psi hydrogen, 7 hours reaction time.

The glycerol conversion using fresh catalyst was reported to be 46% with about 90% selectivity to 1,2PD and when the spent catalyst was used, the glycerol conversion was only 10% although a high 1,2PD selectivity was obtained (97%). This was explained in that the deactivation was due to sintering of the catalyst resulting in a larger particle size.

It was mentioned in the previous section that Xia *et al*. reported a $Cu/MgO/ZnO/Al_2O_3$ catalyst prepared via Na_2CO_3 and NaOH coprecipitation, an exceptionally high 1,2PD selectivity was obtained [64]. However, in this report, catalyst deactivation was also observed; the glycerol conversions were 39.7%, 34.2%, 25.6% and 25.3% for the reactions using fresh, first recycled, second recycled and third recycled catalysts respectively.

Many researchers have reported different ways of preventing catalyst deactivation. Bienholz *et al*. [80] also reported a $Cu/ZnO/Ga_2O_3$ catalyst showing a very high activity for the reactions. In this report, a catalyst with a Cu/Zn/Ga molar ratio of 2/4/1 prepared using Na_2CO_3 could give 96% glycerol conversion with 82% selectivity to 1,2PD after 7 hours. The reaction conditions were 1.7wt% of catalyst, 80wt% aqueous glycerol, 200°C, 725psi hydrogen, 7 hours reaction time. It was also reported that Ga efficiently prevented catalyst deactiviation. By carrying out the recycling experiments, it was reported that the catalyst activity was stable for 4 runs as shown in Table 2-1. However, Ga is a very expensive metal compared to Cu, Zn and Al. It was suggested that the promoting effect of Ga_2O_3 on the catalyst stability was due to the presence of a component which isolated the individual metal particles, preventing their sintering. The same effect was also reported by adding ZrO reported by Duran-Martin *et al.* in 2013 [90].

Table 2-1 Recycling Experiment for $Cu/ZnO/Ga_2O_3$ catalyst[a] [80].

Run	Conversion	Selectivity
1	57	80
2	53	82
3	57	83
4	52	85

[a]Conditions: 0.3 g of Cu/ ZnO/Ga_2O_3, 200°C, 8 g of 90 wt % aqueous glycerol, 5 hours.

2.2.2 Ru Based Catalysts

Supported ruthenium (Ru) catalysts have been reported to have relatively higher activity for this process compared to Cu catalysts [94-97]. This type of catalyst shows a much faster reaction rate compared to a copper based catalyst. However, it was also found that Ru based catalysts could promote excessive C-C cleavage, resulting in a higher selectivity to ethylene glycol. Then ethylene glycol also becomes another major by-product, which has a lower value than 1,2PD.

Miyazawa *et al.* in 2007 developed a Ru/C catalyst in combination with an ion-exchange resin (Amberlyst 15) [95], in which the selectivity was improved. Alhanash *et al.* in 2008 reported that a Ru catalyst supported on heteropoly acid ($Cs_{2.5}H_{0.5}[PW_{12}O_{40}]$) gave a high 1,2PD selectivity (87.6%) under exceptionally mild conditions (150℃ and 80psi of H_2) [98]; however, the glycerol conversion was reported to be only 31%. Balaraju *et al.* in 2009 reported that in cooperation with niobium oxide (N_2O_5), the selectivity to 1,2PD was 66.5% at 180℃ and 870psi of H_2 after 8 hours and the conversion was 62.8% [96].

In 2011, van Ryneveld *et al*. reported a Ru/C catalyst for glycerol hydrogenolysis and the results were compared with Pd/C and Pt/C catalysts [99]. It was reported that at very low temperature (130°C), but relatively high hydrogen pressure (1160psi) with 20wt% aqueous glycerol, the conversion of glycerol was 49.2% after 24 hours and the selectivity to 1,2PD was only 74% with 6% selectivity to ethylene glycol. When the glycerol concentration was increased from 20% to 60%, the ethylene glycol selectivity was increased from 5.1% to 10.1%. Supported Pd and Pt catalysts were also reported and the activity was not as high as a Ru based catalyst. In this report, a reaction mechanism involving by-product formation, when hydrogen was insufficient, has been proposed. The by-products were caused by condensation reactions of acetol with glycerol, 1,2PD and ethylene glycol to form some cyclic products (C5 or C6). When hydrogen is insufficient to hydrogenate all the acetol, the high concentration of acetol will cause these condensation reactions as shown in Scheme 2-5.

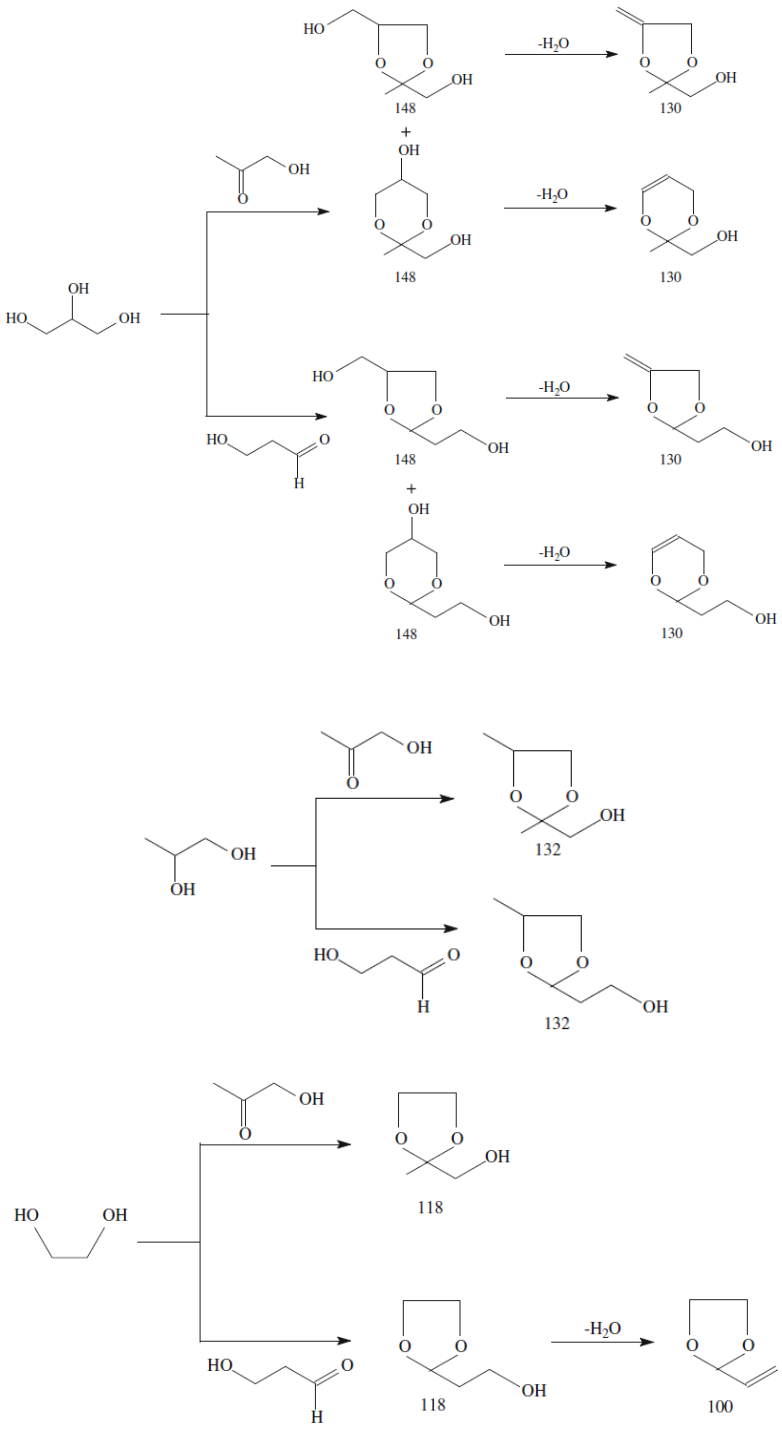

Scheme 2-5 Side Reactions Caused by Acetol [99]*.

*Reprinted from Ryneveld *et al*. *Catalysis Letters*, vol. 141, pp. 958-967 with permission from the Springer Science + Business Media.

A Cu-Ru bimetallic catalyst has also been investigated to utilize the advantages of both metals. Jiang *et al.* in 2009 reported a Cu-Ru bimetallic catalyst supported on natural clay [100], which is a type of environmentally benign material; with a Ru:Cu molar ratio of 3:1, the conversion was 81.6% and the selectivity to 1,2PD was 87.3% after 18 hours at 210 ºC and 362psi hydrogen pressure.

Wu *et al*. in 2011 also reported a Ru catalyst supported on carbon nanotubes for this process [92]. It was found that different types of supports could also affect the catalytic activity of the Ru catalyst. Using Ru/C at 200°C and 580psi, after 6 hours, the glycerol conversion was found to be 55.7% and the 1,2PD selectivity was only 59.4% and the selectivity to ethylene glycol was 15.7%; for the Ru supported on MWCNT (multi-wall carbon nanotube), under the same rection conditions, the conversion was improved to 65.5% and the 1,2PD selectivity was 72.2%, the ethylene glycol selectivity was only 7.6%, which was still high compared to a Cu based catalyst. To further improve the selectivity to 1,2PD, a bi-metallic Cu-Ru/MWCNT catalyst was also used since copper could give a very good 1,2PD selectivity and Ru could increase the reaction rate. The experimental results showed that the glycerol conversion was 99.8% and the 1,2PD selectivity was 86.5% which were very high, and no ethylene glycol was found (0% selectivity). It can be concluded that Ru promoted by Cu can really improve the 1,2PD selectivity and lower the yield of ethylene glycol.

Ru/SiO_2 catalysts have also been frequently reported. In 2011, Vasiliadou and Lemonidou reported a $Ru(5wt\%)/SiO_2$ catalyst and a bi-metalic $Cu\text{-}Ru/SiO_2$ catalyst [89]. Using a Ru/SiO_2 catalyst, the selectivity of ethylene glycol was very high (28.7%) and selectivity of 1,2PD was only 60.5% (reaction conditions: 0.6wt% catalyst, 240°C, 1160psi H_2, 5hours, pure glycerol feed). If Cu was added to the catalyst ($Ru\text{-}Cu/SiO_2$), the glycerol conversion was increased from 21.7% to 39.2% and the selectivity to 1,2PD was increased from 60.5% to 85.9% and the selectivity to ethylene glycol was decreased from 28.7% to 6.9%. The same group in 2011 also investigated the effect of reaction conditions (temperature and hydrogen

pressure) using a Ru/SiO_2 catalyst [101]. The experimental data showed that when the temperature increased, the glycerol conversion and selectivity to 1,2PD increased and the selectivity of ethylene glycol decreased. The drop in formation of ethylene glycol agrees with the results reported by Wu *et al*. [92].

Ru based catalysts using other supports have also been reported. For example, Lee and Moon in 2011 reported a Ru supported on $CaO/MgO/Al_2O_3$ catalyst [102]. In the report a hydrotalcite-like $CaO/MgO/Al_2O_3$ was prepared by $(NH_4)_2CO_3$ co-precipitation, Ru was loaded on the support by impregnation. Under very mild conditions (100°C, 363psi hydrogen, 3wt% catalyst, 20% aqueous glycerol feed, 19 hours), the conversion was 58.5% with a 85.5% selectivity to 1,2PD, and the selectivity to ethylene glycol was 6.6%. A $Ru/\gamma\text{-}Al_2O_3$ catalyst has also been investigated. Under the same reaction conditions, the glycerol conversion was similar (45.6%), but the selectivity to ethylene glycol was significantly higher (22.3%). Recently Hamzah *et al*. reported Ru catalysts with different types of support (TiO_2, bentonite and their mixture) for a glycerol hydrogenolysis process [57]. The mixed bentonite and TiO_2 gave the best results under a very mild condition (150°C, 290psi, and 7hours reaction). It can be seen that supports can affect the yield of ethylene glycol significantly, which also has been reported by Wu *et al*. [92].

In conclusion, the Ru based catalyst catalyze glycerol hydrogenolysis reactions under very mild conditions (100-180°C, less catalyst loading and lower hydrogen pressure 300psi to 500psi) and provide faster reaction rates (less reaction time and high glycerol conversion) compared with a Cu based catalyst. However, the low selectivity is mainly caused by a high yield of ethylene glycol. Different types of support can also affect the selectivity to 1,2PD. In general a support with stronger acidic sites can provide a higher 1,2PD yield. It is also known that higher temperature does not favor the yield of ethylene glycol. In order to improve the selectivity to 1,2PD, a bi-metalic catalyst (supported Ru-Cu) is usually used. However, Ru is also an expensive metal compared with Cu and Ni.

Recently, Re was found to have a promotion effect to improve the activity of supported Ru catalysts. Ma *et al.* [103-105] reported that with the addition of Re, the glycerol conversion could reach 59.4% and selectivity of the catalyst to 1,2PD was 56.6%, with a selectivity of 7.2% to 1,3PD; without adding Re, the glycerol conversion was only to be 29.7% with 50.9% selectivity to 1,2PD. Nano-size supported Ru was also investigated by Wang *et al.* in 2009, it was found that by supporting Ru on carbon nanotubes, the conversion of glycerol was reported to be 42.3% with 60.2% of selectivity to 1,2PD after 12 hours at 200 ºC [97].

2.2.3 Promoting Effect of Pd on Cu Based Catalyst

It is known that when the hydrogen pressure is low, the low 1,2PD selectivity is due to side reactions of acetol. It has been reported that Pd is used as a promoter for a Cu based catalyst since Pd is an active metal for hydrogenation reactions. Xia *et al*. reported the promoting effect of Pd on the $Cu/MgO/Al_2O_3$ [82]. It was reported that by adding Pd, the high selectivity could still be maintained at a lower hydrogen pressure (since the selectivity highly depends on the hydrogen pressure). By adding 4% Pd on the $Cu/MgO/Al_2O_3$ catalyst ($Pd_{0.04}/Cu_{0.4}/Mg_{5.6}/Al2/O_{8.6}$) the selectivity to 1,2PD was 97.2% at 290psi hydrogen and the glycerol conversion was 88%, while without 4% Pd loaded ($Cu_{0.4}/Mg_{5.6}/Al_2/O_{8.6}$), to obtain a 98.0% 1,2PD selectivity the hydrogen pressure was reported to be 435psi and the glycerol conversion was only 80% as reported by Yuan *et al*. [81].

Kim *et al*. in 2012 reported a promoting effect of Pd on a Cu-Cr catalyst [106]. In their report, when the Cu-Cr catalyst was used without Pd loading the experimental conditions were 220ºC and 870psi H_2, with 90wt% aqueous glycerol, 2wt% of catalyst and 12 hours reaction time, and the glycerol conversion was 76% and the 1,2PD selectivity was 79%. When 0.5% Pd was loaded, the glycerol conversion and 1,2PD selectivity were increased to 83% and 91% respectively; the rate constant of the reaction was almost doubled when Pd was loaded. From an H_2 TPD experiment, it was found that when Pd was loaded onto a Cu-Cr catalyst, the

capacity for adsorbed hydrogen on the catalyst surface was significantly improved. Therefore, it was found that the promoting effect of Pd was due to hydrogen spillover behavior. When hydrogen is adsorbed onto the catalyst, it can dissociate into hydrogen atoms and the Pd can provide hydrogen atoms to the catalytic active sites via spillover, and the spillover of hydrogen can exhibit higher diffusivity and activity compared with molecular hydrogen.

2.3 Glycerol Hydrogenolysis to Produce 1,2-propanediol without Molecular Hydrogen Added

Literature reports and patents have shown that high hydrogen pressure was required ($\geqslant$ 200psi) to produce 1,2PD from glycerol; some of the reactions were carried out at over 1500psi. This high hydrogen pressure may cause a significant cost issue related to the purchase, transportation and storage of gaseous hydrogen as well as the cost of high pressure hydrogen reactors. Safety is another concern due to the high pressure operation because hydrogen can easily leak and cause explosion on contact with air and also hydrogen can easily embrittle metals. Liquid hydrogen also poses additional difficulties in handling due to extremely high pressure and low temperature. Therefore, many researchers are focusing on glycerol hydrogenolysis processes to produce 1,2PD without adding molecular hydrogen.

2.3.1 Glycerol Steam Reforming as a Hydrogen Source

Currently steam reforming of glycerol to produce hydrogen has received a lot of attention from researchers. Therefore, some researchers have been investigating catalysts that can catalyze this process using *in situ* hydrogen produced via glycerol steam reforming. D'Hondt *et al.* in 2008 firstly proposed a supported Pt catalyst that can convert glycerol to 1,2PD in the absence of added hydrogen [41, 42]. A mechanism for this process was also reported as shown in Scheme 2-3 where the *in situ* hydrogen was formed by a liquid steam reforming of

glycerol with a CO_2 by-product. Then the hydrogen was used for acetol hydrogenation, which was formed by dehydration of glycerol. The reaction was carried at 230ºC under an inert atmosphere using a Pt supported on NaY catalyst and the glycerol conversion was reported to be 85.4% with 64% selectivity to 1,2PD.

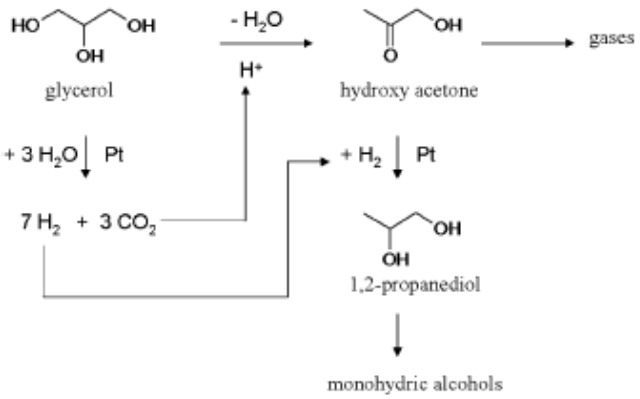

Scheme 2-6 Reaction Pathway of Converting Glycerol to 1,2PD in Absence of Added Hydrogen Using Pt/NaY as the Catalyst [41]*.

*Reprinted D'Hondt et al., *Chemical Communication,* vol. 11, pp. 1511-1513, 2009 with permission from the Royal Society of Chemistry.

In 2012, Barbelli *et al.* reported the same process using a 1% Pt supported on silica catalyst, where the Pt loading was lower than what D'Hondt *et al*. reported [107]. In Barbelli *et al*. report, at 200°C, with a 10% aqueous glycerol feed, after 2 hours, the conversion of glycerol was only 1%, and at 225°C, the conversion was only 3% which was very low. With 0.2 mol% of Sn added as a promoter ($PtSn_{0.2}/SiO_2$), the conversion was significantly improved from 1% to 54%, and the selectivity to 1,2PD was reported to be 59% which was similar to the data reported by D'Hondt *et al*. The by-products were reported to be ethylene glycol, acetol, ethanol, 1-propanol and methanol.

In 2012 Pendem *et al*. reported a glycerol hydrogenolysis process using supported Pt catalysts [59]. In this report, various supports were used and a 3% Pt supported on hydrotalcite was found to have the highest activity for this process. The reaction conditions

were 10wt% aqueous glycerol, 1wt% catalyst loading and a 250°C reaction temperature; after 3 hours the glycerol conversion was 98.4% and the 1,2PD selectivity was 70.2%. It was also found that when the catalyst was recycled and reused, the glycerol conversion was 93.1% and the 1,2PD selectivity was 67.6%, which were only slightly decreased compared with the results using a fresh catalyst.

From the reported data, it is noticed that in order to get higher glycerol conversion and more hydrogen produced, Pt based catalysts are usually used. However, Pt is an expensive metal, and hence will result in a high production cost for the 1,2PD hydrogenolysis process. In order to lower the cost of the catalyst, Maglinao and He in 2011 reported a process in which Raney Nickel was used as the catalyst [108]. In their report, at 230°C with a 50wt% aqueous glycerol feed, after 105min of reaction, the glycerol conversion was 99% but the yield of 1,2PD was only 18%. It was interesting that at 15min, the yield of 1,2-propanediol was at the maximum which was 30%, the byproducts were mainly acetol and lower alcohols such as n-propanol, iso-propanol, ethanol and methanol.

From the reports published about this process, using the *in situ* hydrogen produced from glycerol steam reforming as the hydrogen source has its advantages and disadvantages. The advantage is that no other reactant feed is needed since glycerol itself is the raw material for both hydrogen and 1,2-propanediol production. However, to make this process feasible, a Pt supported catalyst is usually used, which is very expensive; also the selectivity is much lower compared with when molecular hydrogen is used. Since steam reforming of glycerol involves C-C cracking, the by-products were reported to be some lower alcohols and methane.

2.3.2 Iso-propanol as a Hydrogen Donor

Another process without the addition of molecular hydrogen has been reported, in which the hydrogen atom is donated from iso-propanol, therefore producing acetone as the by-product. This process was first reported by Musolino *et al*. in 2009 using a Pd/Fe_2O_3 catalyst [109] as

shown in Scheme 2-7. The hydrogen atom in the hydroxyl group of 2-propanol was absorbed by the Pd metal, then the hydrogenation of acetol proceeded utilizing the adsorbed hydrogen atom donated from 2-propanol. In this report, the Pd(10wt%) Fe_3O_4 prepared by Na_2CO_3 co-precipitation was used. In this process, a 12wt% glycerol iso-propanol mixture was used as the feedstock, and the reaction conditions were: 180°C, and the reaction time was 24 hours. The glycerol conversion was 100% with 84% 1,2-PD selectivity which was very high compared with the results using glycerol steam reforming as the hydrogen source. If ethanol was used, at 180ºC after 24 hours, the conversion was reported to be 100% and the selectivity to 1,2PD was 90%.

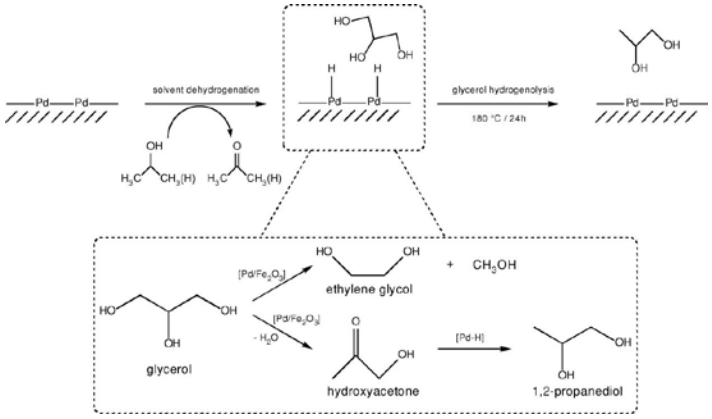

Scheme 2-7 Reaction Pathway of Converting Glycerol to 1,2PD in the Absence of Added Hydrogen Using a Pd/Fe_2O_3 Catalyst and Iso-propanol as the Hydrogen Resouce [109]*.

Reprinted Musolino *et al*., *Chemical Communications*, pp. 6011-6012, 2008 with permission from the Royal Society of Chemistry.

However, Pd is also an expensive metal and 10% loading is very high; the cost of catalyst is even higher than Pt based catalyst. Therefore, Ganarias *et al*. in 2011 reported the same process using a $Ni\text{-}Cu/Al_2O_3$ catalyst [110]. In this report, temperatures of 320°C and 450°C were used, which were much higher than the temperature reported using a Pd based catalyst. After 24 hours, at 320°C the glycerol conversion was 41.2% with 48.3% 1,2PD selectivity; at 450°C, the glycerol conversion was 57.3% with 62.1% 1,2PD selectivity.

The advantage of this process is higher selectivity since this process does not involve too much C-C cleavage. The by-products were mainly acetol, 1-propanol and ethylene glycol, with less lower alcohol produced compared with that when using glycerol steam reforming as the hydrogen source. The disadvantages of this process are: acetone is formed as a by-product causing a high production cost for the downstream separation process; lower hydrogen utilization since one mole of iso-propanol can only donate one mole of hydrogen atoms, which can result in a high cost of solvent because the solvent is not re-useable; in order to have a high 1,2PD selectivity, high loading of Pd is needed resulting in a high catalyst cost.

2.3.3 Formic Acid as Hydrogen Donor

Some researchers have developed a glycerol hydrogenolysis process to produce 1,2PD using formic acid as the hydrogen donor. The advantages of using formic acid are that it can be obtained from renewable resources from non-food biomass. Formic acid is also considered as a promising hydrogen storage compound as it can be obtained through CO_2 hydrogenation.

Gandarias *et al*. in 2012 reported this process using a Ni-Cu/Al_2O_3 catalyst [111] as shown in Scheme 2-8. In this report, a semi-batch process with formic acid pumping into the reaction mixture was developed. The reaction conditions were 20wt% aqueous glycerol, 220°C reaction temperature and 0.02mL/min formic acid feed rate, after 10 hours the glycerol conversion was 33.5% and the 1,2PD selectivity was 85.9%.

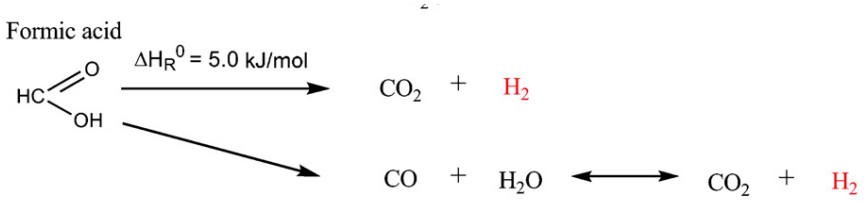

Scheme 2-8 Reaction Pathway of Converting Glycerol to 1,2PD in Absence of Added Hydrogen Using Formic Acid as the Hydrogen Resouce [111]*.

*Reprinted Gandarias et al., *Catalysis Today*, vol. 195, pp. 22-31, 2012. with permission from the Elsevier Limited.

Gandarias *et al*. in 2012 reported the same process by further optimizing the Ni/Cu ratio and reaction conditions [54]. In this report, $Ni_{20}Cu_{15}$ was reported to be the optimized composition. When the formic acid feed rate was 3.6mmolg-cat^{-1}h^{-1} at 220°C, after 16 hours the glycerol conversion was 49.3% and 1,2PD selectivity was 75.4%. The carbon balance in the liquid solution was 99.1%, it was suggested that glycerol was not consumed for steam reforming.

In 2013 Gandarias *et al*. reported the same process and the experimental results were compared with the process in which molecular hydrogen was used [112]. Under the same conditions, it was found that when hydrogen was initially fed, the 1,2PD selectivity was not significantly improved but the glycerol conversion was increased, i.e. when 45 bar nitrogen was added into the reaction the glycerol conversion was 55.2% and the 1,2PD selectivity was 84.6% while when 45 bar hydrogen was added the glycerol conversion was increased to 69.2% and the 1,2PD selectivity was unchanged at 84.6%.

Martin *et al*. in 2013 published a review article for glycerol hydrogenolysis using *in situ* hydrogen [113]. More reported numerical results regarding this process are listed in Table A-2 in Appendix A.

2.4 Catalyst Development for Production of 1,3-propanediol (1,3PD) from Glycerol

The conversion of glycerol into 1,3-propanediol (1,3PD) has also been investigated since 1,3-propanediol is much more valuable as introduced in Chapter 1. 1,3PD is usually used in the production of polymethylene terephthalates (PTT) and polyurethanes. However, the process is much more challenging compared with the production of 1,2PD. Reported yields of 1,3PD from glycerol hydrogenolysis processes are very low so far.

In 2010, Nakagawa *et al*. reported that a Ir-ReO_x (Re:Ir = 1) catalyst was active to give a high yield of 1,3PD [114] under mild reaction conditions (0.75wt% catalyst, 120°C, 1160psi, 24 hours). However, in order to obtain high acidity, sulfuric acid was also added which causes environmental pollution problems in case of spillage, equipment corrosion and additional cost for the downstream neutralization process. The conversion of glycerol was reported to be 62.8% and selectivity to 1,3PD was 49% and selectivity to 1,2PD was 10%. Because of the acidity provided by sulfuric acid, a high selectivity to 1-propanol of 33% was found.

In 2011, Amada *et al*. reported the effect of Re:Ir ratio [115] under the same experimental conditions as Nakagawa *et al.* reported [114] for the process of 1,3PD production. In their report, when Re:Ir = 2, the results were optimal providing 58.6% glycerol conversion, with a selectivity to 1,3PD and 1,2PD of 44.6% and 5.4% respectively, and the selectivity to 1-propanol was still high (40.7%). Also it was mentioned that without sulfuric acid addition, the glycerol conversion dropped to about half.

Supported platinum catalysts have frequently been reported for 1,3PD production from glycerol. Oh *et al*. in 2011 reported a Pt-sulfated zirconia catalyst [116]. In their report, it was stated that super acidic sites were required to have a high 1,3PD yield; when platinum was loaded on zirconia strong Bronsted acidic sites were found based on NH_3 TPD and FTIR results. To carry out the experiment, 1,3-dimethyl-2-imidazolidinone (DMI) was used as the solvent (3mmol glycerol in 0.2ml DMI), the reaction conditions were: 180°C, 1160psi hydrogen, 24 hours,with 35wt% catalyst); the glycerol conversion was 66.5% and the yield of 1,3PD was 55.6% which is the highest reported to date. However, without the solvent (only aqueous glycerol as the feedstock), the conversion was 62.9% which was similar to the value with solvent however, the yield of 1,3PD was only 12.3%. Therefore, the solvent plays a very important role on the selectivity toward 1,3PD. It was also reported that the DMI was not degraded after each reaction, so it could be separated for subsequent usage.

Gong *et al*. in 2010 reported a $Pt/WO_3/TiO_2/SiO_2$ catalyst [117]. In this report, aqueous glycerol was used as the feedstock and the conversion was only 15.3% with a fairly high 1,3PD selectivity (50.5%). Recently Zhu *et al*. in 2012 reported a $Pt\text{-}H_4SiW_{12}O_{40}/SiO_2$ catalyst to produce 1,3PD using a fixed bed reactor [118]. At 200°C and 725psi hydrogen, when 10% aqueous glycerol was fed at WHSV = $0.03h^{-1}$, the glycerol conversion was 88.5% however the 1,3PD selectivity was only 27.2%. By varying the reaction condition, it was found that high temperature and high hydrogen pressure decreased the 1,3PD selectivity.

No report has been published about 1,3PD production without external hydrogen added. However, Ouyang *et al*. in 2011 published a report [119], in which a mathematical model was developed applying some thermodynamic parameters to simulate the process of 1,3PD production using *in situ* hydrogen from glycerol steam reforming. The results showed that this process was thermodynamically feasible. However, based on the experimental results, over 1000psi of hydrogen is always needed; therefore, the process using *in situ* hydrogen produced from glycerol steam reforming is very challenging.

In conclusion, in order to have a high yield of 1,3PD from hydrogenolysis of glycerol, the acidity of the catalyst plays a key role. Higher acidic strength and more acidic sites can give higher 1,3PD selectivity and higher glycerol conversion. Based on current publications, in order to obtain high 1,3PD selectivity, a supported Pt on solid acid catalyst is usually used with a special liquid solvent added (DMI or sulfuric acid).

Chapter Three
Experimental Apparatus and Methods

In this chapter, the procedure of catalyst preparation and loading of different promoters are introduced. The analytical methods employed in this work are outlined including the quantitative analysis of liquid products by gas chromatography and the gas products by a residual gas analyzer (RGA). The specifications of the bench scale autoclave reaction for glycerol hydrogenolysis to produced 1,2-propanediol (1,2PD) and the procedures of liquid sampling and gas sampling are explained. The detailed catalyst characterization techniques are described including temperature programmed desorption (TPD), X-Ray diffraction (XRD), thermogravimetric analysis (TGA), BET surface area and Transmission Electron Microscopy (TEM).

3.1 Catalyst Preparation Methods

In this section, the procedures of preparing catalysts via different preparation methods including the methods of loading different promoters are introduced.

3.1.1 Oxalate Gel-coprecipitation

Ethanol was purchased from Fisher Scientific Canada (HPLC grade). The other chemicals were purchased from Sigma Aldridge Co. Canada and all the gases were purchased from Praxair Canada Inc. To prepare the $Cu/ZnO/Al_2O_3$ catalysts by oxalate gel-coprecipitation,

20% excess ethanol solution of 0.5M oxalic acid (anhydrous, ⩾97.0%) was rapidly injected into an ethanol solution mixture of $Cu(NO_3)2 \cdot 2.5H_2O$ (⩾98.0%), $Zn(NO_3)_2 \cdot 6H_2O$ (⩾98.0%), $Al(NO_3)_3$•9H2O (⩾98.0%) with designated molar ratio under vigorous stirring, the total metal concentration was 0.5M [78, 79]. The slurry was then aged under stirring for 2 hours and the precipitate was filtered and dried in air at 110ºC for 24 hours. The dried particles were ground and screened via a sieve with 250μm opening and then calcined in air at 150ºC for 1 hour, 200ºC for 1 hour, 250ºC for 1 hour, 300ºC for 1 hour and 360ºC for 4 hours [120].

To prepare $Cu/MgO/Al_2O_3$ catalysts via the gel-coprecipitation method, the procedures were the same as described in the previous paragraph except replacing $Zn(NO_3)_2 \cdot 6H_2O$ by $Mg(NO_3)_2$•$6H_2O$ (⩾99.0%) which was purchased from Sigma Aldridge Co. Canada.

To add Ni into the catalysts via a gel-coprecipitation method, $Ni(NO_3)_2$•$6H_2O$ (⩾99.0%) purchased from Sigma Aldridge Co. Canada was used as a Ni precursor. A designated amount of $Ni(NO_3)_2$ was mixed with the metal nitrate solution. Other procedures were the same as described in the previous paragraph.

3.1.2 Na_2CO_3 Co-precipitation

For a comparative study, the $Cu/ZnO/Al_2O_3$ catalysts were prepared by a conventional Na_2CO_3 coprecipitation method [47, 70]. An aqueous solution of 0.5M Na_2CO_3 purchased from Sigma Aldridge Co. Canada was added drop-wise into an aqueous mixture of 0.5M of the metal nitrate with a designated molar ratio under vigorous stirring until the pH reached 9.0. The slurry was then aged under stirring for 1 hour. The precipitate was then filtered and washed with de-ionized water until the pH of the filtrate reached 7.0. The washed precipitate was dried in air at 110ºC for 24 hours. The dried particles were ground and screened with a sieve with a 250μm opening and then calcined in air at 650ºC for 4 hours.

3.1.3 Impregnation

The catalysts were also prepared by an impregnation method. A designated amount of support was aged for a metal nitrates aqueous solution (0.5M) for 4 hours in a round bottom flask. The flask containing the impregnated solution was then placed in an oil bath at 110ºC under vigorous stirring to evaporate the water. The particles were dried in air at 110ºC for 24 hours and calcined in air at 450ºC for 4 hours.

3.1.4 Loading Pd on Calcined Cu/Zn/Al or Cu/Mg/Al Catalysts

The $Cu/ZnO/Al_2O_3$ or $Cu/MgO/Al_2O_3$ catalysts with a designated ratio prepared via a gel-coprecipitation method was used as the support for Pd. The catalysts were prepared via an impregnation method. Palladium (II) acetate (98%) purchased from Sigma Aldridge Co. Canada was used as the precursor. A pre-calculated amount of palladium (II) acetate was weighed and transferred into a round bottom flask. A designated amount of acetone (98%) required to meet 35ml of solvent per gram of catalyst support [121] was added into the round bottom flask under vigorous stirring until the palladium (II) acetate was completely dissolved in the solvent. Then the calculated amount of catalyst support was weighed and transferred into the round bottom flask with the palladium (II) acetate solution and aged for 4 hours. The flask containing the impregnation solution was then placed in an oil bath at 70ºC under vigorous stirring to evaporate the acetone solvent. The particles were dried under air at 110ºC for 24 hours and calcined in air at 360ºC for 4 hours.

3.2 Autoclave Experimental Apparatus

In this section, the experimental apparatus for the experiments carried out in an autoclave are introduced including the catalyst reduction and reaction systems.

3.2.1 Catalyst Reduction Apparatus

Before each experiment was carried out, the catalyst was reduced in a quartz tubular reactor. The reactor is enclosed in a furnace controlled by a temperature controller as shown in Figure 3-1. The pre-weighed catalyst particles were placed on a catalyst bed made from quartz in the tubular reactor and the reactor was placed into the furnace; a thermocouple was placed into the tube below the catalyst bed. The reactor was heated to the designated temperature under a continuous high purity helium flow. After the desired temperature was reached, the three-way valve was adjusted to let a continuous high purity hydrogen gas flow upward through the catalyst bed for 3 hours. Then the furnace was turn off and the catalyst particles were cooled to room temperature under a helium flow.

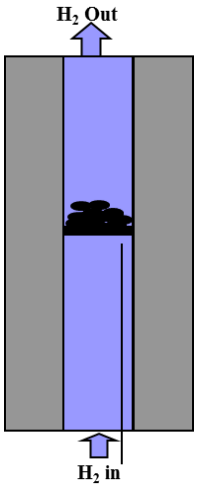

Figure 3-1 Schematic Flow Diagram of the Catalyst Reduction Apparatus.

3.2.2 Autoclave Apparatus

A 300mL Parr Instrument 4560 Series mini bench top reactor, which is illustrated in Figure 3-2, was used for the catalyst activity tests. The reactor was constructed of hastelloy with a PTFE o-ring seal on the top of the reactor. The maximum operating conditions were rated to be 360ºC and 3000psig. An impeller connected to a magnetic drive was used for mixing. The

reactor temperature was monitored by a thermocouple and the temperature was controlled by a Parr Instrument 4848 Series reactor controller. Over-pressure protection was provided by a rupture disk made from Au and rated to fail at 2500 psi (purchased from Fike Corp). A sampler was equipped for taking liquid samples at different time intervals during the reaction. A three-way valve sealed with an inlet septa purchased from Agilent Technologies was used to take the gas samples.

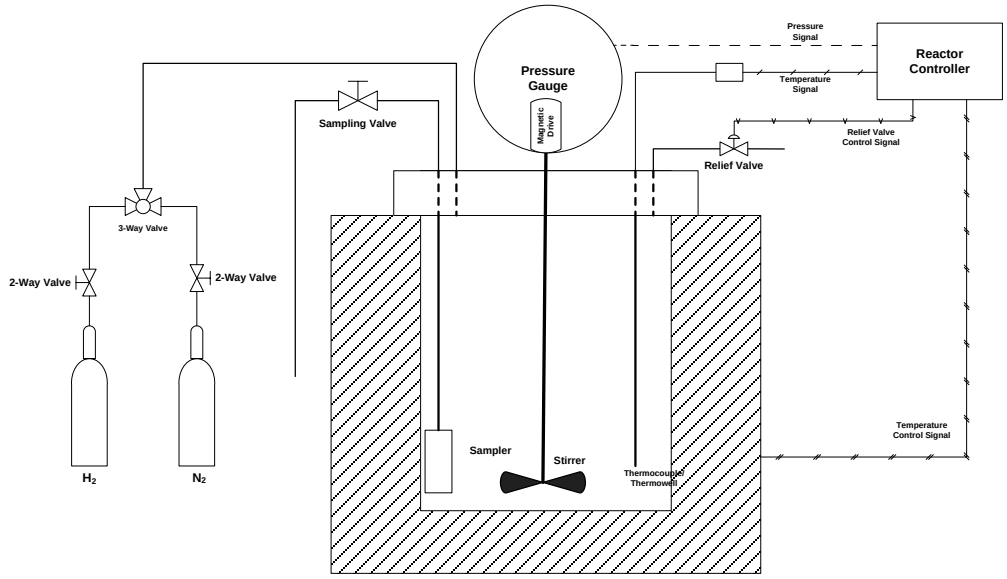

Figure 3-2 Schematic Flow Diagram of an Autoclave Reactor System.

3.3 Products Analytical Apparatus and Method

In this section, the apparatus for product analysis and the calculations for conversion and selectivity are defined.

3.3.1 Gas Chromatography (GC)

All the liquid samples were analyzed by an Agilent Technology's 6890N Gas Chromatograph equipped with a flame ionization detector (FID). All the samples were

injected automatically by using an Agilent Technology's 7863 Series auto-injector equipped with a 5μL syringe. A J&W Scientific DB-WAX megabore capillary column (30m x 0.53mm I.D. x 10μm film thickness) was used for separation of the different species. The GC method parameters are listed in Table 3-1.

Table 3-1 Detailed GC Method.

Inlet	Volume Injected	1 μL
	Inlet Temperautre	300 °C
	Carrier Gas	He
	Inlet Pressure	5 psi
	Total Flow	100 mL/min
Oven Temperature Profile	Initial Temperautre	100 °C
	Hold	2 min
	Ramp1	1 °C /min to 105 °C
	Ramp2	10 °C /min to 200 °C
	Hold	15 min
FID Detector	Detector Temperautre	300 °C
	H_2 Flow	40 mL/min
	Air Flow	450 mL/min
	Makeup Gas	He
	Makeup Flow	45 mL/min

1,4-butanediol was chosen as the internal standard since it is not one of the product species and it exhibits similar properties to the components because it contains two hydroxyl groups. An internal standard solution was prepared by adding 5g of 1,4-butanediol into 1L of n-butanol. The standards were purchased from Sigma Aldridge Co. Canada. Before the experimental samples were injected into the GC, a calibration for each sample standard was carried out. A typical chromatogram of one calibration standard with all possible products is illustrated in Figure 3-3; the species in an unknown sample can be determined based on the retention time of standards as listed in Table 3-2.

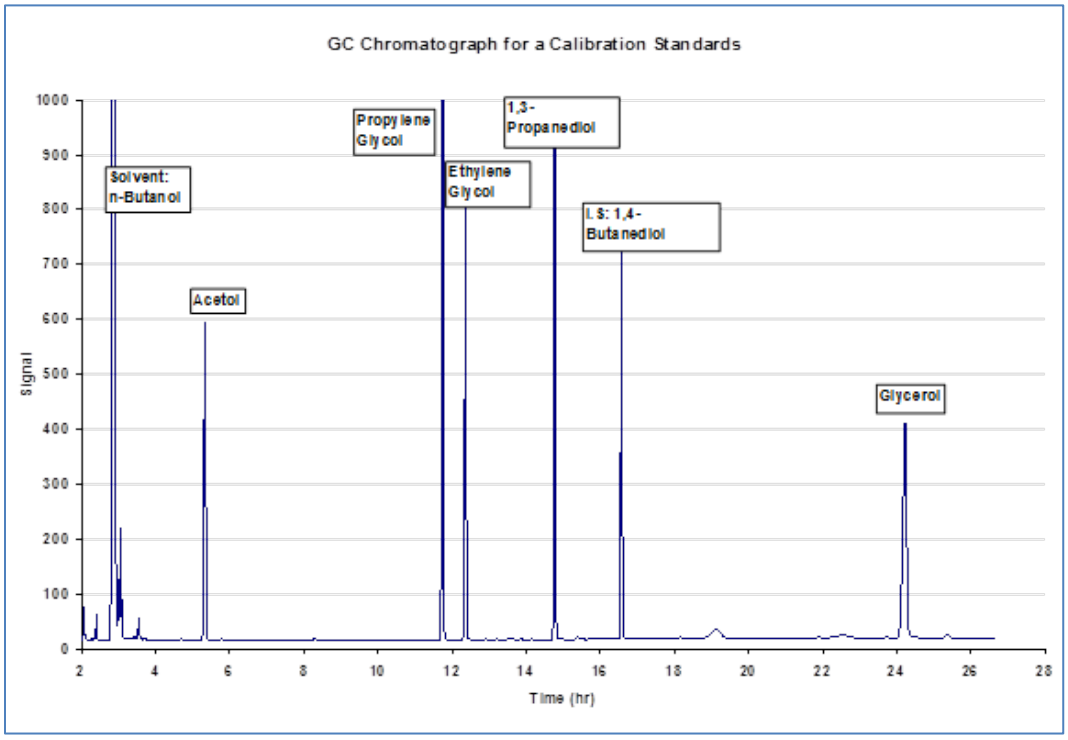

Figure 3-3 A Typical Chromatogram of a GC Calibration Standard (0.05g of each compound in 5mL of internal standard solution)

A multiple-point internal standard method was used for the GC calibration. Which involved 6 calibration standards which contained different amounts of each product species (50mg, 100mg, 150mg, 200mg, 250mg, 600mg) in 5mL of internal standard solutions which were prepared for analysis. Then the response factor of each component was calculated according to Equation 3-1. The calibrated response factor of each species is listed in Table 3-2 and the calibration curves are shown in Appendix B.

$$\frac{m_i}{m_{I.S.}} = k_i \frac{A_i}{A_{I.S.}} \qquad \textbf{Equation 3-1}$$

where,

m_i, A_i -- mass and area of each species respectively

$m_{I.S.}$, $A_{I.S.}$ -- mass and area of internal standard respectively

k_i -- response factor of each species

Table 3-2 Retention Time and Response Factor for Each Compound.

Compound	n-Butanol	Acetol	1,2PD	EG	1,3PD	1,4-Butanediol	Glycerol
Retention Time (min)	2.887	5.322	11.739	12.357	14.772	16.566	24.192
Response Factor		2.014	1.232	1.672	1.222		1.554

The liquid samples taken from the autoclave experiments were first centrifuged in an IEC CL31 multispeed centrifuge, purchased from Thermo Electron Corp., at 8000RPM for 10 minutes to separate the large particles from the liquid product samples. Then the centrifuged liquid samples were filtered through a polyethersulfone syringe membrane with a 0.2μm pore size to further separate the fine particles remaining in the liquid samples. Approximately 120mg of liquid sample was added into a 1ml GC vial mixed with 1ml of an internal standard solution. Equation 3-2 was used to calculate the mass of each species in the sample. The glycerol conversion, 1,2PD selectivity and yield of each product were calculated on a carbon basis using Equation 3-3 - Equation 3-5.

$$m_i = m_{I.S.} k_i \frac{A_i}{A_{I.S.}} \qquad \textbf{Equation 3-2}$$

$$Conv_{Glycerol}\% = 100\% - \frac{n_{Glycerol}}{\sum n_{carbon\cdot species} + n_{EG} + n_{others}} \times 100\% \qquad \textbf{Equation 3-3}$$

$$Selectivity_{12PD}\% = \frac{n_{12PD}}{\sum n_{carbon\cdot species} - n_{Glycerol} + n_{EG} + n_{others}} \times 100\% \qquad \textbf{Equation 3-4}$$

$$Yield_i\% = \frac{n_i}{\sum n_{carbon\cdot species} + n_{EG} + n_{others}} \times 100\% \qquad \textbf{Equation 3-5}$$

3.3.2 Refinery Gas Analyzer (RGA)

Gas samples were analyzed by a calibrated Agilent Refinery Gas Analyzer (RGA, 3000 Micro C). Gas samples were injected into the sample inlet of the RGA and then an internal vacuum pump drew the samples into four independent GC modules simultaneously. Table 3-3 lists the detailed configuration and separation of gases on the RGA. Each GC module houses a silicon micro injector, a temperature-controlled capillary column, and a micro thermal conductivity detector (TCD).

Table 3-3 Configuration and gas separation of RGA.

Channels	**A**	**B**	**C**	**D**
Injector Type	Backflush	Backflush	Backflush	Firmed volume
Carrier Gas	Argon	Helium	Helium	Helium
Column Type	Molecular Sieve	Plot U	Alumina	OV-1
Detector Type	TCD	TCD	TCD	TCD
Inlet Type	Heated	Heated	Heated	Heated
Gas separated	H_2, O_2, N_2, CH_4, CO	CO_2, C_2, H_2S, COS	C_3, $C_4^=$, C_5	i-C_4, C_6

3.4 Methods and Procedures for Catalyst Characterization Techniques

In order to study the physicochemical properties of the catalysts and the relationship between the catalyst structures and catalytic activity, some catalyst characterization experiments were carried out. In this section, the methods and procedures for the catalyst characterization techniques are introduced.

3.4.1 NH_3 Temperature Programmed Desorption (TPD)

An Altamira AMI-200 Catalyst Characterization System was used for the TPD experiments. The catalyst powder was pressed into thin wafers. The wafers were then broken down and screened through a sieve. The particles with sizes between 250μm and 500μm were collected for the TPD analysis. Approximately 120mg of catalyst was weighed and placed within a quartz U-tube reactor with a small amount of quartz wool placed on both ends of the catalyst sample. The U-tube was then secured to the sample station and enclosed by a furnace integrated with a thermocouple. The flow diagram for this system is shown in Figure 3-4.

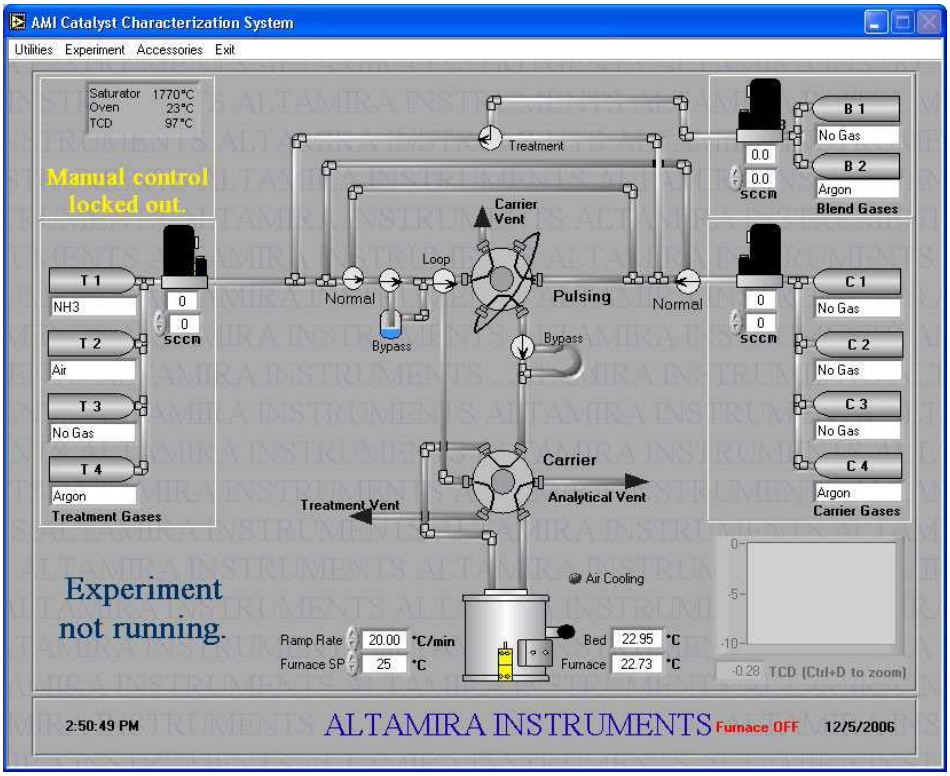

Figure 3-4 Schematic Flow Diagram of the Altamira AMI-200 Catalyst Characterization System (Screen print out from AMI-200 Human-Machine Interface).

The catalyst was reduced under a flow of 5% H_2 balanced with Argon at a volumetric flow rate of 30ml/hr at 300°C for 3 hours as Figure 3-5A shows. After reduction, the catalyst was cooled down to 25°C, 20 pulses of 5% NH_3 balanced with Argon at a flow rate of 30ml/min for 60s were injected into the U tube to saturate all the acidic sites of the catalyst (Figure 3-

5B). Then the catalyst was heated to 1000°C at a heating rate of 10°C/min for NH_3 desorption (Figure 3-5C). After the catalyst TPD experiment, 10 pulses of a known volume (i.e. the sample loop volume of 524.0 mL) of 5% NH_3 balanced with Argon were injected directly into TCD without being passed through the U tube for calibration; the number of moles of ammonia injected can be calculated using the ideal gas law. The number of moles of NH_3 desorbed during the desorption step can be calculated using Equation 3-6 and Equation 3-7.

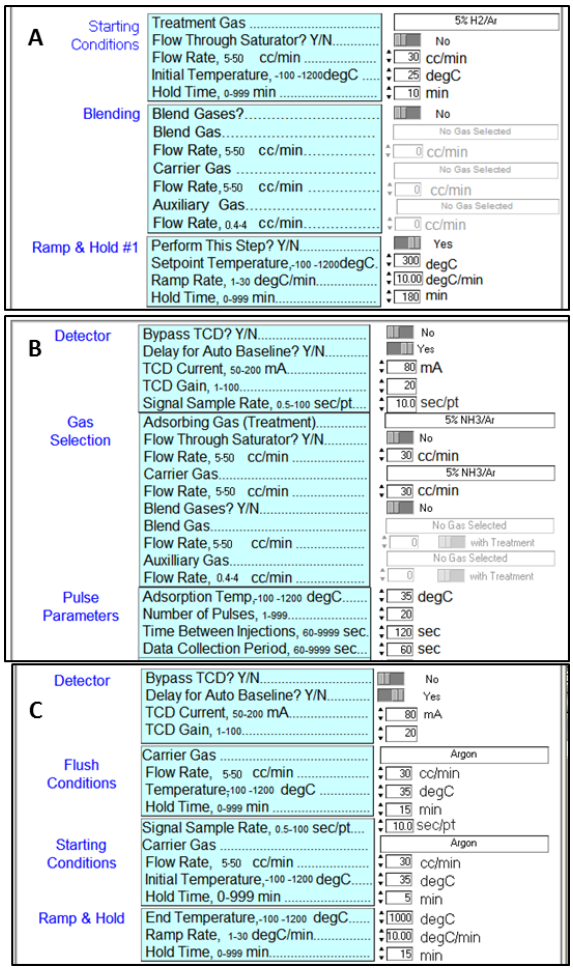

Figure 3-5 Method for NH_3 TPD: A) Catalyst Reduction; B) NH_3 Saturation; C) Temperature Programmed Desorption.

$$Calibration\_Value = \frac{0.524ml \times 5.16\% NH_3}{mean\_calibration\_area}$$ **Equation 3-6**

$$Uptake(\mu mole/gcat) = \frac{analytical\_area \times calibration\_value}{sample\_weight \times 24.5}$$ **Equation 3-7**

3.4.2 CO_2 TPD

For a CO_2 TPD experiment, the catalyst was loaded and reduced as described in the previous section for NH_3 TPD. After reduction, the catalyst was cooled down to 35°C; a stream of 5% CO_2 balanced with Argon was passed over the catalyst for 60min at 35°C to saturate the catalyst as shown in Figure 3-6A. Then the catalyst was heated to 1000°C at a heating rate of 10°C/min for CO_2 desorption (Figure 3-6B). After the desorption, 10 pulses of a known volume (i.e. the sample loop volume of 524.0 mL) of 5% CO_2 balanced with Argon were injected directly into TCD without being passed through the U tube for calibration; the number of moles of CO_2 injected can be calculated using the ideal gas law. The number of moles of CO_2 desorbed during the TPD step can be calculated using Equation 3-6 and Equation 3-7.

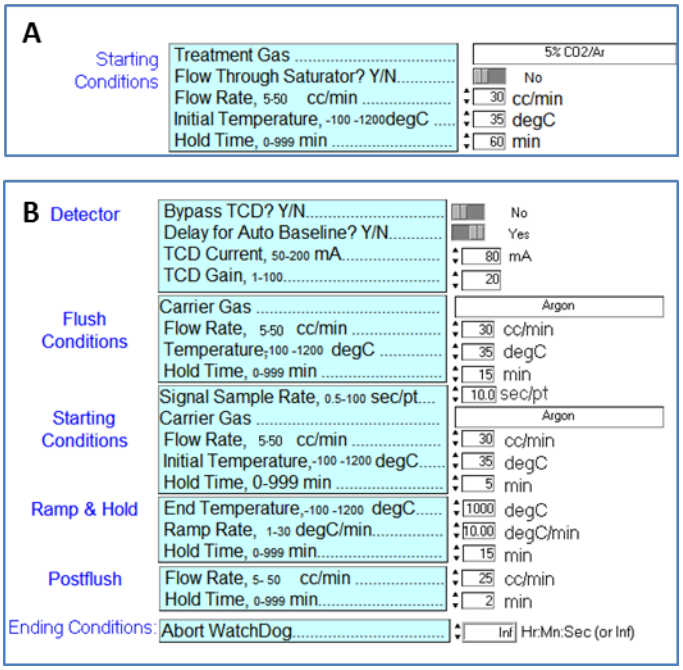

Figure 3-6 Method for CO_2 TPD: A) CO_2 Saturation; B) Temperature Programmed Desorption.

3.4.3 H_2 TPD

Hydrogen temperature programmed desorption experiments have been carried out to test the hydrogen adsorption capacity of the catalysts which could affect the catalytic activity for hydrogenation. The catalyst was loaded and reduced as described in Section 3.4.1 for the NH_3 TPD experiments. After the catalyst was cooled to 35°C a stream of 5% H_2 balanced with Argon was passed over the catalyst for 60min at 35°C to saturate the catalyst as shown in Figure 3-7A. Then the catalyst was heated to 1000°C at a heating rate of 10°C/min for H_2 desorption (Figure 3-7B). After the desorption step, 10 pulses of a known volume (i.e. the sample loop volume of 524.0 mL) of 5% H_2 balanced with Argon were injected directly into the TCD without being passed through the U tube for calibration; the number of moles of H_2 injected can be calculated using the ideal gas law. The number of moles of H_2 desorbed during the TPD step can be calculated using Equation 3-6 and Equation 3-7.

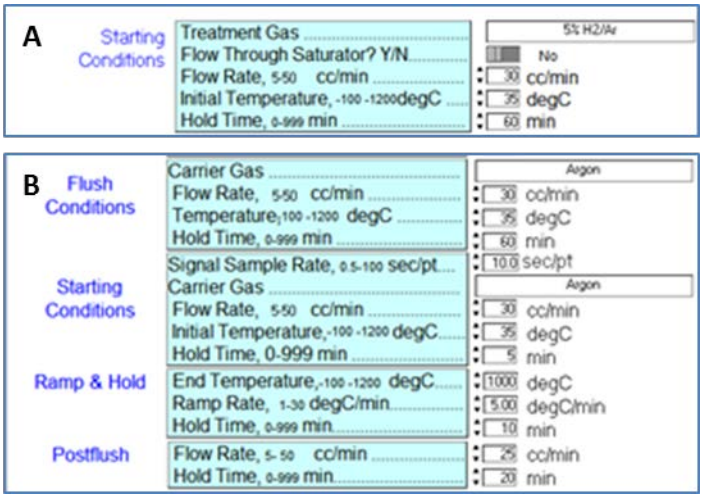

Figure 3-7 Method for H_2 TPD: A) H_2 Saturation; B) Temperature Programmed Desorption.

3.4.4 H_2 Temperature Programmed Reduction (TPR)

Temperature programmed reduction (TPR) experiments have been carried out to test the appropriate reduction temperature for each catalyst. In an H_2 TPD experiment introduced in the previous section, the hydrogen was adsorbed and desorbed on a pre-reduced catalyst and the amount of hydrogen adsorbed can be calculated. In a TPR experiment, the catalyst was reduced while the temperature was increased to find the optimum reduction temperature. The catalyst was first heated to 200°C and kept at 200°C for 60 minutes under a stream of 30ml/min Argon flow to remove all the moisture and other species absorbed on the catalyst surface (Figure 3-8A). Then the catalyst was heated under a stream of 30ml/min 5% H_2 balanced with Argon at a heating rate of 5°C/min until 800°C was reached and then the temperature was held at 800°C for 15 minutes (Figure 3-8B).

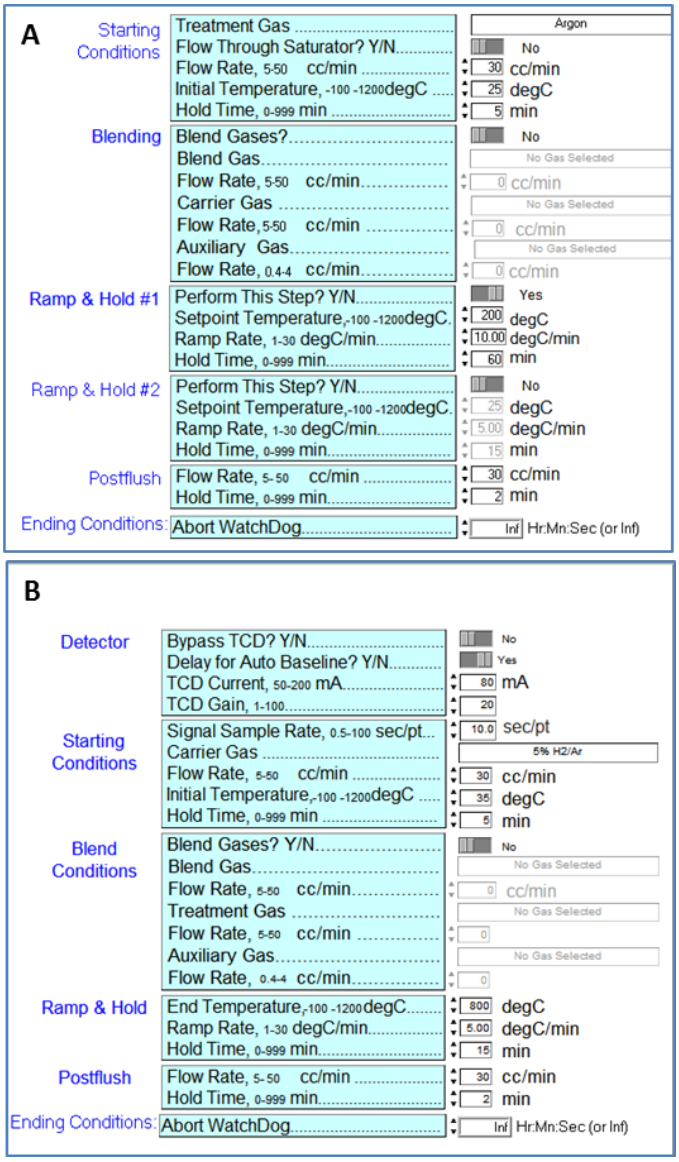

Figure 3-8 Method for TPR: A) Moisture Removal; B) Temperature Programmed Reduction.

3.4.5 BET Surface Area

BET surface areas of the catalysts were determined by a Gemini 2375 instrument using nitrogen physisorption at 77 K, taking 0.162 nm^2 as the cross sectional area for di-nitrogen. Catalyst samples were dried in air at 110°C overnight and cooled down to room temperature before BET analysis.

3.4.6 Thermal Gravimetric Analysis (TGA) / Differential Thermal Analysis (DTA)

An SDT Q600 was used for TGA and DTA thermal analysis. The panel was filled with around 15mg of catalyst sample. Then the sample was heated under 100ml/min air flow from room temperature to 1000 ºC.

3.4.7 X-Ray Diffraction (XRD)

The XRD patterns were obtained on a Bruker D8 Focus model. The vacuum tube parameters were set to 40 kV potential and 30 mA current intensity. The Cu kα radiation wave length was set to 1.54 Å; the 2θ angle range was set at 20^{o}-80^{o} with a ramp of 0.02^{o} per minute.

3.4.8 Transmission Electron Microscopy (TEM)

Catalyst powders were diluted with ethanol and sonicated in order to be well dispersed. One drop of the solution was deposited on a holey-carbon film supported on Cu grids. Specimens were examined using a JEOL 2010 TEM operated at an accelerating voltage of 200keV.

3.4.9 Inductively coupled plasma (ICP)

The metal content of the catalysts were determined using a prodigy high dispersion ICP purchased from Teledyne Leeman Labs. 10mg of each sample was dissolved in 50ml of HF solution before each test.

Chapter Four
Glycerol Hydrogenolysis to Produce 1,2-propanediol with Molecular Hydrogen Feed

The experiments of glycerol hydrogenolysis to produce 1,2-propanediol (1,2PD) with molecular hydrogen have been carried out. Different catalyst preparation methods have been investigated for $Cu/ZnO/Al_2O_3$ catalysts. Based on the method which showed the best catalytic activity the ratio of the three metals has been studied to find the optimum composition to provide the highest activity for the production of 1,2PD. Experimental conditions such as hydrogen pressure, temperature, glycerol concentration, types of solvent, have been optimized. The effect of Pd and Mg have been investigated. Pseudo-first-order kinetics have been applied to estimate the reaction rate. It was found that the catalysts prepared via oxalate gel-coprecipitation had the highest activity for glycerol hydrogenolysis and the addition of alumina could prevent the deactivation of the catalysts and improve the catalyst stability.

4.1 Effect of the Catalyst Preparation Method on $Cu/ZnO/Al_2O_3$ Catalysts

Experiments have been carried out using $Cu/ZnO/Al_2O_3$ catalysts prepared by three different preparation methods, which were oxalate gel-coprecipitation (OA), Na_2CO_3 coprecipitation (Na) and impregnation (IMP). The molar ratio of Cu/Zn/Al catalysts prepared by oxalate gel-coprecipitation and Na_2CO_3 coprecipitation was 25/25/50 and the molar ratio for the catalyst prepared by impregnation was 15/15/70. All the catalysts were pre-reduced using a hydrogen

stream (ultra-high purity) at 300ºC for 3 hours, which has been reported very frequently [47]. The experimental conditions for hydrogenolysis were: 200ºC, 500RPM, 400psi H_2, 5wt% catalyst with respect to glycerol weight, 80% aqueous glycerol, and 24 hours reaction time. Figure 4-1 shows the glycerol conversion and 1,2PD selectivity over the reaction time using different catalysts. From Figure 4-1A it can be seen that the glycerol conversion over the reaction time is the highest using the catalyst prepared by oxalate gel-coprecipitation. Using the catalyst prepared by Na_2CO_3 coprecipitation, the glycerol conversion is lower; while the catalyst prepared by impregnation method shows the lowest glycerol conversion. As shown in Figure 4-1B, the 1,2PD selectivities using different catalysts are not much different, which are between 92% and 94%. Table 4-1 and Figure 4-2 summarize the glycerol conversion and the yield of all other by-products. Using the catalyst prepared by oxalate gel-coprecipitation the glycerol conversion and 1,2PD selectivity are about 93.0% and 94.8% respectively; and they are higher than that obtained using the catalyst prepared by Na_2CO_3 coprecipitation which gives 77.0% glycerol conversion and 92.4% 1,2PD selectivity. The catalyst prepared by the impregnation method shows the lowest activity, i.e. the glycerol conversion is only 17.2%, even though the 1,2PD selectivity is similar to that obtained using the catalysts prepared by Na_2CO_3 coprecipitation and oxalate gel-coprecipitation, the 1,2PD yield is very low.

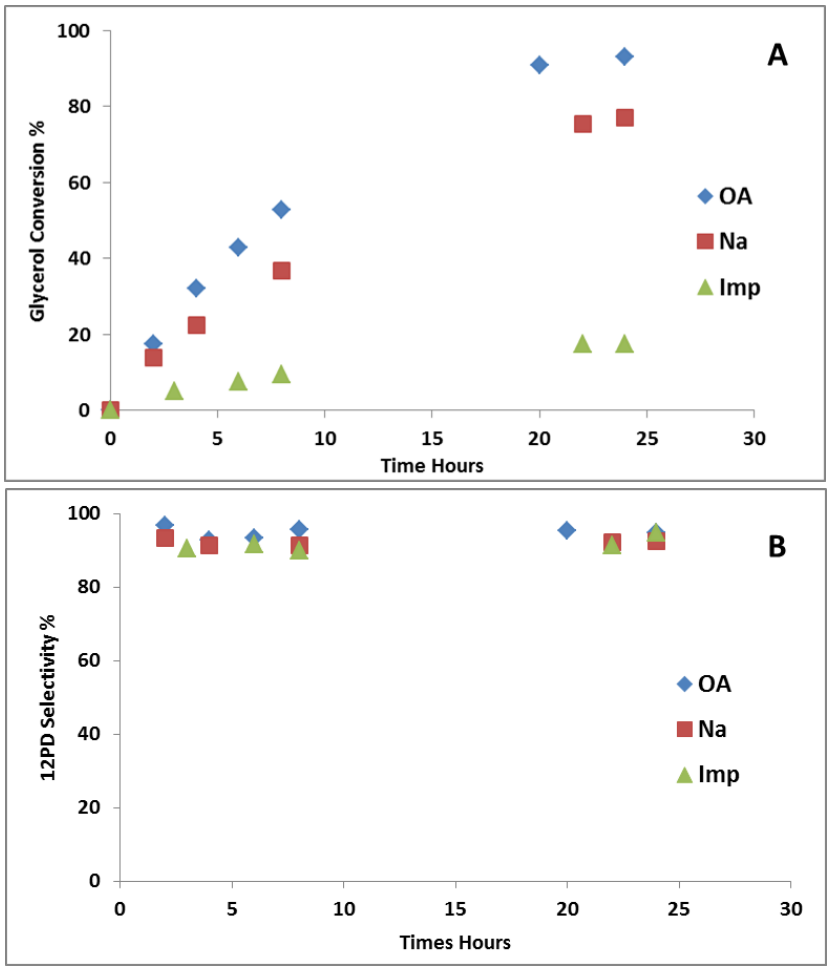

Figure 4-1 Glycerol Conversion and 1,2PD Selectivity Comparison Using the Cu/ZnO/Al_2O_3 Catalysts by Different Preparation Methods: A) Glycerol Conversion; B) 1,2PD Selectivity. Experimental Conditions: 200ºC, 500RPM, 400psi H_2, 5wt% catalyst with respect to glycerol weight, 80wt% aqueous glycerol. Metal Composition: Cu/Zn/Al-(OA and Na) = 25/25/50 (molar), Cu/Zn/Al-(IMP) = 15/15/70 (molar), support: γ-Al_2O_3.

Table 4-1 Effect of Preparation Method on Product Yield[a].

Catalysts	Glycerol Conversion	1,2PD Selectivity	1,2PD Yield	Acetol Yield	EG Yield	PrOH Yield	Others Yield
OA[1]	93.04	94.78	88.18	0.39	4.16	0.30	0.00
Na[2]	77.02	92.44	71.20	0.52	5.06	0.25	0.00
Imp[3]	17.16	94.53	16.22	0.46	0.39	0.09	0.00

[a.] Reaction conditions: 200ºC, 400psi H_2, 500RPM, 80wt% aqueous glycerol, 5wt% catalyst with respect to glycerol weight, 24 hours reaction time.

[1.] $Cu/ZnO/Al_2O_3$ Catalyst Prepared by Oxalate Gel-coprecipitation Cu/Zn/Al = 25/25/50 (molar)

[2.] $Cu/ZnO/Al_2O_3$ Catalyst Prepared by Na_2CO_3 Coprecipitation Cu/Zn/Al = 25/25/50 (molar)

[3.] $Cu/ZnO/Al_2O_3$ Catalyst Prepared by Impregnation Cu/Zn/Al = 15/15/70 (molar)

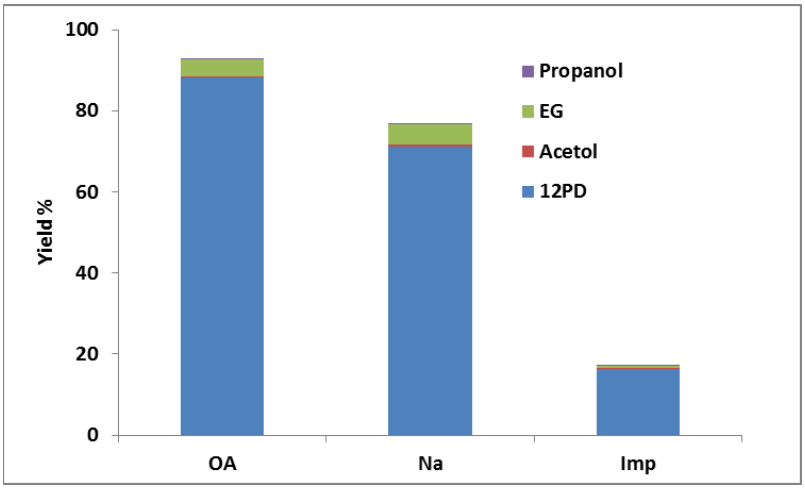

Figure 4-2 Effect of Preparation Method on Product Yield. Experimental Conditions: 200ºC, 500RPM, 400psi H_2, 5wt% catalyst with respect to glycerol weight, 80wt% aqueous glycerol. Metal Composition: Cu/Zn/Al-(OA and Na) = 25/25/50 (molar), Cu/Zn/Al-(IMP) = 15/15/70 (molar), support: γ-Al_2O_3.

Pseudo-first-order kinetics have been used to calculate the first order rate constant of the catalysts prepared by the different preparation methods. Sample calculations are obtained from Equation 4-1 and Equation 4-2 and the results are shown in Figure 4-3**.**

$$-\frac{d[GL]}{dt} = k[GL] \Rightarrow Ln[GL] = -kt + Ln[GL_{t=0}] \qquad \textbf{Equation 4-1}$$

Assume [GL] = $[GL]_{t=0}$ – [1,2PD]

$$Ln\{[GL]_{t=0} - [12PD]\} = -kt + Ln[GL_{t=0}] \qquad \textbf{Equation 4-2}$$

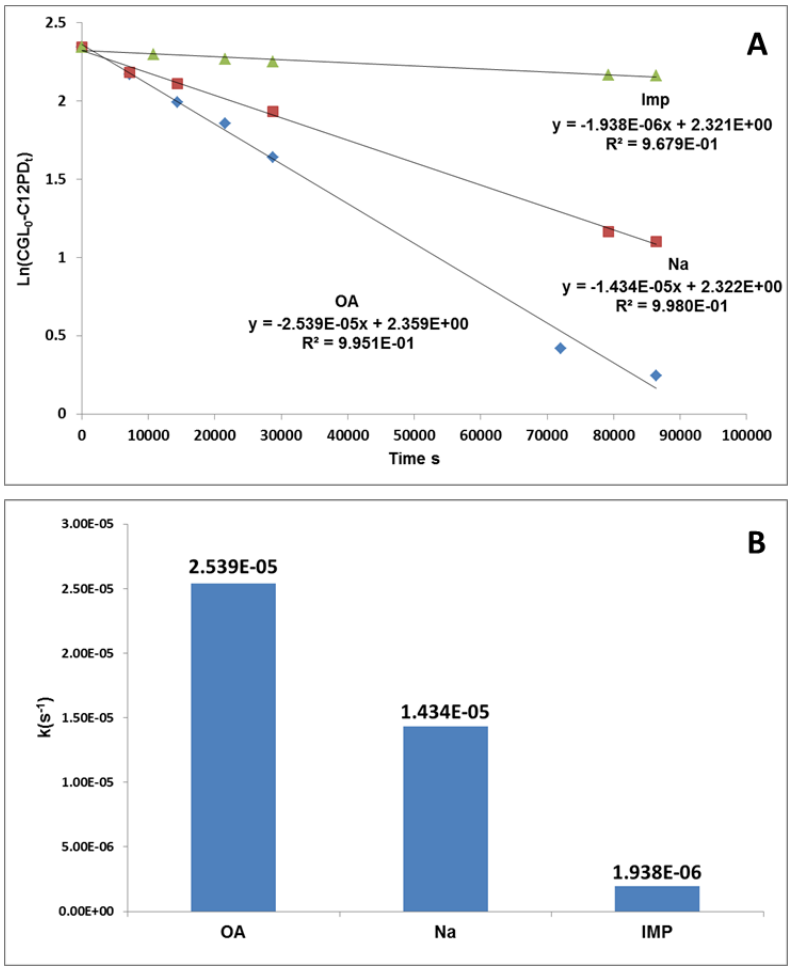

Figure 4-3 Pseudo-First-Order Kinetics Analyses for the Cu/ZnO/Al_2O_3 Catalysts Prepared by Different Preparation Methods. Experimental Conditions: 200ºC, 500RPM, 400psi H_2, 5wt% catalyst with respect to glycerol weight, 80% aqueous glycerol. Catalyst Composition: Cu/Zn/Al-(OA and Na) = 25/25/50 (molar), Cu/ZnO/Al_2O_3-Imp: Cu/Zn/Al-(IMP) = 15/15/70 (molar), support: γ-Al_2O_3.

The Cu/ZnO/Al_2O_3 catalyst prepared by the oxalic acid co-precipitation is the most active catalyst since the pseudo-first-order rate constant is the largest, which is calculated to be

$2.539x10^{-5}s^{-1}$; the rate constant of the catalyst prepared by Na_2CO_3 co-precipitation is $1.434x10^{-5}s^{-1}$, which is much smaller and the $Cu/ZnO/Al_2O_3$ catalyst prepared by the oxalate gel-coprecipitation; the catalyst prepared by the impregnation has the smallest rate constant which is only $1.938x10^{-6}s^{-1}$. Therefore, the preparation methods affect the catalytic activity significantly. It has been reported that the $Cu/ZnO/Al_2O_3$ catalysts prepared by the oxalate gel-coprecipitation method can generate much smaller Cu particles to provide more active sites, so that the reaction rate is faster [78, 79, 122]. Furthermore, the catalysts prepared by the oxalate gel-coprecipitation can generate stronger acidity and more acidic sites based on the NH_3 TPD results, and it might be able to facilitate the glycerol dehydration step to increase the reaction rate. The details will be explained in Section 6.1.1.

4.2 Cu/Zn/Al Composition Study

The optimum molar ratio of Cu to Zn was reported to be 1/1 in most of the reported literature on the activity of Cu/ZnO catalysts for the production of 1,2PD from glycerol [47, 67, 76, 123]; therefore, the effect of alumina content was studied by keeping the Cu/Zn molar ratio at 1/1. 0%, 10%, 30%, 50% and 70% of aluminum content (molar) were tested to find out the effect of aluminum content and the optimum composition. The final product yields are shown in Figure 4-4 and Table 4-2. The selectivity to 1,2PD is similar for all the catalysts which is over 90%. The glycerol conversion increases from 84.7% to 93.0% when the aluminum content is increased from 0% to 50%; when the aluminum content is further increased to 70%, the glycerol conversion dropped to 87.3%. Therefore, the optimum aluminum content is 50%. In order to check if the experimental result differences are due to the aluminum content rather than experimental error, experiments using a Cu/ZnO catalyst without aluminum added and 50% aluminum added have been repeated 3 times. A statistical analysis has been carried out using a t-distribution. The results show that the improvement of the activity is significant due to the addition of aluminum.

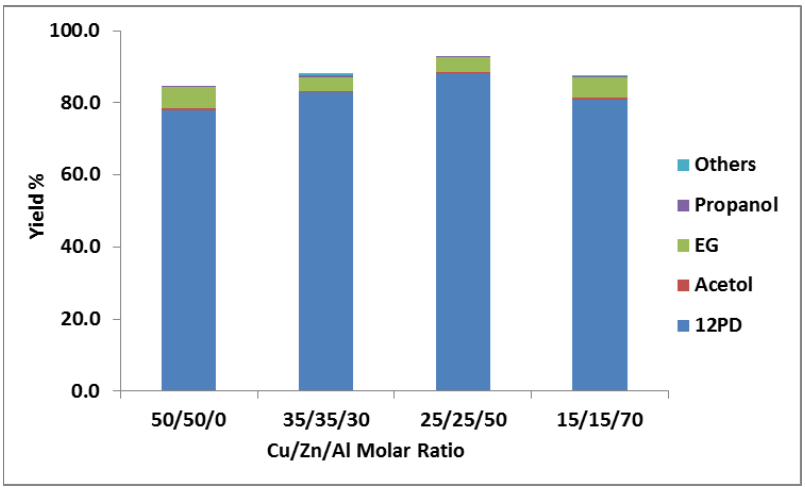

Figure 4-4 Effect of Alumina Content on Product Yield. Experimental Condition: 200ºC, 500RPM, 400psi H_2, 5wt% catalyst with respect to glycerol weight, 80% aqueous glycerol.

Table 4-2 Effect of Alumina Content on Product Yield[a].

	Glycerol Conversion	1,2PD Selectivity	1,2PD Yield	Acetol Yield	EG Yield	PrOH Yield	Others Yield
50/50/0[b]	84.71±3.81	91.80±2.19	77.76±5.06	0.61±0.49	6.01±1.10	0.32±0.16	0.00
35/35/30	88.21	93.87	82.80	0.50	3.62	0.67	0.63
25/25/50[b]	93.04±2.48	94.78±1.09	88.18±2.30	0.39±0.27	4.16±1.27	0.30±0.05	0.00
15/15/70	87.29	92.60	80.83	0.57	5.57	0.32	0.00

[a]Experimental Condition: 200ºC, 500RPM, 400psi H_2, 5wt% catalyst with respect to glycerol weight, 80% aqueous glycerol 24hours reaction time.
[b]95% Confident Interval with t-distribution

Figure 4-5 shows the glycerol conversion and 1,2PD selectivity during the reaction time for the catalysts with a Cu/Zn/Al ratio of 50/50/0, 35/35/30 and 25/25/50. As the aluminum molar ratio is increased from 0% to 50%, the glycerol conversion also increases over the reaction time. The experiment with a Cu/Zn/Al ratio of 25/25/50 shows the highest reaction rate and highest final glycerol conversion compared to the others and can be explained on the basis of the highest pseudo-first-order kinetic rate constant as shown in Figure 4-6. The selectivity to 1,2PD for all the catalysts over the reaction time does not change significantly. It is found that with aluminum added up to 50mol%, the catalytic activity is improved. It has been reported that with aluminum addition, the particles are very well mixed and

homogeneously distributed throughout the catalyst, and the aluminum in the catalyst is able to isolate the individual metal particles, avoiding their sintering [80, 124]. This will be further explained in Section 4.6 for catalyst lifetime and in Section 6.7 for XRD analysis.

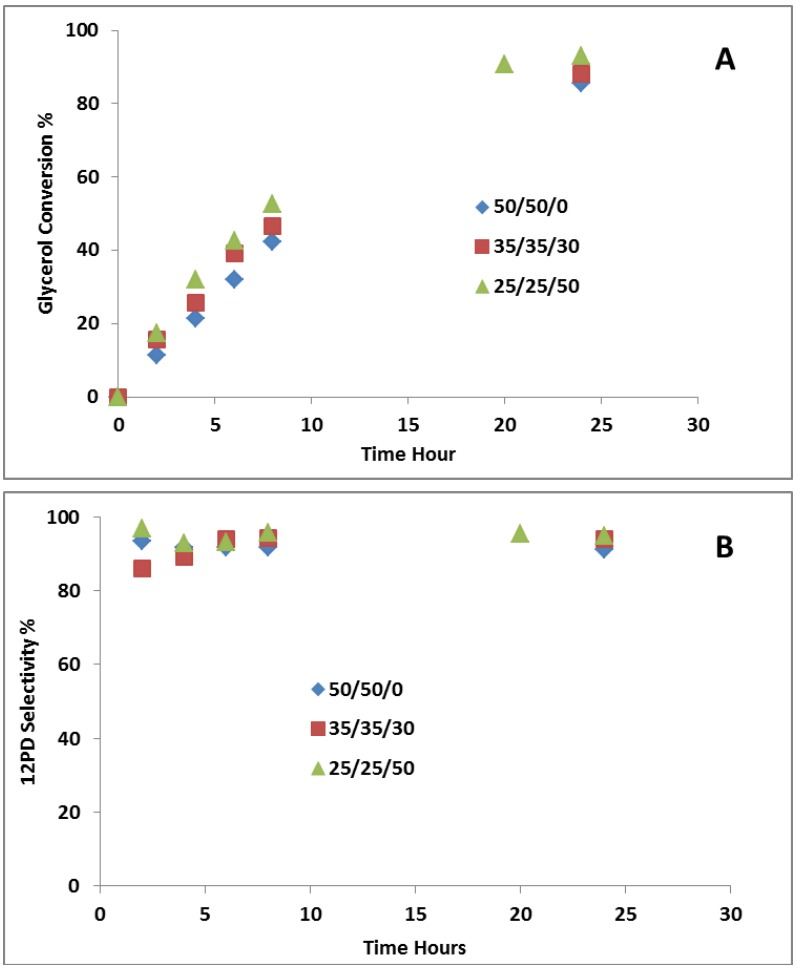

Figure 4-5 Glycerol Conversion and 1,2PD Selectivity Comparison Using the Cu/ZnO/Al_2O_3 Catalysts with Different Aluminum Content: A) Glycerol Conversion; B) 1,2PD Selectivity. Experimental Conditions: 200ºC, 500RPM, 400psi H_2, 5wt% catalyst with respect to glycerol weight, 80% aqueous glycerol.

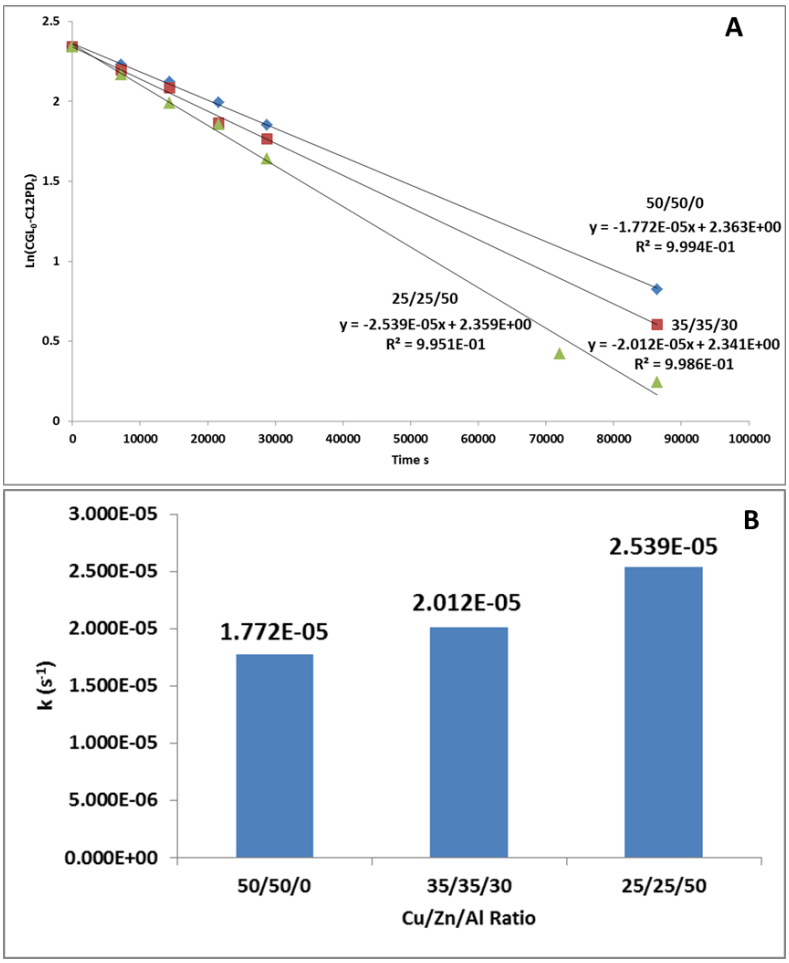

Figure 4-6 Pseudo-First-Order Kinetics Analyses for the Cu/ZnO/Al_2O_3 Catalysts Prepared by Oxalate Gel-coprecipitation with Different Aluminum Molar Content. Experimental Conditions: 200ºC, 500RPM, 400psi H_2, 5wt% catalyst with respect to glycerol weight, 80% aqueous glycerol.

Keeping 50% aluminum content, the Cu/Zn ratio was also varied to confirm that 1/1 is the optimum ratio. The experiments with three different Cu/Zn ratios were carried out, which were Cu/Zn = 1/2 (16.67/33.33/50), Cu/Zn = 1/1 (25/25/50) and Cu/Zn = 2/1 (33.33/16.67/50). The yields of final products are shown in Table 4-3. When Cu/Zn=1/1, the glycerol conversion is the highest among these catalysts with the three ratios. The 1,2PD selectivity for the catalyst with Cu/Zn= 1/2 is slightly higher than the other two, and the yield

of 1,2PD is the highest when Cu/Zn=1/1. It is also observed that by varying the Cu/Zn ratio from 1/2 to 2/1, the difference on 1,2PD yield is not significant.

Table 4-3 Effect of Cu/Zn Molar Ratio on Product Yield[a].

	Glycerol Conversion	1,2PD Selectivity	1,2PD Yield	EG Yield	Acetol Yield	PrOH Yield	Others Yield
Cu/Zn/Al = 17/33/50	71.30	91.27	65.08	0.31	5.29	0.62	0.00
Cu/Zn/Al = 25/25/50	77.24	88.54	68.39	0.36	7.64	0.85	0.00
Cu/Zn/Al = 33/17/50	73.74	89.08	65.69	0.31	7.02	0.72	0.00

[a]Experimental Condition: 200ºC, 500RPM, 400psi H_2, 5wt% catalyst with respect to glycerol weight, 50% aqueous glycerol 24hours reaction time.

4.3 Effect of Hydrogen Pressure Using a Cu/ZnO/Al_2O_3 Catalyst

The experiments were carried out at 200psi 300psi and 400psi hydrogen pressure to study the effect of hydrogen pressure on the overall reaction. The glycerol conversion and 1,2PD selectivity during the reaction time are shown in Figure 4-7. In Figure 4-7A, it can be observed that when the pressure is higher the glycerol conversion and reaction rate are higher which is shown in Figure 4-8. The glycerol conversion rate strongly depends on hydrogen pressure possibly because that glycerol hydrogenolysis involves two consecutive reactions which are glycerol dehydration and acetol hydrogenation. The glycerol dehydration step is believed to be the rate-determining-step; the detailed explanation will be provided in Section 4.8 for acetol hydrogenation. Therefore, when hydrogen pressure is high, the acetol, which is the intermediate, can be effectively reacted driving the reaction equilibrium of the rate-determing-step in the forward direction. In that case, the overall rate of reaction is faster. It can also be observed in Figure 4-9 that when hydrogen pressure is low, the concentration of acetol is higher than when the hydrogen pressures are high. Figure 4-8B shows plots of the relationship between the pseudo-first-order rate constant and the hydrogen pressure; a linear relationship can be observed with a R^2 value of 0.9889. Therefore, the overall glycerol hydrogenolysis reaction is a first order reaction with respect to hydrogen pressure and the rate constant increases linearly with increasing hydrogen pressure.

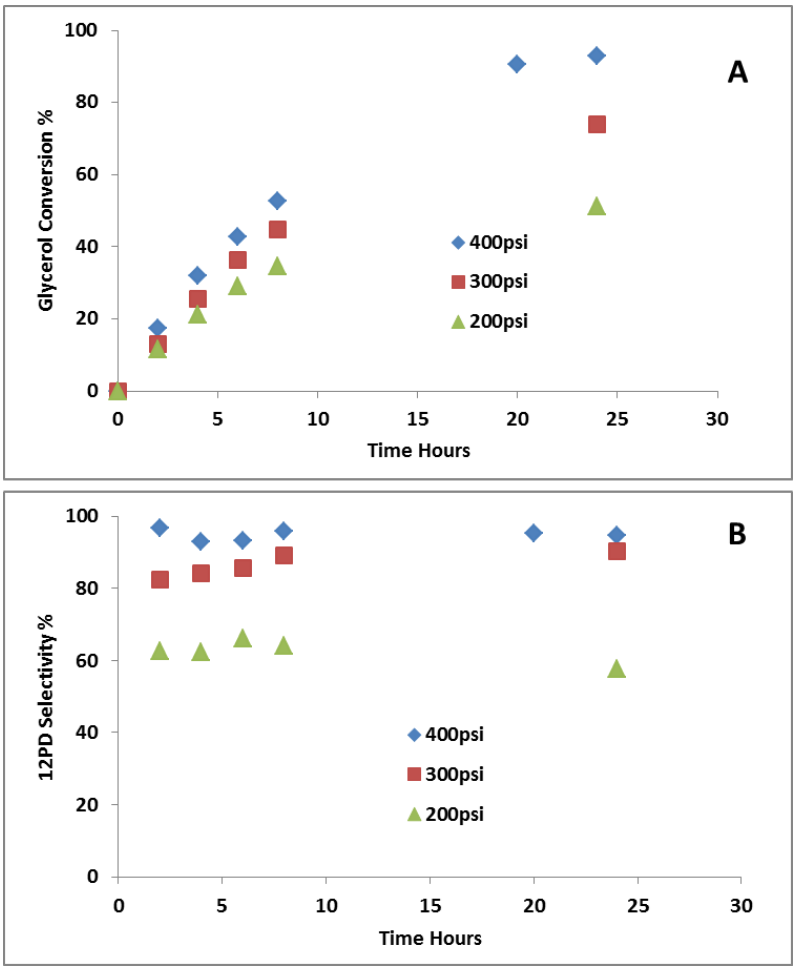

Figure 4-7 Effect of Hydrogen Pressure on Glycerol Conversion and 1,2PD Selectivity during the Reaction Time: A) Glycerol Conversion; B) 1,2PD Selectivity. Experimental Condition: 200ºC, 500RPM, 5wt% catalyst with respect to glycerol weight, 80% aqueous glycerol, Cu/Zn/Al = 25/25/50 (molar).

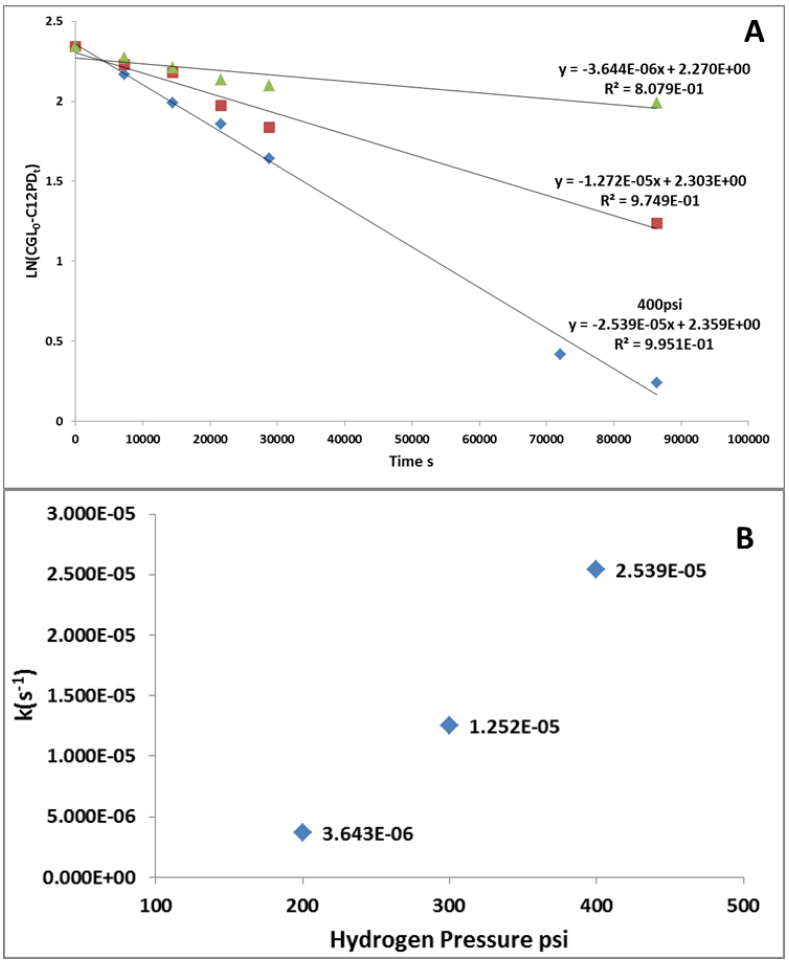

Figure 4-8 Pseudo-First-Order Kinetics Analyses for the $Cu/ZnO/Al_2O_3$ Catalysts at Different Hydrogen Pressures. Experimental Condition: 200ºC, 500RPM, 5wt% catalyst with respect to glycerol weight, 80% aqueous glycerol, Cu/Zn/Al = 25/25/50.

In Figure 4-7B as well as in Table 4-4, it is noticed that the 1,2PD selectivity strongly depends on hydrogen pressure. When the hydrogen pressure is increased from 200psi to 400psi, the 1,2PD selectivity increases from 57.7% to 94.8%. The low 1,2PD selectivity is due to many unknown by-products formed as detected by GC and shown in Figure 4-10**.** It is observed that when hydrogen pressure is increased from 200psi to 400psi, the signal is less complex and at 400psi, no other by-products formation is observed and only the peaks for acetol, 1,2PD, ethylene glycol and un-reacted glycerol are found. It has been reported that the unknown by-products are formed by side reactions due to the presence of acetol contacting

the catalysts since acetol is a very active species [125]. It was also reported by van Ryneveld *et al.* in 2011 that the by-products were formed via side reactions between acetol and glycerol, ethylene glycol or 1,2PD [99]. More observations supporting that the by-products are formed by side reactions with acetol will be provided in Section 4.8 for acetol hydrogenation. Therefore, a higher hydrogen pressure could improve the selectivity to 1,2PD since it can rapidly hydrogenate acetol to 1,2PD and thus eliminate the side reactions due to acetol. However, higher hydrogen pressure might facilitate the C-C cleavage to cause a higher yield of ethylene glycol as shown in Table 4-4. 400psi was chosen as the optimum hydrogen pressure since it gave the highest 1,2PD selectivity and yield of 1,2PD and almost no unknown by-products were observed in the final product.

The dependence of hydrogen for this process was also calculated based on $k'=k.[P_{H2}]^n$ where k' is the calculated pseudo-first order rate constant and n is the order of hydrogen. After plugging the data from Figure 4-8, the reaction order of hydrogen was calculated to be 2.26.

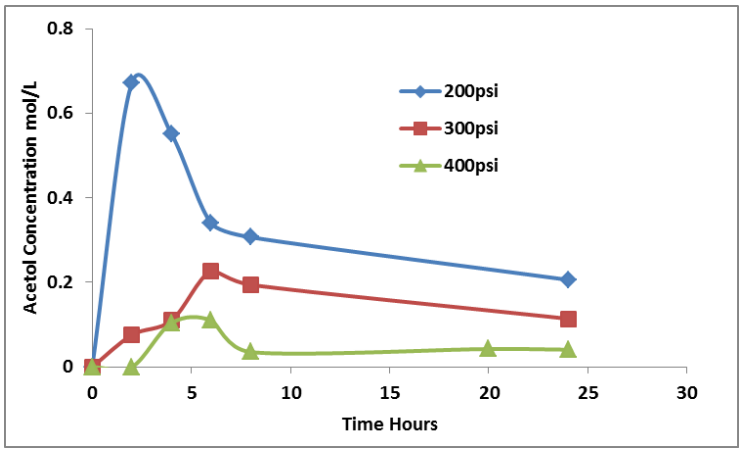

Figure 4-9 Acetol Concentration during the Reaction Time at Different Hydrogen Pressures. Experimental Condition: 200ºC, 500RPM, 5wt% catalyst with respect to glycerol weight, 80% aqueous glycerol, Cu/Zn/Al = 25/25/50.

Table 4-4 Effect of Hydrogen Pressure on Product Yield[a].

	Glycerol Conversion	1,2PD Selectivity	1,2PD Yield	Acetol Yield	EG Yield	PrOH Yield	Others Yield
400psi	93.04	94.78	88.18	0.39	4.16	0.30	0.00
300psi	74.02	90.15	66.73	2.19	1.09	0.78	3.23
200psi	51.32	57.71	29.62	1.98	0.96	0.97	17.79

[a] Experimental Condition: 200ºC, 500RPM, 5wt% catalyst with respect to glycerol weight, 80% aqueous glycerol, Cu/Zn/Al = 25/25/50, 24 hours reaction time.

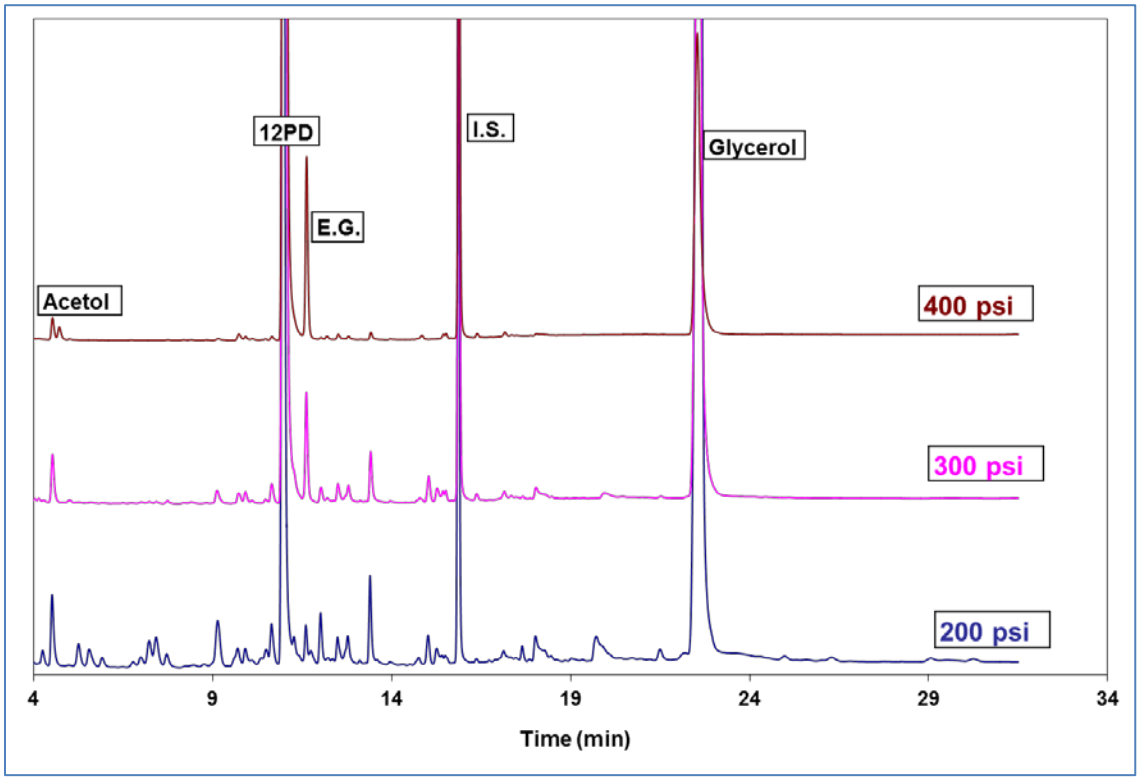

Figure 4-10 GC Profile of the Final Products at Different Hydrogen Pressures. Experimental Condition: 200ºC, 500RPM, 5wt% catalyst with respect to glycerol weight, 80% aqueous glycerol, Cu/Zn/Al = 25/25/50 Catalyst, 24 hours reaction time.

4.4 Effect of Glycerol Concentration Using $Cu/ZnO/Al_2O_3$ Catalyst

The effect of aqueous glycerol feed concentration on the production of 1,2PD was investigated. It has been reported that water is an inhibitor in the process and it is always

preferable to reduce the water content from the initial reaction mixture to drive the equilibrium toward the products [28, 68]. In addition, as the concentration of glycerol decreases, the size of the reactor will have to be enlarged to produce the same amount of product. Therefore, experiments with different water content were carried out to study the initial glycerol concentration effect on the overall reaction. The experiments with 4 different initial glycerol concentrations were carried out, which were 100%, 80%, 60% and 50%. The glycerol conversion and 1,2PD selectivity over the reaction time are shown in Figure 4-11.

It can be seen from Figure 4-11A that when the glycerol concentration is increased from 50% to 80%, the glycerol conversion and the reaction rate increase as shown in Table 4-5. This is possibly due to the fact that as the water content is reduced, the equilibrium is driven in the forward direction. From Figure 4-11B, it can be seen that the glycerol initial concentration does not have a significant effect on the selectivity to 1,2PD and when the glycerol concentration is 80%, the 1,2PD selectivity is slightly higher (Table 4-5). When the glycerol concentration is further increased to 100%, the glycerol conversion significantly decreases as shown in Figure 4-11A. Dasari in 2006 reported that when pure glycerol was used the degradation of reaction product occurred due to polymerization, so it was essential to have 10%~20% water [17]. Therefore, 80% aqueous glycerol is considered as the optimum glycerol concentration in the reaction mixture.

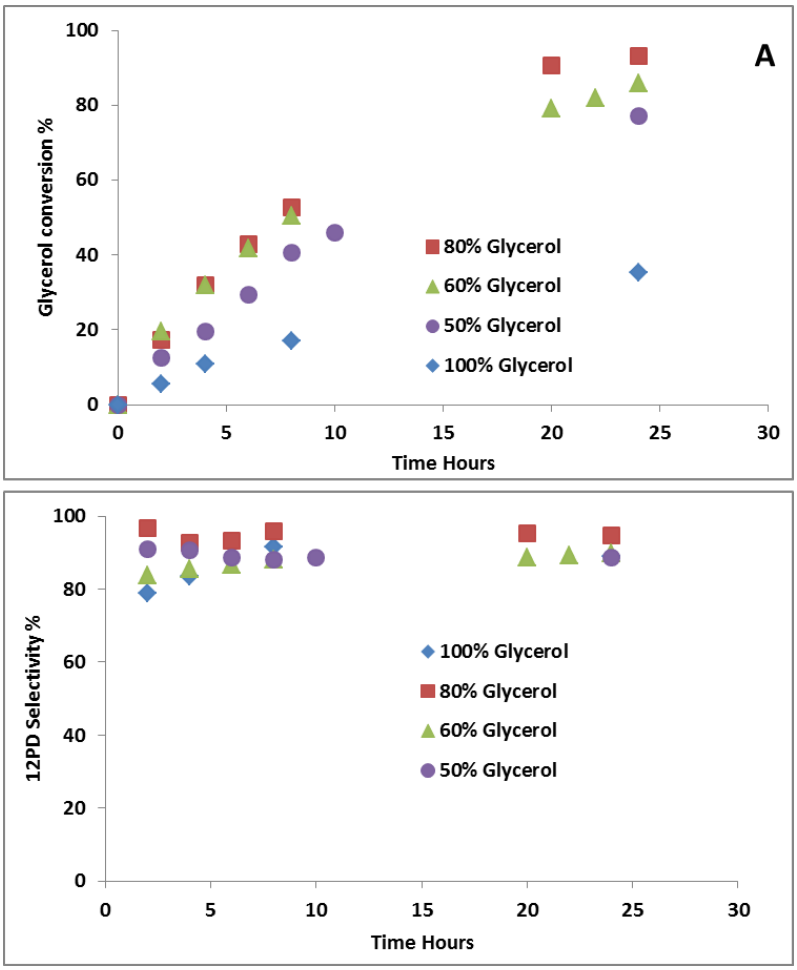

Figure 4-11 Effect of Initial Glycerol Concentration on Glycerol Conversion and 1,2PD Selectivity during the Reaction Time: A) Glycerol Conversion; B) 1,2PD Selectivity. Experimental Condition: 200ºC, 400psi H_2, 500RPM, 5wt% catalyst with respect to glycerol weight, Cu/Zn/Al = 25/25/50.

Table 4-5 Effect of Glycerol Concentration on Product Yield[a]

Glycerol Concentration	Glycerol Conversion	1,2PD Selectivity	1,2PD Yield	EG Yield	Acetol Yield	PrOH Yield	Others Yield	Rate Constant
100%	35.27	88.99	31.38	0.75	0.39	0.65	2.10	$5.90^{-6}s^{-1}$
80%	93.04	94.78	88.18	4.16	0.39	0.30	0.00	$2.54^{-5}s^{-1}$
60%	85.18	89.75	76.45	7.34	0.53	0.87	0.00	$1.59^{-5}s^{-1}$
50%	77.24	88.54	68.39	7.64	0.36	0.85	0.00	$1.33^{-5}s^{-1}$

[a]Experimental Condition: 200ºC, 400psi H_2, 500RPM, 5wt% catalyst with respect to glycerol weight, Cu/Zn/Al = 25/25/50, 24 hours reaction time.

4.5 Effect of Solvent Using a $Cu/ZnO/Al_2O_3$ Catalyst

In most biodiesel plants methanol is used for the transesterification reaction since it is cheaper compared with ethanol and butanol and also has a smaller molecular size facilitating mass transfer of methanol within the pores of the catalysts [126-128]. Crude glycerol always contains a certain amount of methanol [129]. In order to investigate the effect of methanol on the catalytic activity, an experiment with 80% glycerol and 20% methanol (by weight) was carried out and the experimental results are shown in Figure 4-12.

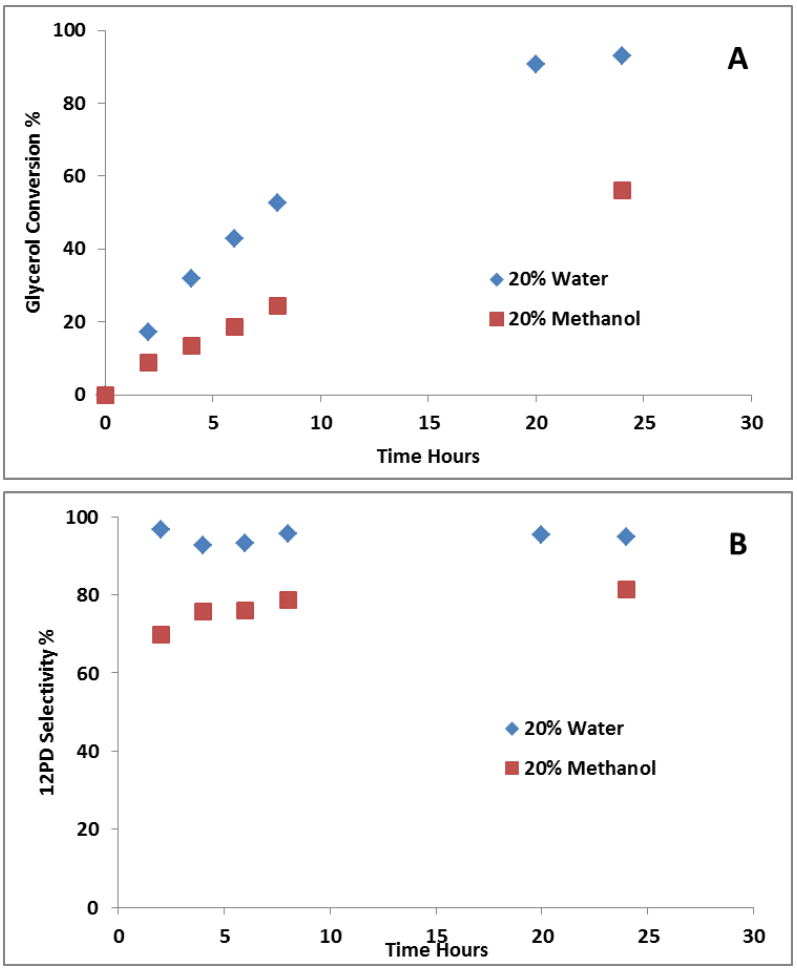

Figure 4-12 Effect of Methanol as the Solvent on Glycerol Conversion and 1,2PD Selectivity during the Reaction Time: A) Glycerol Conversion; B) 1,2PD Selectivity. Experimental Condition: 200ºC, 400psi H_2, 500RPM, 5wt% catalyst with respect to glycerol weight, 80% glycerol, Cu/Zn/Al = 25/25/50.

From the results, it can be observed that methanol as a solvent has a negative effect on the overall reaction. The glycerol conversion is much lower over the reaction time when methanol is used as the solvent as shown in Figure 4-12A. The reaction rate is much slower when methanol is used as the solvent, as shown in Figure 4-13. The calculated pseudo-first-order rate constant is $7.021 \times 10^{-6} s^{-1}$ when methanol is used as the solvent, while when water is used as the solvent, the rate constant is about 3.6 times higher being $2.539 \times 10^{-5} s^{-1}$. The conversion of glycerol when water is used as the solvent (93.04%) is much higher than that when methanol is used as shown in Table 4-6**.** From Figure 4-12B as well as Table 4-6, it can also be noticed that the 1,2PD selectivity is also much higher when water is used as the solvent. The yield of other by-products is 4.6% indicating when methanol is used as the solvent, the hydrogen pressure is not sufficient and the acetol yield is also observed to be much higher. It is possible that the solubility of hydrogen is lower in methanol than in water which has been often reported [130-133]. Figure 4-14 illustrates the GC profile for the final products when 20% methanol is used as the solvent and the results are compared with the profile for the products when 20% water is used as the solvent at low hydrogen pressure (200psi). It can be observed that the retention time for the production of the unknown by-products for these two samples match each other very well. Therefore, the formation of by-products when methanol is used as the solvent is due to insufficient hydrogen dissolved in the solution for the hydrogenation reaction.

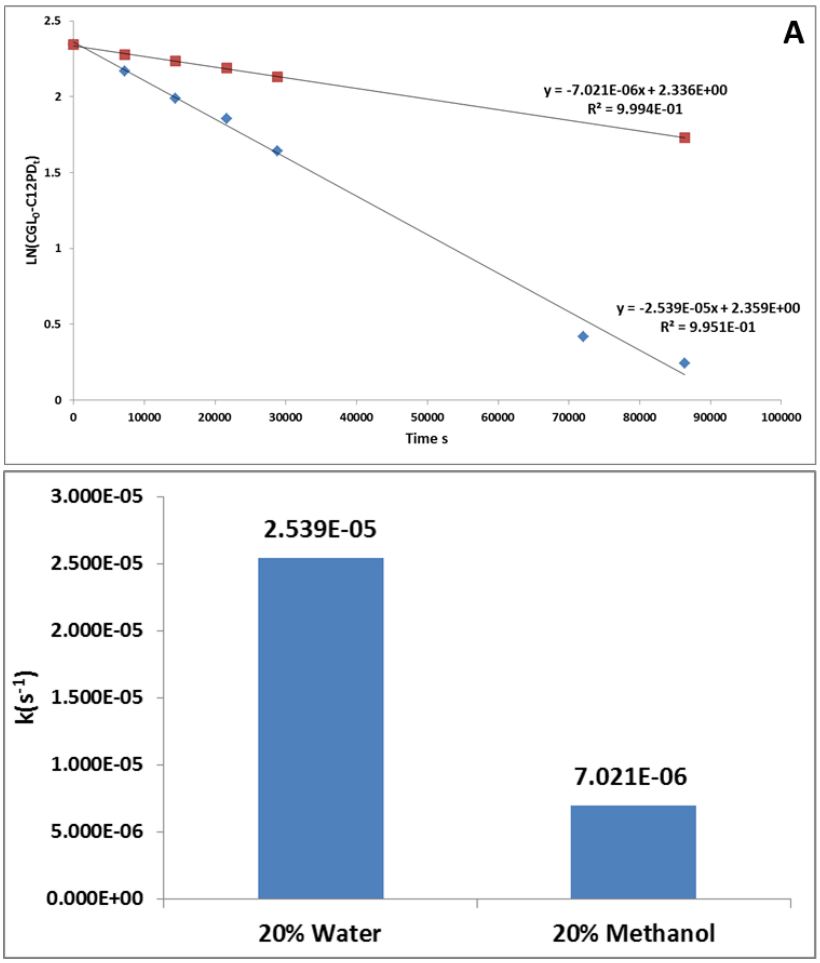

Figure 4-13 Pseudo-First-Order Kinetics Analyses for the $Cu/ZnO/Al_2O_3$ Catalysts Using Different Solvent. Experimental Condition: 200ºC, 400psi H_2, 500RPM, 5wt% catalyst with respect to glycerol weight, 80% aqueous glycerol, Cu/Zn/Al = 25/25/50, 24 hours reaction time.

Table 4-6 Effect of Type of Solvent on Product Yield[a].

	Glycerol Conversion	1,2PD Selectivity	1,2PD Yield	Acetol Yield	EG Yield	PrOH Yield	Others Yield
20% Water	93.04	94.78	88.18	0.39	4.16	0.30	0.00
20% Methanol	56.20	81.35	45.71	1.25	3.95	0.69	4.59

[a]Experimental Condition: 200ºC, 400psi H_2, 500RPM, 5wt% catalyst with respect to glycerol weight, 80% aqueous glycerol, Cu/Zn/Al = 25/25/50, 24 hours reaction time.

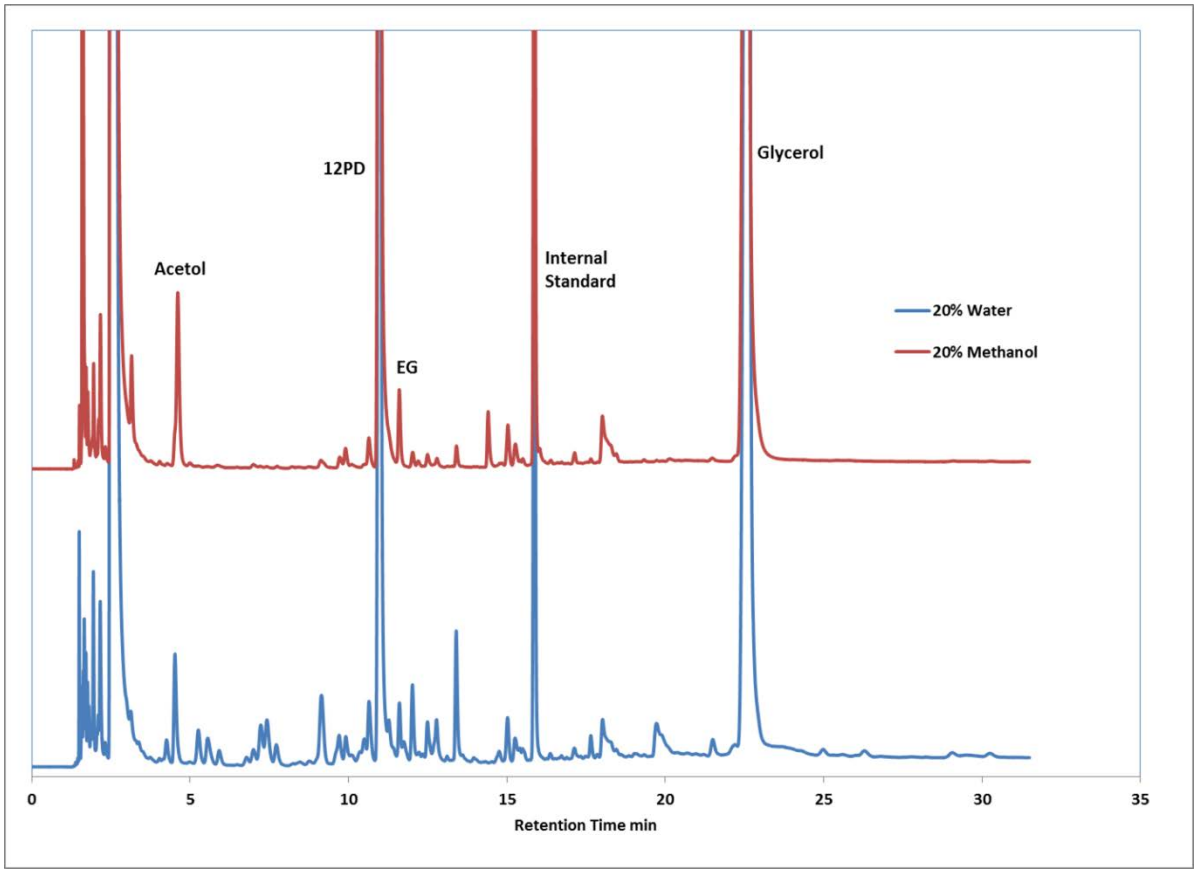

Figure 4-14 GC Profile of the Final Products Using Different Solvent. Blue: 20% Water at 200psi H_2; Red: 20% Methanol at 400psi H_2. Experimental Condition: 200ºC, 400psi H_2, 500RPM, 5wt% catalyst with respect to glycerol weight, 80% aquous glycerol, Cu/Zn/Al = 25/25/50.

Currently in most biodesil plants, homogeneous NaOH or KOH is used for the transesterification reactions. Therefore, there is always a certain amount of catalyst residual remaining in the crude glycerol [129]. In order to investigate the effect of the residual base on the overall reaction, experiments with NaOH addition at different hydrogen pressures have been carried out. The reactions were conducted at 200ºC, and the stirring speed was set to 500RPM, with 5wt% of catalyst with respect to the glycerol feed. 5wt% NaOH with respect to total reactant mixture weight was added, and the experiments at two hydrogen pressures were conducted, which were 400psi and 600psi. The yields of the different products after 24 hours reaction time are listed in Table 4-7. It can be observed that the

presence of NaOH has a negative effect on the overall reaction since at 400psi hydrogen pressure, the final glycerol conversion drops from 93.04% when no NaOH is added to only 81.9% with 5wt% NaOH addition, and the selectivity to 1,2PD drops from 94.8% to 86.3%. Furthermore the yield of other undesired by-products is 6.9%. When the hydrogen pressure is increased from 400psi to 600psi, the glycerol conversion is only slightly improved from 81.9% to 84.5%, and the selectivity to 1,2PD is not changed significantly. It was also noticed that with the addition of NaOH, no acetol was detected in the final products but still around 6% of other by-products were formed. Figure 4-15 illustrates the GC profile for the final products when 5% NaOH was used and the results are compared with the profile for the products when no NaOH was used at low hydrogen pressure (200psi). It can be observed that the retention time of the unknown by-products for these two samples match each other very well. Therefore, the formation of by-products when NaOH is added is due to side reactions of acetol. It is possible that NaOH can catalyze the side reactions with acetol; therefore, acetol can be rapidly reacted and no acetol is found in the final products.

Table 4-7 Effect of NaOH on Product Yield[a].

	Glycerol Conversion	1,2PD Selectivity	1,2PD Yield	EG Yield	Acetol Yield	PrOH Yield	Others Yield
No NaOH 400psi	93.04	94.78	88.18	4.16	0.39	0.30	0.00
5% NaOH 400psi	81.90	86.28	70.66	3.64	0.00	0.72	6.88
5% NaOH 600psi	84.51	86.03	72.70	4.82	0.00	1.30	5.69

[a]Condition: 200ºC, 400psi H_2, 500RPM, 5wt% catalyst with respect to glycerol weight, 80% aquous glycerol, Cu/Zn/Al = 25/25/50, 24 hours reaction time, 5wt% NaOH with respect to total reactant weight.

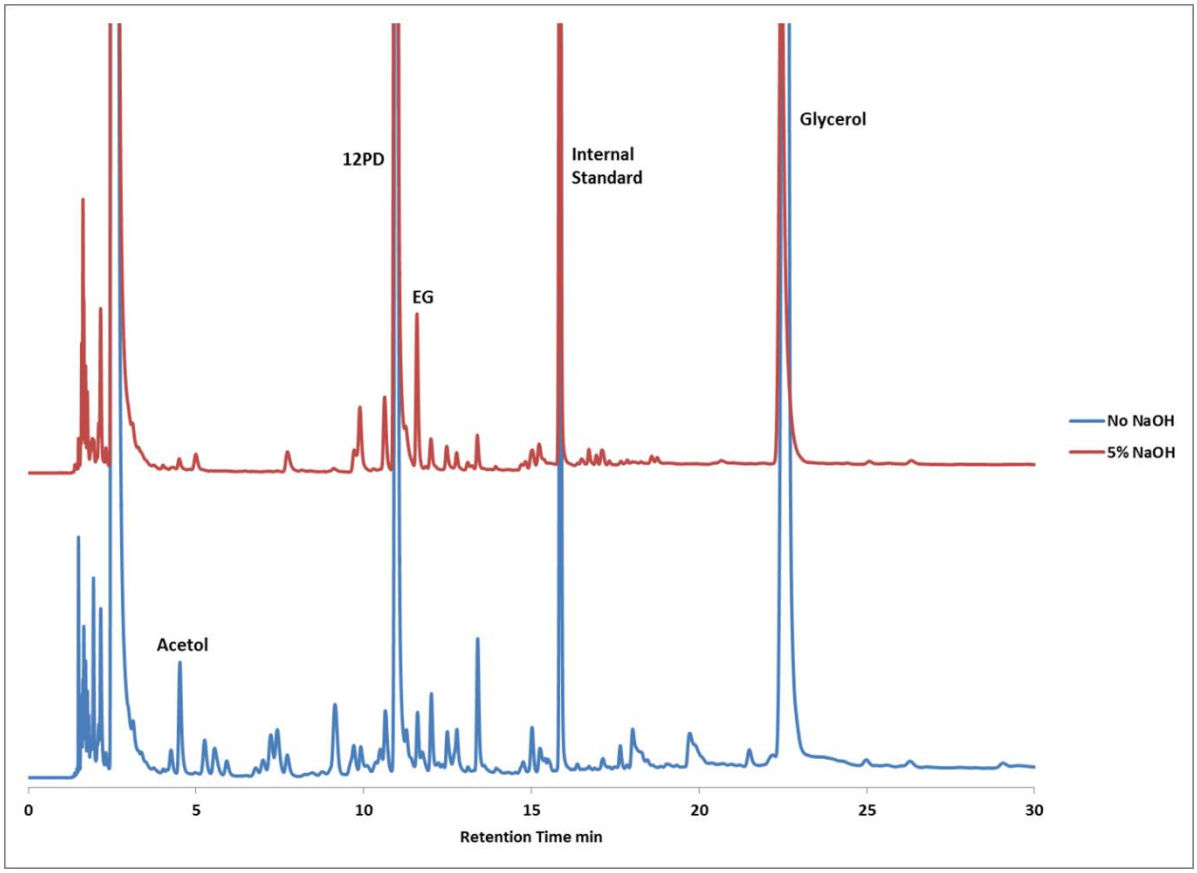

Figure 4-15 GC Profile of the Final Products with NaOH Added. Condition: 200ºC, 400psi H_2, 500RPM, 5wt% catalyst with respect to glycerol weight, 80% aquous glycerol, Cu/Zn/Al = 25/25/50, 24 hours reaction time, 5wt% NaOH with respect to total reactant weight.

4.6 Effect of Al on Cu/ZnO/Al_2O_3 Catalyst Lifetime

The deactivation of Cu based catalysts for glycerol hydrogenolysis processes has been frequently reported and many researchers have done extensive research to improve the lifetime of the catalysts [68, 80, 89]. In most of the literature deactivation of Cu based catalysts by sintering is reported as being the main reason causing the loss of activity. It has been reported that adding another metal oxide such as Al_2O_3, Ga_2O_3, and ZrO_2 can improve the stability of the Cu/ZnO catalysts [80, 124, 134, 135]. Since Al_2O_3 has the lowest cost and it is non-toxic, experiments on catalyst lifetime have been carried out to study the effect of Al_2O_3 on catalyst stability. The spent catalysts were recycled by filtering the final reaction

mixture. The filtered particles were rinsed with ethanol three times and dried in air at 110ºC overnight. Then the particles were calcined in air at 360ºC for 4 hours. Some fresh catalyst was added to make up the loss during the recycling process. The calcined particles were reduced in air at 300ºC for 3 hours before the experiment. The experiments were carried out at 200ºC, with 5wt% catalyst with respect to glycerol weight being added, and 50wt% aqueous glycerol was used as the reactant mixture.

The glycerol conversion and 1,2PD selectivity over the reaction time when using the fresh and recycled $Cu/ZnO/Al_2O_3$ catalysts are shown in Figure 4-16 and Table 4-8. It can be observed that after 4 times of recycling, no obvious deactivation is found since the glycerol conversions and 1,2PD selectivity during the reaction time using the recycled catalyst are not significantly lowered. The reaction rate is also not lowered using spent catalyst up to the forth recycling as shown in Figure 4-17. The glycerol conversion drops slightly from 77.2% to 73.6% and the selectivity to 1,2PD does not change after 4^{th} recycling being maintained at 88.6%. Therefore, after 4 times recycling there is no significant loss in catalyst activity. It was reported that when Al was added to the Cu/ZnO catalyst, it was able to isolate the individual metal particles, avoiding their sintering [80, 124]. It can also be observed in the Section 6.7 concerned with the TEM analysis that when Al is added, the particle size distribution for the spent catalyst is not significantly changed compared with the fresh catalyst.

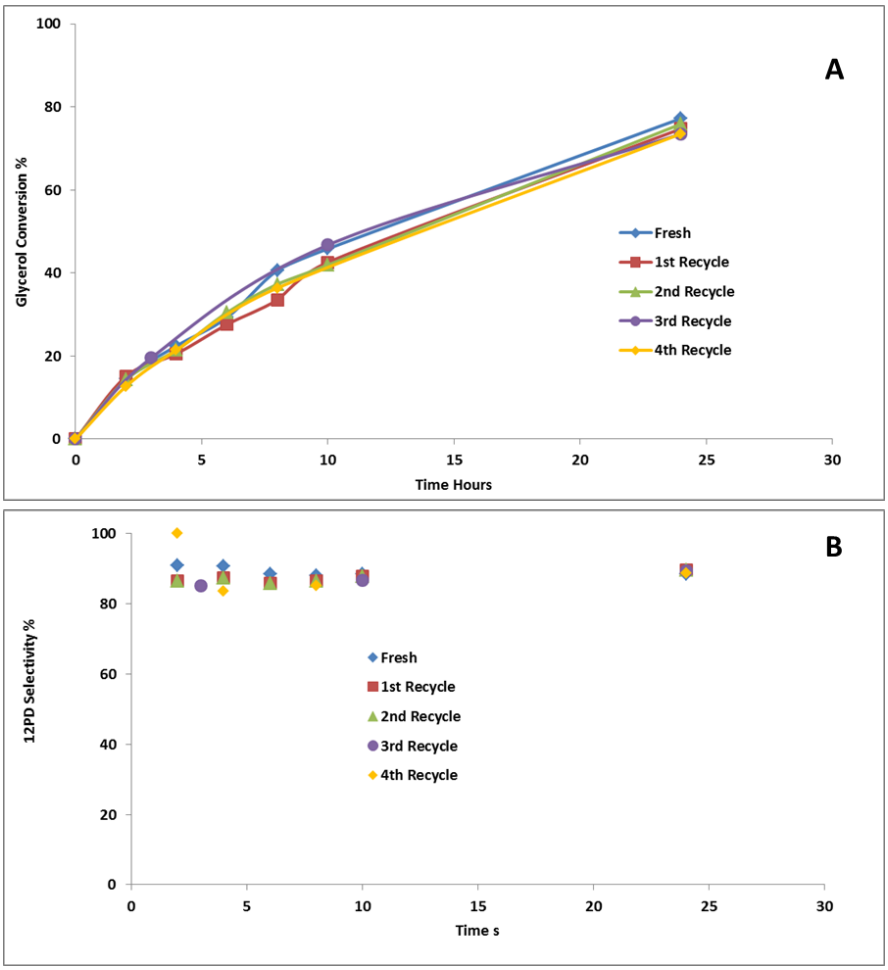

Figure 4-16 Glycerol Conversion and 1,2PD Selectivity during the Reaction Time using Fresh and Recycled Catalysts: A) Glycerol Conversion; B) 1,2PD Selectivity. Experimental Condition: 200ºC, 400psi H_2, 500RPM, 5wt% catalyst with respect to glycerol weight, 50% aqueous glycerol, Cu/Zn/Al = 25/25/50.

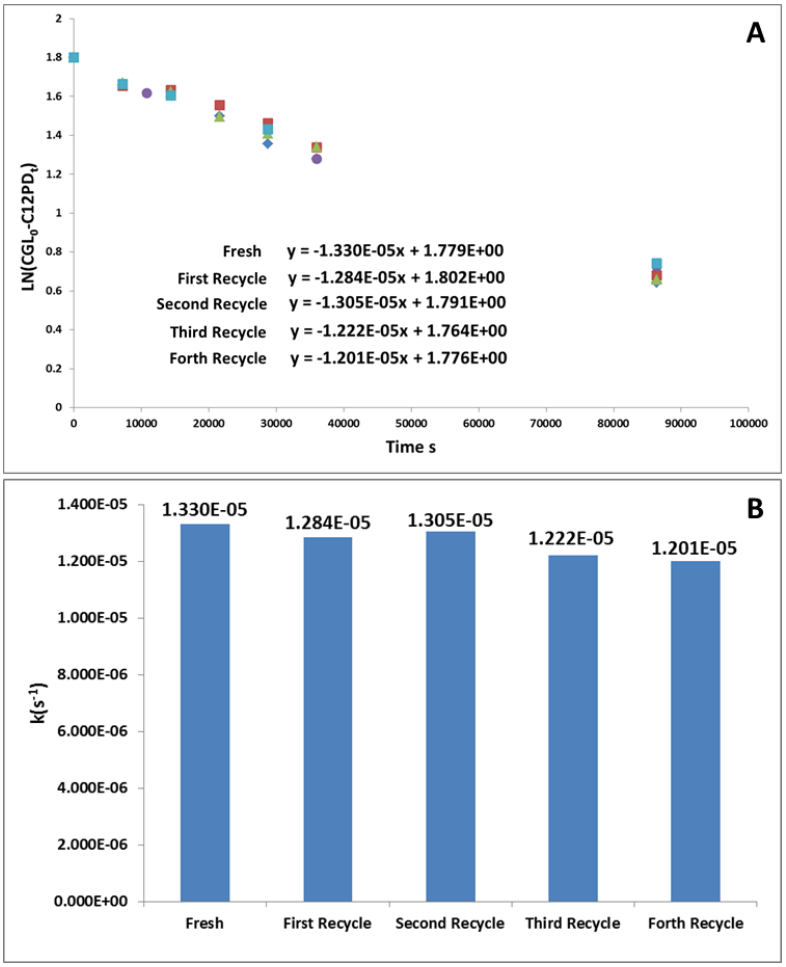

Figure 4-17 Pseudo-First-Order Kinetics Analyses for the Fresh and Recycled $Cu/ZnO/Al_2O_3$ Catalysts. Experimental Condition: 200ºC, 400psi H_2, 500RPM, 5wt% catalyst with respect to glycerol weight, 50% aqueous glycerol, Cu/Zn/Al = 25/25/50.

Table 4-8 Product Yield Using Fresh and Recycled $Cu/ZnO/Al_2O_3$ Catalysts[a].

	Glycerol Conversion	1,2PD Selectivity	1,2PD Yield	EG Yield	Acetol Yield	PrOH Yield	Others Yield
Fresh	77.24	88.54	68.39	0.36	7.64	0.85	0.00
First Recycle	75.14	90.14	67.74	0.00	6.54	0.87	0.00
Second Recycle	75.91	89.53	67.96	0.00	7.11	0.83	0.00
Third Recycle	73.95	89.37	66.09	0.43	7.42	0.00	0.00
Forth Recycle	73.56	88.64	65.20	0.45	6.86	1.05	0.00

[a]Condition: 200ºC, 400psi H_2, 500RPM, 5wt% catalyst with respect to glycerol weight, 50% aqueous glycerol, Cu/Zn/Al = 25/25/50, 24 hours reaction time

Figure 4-18 shows the glycerol conversion and 1,2PD selectivity during the reaction time using the fresh and recycled Cu/Zn catalysts for comparison to investigate the effect of Al on the stability of the catalyst. Figure 4-18A shows that the glycerol conversion using fresh Cu/ZnO catalyst during the reaction time is much higher than that using the first recycled catalyst, and when the catalyst is reused a second time, the glycerol conversion is very low and the final conversion at 24 hours is only 17.8% while the glycerol final conversion using fresh Cu/ZnO catalyst is 46.44% as shown in Table 4-9. From Figure 4-18B, it is noticed that even the conversion of glycerol decreases significantly when the catalyst is recycled and reused, the 1,2PD selectivity is not seriously affected. It can be explained in that the 1,2PD selectivity strongly depends on hydrogen pressure, when the catalyst is deactivated, and the activity of glycerol dehydration is lower; as the hydrogen pressure is sufficient for acetol hydrogenation. The deactivation of Cu/ZnO catalyst has been often reported [68, 80, 89]. The most commonly reported reason for catalyst deactivation is sintering and it is also observed in Section 6.7 from the TEM analysis for the Cu/ZnO spent catalyst; the particle size is much larger and the distribution is much wider than that of a fresh catalyst indicating that severe sintering occurred. Figure 4-19 shows that when the Cu/ZnO catalyst is recycled, the reaction is slower since the rate constant is lower. The reason is because when the catalyst is sintered, the particle size is larger resulting in fewer active sites for the reaction.

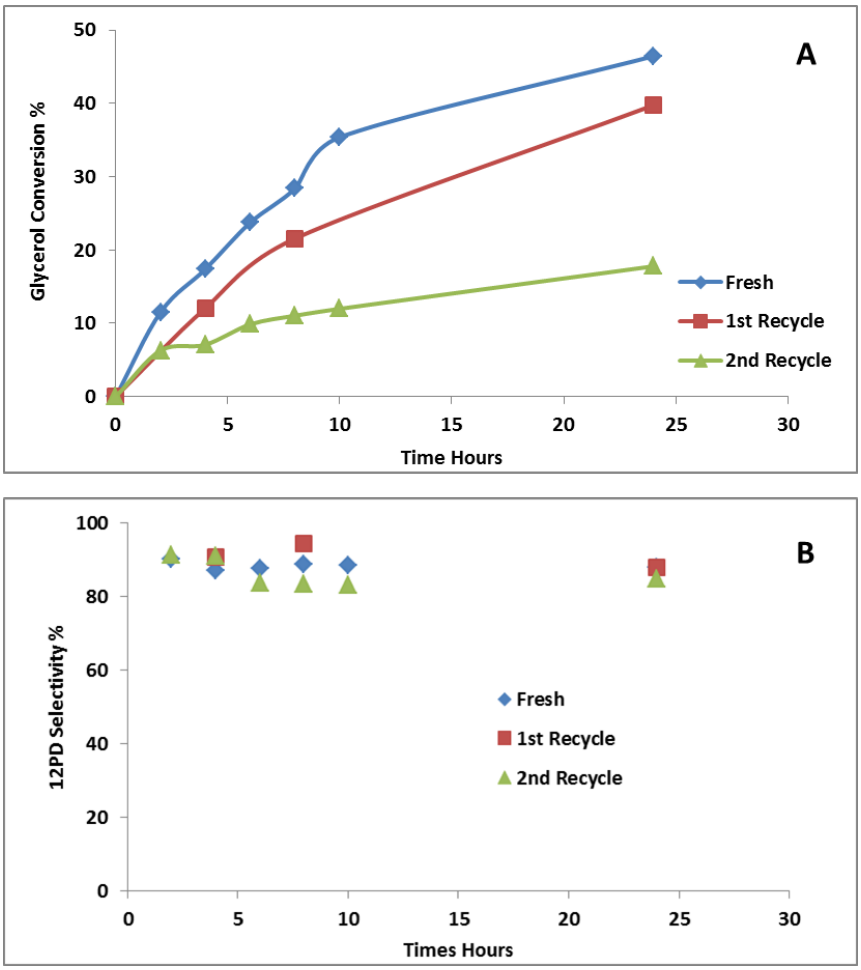

Figure 4-18 Glycerol Conversion and 1,2PD Selectivity during the Reaction Time using Fresh and Recycled Catalysts: A) Glycerol Conversion; B) 1,2PD Selectivity. Experimental Condition: 200ºC, 400psi H_2, 500RPM, 5wt% catalyst with respect to glycerol weight, 50% aqueous glycerol, Cu/Zn = 50/50.

Table 4-9 Product Yield Using Fresh and Recycled Cu/ZnO Catalysts[a].

	Glycerol Conversion	1,2PD Selectivity	1,2PD Yield	EG Yield	Acetol Yield	PrOH Yield	Others Yield
Fresh	46.44	87.79	40.77	0.00	4.37	0.84	0.46
First Recycle	40.09	88.31	35.40	0.43	2.47	0.86	0.93
Second Recycle	17.77	84.77	15.07	0.00	1.22	0.77	0.72

[a]Condition: 200ºC, 400psi H_2, 500RPM, 5wt% catalyst with respect to glycerol weight, 50% aqueous glycerol, Cu/Zn = 50/50, 24 hours reaction time.

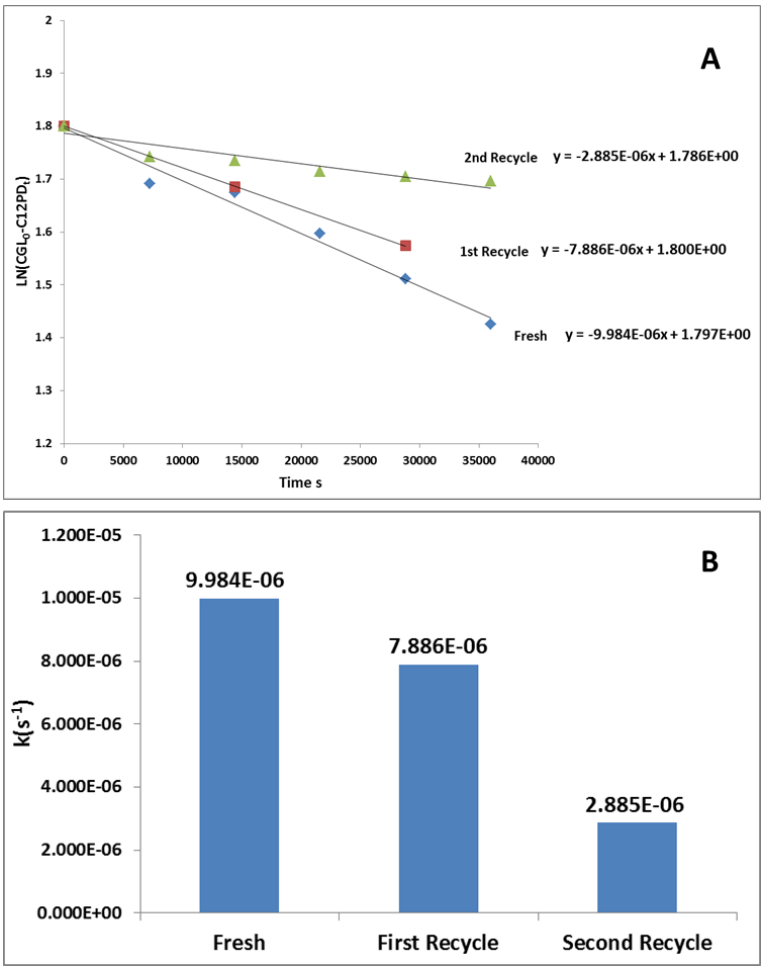

Figure 4-19 Pseudo-First-Order Kinetics Analyses for the Fresh and Recycled Cu/ZnO Catalysts. Experimental Condition: 200ºC, 400psi H_2, 500RPM, 5wt% catalyst with respect to glycerol weight, 50% aqueous glycerol, Cu/Zn = 50/50.

It has been reported by Bienholz *et al.* in 2010 that the water content plays an important role on the catalyst activity [68]. In their report, when the water content was increased from 0% (pure glycerol) to 50%, the glycerol conversion dropped from 46% to only 5%. It was explained that water could cause a formation of larger Cu particles and hence smaller total Cu surface area. Figure 4-20 compares the catalytic activity with Al and without Al using different water content in the reactant mixture. It can be observed that when Al is added, the glycerol conversion only drops from 93% to 77% when the water content is increased from

20wt% to 50wt%; however, when Al is not used, the glycerol conversion drops from 86% to 46% when the water content is increased from 20wt% to 50wt%. This suggests that Al can also improve the water tolerance of the catalyst so that it can be used with various water contents. Figure 4-21 shows that when the water content is increased from 20wt% to 50wt%, the rate constants decreased. This is possibly due to that higher water content can inhibit the glycerol dehydration step resulting in a lower reaction rate.

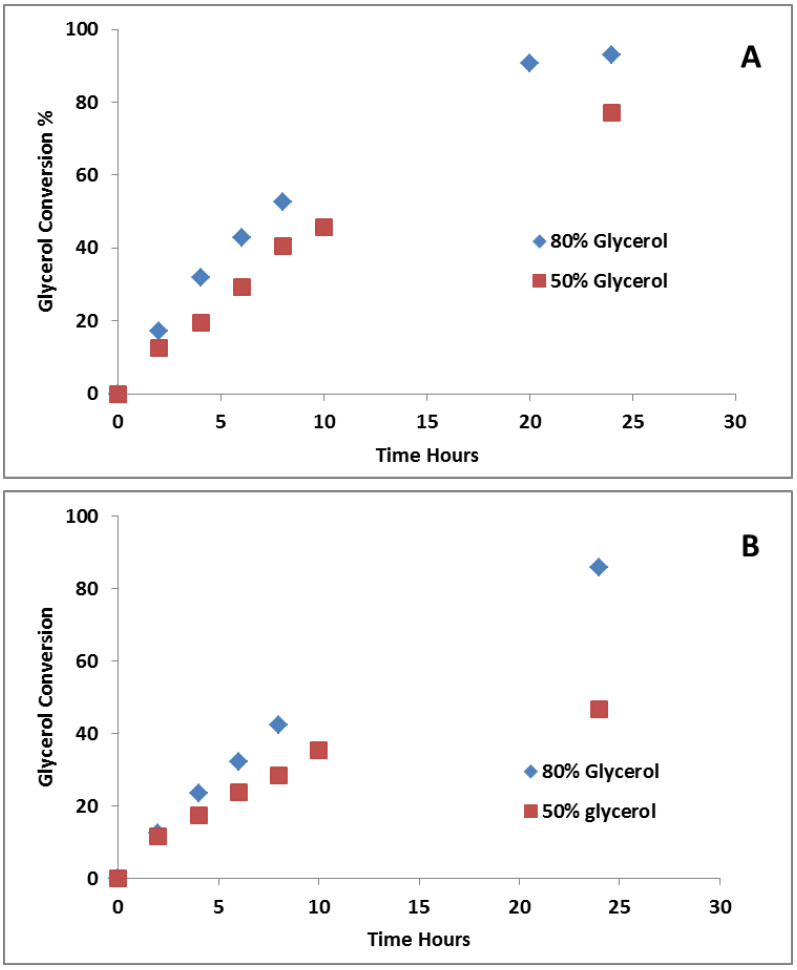

Figure 4-20 Effect of Al on Glycerol Conversion using Different Water Content: A) Cu/Zn/Al = 25/25/50; B) Cu/Zn = 50/50. Experimental Condition: 200ºC, 400psi H_2, 500RPM, 5wt% catalyst with respect to glycerol weight.

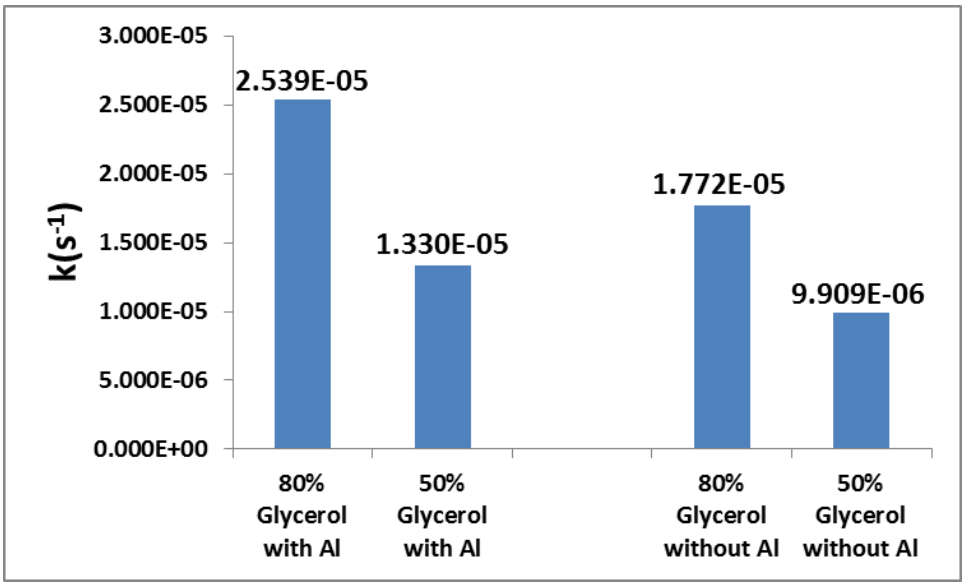

Figure 4-21 Pseudo-First-Order Kinetics Analyses for Effect of Al on Glycerol Conversion using Different Water Content. Experimental Condition: 200ºC, 400psi H_2, 500RPM, 5wt% catalyst with respect to glycerol weight, with Al: Cu/Zn/Al=25/25/50, without Al: Cu/Zn=50/50.

4.7 Effect of Temperature and Kinetic Study Using Cu/ZnO/Al_2O_3 Catalyst

Experiments at different temperatures using a Cu/ZnO/Al_2O_3 catalyst have been carried out to study the effect of temperature on the reaction rate to obtain the activation energy. Three temperatures were selected for the reactions which were 180ºC, 200ºC and 220ºC. The experimental results are shown in Figure 4-22. It can be observed that at higher temperature, the glycerol conversion at the beginning of the reaction time is higher. It is also found that at 220ºC the final conversion of glycerol after 24 hours (74.1%) is slightly lower than that at 200ºC (77.4%) also listed in Table 4-10. One possible reason is because at higher temperature, the rate of glycerol dehydration is higher and more acetol is formed; the other reason might be when the temperature is higher the solubility of hydrogen in the reaction mixture is lower and the hydrogen supplied in the reaction mixture is not sufficient to convert all the acetol to 1,2PD. Therefore, the 1,2PD selectivity at 220ºC is also lower than those

obtained at 200ºC and 180ºC since the selectivity to 1,2PD strongly depends on hydrogen pressure.

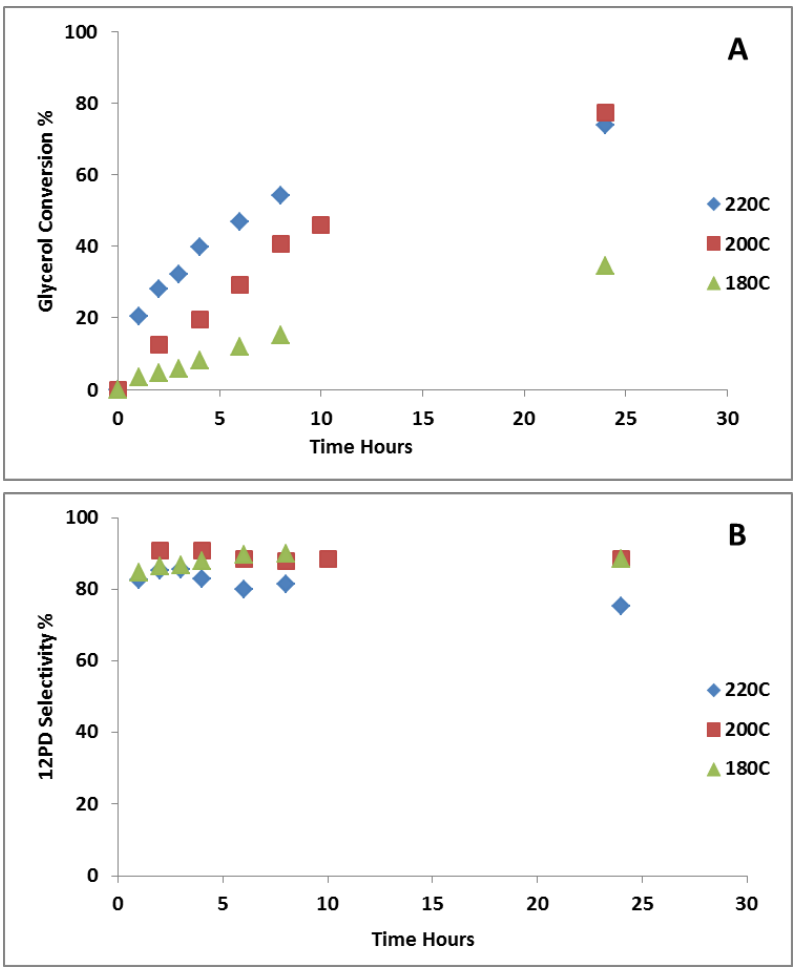

Figure 4-22 Effect of Temperature on Glycerol Conversion and 1,2PD Selectivity during the Reaction Time: A) Glycerol Conversion; B) 1,2PD Selectivity. Experimental Condition: 400psi H_2, 500RPM, 5wt% catalyst with respect to glycerol weight, 50% aqueous glycerol, Cu/Zn/Al = 25/25/50.

Table 4-10 Effect of Temperature on Product Yield[a].

	Glycerol Conversion	1,2PD Selectivity	1,2PD Yield	EG Yield	Acetol Yield	PrOH Yield	Others Yield
220ºC	74.11	75.43	55.90	2.80	1.78	5.04	8.58
200ºC	77.24	88.54	68.39	7.64	0.36	0.85	0.00
180ºC	34.34	88.37	30.35	3.70	0.00	0.30	0.00

[a]Conditions: 400psi H_2, 500RPM, 5wt% catalyst with respect to glycerol weight, 50% aqueous glycerol, Cu/Zn/Al = 25/25/50, 24 hours reaction time.

It can be seen from Figure 4-22 the reaction rate is strongly temperature dependent. Based on the Arrhenius Equation, the activation can be calculated using Equation 4-3. By plotting ln(k) versus 1/T, the intersect of the estimated linear trend line is $\ln(A_0)$ and the slope of the line is -Ea/R where R is the gas constant ($8.314 JK^{-1}mol^{-1}$). The fitting of the kinetic parameters is shown in Figure 4-24. The pre-exponential factor is calculated to be 24270.1 and the activation energy is calculated to be 69387J/mol or 69.39kJ/mol, which indicates that the reaction with this catalyst is chemically kinetically controlled.

$$k = A_0 e^{-Ea/RT} \Rightarrow \ln(k) = \ln(A_0) - \frac{Ea}{R}\frac{1}{T} \qquad \textbf{Equation 4-3}$$

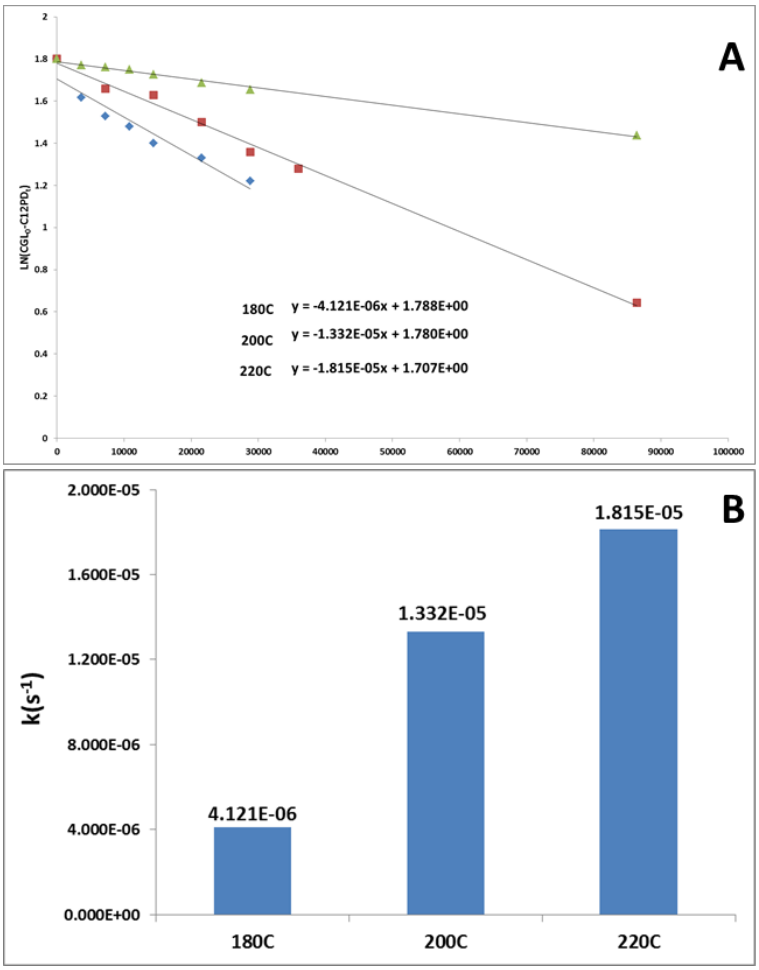

Figure 4-23 Pseudo-First-Order Kinetics Analyses for the Cu/Zn/Al Catalyst at Different Temperatures. Experimental Condition: 400psi H_2, 500RPM, 5wt% catalyst with respect to glycerol weight, 50% aqueous glycerol, Cu/Zn/Al = 25/25/50.

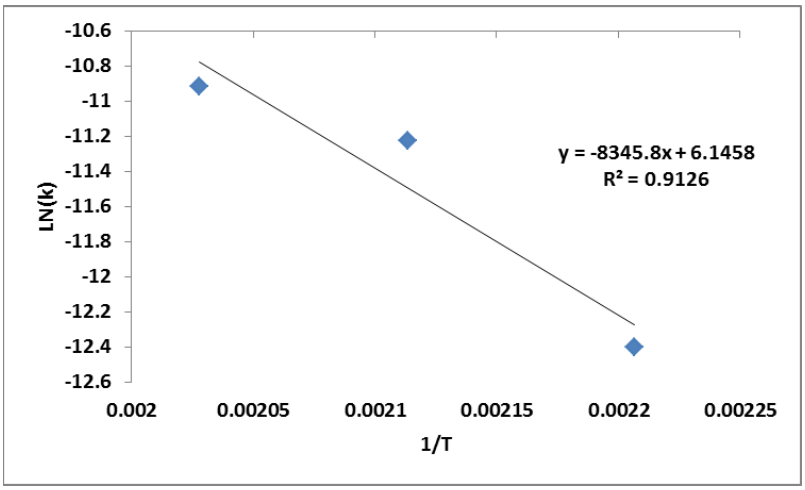

Figure 4-24 Effect of Temperature on Rate Constant. Experimental Condition: 400psi H_2, 500RPM, 5wt% catalyst with respect to glycerol weight, 50% aqueous glycerol, Cu/Zn/Al = 25/25/50.

4.8 Acetol Hydrogenation

Acetol hydrogenation reactions were carried out to investigate the effect of acetol on the selectivity to 1,2PD. 20wt% aqueous acetol solution was used as the reactant mixture. The experiments were carried out at 3 different hydrogen pressures which were 400psi, 600psi and 800psi, and at 200ºC, 20wt% aqueous acetol was used as the reactant, 5wt% catalyst (Cu/Zn/Al=25/25/50) with respect to acetol weight was loaded. The conversion of acetol and 1,2PD selectivity over the reaction time are shown in Figure 4-22A and 4-22B respectively. Pseudo-first-order kinetics was used to calculate the first order rate constant for acetol hydrogenation. The sample calculation is according to Equation 4-4**.**

$$-\frac{d[Acetol]}{dt} = k[Acetol] \Rightarrow \ln[Acetol] = -kt + \ln[Acetol_{t=0}] \qquad \textbf{Equation 4-4}$$

From Figure 4-25A, it can be seen that when the hydrogen pressure is higher, the acetol conversion is higher and the hydrogenation rate is higher since a higher rate constant is observed in Figure 4-26. The rate constant at 400psi is calculated to be $1.297 \times 10^{-4} s^{-1}$ which is almost one order of magnitude higher than that obtained for glycerol hydrogenolysis.

Therefore, the acetol hydrogenation reaction is much faster and the rate-limiting-step of glycerol hydrogenolysis is glycerol dehydration. It is observed in Figure 4-25B that the 1,2PD selectivity is increased when the hydrogen pressure is increased; this might be because if the hydrogenation rate is higher, the concentration of un-hydrogenated acetol is lower as shown in Figure 4-25C; hence less by-products will be formed due to side reactions. The pseudo-first-order rate constant increases linearly when the hydrogen pressure is increased as shown in Figure 4-26B; therefore, the hydrogenation reaction is approximately first order with respect to hydrogen pressure.

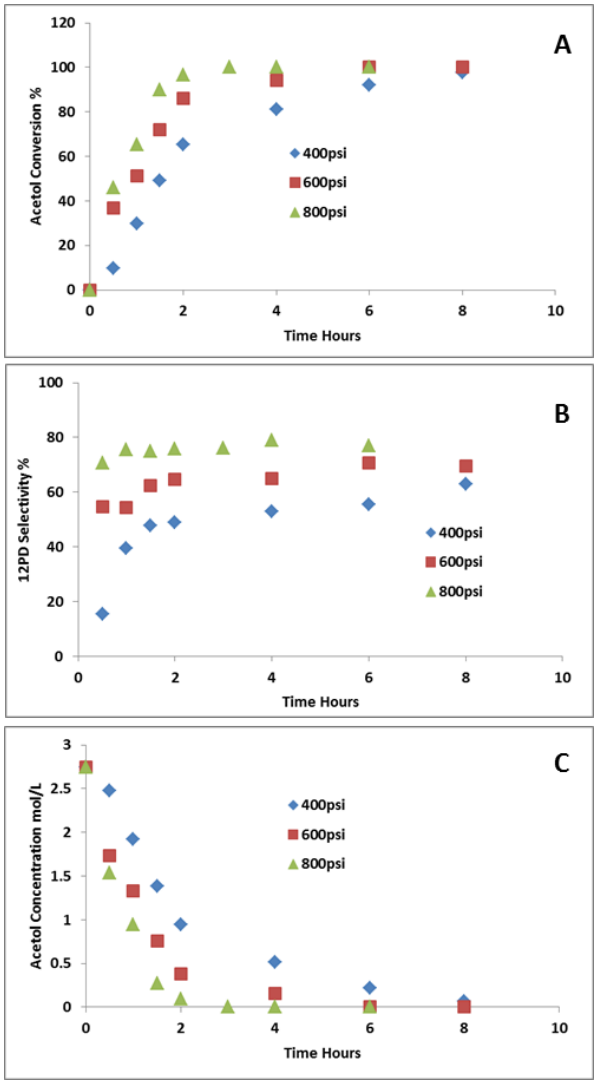

Figure 4-25 Effect of Hydrogen Pressure on Acetol Conversion and 1,2PD Selectivity over the Reaction Time: A) Acetol Conversion; B) 1,2PD Selectivity; C) Acetol Concentration. Experimental Condition: 200ºC, 500RPM, 5wt% catalyst with respect to acetol weight, 20% aqueous acetol, Cu/Zn/Al = 25/25/50.

Table 4-11 Effect of Acetol on Product Yield[a].

	Acetol Conversion	1,2PD Selectivity	1,2PD Yield	Others Yield
400psi	97.70	63.08	61.63	36.07
600psi	100.00	69.51	69.51	30.49
800psi	100.00	77.12	77.12	22.88

[a]Conditions: 200ºC, 500RPM, 5wt% catalyst with respect to acetol weight, 20wt% aqueous acetol, Cu/Zn/Al = 25/25/50, 8 hours reaction time.

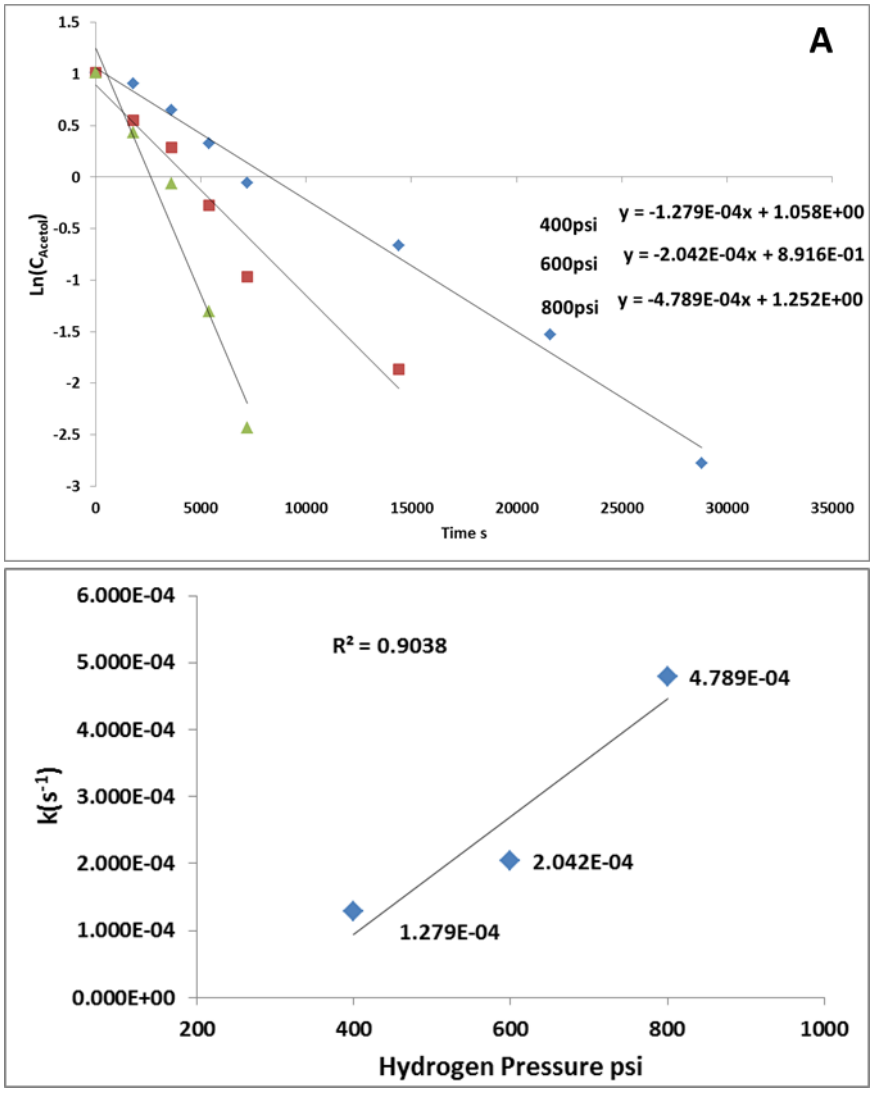

Figure 4-26 Pseudo-First-Order Kinetics Analysis for Acetol Hydrogenation at Different Hydrogen Pressures. Experimental Condition: 200ºC, 500RPM, 5wt% catalyst with respect to acetol weight, 20wt% aqueous acetol, Cu/Zn/Al = 25/25/50.

In order to further investigate the effect of acetol concentration on the selectivity to 1,2PD, experiments were carried out with different acetol concentrations which were 10wt% and 20wt% under 400psi hydrogen pressure, 5wt% catalyst with respect to acetol weight was loaded and the reactions were conducted at 200ºC. When the acetol feed concentration was low the selectivity to 1,2PD was higher (Figure 4-27B) because less by-products were

formed. Therefore, the 1,2PD selectivity is strongly dependent on the acetol concentration in the reaction mixture. As shown in Figure 4-27A, the rate constant for the reactions with 20% acetol is slightly higher than that with 10% acetol.

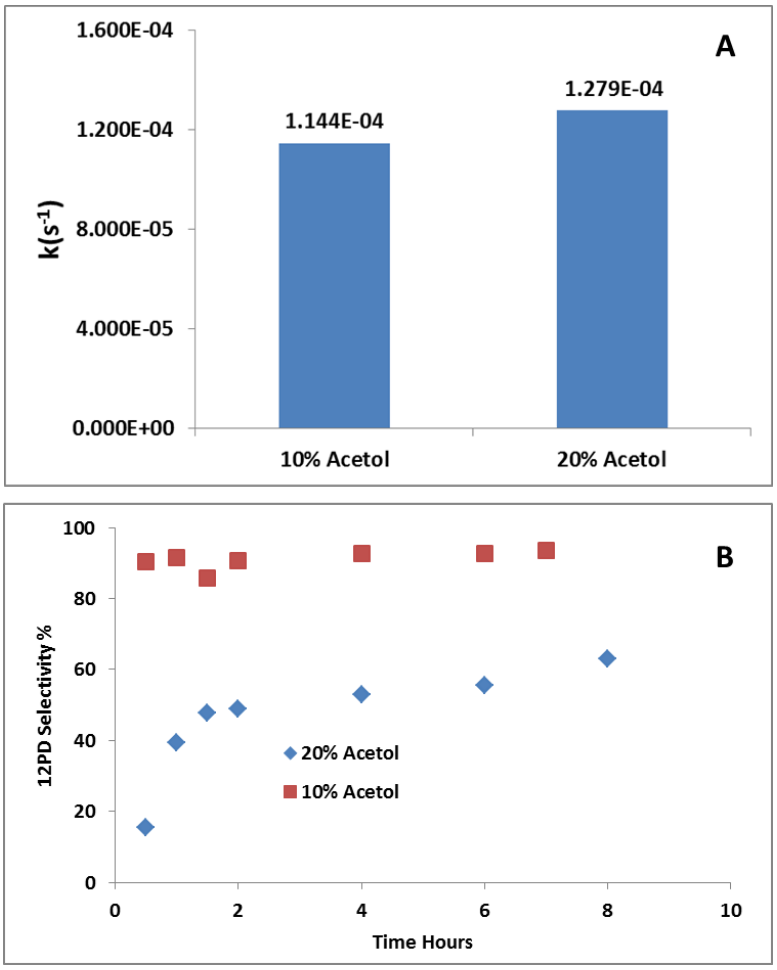

Figure 4-27 Effect of Hydrogen Pressure on Reaction Rate and 1,2PD Selectivity during the Reaction Time: A) Pseudo-first-order Reaction Rate Fitting; B) 1,2PD Selectivity. Experimental Condition: 200ºC, 500RPM, 5wt% catalyst with respect to acetol weight, Cu/Zn/Al = 25/25/50.

It has been previously discussed that in a glycerol hydrogenolysis process when the hydrogen pressure is low, the un-desired by-products are likely due to side reaction caused by the presence of the intermediate acetol. Figure 4-25 compares the retention time of the final products from glycerol hydrogenolysis when hydrogen pressure is low (200psi) with the

acetol hydrogenation. It can be seen that the retention times of the undesired by-products for both reactions match each other very well. This confirms that the by-product formation is due to insufficient hydrogen supplied to rapidly hydrogenate the acetol to 1,2PD and the side reactions occurred when the acetol concentration is high. Therefore, the selectivity to 1,2PD could be improved by either increasing the hydrogen supply or improving the activity of the hydrogenation catalyst. From the GC profile of the final product, it is noticed that no ethylene glycol is detected for acetol hydrogenation as shown in Figure 4-28. It is apparent that ethylene glycol is formed via C-C cleavage of glycerol; this observation is in agree with the report by Tanielyan *et al.* in 2013 [45] in Section 2.1.

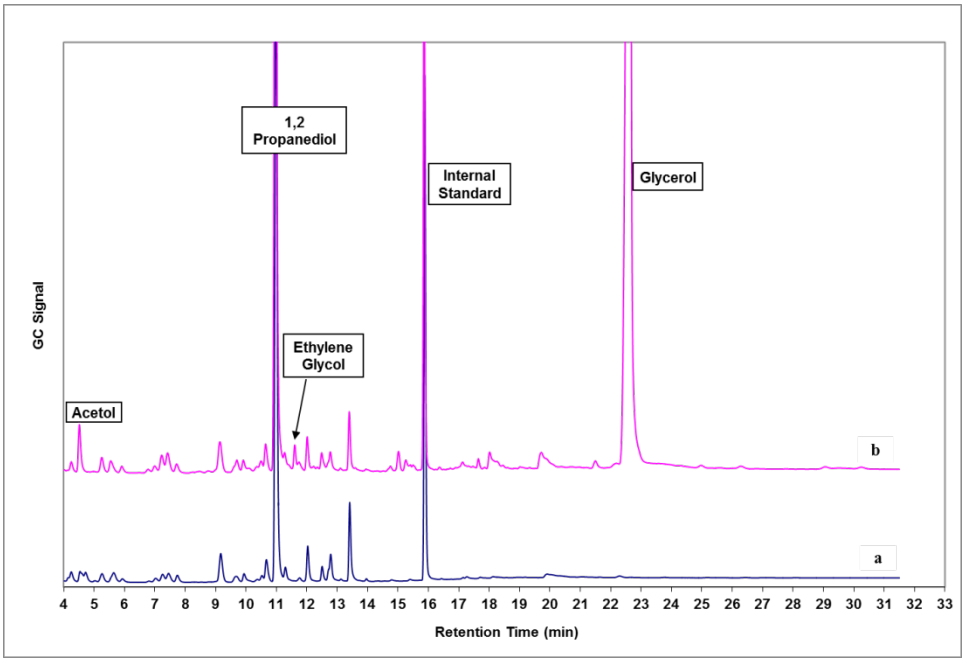

Figure 4-28 GC Profile of the Final Products for glycerol hydrogenolysis and acetol hydrogenation: a) Acetol Hydrogenation: 200ºC, 500RPM, 20% aqueous acetol, 5wt% catalyst with respect to acetol weight, 8 hours reaction time, Cu/Zn/Al=25/25/50 catalyst, 400psi H_2 Pressure. b) Glycerol Hydrogenolysis: 200ºC, 500RPM, 80% aqueous glycerol, 5wt% catalyst with respect to glycerol weight, 24 hours reaction time, Cu/Zn/Al=25/25/50, 200psi H_2 Pressure.

4.9 Effect of Ni on a $Cu/ZnO/Al_2O_3$ Catalyst

It has been reported that Ni is widely used in hydrogenation processes and it is less costly compared to the precious hydrogenation metals such as platinum, palladium and ruthenium [136, 137]. Ni was loaded on a $Cu/ZnO/Al_2O_3$ catalyst in 2 different ways. First of all, Ni was loaded on the $Cu/ZnO/Al_2O_3$ catalyst via oxalic acid co-precipitation. The catalyst preparation procedures are described in Section 3.1.1. The other way was just to mix a pre-calculated amount of NiO purchased from Sigmal Aldridge Co. Canada with the $Cu/ZnO/Al_2O_3$ catalyst prepared by oxalage gel-coprecipitation method physically.

The catalyst was used for acetol hydrogenation to investigate the improvement of the hydrogenation activity by addition of Ni. 20wt% aqueous acetol solution was used as the reactant mixture, 400psi hydrogen pressure, 5wt% catalyst with respect to acetol at 200ºC were chosen for the reaction conditions. Figure 4-29 shows the acetol conversion and 1,2PD selectivity during the reaction time and Figure 4-30 shows the pseudo-first-order rate constant for each catalyst. It can be observed that using the catalysts with 5mole% Ni loaded in both ways, the acetol conversions and the reaction rates are higher than that without Ni. Compared with the $Cu/ZnO/Al_2O_3$ catalyst without Ni, the reaction rate is increased by 100% when 5mole% Ni is added. By comparing the two different Ni loading methods, using the catalyst with 5mole% Ni loaded by co-precipitation a higher rate constant ($2.721x10^{-4}s^{-1}$) is obtained compared with that obtained by physically mixing ($2.272x10^{-4}s^{-1}$). This may be due to the fact that for the catalyst prepared by co-precipitation method, the metals are very well mixed; therefore, the catalyst activity can be improved. With Ni loaded, the 1,2PD selectivity is also higher than that without Ni loaded. The results have shown that with Ni loaded, the hydrogenation rate is higher; the concentration of the un-reacted acetol in the reaction mixture is lower and less amounts of by-products are formed via the side reactions. Since Ni can improve the hydrogenation activity of the catalyst, the selectivity to 1,2PD is improved

and the Ni loading using the co-precipitation method apparently has a better enhancement effect on the catalytic acitivity than physical mixing.

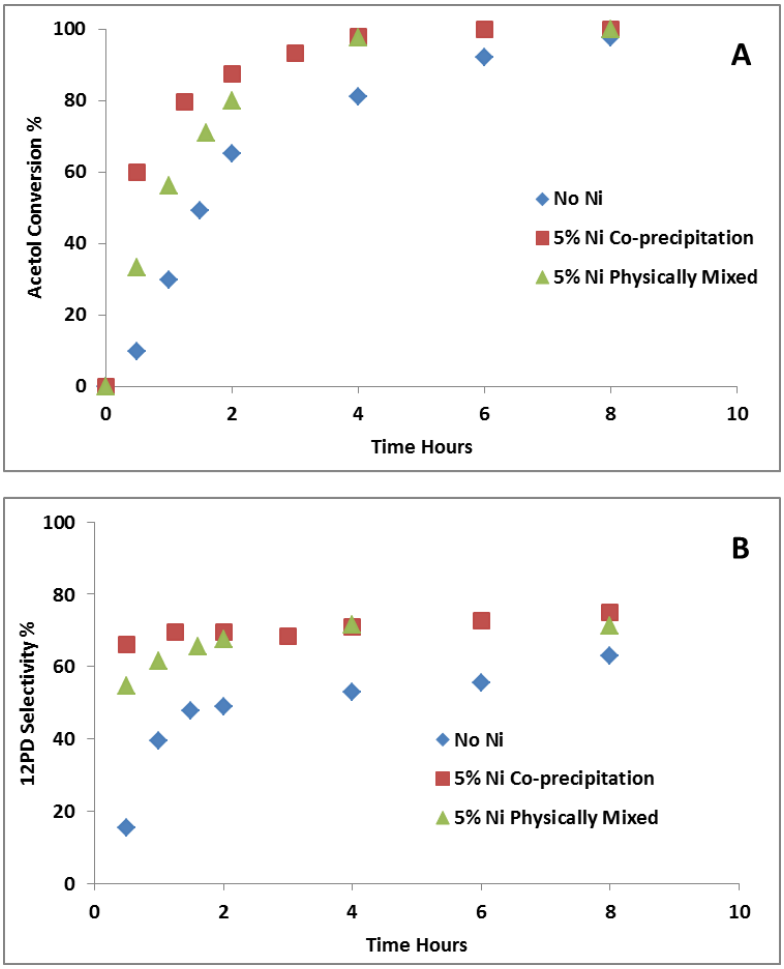

Figure 4-29 Effect of Ni Loading on Acetol Conversion and 1,2PD Selectivity during the Reaction Time: A) Acetol Conversion; B) 1,2PD Selectivity. Experimental Condition: 200ºC, 500RPM, 5wt% catalyst with respect to acetol weight, 20% aqueous acetol. Ni/Cu/Zn/Al=5/22.5/22.5/50 (molar).

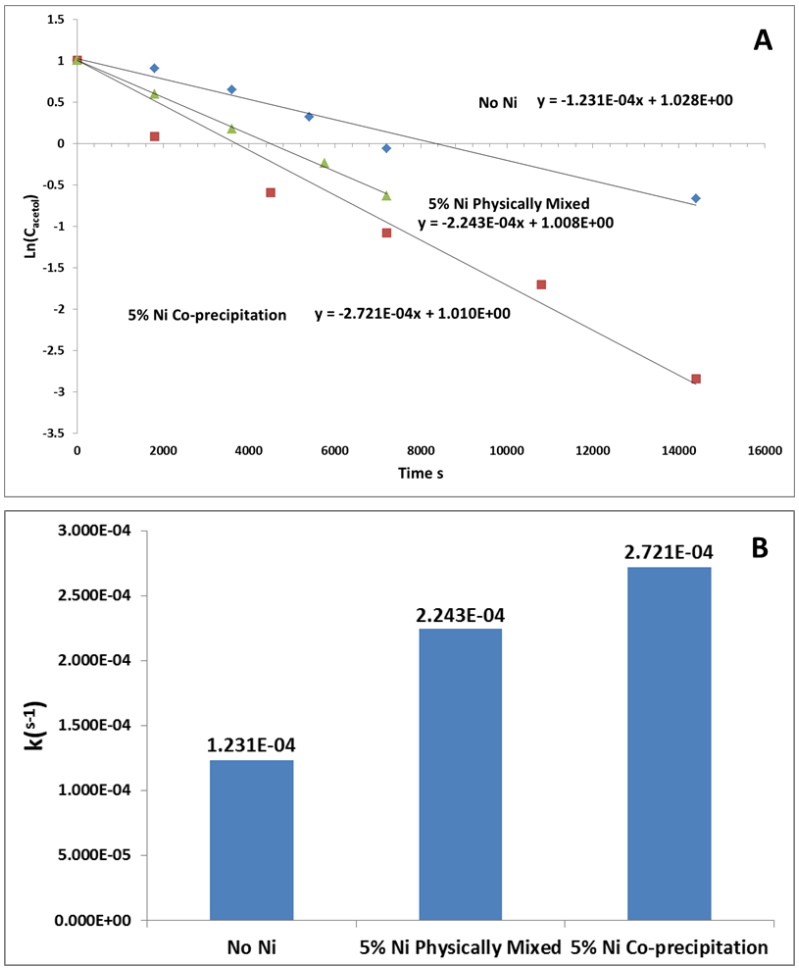

Figure 4-30 Pseudo-First-Order Kinetics Analyses for the Effect of Ni on Acetol Hydrogenation. Experimental Condition: 200ºC, 500RPM, 5wt% catalyst with respect to acetol weight, 20% aqueous acetol. Ni/Cu/Zn/Al=5/22.5/22.5/50 (molar).

Knowing that Ni can improve the hydrogenation activity of the $Cu/ZnO/Al_2O_3$ catalyst, the effect of Ni loading for glycerol hydrogenolysis reactions was investigated. As shown in Figure 4-31 and Figure 4-32, the glycerol conversion and the reaction rate with Ni added are slightly lower than that without Ni loaded. It is found that some acidic sites are lost when Ni is added based on the NH_3 TPD results (see Section 6.1); therefore, the activity of the catalysts for glycerol dehydration is also inhibited causing a slower reaction rate since glycerol dehydration is the rate-determining-step of the overall reaction. Details of the

change of acidity with Ni added will be presented in Section 6.1 for the NH_3 TPD analysis. From Figure 4-31B, it can be observed that the selectivity to 1,2PD is very similar for all these three catalysts as shown in Table 4-12. By comparing the catalysts with different Ni loading methods, it is found that these two loading methods do not make significant differences since the glycerol conversion, 1,2PD selectivity and reaction rate are not significantly improved after Ni is added.

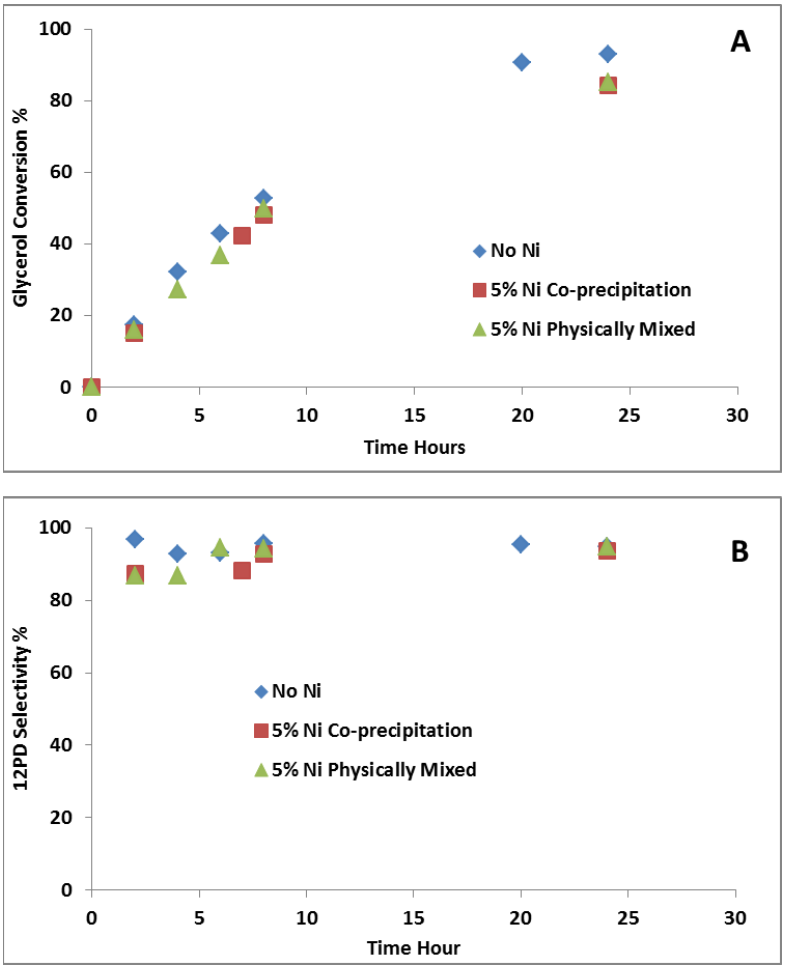

Figure 4-31 Effect of Ni Loading on Glycerol Conversion and 1,2PD Selectivity during the Reaction Time: A) Glycerol Conversion; B) 1,2PD Selectivity. Experimental Condition: 200ºC, 500RPM, 5wt% catalyst with respect to glycerol weight, 80wt% aqueous glycerol. Ni/Cu/Zn/Al=5/22.5/22.5/50 (molar).

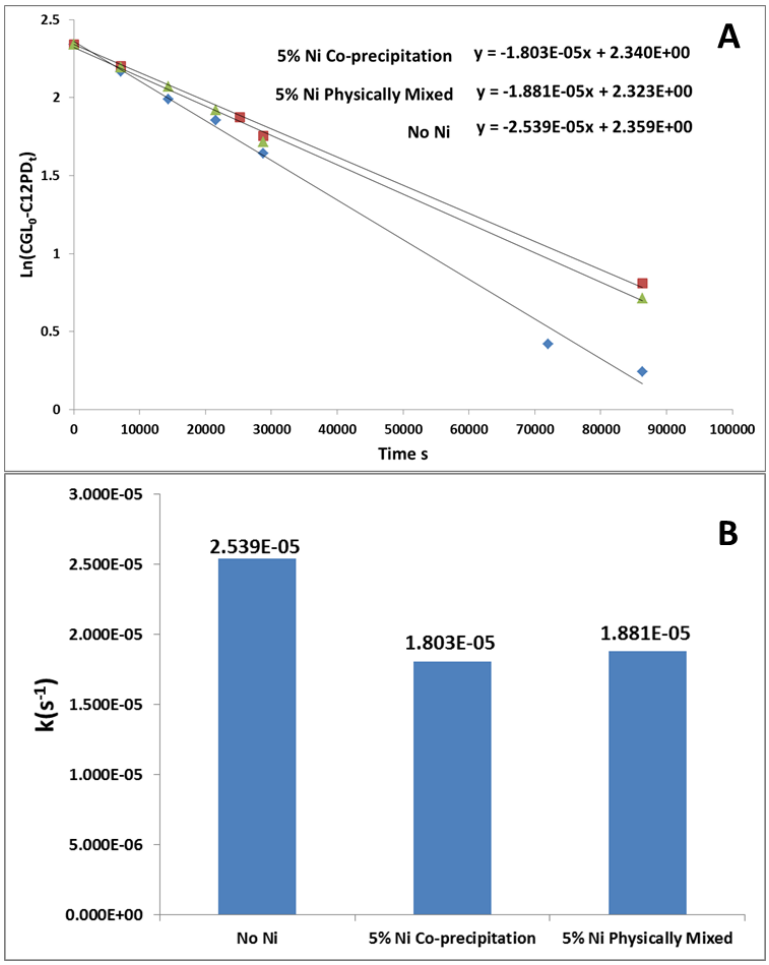

Figure 4-32 Pseudo-First-Order Kinetics Analyses for the Effect of Ni on Glycerol Hydrogenolysis. Experimental Condition: 200ºC, 500RPM, 5wt% catalyst with respect to glycerol weight, 80wt% aqueous glycerol. Ni/Cu/Zn/Al=5/22.5/22.5/50 (molar).

Table 4-12 Effect of Ni on Product Yield for a Glycerol Hydrogenolysis Process[a].

	Glycerol Conversion	1,2PD Selectivity	1,2PD Yield	EG Yield	Acetol Yield	PrOH Yield	Others Yield
No Ni	93.04	94.78	88.18	4.16	0.39	0.30	0.00
5% Ni Co-precipitation	84.12	93.66	78.78	3.61	0.46	0.60	0.67
5% Ni Physically Mixed	85.02	94.79	80.60	3.26	0.20	0.57	0.59

[a]Condition: 500RPM, 5wt% catalyst with respect to glycerol weight, 80wt% gelycerol, 400psi Hydrogen, 24 hours reaction time, 200ºC. Ni/Cu/Zn/Al=5/22.5/22.5/50 (molar).

4.10 2wt% Pd Supported on a $Cu/MgO/Al_2O_3$ Catalysts

The $Cu/MgO/Al_2O_3$ catalyst is found to have a higher activity than $Cu/ZnO/Al_2O_3$ for the glycerol hydrogenolysis process via *in situ* hydrogen produced by methanol steam reforming and Pd as a promoter can improve the catalyst activity, which will be described in Chapter 5. In order to investigate the $Cu/MgO/Al_2O_3$ catalyst activity on glycerol for the hydrogenolysis process with molecular hydrogen added and the effect of Pd as a promoter, experiments were carried out using a $Cu/MgO/Al_2O_3$ catalyst with an optimum molar ratio (Cu/Mg/Al=22.5/67.5/10) via the oxalate gel-coprecipitation method and the $Cu/MgO/Al_2O_3$ catalyst with 2wt% Pd loaded by an impregnation method. The detailed preparation method procedure is described in Section 3.1**.** The experimental conditions were: 200ºC, 500RPM, 5wt% catalyst with respect to glycerol weight, 50wt% aqueous glycerol and 24 hours reaction time. The glycerol conversion and 1,2PD selectivity are compared with those using $Cu/ZnO/Al_2O_3$ as shown in Figure 4-33.

From Figure 4-33A, it can be observed that at the beginning of the reaction, the glycerol conversion over the reaction time when using the $Cu/MgO/Al_2O_3$ catalyst is higher than that when using the $Cu/ZnO/Al_2O_3$ catalyst; as the reaction goes on, the increase of glycerol conversion is slower and the final conversion using $Cu/MgO/Al_2O_3$ after 24 hours is lower than when using the $Cu/ZnO/Al_2O_3$ catalyst as shown in Table 4-13**.** This is likely due to catalyst deactivation occurring during the reaction time with the $Cu/MgO/Al_2O_3$ catalyst. Therefore, at the early stage, the reaction using the $Cu/MgO/Al_2O_3$ catalsyt is faster than that using the $Cu/ZnO/Al_2O_3$ as shown in Figure 4-34 and the calculated pseudo-first-order rate constant is higher using the $Cu/MgO/Al_2O_3$ catalyst ($2.469x10^{-5}s^{-1}$) than when using the $Cu/ZnO/Al_2O_3$ catalyst ($1.456x10^{-5}s^{-1}$); but the final glycerol conversion using the $Cu/ZnO/Al_2O_3$ catalyst (77.2%) is higher than when using the $Cu/MgO/Al_2O_3$ catalyst (63.1%). When 2wt% Pd is loaded on the $Cu/MgO/Al_2O_3$ catalyst, the glycerol conversion over the reaction time is higher than when using the $Cu/ZnO/Al_2O_3$ catalyst. For the

Cu/MgO/Al_2O_3 catalyst the reaction rate shows about a 100% increase compared with the Cu/ZnO/Al_2O_3 catalyst as shown in Figure 4-34. As listed in Table 4-13, the final glycerol conversion using the 2wt%Pd-Cu/MgO/Al_2O_3 catalyst is also higher. The 1,2PD selectivity using these catalysts is not significantly different, being between 88% and 90%, indicating that 400psi hydrogen pressure is sufficient for the hydrogenolysis because no other unknown by-product was detected by GC as shown in Table 4-13.

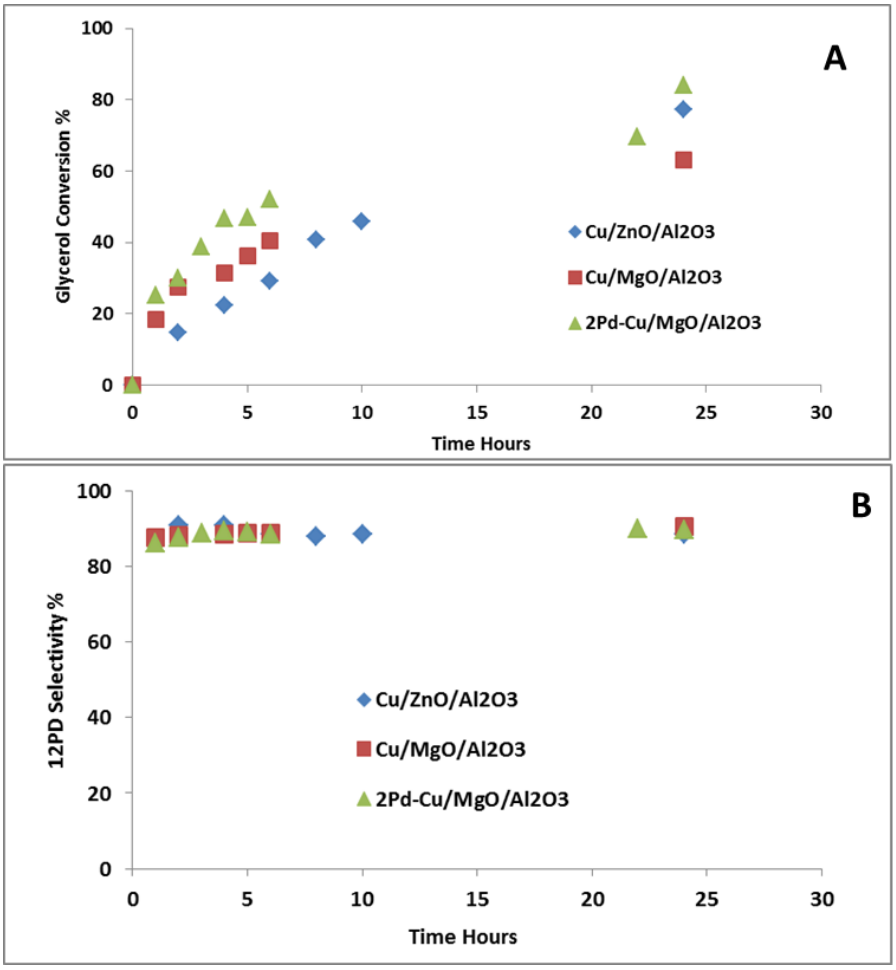

Figure 4-33 Glycerol Conversion and 1,2PD Selectivity during the Reaction Time: A) Glycerol Conversion; B) 1,2PD Selectivity. Experimental Condition: 200ºC, 500RPM, 5wt% catalyst with respect to glycerol weight, 50wt% aqueous glycerol, Cu/Zn/Al=25/25/50, Cu/Mg/Al=22.5/67.5/10.

Table 4-13 Products Yield Comparison between $Cu/MgO/Al_2O_3$ and $Cu/ZnO/Al_2O_3$[a].

	Glycerol Conversion	1,2PD Selectivity	1,2PD Yield	EG Yield	Acetol Yield	PrOH Yield	Others Yield
Cu/Zn/Al	77.24	88.54	68.39	7.64	0.36	0.85	0.00
Cu/Mg/Al	63.07	90.37	57.00	5.39	0.69	0.00	0.00
2Pd-Cu/Mg/Al	83.91	89.60	75.18	7.58	0.46	0.11	0.58

[a]Condition: 500RPM, 5wt% catalyst with respect to glycerol weight, 50wt% glycerol, 400psi Hydrogen, 24 hours reaction time, 200ºC, Cu/Zn/Al=25/25/50, Cu/Mg/Al=22.5/67.5/10.

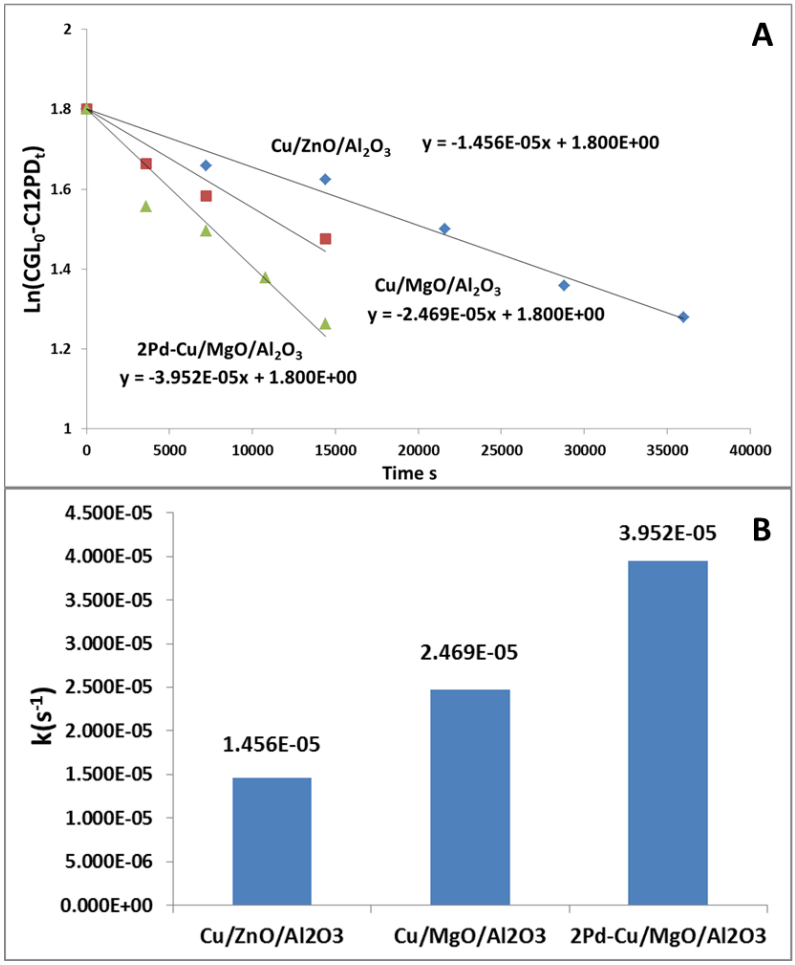

Figure 4-34 Pseudo-First-Order Kinetics Analyses for Cu/Zn/Al, Cu/Mg/Al and 2wt%Pd-Cu/Mg/Al Catalysts. Experimental Condition: 200ºC, 500RPM, 5wt% catalyst with respect to glycerol weight, 50wt% aqueous glycerol, Cu/Zn/Al=25/25/50, Cu/Mg/Al=22.5/67.5/10.

In order to investigate the stability of 2wt% Pd-Cu/MgO/Al_2O_3 catalyst for the glycerol hydrogenolysis process, the spent catalyst has been recycled and reused. The glycerol conversion and the 1,2PD selectivity are shown in Figure 4-35. An obvious activity deactivation is observed since the glycerol conversion using the spent catalyst is significantly lower than that using fresh catalyst. The reaction rate drops by 50% as shown in Figure 4-36.

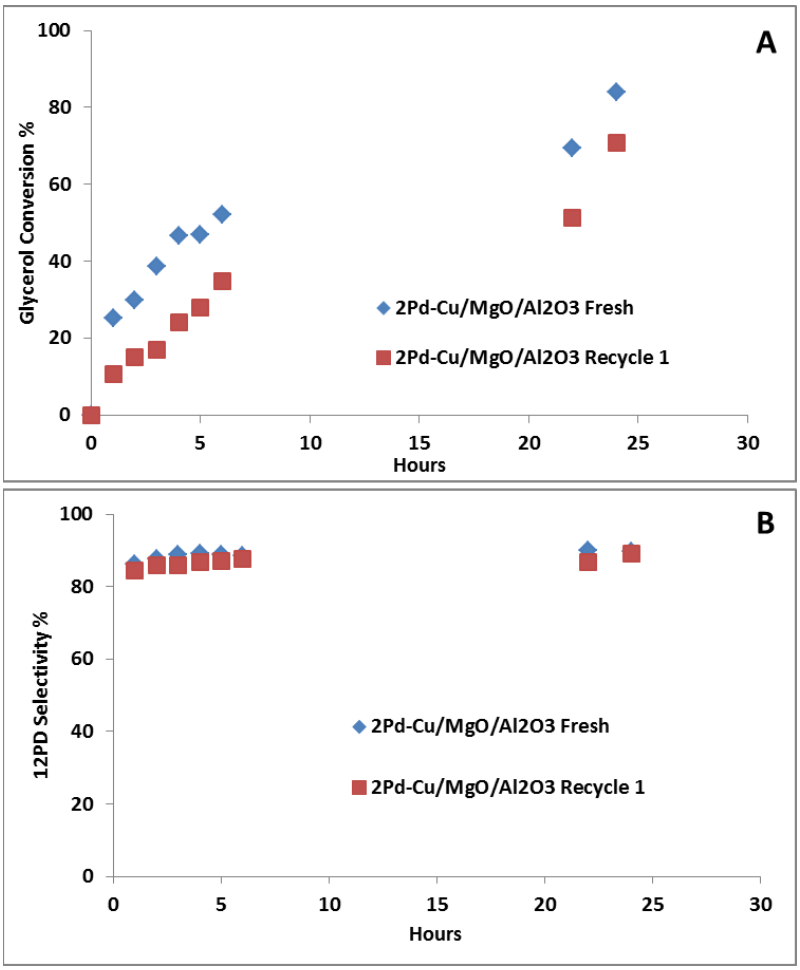

Figure 4-35 Glycerol Conversion and 1,2PD Selectivity during the Reaction Time using Fresh and Recycled Catalysts: A) Glycerol Conversion; B) 1,2PD Selectivity. Experimental Condition: 200ºC, 400psi H_2, 500RPM, 5wt% catalyst with respect to glycerol weight, 50% aqueous glycerol, 2wt% Pd on Cu/MgO/Al_2O_3 (Cu/Mg/Al=22.5/67.5/10).

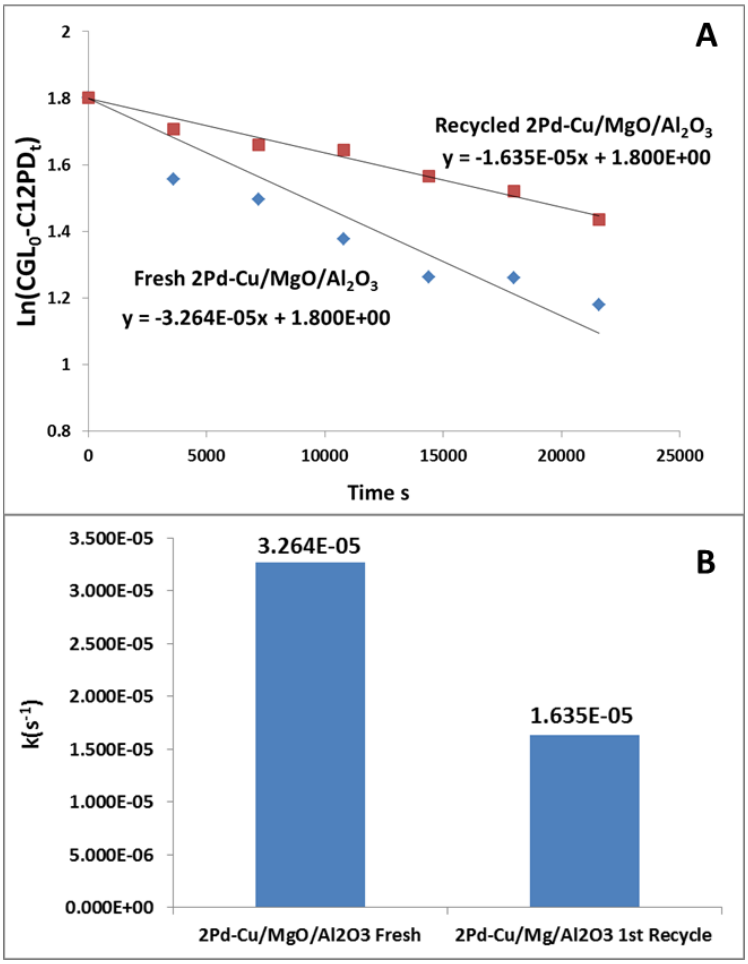

Figure 4-36 Pseudo-First-Order Kinetics Analyses for the Fresh and Recycled 2wt% Pd-Cu/MgO/Al_2O_3 Catalysts. Experimental Condition: 200ºC, 400psi H_2, 500RPM, 5wt% catalyst with respect to glycerol weight, 50% aqueous glycerol, 2wt% Pd on Cu/MgO/Al_2O_3 (Cu/Mg/Al=22.5/67.5/10).

4.11 Effect of Temperature and Kinetic Study Using 2wt% Pd-Cu/MgO/Al_2O_3 Catalyst

The experiments at different temperatures using the 2wt% Pd supported on Cu/MgO/Al_2O_3 catalyst have been carried out to study the effect of temperature on the glycerol hydrogenolysis process and to obtain the activation energy. Three temperatures, namely, 180ºC, 200ºC and 220ºC, have been selected for the reaction study. The glycerol conversion

and the 1,2PD selectivity during the reaction time are shown in Figure 4-37. It can be observed that at higher temperature, the glycerol conversion is higher. It is noticed in Figure 4-37B that the selectivity to 1,2PD at 220ºC is lower than at 200ºC and 180ºC. This observation is similar with what was found when using the Cu/ZnO/Al_2O_3 catalyst at a high temperature. It is possibly due to that the solubility of hydrogen in the reaction mixture is lower at a higher temperature; and also that at higher temperature more acetol is formed causing a higher acetol concentration in the solution; therefore, the 1,2PD selectivity is lower.

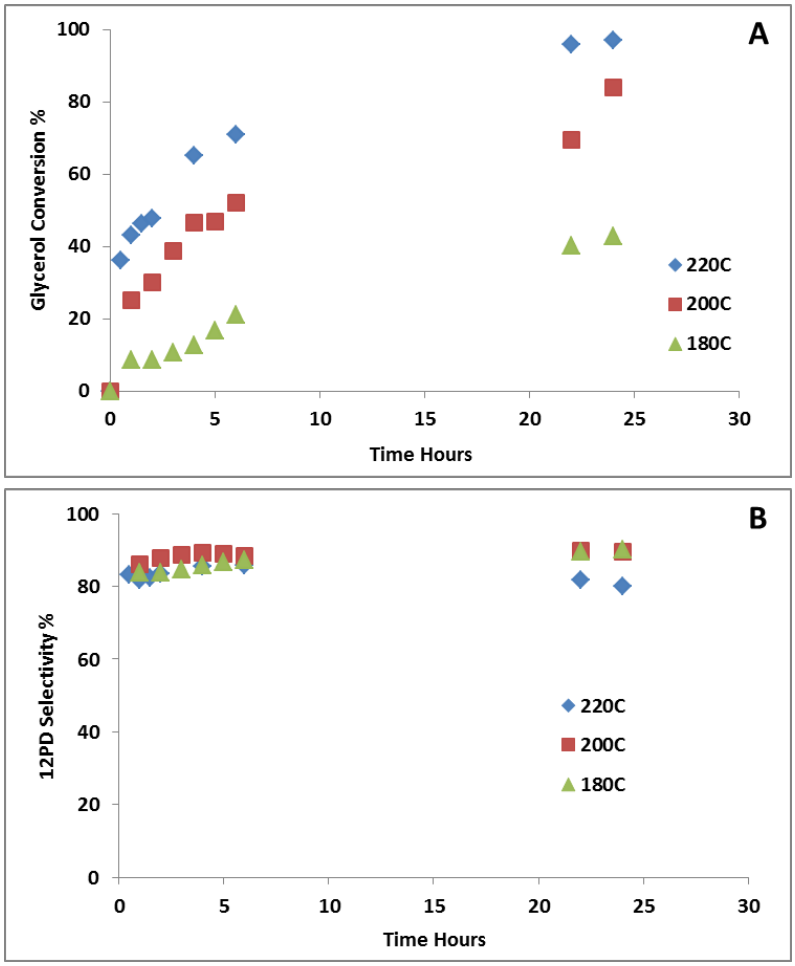

Figure 4-37 Effect of Temperature on Glycerol Conversion and 1,2PD Selectivity during the Reaction Time: A) Glycerol Conversion; B) 1,2PD Selectivity. Experimental Condition: 400psi H_2, 500RPM, 5wt% catalyst with respect to glycerol weight, 50% aqueous glycerol, 2wt% Pd on Cu/MgO/Al_2O_3 (Cu/Mg/Al=22.5/67.5/10) Catalyst.

Table 4-14 Effect of Temperature on Product Yield Using a 2wt%Pd-Cu/MgO/Al_2O_3 Catalyst[a].

	Glycerol Conversion	1,2PD Selectivity	1,2PD Yield	Acetol Yield	EG Yield	PrOH Yield	Others Yield
220˚C	96.87	80.03	77.52	1.83	5.52	1.11	10.88
200˚C	83.91	89.60	75.18	0.46	7.58	0.11	0.58
180˚C	42.87	90.00	38.58	0.00	3.99	0.00	0.30

[a]Conditions: 400psi H_2, 500RPM, 5wt% catalyst with respect to glycerol weight, 50% aqueous glycerol, 2wt% Pd on Cu/MgO/Al_2O_3 (Cu/Mg/Al=22.5/67.5/10) Catalyst, 24 hours reaction time.

It can be observed in Figure 4-38 that the reaction is faster when the temperature is higher since the reaction rate is higher. Based on Arrhenius Equation, the activation can be calculated using Equation 4-3. By plotting ln(k) versus 1/T, the intersect of the estimated linear trend line is ln(k_0) and the slop of the line is –Ea/R where R is the gas constant with the value of 8.314$JK^{-1}mol^{-1}$. The fitting of the kinetic parameters is shown in Figure 4-39. The pre-exponential factor is calculated to be $113.464x10^6$ and the activation energy is calculated to be 113619.12J/mol or 113.62/mol. It indicates that the reaction with this catalyst is chemically kinetically controlled. It is introduced in Section 4.7 that the activation energy by using Cu/ZnO/Al_2O_3 catalyst is 69.39kJ/mol. Hence the reaction using 2wt%Pd-Cu/MgO/Al_2O_3 catalyst is more kinetically controlled. Therefore, a higher temperature is necessary when a faster reaction rate is needed.

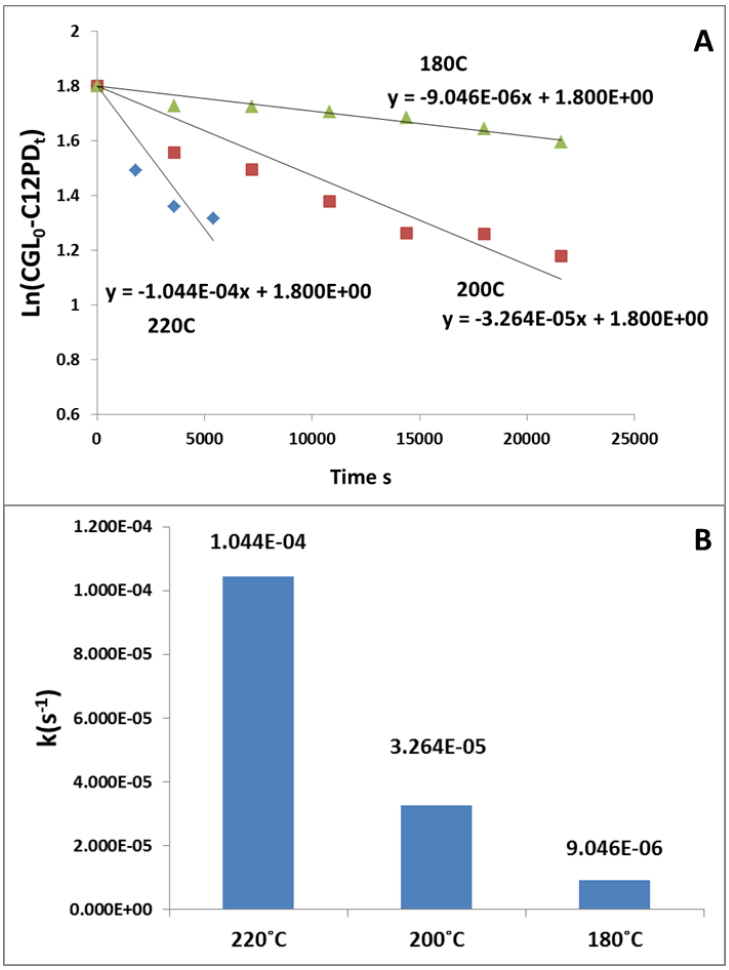

Figure 4-38 Pseudo-First-Order Kinetics Analyses for the 2wt% Pd on $Cu/MgO/Al_2O_3$ Catalyst at Different Temperatures. Condition: 400psi H_2, 500RPM, 5wt% catalyst with respect to glycerol weight, 50% aqueous glycerol, 2wt% Pd on $Cu/MgO/Al_2O_3$ (Cu/Mg/Al=22.5/67.5/10) Catalyst.

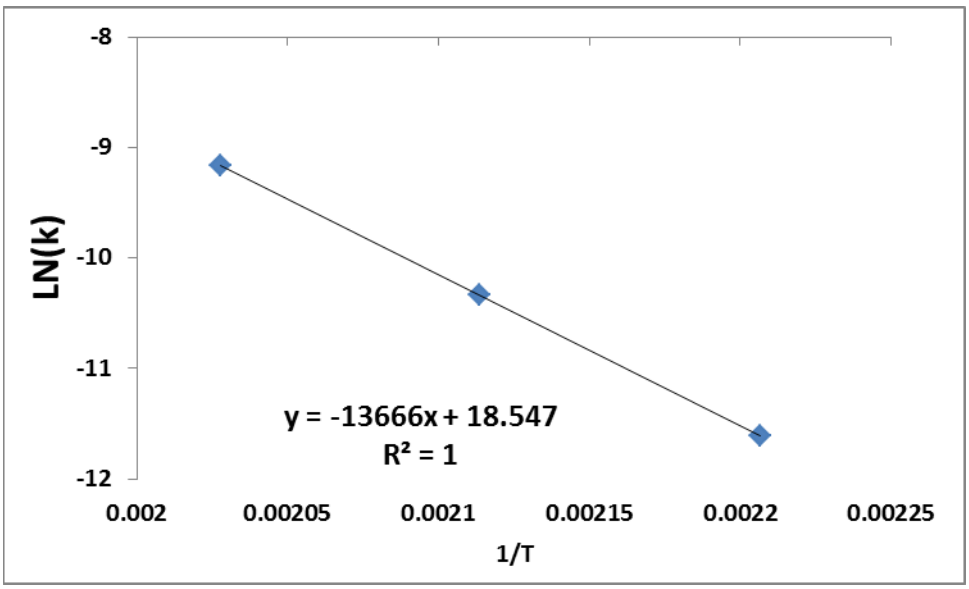

Figure 4-39 Effect of Temperature on Rate Constant. Catalyst: 2wt% Pd on Cu/MgO/Al_2O_3 (Cu/Mg/Al=22.5/67.5/10).

It is observed in Table 4-14 that the selectivity to 1,2PD at 220ºC is lower than at lower temperatures and the yield of other unknown by-products is 10.9%. This is attributed to insufficient hydrogen in the reaction mixture. Therefore, an experiment at higher hydrogen pressure (600psi) was carried out to investigate if the 1,2PD selectivity can be improved. The glycerol conversion and 1,2PD selectivity during the reaction time are shown in Figure 4-40. From Figure 4-40A, it is observed that the glycerol conversion during the reaction time are similar at both hydrogen pressures. However, the 1,2PD selectivity at 600psi hydrogen pressure is higher than that at 400psi as shown in Figure 4-40B. When the hydrogen pressure is increased from 400psi to 600psi, the yield of other by-products after 24 hours due to side reactions by acetol drops from 10.9% to only 3.5% respectively and the yield of acetol in the final product mixture also drops from 1.8% to 0.5% respectively. It is found that at 220ºC, the reaction rate does not change significantly by increasing the hydrogen pressure from 400psi to 600psi (Figure 4-41) but the selectivity of 1,2PD is improved and less other by-products are formed. This is possibly attributed to that when the hydrogen pressure is not high enough to effectively hydrogenate acetol at higher temperature, the rates of the side

reactions are also increased causing a high glycerol conversion rate. From Table 4-15 it is also observed that at 600psi hydrogen pressure, the ethylene glycol yield (9.2%) is higher than that at 400psi (5.5%)

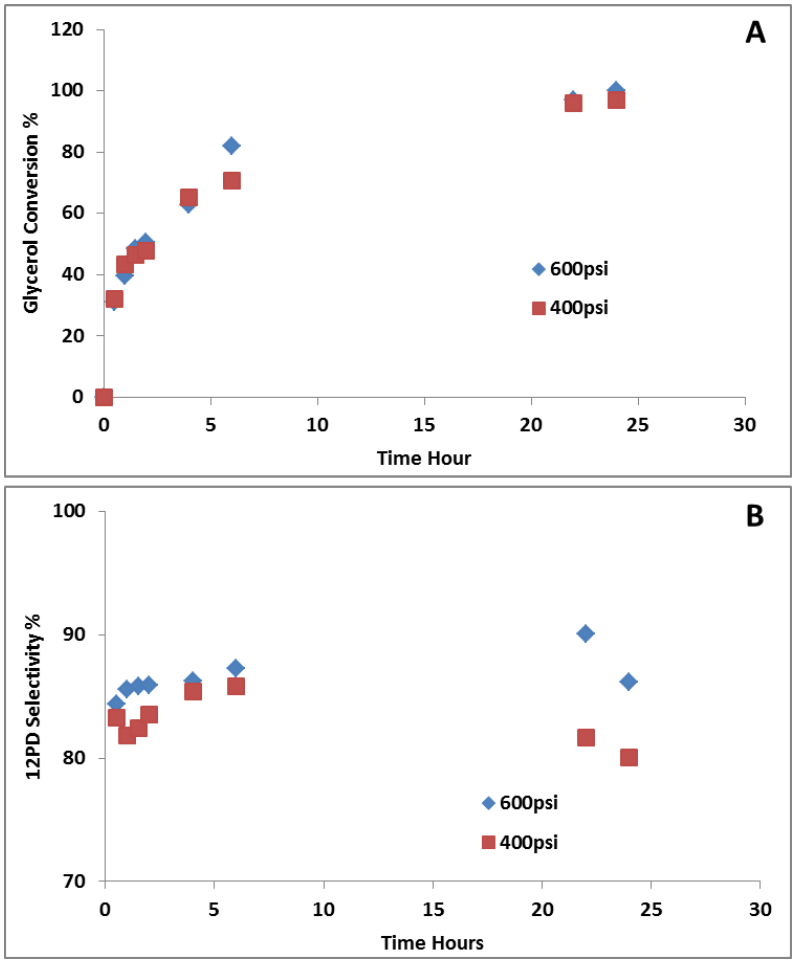

Figure 4-40 Effect of Hydrogen Pressure on Glycerol Hydrogenolysis Using Pd-Cu/MgO/Al_2O_3 Catalyst: A) Glycerol Conversion; B) 1,2PD Selectivity. Experimental Condition: 220ºC 400psi H_2, 500RPM, 5wt% catalyst with respect to glycerol weight, 50% aqueous glycerol, 2wt% Pd on Cu/MgO/Al_2O_3 (Cu/Mg/Al=22.5/67.5/10) Catalyst.

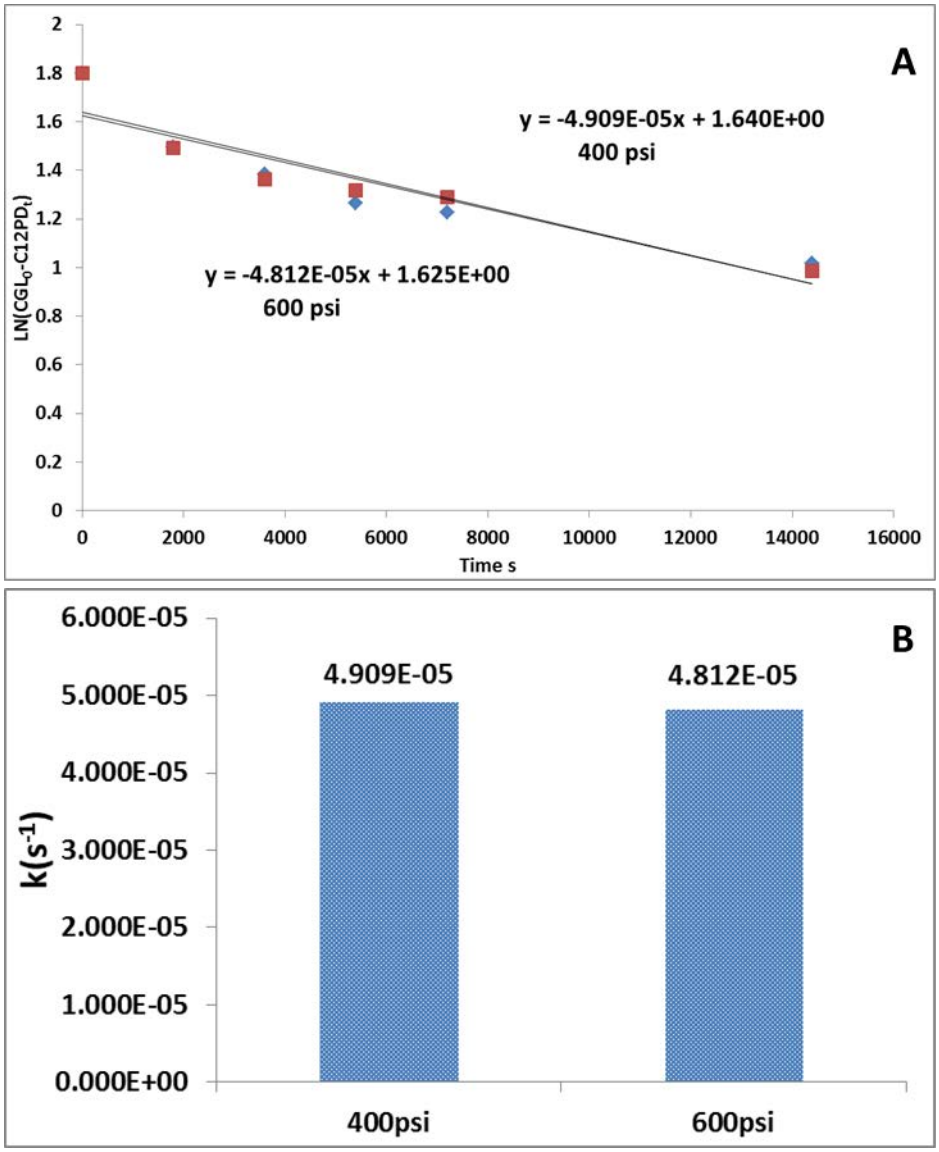

Figure 4-41 Pseudo-First-Order Kinetics Analyses for the 2wt% Pd on $Cu/MgO/Al_2O_3$ (Cu/Mg/Al=22.5/67.5/10) Catalyst at Different Hydrogen Pressures

Table 4-15 Effect of Hydrogen Pressure on Product Yield Using 2wt%Pd-$Cu/MgO/Al_2O_3$ Catalyst[a]

	Glycerol Conversion	1,2PD Selectivity	1,2PD Yield	Acetol Yield	EG Yield	PrOH Yield	Others Yield
600psi	100.00	86.13	86.13	0.54	9.22	0.63	3.49
400psi	96.87	80.03	77.52	1.83	5.52	1.11	10.88

[a]Condition: 220ºC 400psi H_2, 500RPM, 5wt% catalyst with respect to glycerol weight, 50% aqueous glycerol, 2wt% Pd on $Cu/MgO/Al_2O_3$ (Cu/Mg/Al=22.5/67.5/10) Catalyst.

4.12 Conclusions

The autoclave experiments of glycerol hydrogenolysis to produce 1,2PD with a molecular hydrogen feed have been carried out.

Three different preparation methods were attempted to prepare a $Cu/ZnO/Al_2O_3$ catalyst, and the catalyst prepared by oxalate gel-coprecipitation method was found to have the highest activity.

The experiments were carried out under different hydrogen pressures using a $Cu/ZnO/Al_2O_3$ catalyst prepared by oxalate gel-coprecipitation and it was found that the 1,2PD selectivity strongly depended on hydrogen pressure; when the hydrogen pressure was low, some unknown by-products were formed. This by-product formation was most likely due to side reactions with acetol.

Acetol hydrogenation experiments have been carried out. The kinetic data suggests that the acetol hydrogenation step is significantly faster than the overall reaction and hence the glycerol dehydration step is the rate-determining-step. It was also observed that the by-products formed during the acetol hydrogenation reaction were exactly the same as those formed during glycerol hydrogenolysis when the hydrogen pressure was low; this further suggests that the by-products were formed via the side reactions with acetol.

The metal composition of the $Cu/ZnO/Al_2O_3$ catalyst has been optimized by varying the molar ratio of the three metals and the Cu/Zn/Al metals molar ratio of 25/25/50 gave the highest activity. It was also found that with aluminum added, the catalyst not only gave a higher activity but also had a better stability as found in the catalyst recycling experimental results. Using the $Cu/ZnO/Al_2O_3$ catalyst, no obvious activity loss after four times of recycling was observed; while when using the Cu/ZnO catalyst without adding Al a significant deactivation was observed when the catalyst was recycled and reused.

Ni has been loaded onto the $Cu/ZnO/Al_2O_3$ catalyst and experiments with Ni loaded have been carried out to study the promoting effect of Ni. It was found that with Ni added, the hydrogenation activity of the catalyst was improved; however, no significant improvement was found for the hydrogenolysis reaction.

Experiments have been carried out using 2wt% Pd supported on a $Cu/MgO/Al_2O_3$ catalyst. This catalyst gave a higher reaction rate and higher 1,2PD selectivity compared with the $Cu/ZnO/Al_2O_3$ catalyst. However, a significant deactivation was observed using the spent catalyst.

Three different temperatures, 180ºC, 200ºC and 220ºC respectively, have been chosen for the reactions using both $Cu/ZnO/Al_2O_3$ and 2wt%Pd on $Cu/MgO/Al_2O_3$ catalysts to study the temperature effect on the glycerol hydrogenolysis process. It was found that the reaction rate was higher at higher temperature but that the 1,2PD selectivity was lower when the reaction was carried out at 220ºC for the reaction carried at 400psi hydrogen pressure. The activation energies for the reactions using both catalysts have been calculated. Using the $Cu/ZnO/Al_2O_3$ catalyst, the activation energy was 69.39kJ/mole; when using the 2wt%Pd on $Cu/MgO/Al_2O_3$ catalyst, the activation energy was 113.62kJ/mol. This suggested that the reaction was chemically kinetically controlled using both catalysts and that when the 2wt%Pd on $Cu/MgO/Al_2O_3$ catalyst was used, the reaction was more temperature dependent.

Chapter Five
Glycerol Hydrogenolysis Using the *in situ* Hydrogen Produced via Methanol Steam Reforming

Experiments of glycerol hydrogenolysis to produce 1,2PD via *in situ* hydrogen produced via methanol steam reforming have been carried out. Different catalyst preparation methods have been investigated for $Cu/ZnO/Al_2O_3$ catalysts. The method which gave the best catalytic activity was used to optimize the metal composition and experimental conditions. The effect of Ni as a promoter was also investigated. A $Cu/MgO/Al_2O_3$ catalyst was used in the reaction system and the metal composition and experimental conditions were also optimized. Pd was used as a promoter to study its promoting effect on a $Cu/MgO/Al_2O_3$ catalyst. A series of factorial design experiments were carried out to investigate the effect of different experimental conditions and interactions between various factors such as: temperature, pressure, stirring speed, glycerol concentration, water to methanol molar ratio, catalyst weight and the loading of Pd.

5.1 $Cu/ZnO/Al_2O_3$ Catalyst

$Cu/ZnO/Al_2O_3$ catalyst has been reported to be most frequently used for methanol steam reforming because it is easy and safe to handle, low cost and exhibits high activity [138-140]. Also $Cu/ZnO/Al_2O_3$ has shown high activity for glycerol hydrogenolysis to produce 1,2PD as discussed in Chapter 4 and in some literature reports [47, 67, 68].

5.1.1 The Activities of $Cu/ZnO/Al_2O_3$ Catalysts by Different Preparation Methods.

$Cu/ZnO/Al_2O_3$ is usually prepared via co-precipitation and impregnation methods. Two precipitation agents were used for investigation: sodium carbonate (Na) and oxalic acid (OA) [79, 138], with a Cu/Zn/Al molar ratio of 25/25/50. The catalyst was also prepared by an impregnation method; an alumina ring purchased from Saint-Gobain (SA6575) was used as the support and the molar ratio of Cu/Zn/Al is 15/15/70.

It has been reported in Chapter 4 for glycerol hydrogenolysis with molecular hydrogen added that the catalytic activity was high when the molecular ratio of Cu/Zn/Al is 25/25/50; also it was reported by Meher *et al.* in 2009 [47] that the ratio of Cu/Zn/Al at 25/25/50 prepared by Na co-precipitation also showed a higher activity compared with other metal compositions. Therefore, a Cu/Zn/Al ratio of 25/25/50 was used as a starting point. For a methanol steam reforming reaction, the stoichiometric ratio of water to methanol is 1 (Equation 5-1). However, the typical water to methanol molar ratio has been reported to be varied from 1 to 1.4. It was reported that a slightly higher water content can shift the equilibrium toward the product to provide higher methanol conversion and it could also decrease CO formation caused by methanol decomposition [141, 142]. Therefore, 1.2 was chosen as the ratio of water to methanol feed ratio unless otherwise indicated. The experimental results obtained are shown in Figure 5-1.

$$CH_3OH + H_2O \xleftrightarrow{Catalyst} CO_2 \uparrow + 3H_2 \uparrow \qquad \textbf{Equation 5-1}$$

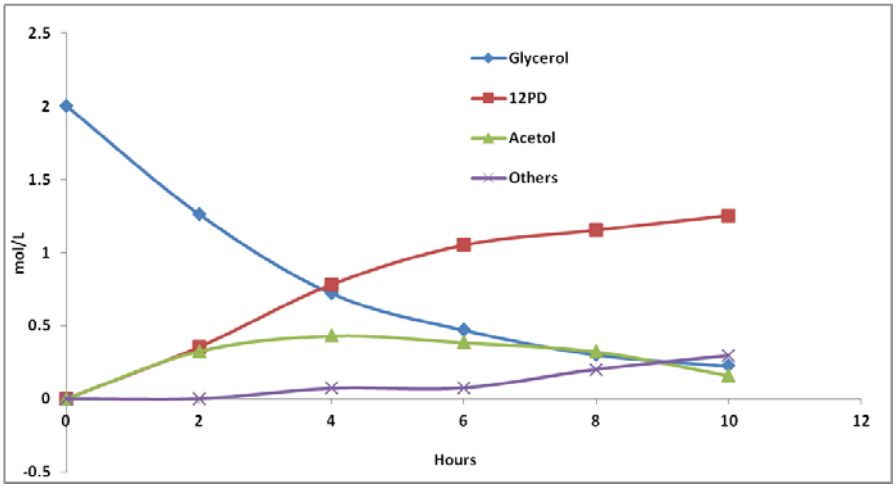

Figure 5-1 Concentration Profiles of Different By-Products Using $Cu/ZnO/Al_2O_3$ Catalyst (OA). Conditions: 220 ºC, 15bar N_2, 20wt% Glycerol, Water/Methanol=1.2, 3wt% catalyst with respect to the total weight of the reaction mixture, 500RPM, Cu/Zn/Al=25/25/50 (OA).

From Figure 5-1, it can be observed that as the reaction proceeds, the concentration of glycerol is decreased and the concentration of 1,2PD is increased. The concentration of acetol as the intermediate increases at the beginning of the reaction and then decreases with reaction time. There are other by-products formed during the reaction time. It has been reported previously that some other by-products were formed most likely due to insufficient hydrogen to rapidly hydrogenate acetol to 1,2PD. To investigate the nature of the by-products formed when hydrogen was produced via methanol steam reforming, the GC graph of the final sample (8^{th} hour) was compared with the chromatograms of the sample obtained when molecular hydrogen was added as shown in Figure 5-2.

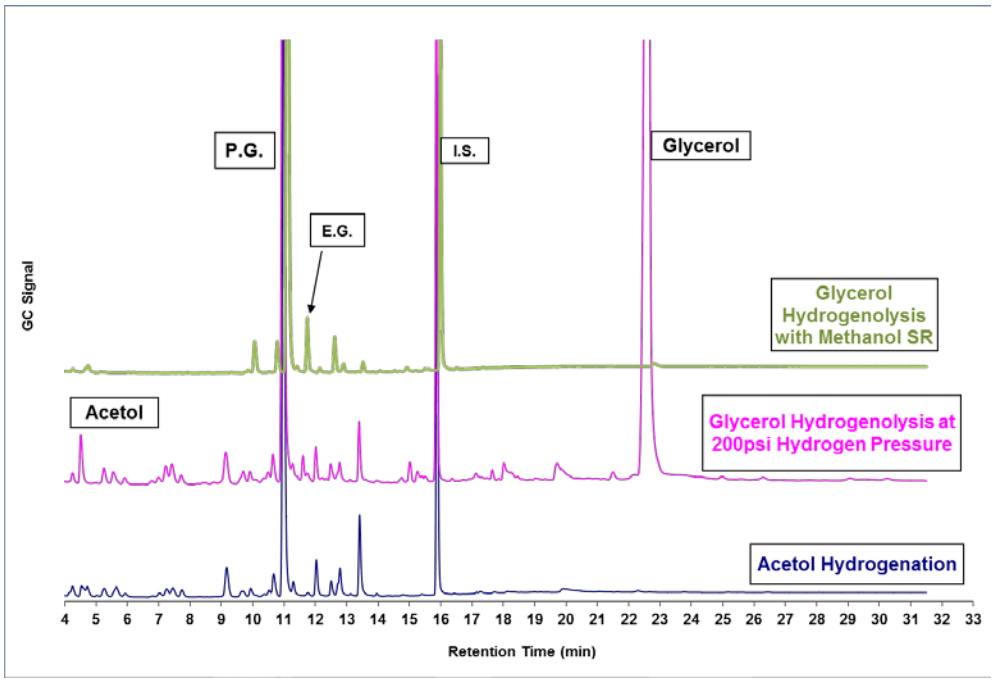

Figure 5-2 Chromatograms of the Final Sample of: (Blue) Acetol Hydrogenation, (Pink) Glycerol Hydrogenolysis with Moledular Hydrogen Added, (Green) Glycerol Hydrogenolysis with Methanol Steam Reforming.

In Figure 5-2, it can be seen that the retention times of by-product formation for the reaction with methanol steam reforming match the other two reactions. Hence indeed *in situ* H_2 was produced for glycerol hydrogenolysis and the the by-product formation is due to insufficient hydrogen produced by methanol steam reforming. Therefore, the selectivity to 1,2PD is believed to be strongly dependent on the methanol conversion.

The $Cu/ZnO/Al_2O_3$ catalysts prepared by Na_2CO_3 coprecipitation and impregnation (IMP) were also used under the same reaction conditions; the results are compared and shown in Figure 5-3 and Table 5-1.

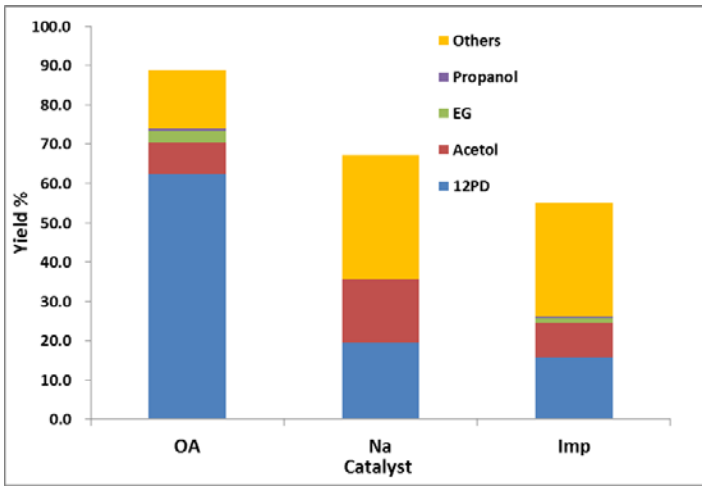

Figure 5-3 Products Distribution for the Catalysts Prepared by 3 Different Preparation Methods. Conditions: 220ºC, 15bar N_2, 20wt% Glycerol, Water/Methanol=1.2, 3wt% catalyst, 500RPM, Cu/Zn/Al=25/25/50 (OA), 8 hours.

Table 5-1 Products Distribution for the Catalysts Prepared by 3 Different Preparation Methods[a].

	Glycerol Conversion	1,2PD Selectivity	1,2PD Yield	Acetol Yield	EG Yield	PrOH Yield	Others Yield
OA	88.8	70.3	62.5	7.9	3.0	0.7	14.7
Na	60.3	29.1	19.6	16.1	0.0	0.0	31.6
Imp	55.1	28.6	15.8	8.9	1.1	0.5	28.8

[a]Conditions: 220ºC, 15bar N_2, 20wt% Glycerol, Water/Methanol=1.2, 3wt% catalyst, 500RPM, Cu/Zn/Al=25/25/50 (OA and Na), Cu/Zn/Al=15/15/70 (Imp), 8 hours.

From Figure 5-3 as well as Table 5-1, it can be seen that the glycerol conversion and 1,2PD selectivity are the highest using the catalyst prepared by an oxalate gel-coprecipitation. Hence the preparation method apparently plays a very important role for both glycerol hydrogenolysis and methanol conversion. This is in agreement with the experimental results discussed in Chapter 4 for glycerol hydrogenolysis with added molecular hydrogen as well as most of the literature reports on methanol steam reforming. For the catalyst prepared by oxalate gel-coprecipitation, Cu particles are very fine and homogenously distributed in the catalyst, therefore, providing higher Cu surface area [78, 79, 120, 122, 138].

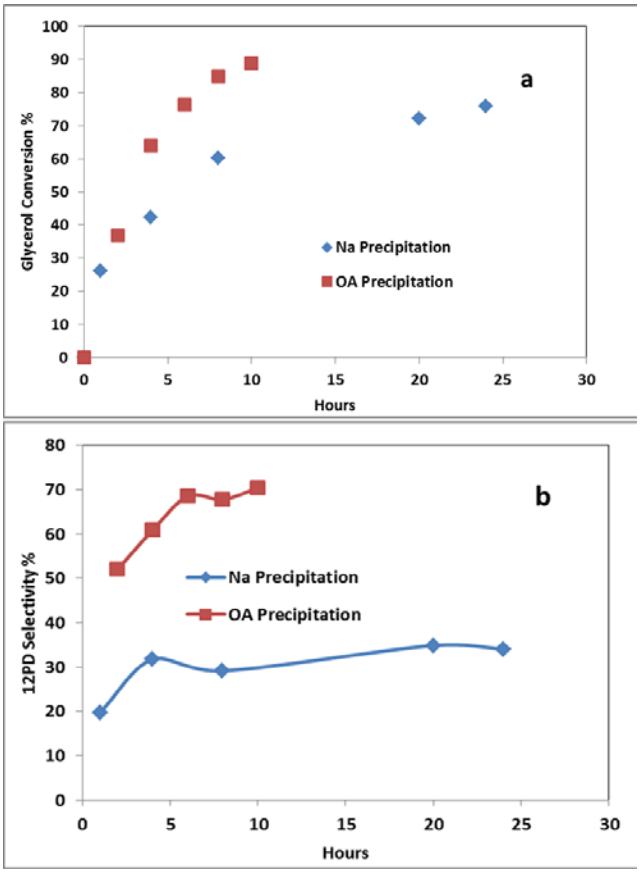

Figure 5-4 Comparison between Catalysts Prepared by Na Coprecipitation and OA Coprecipitation: a) Glycerol Conversion; b) 1,2PD Selectivity. Conditions: 220ºC, 15bar N_2, 20wt% Glycerol, Water/Methanol=1.2, 3wt% catalyst, 500RPM, Cu/Zn/Al=25/25/50.

It can be seen in Figure 5-4a that for the catalyst prepared by oxalate gel-coprecipitation, the glycerol conversion reaches 90% in 10 hours; however, the glycerol conversion only reaches 76% conversion after 24 hours using the catalyst prepared by Na_2CO_3 co-precipitation. This might be attributed to the fact that the catalyst prepared by the oxalate gel-coprecipitation method could provide more Cu sites, which are active for the glycerol hydrogenolysis reactions [143]. In Figure 5-4b, it can be seen that the 1,2PD selectivity using both catalysts increases slightly over the reaction time. This is possibly because at the beginning of the reaction, the hydrogen produced by methanol steam reforming is not sufficient to hydrogenate the acetol produced via glycerol dehydration. As the reactions proceed, the reaction rate of dehydration decreass due to a lower concentration of glycerol remaining in

the reaction mixture while more hydrogen is produced via methanol steam reforming, and the selectivity to 1,2PD therefore increases accordingly. The 1,2PD selectivity over the reaction time using the catalyst prepared by oxalate gel-coprecipitation is always higher than that by Na co-precipitation. One possible reason is that the catalyst by oxalate gel-coprecipitation method is reported to be more active for methanol steam reforming [138, 144-148] than the catalysts prepared by Na_2CO_3 coprecipitation, therefore, more hydrogen can be produced for acetol hydrogenation, and less by-products are formed. The other reason might be that more Cu active sites can facilitate the acetol hydrogenation, therefore acetol can be more rapidly hydrogenated resulting in a high 1,2PD selectivity.

5.1.2 Effect of Catalyst Reduction

For a $Cu/ZnO/Al_2O_3$ catalyst, metallic Cu^0 is reported to be the active site for glycerol hydrogenolysis reactions [106, 143, 149], therefore, the reduction process of the calcined catalyst prior the reaction becomes crucial. Two types of reduction reactors were used as shown in Figure 5-5. Figure 5-5a shows a semi batch reactor in which the catalysts sit at the bottom of the tube, hydrogen flows through a tube extented near the bottom of the tube and a vent valve is on the top of the tube; Figure 5-5b shows a fixed bed flow reactor in which the catalysts sit on a bed in the middle of the tube, and hydrogen flows in from the bottom of the tube and flows out from the top. To further compare the effect of the reactor type on the hydrogenolysis process, an un-reduced catalyst was also tested and the results are shown in Figure 5-6.

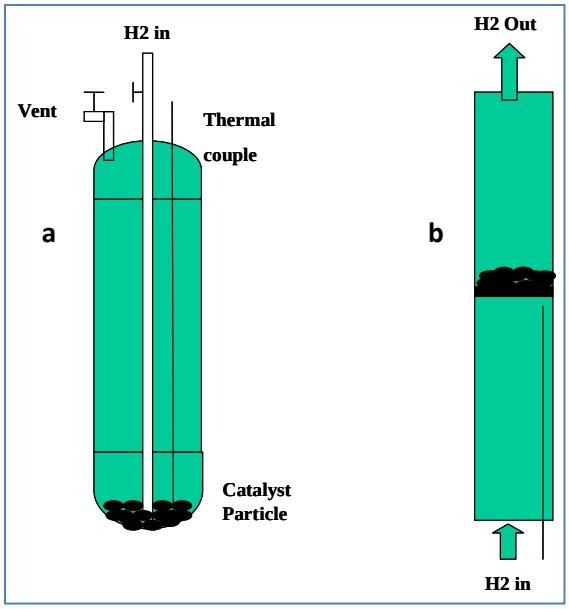

Figure 5-5 Reactors Used for Catalyst Reduction: a) Batch Reactor; b) Flow Reactor.

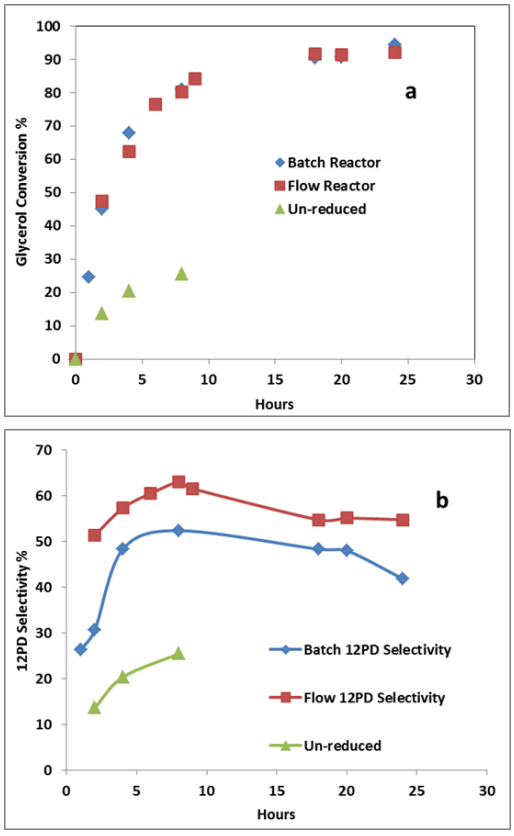

Figure 5-6 Effect of Catalyst Reduction: a) Glycerol Conversion; b) 1,2PD Selectivity. Conditions: 220ºC, 15bar N_2, 20wt% Glycerol, Water/Methanol=1.2, 3wt% catalyst, 500RPM, Cu/Zn/Al=25/25/50, OA Coprecipitation.

From Figure 5-6, it can be seen that, the 1,2PD selectivity using the catalyst reduced in a flow reactor (63.0%) is much higher than that in a batch reactor (52.4%). This indicates that the flow reactor can give a better reduction to provide more Cu^0 sites for methanol steam reforming and glycerol hydrogenolysis. It is also noticed that the glycerol conversions are similar for the catalysts reduced in both reactors; these results suggest that an inefficiently reduced catalyst also has an activity for glycerol dehydration. The results of an un-reduced catalyst as shown in Figure 5-6 also show glycerol conversion (25.4%), but the 1,2PD selectivity is very low (21.9%). Therefore, it appears that CuO also has some activity for glycerol dehydration. The by-product distribution is shown in Figure 5-7 as well as in Table 5-2.

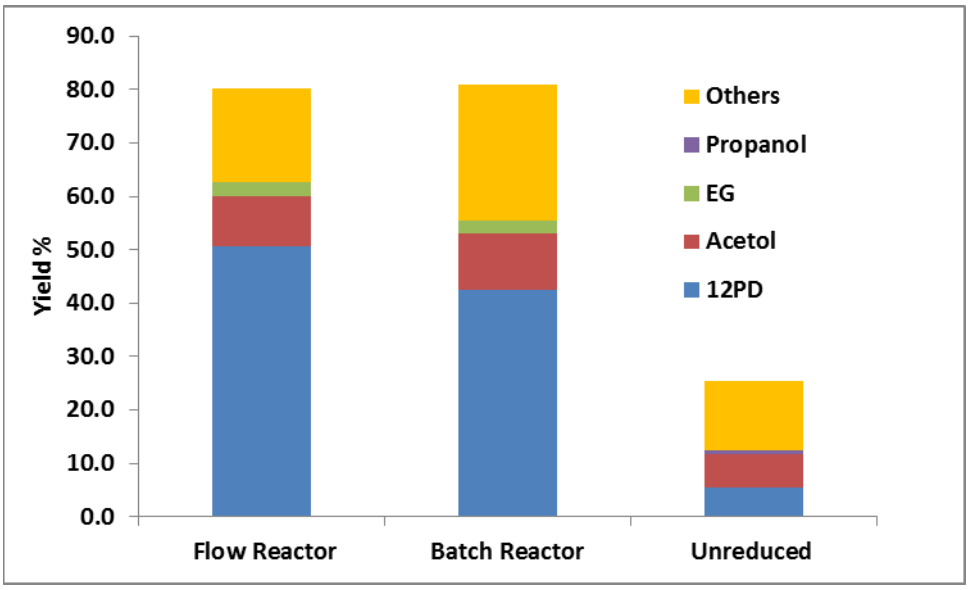

Figure 5-7 Effect of Catalyst Reduction on Product Distribution. Conditions: 220ºC, 15bar N_2, 20wt% Glycerol, Water/Methanol=1.2, 3wt% catalyst, 500RPM, $Cu/ZnO/Al_2O_3$ (Cu/Zn/Al=25/25/50) by oxalate gel-co-precipitation.

Table 5-2 Effect of Catalyst Reduction on Product Distribution[a].

	Glycerol Conversion	1,2PD Selectivity	1,2PD Yield	Acetol Yield	EG Yield	PrOH Yield	Others Yield
Flow Reactor	80.2	63.0	50.5	9.4	2.6	0.0	17.7
Batch Reactor	80.9	52.4	42.4	10.7	2.4	0.0	25.4
Unreduced	25.4	21.9	5.6	6.1	0.0	0.7	13.0

[a]Conditions: 220ºC, 15bar N_2, 20wt% Glycerol, Water/Methanol=1.2, 3wt% catalyst, 500RPM, Cu/ZnO/Al_2O_3 (Cu/Zn/Al=25/25/50) by oxalate gel-co-precipitation.

5.1.3 Study of Reaction Conditions (Temperature and Catalyst Loading)

In most of the literature reports about methanol steam reforming, the methanol conversion is always higher at higher temperature (150ºC to 300ºC) since this is an exothermic reaction. However, for glycerol hydrogenolysis, if the temperature is too high, the selectivity to 1,2PD is lower [28, 67]. The reasons for this are that if the temperature is too high, the 1,2PD will be degraded to lower alcohols and the rate of side reactions will also increase to form some un-desired by-products. The optimum temperature was reported to be between 200ºC and 240ºC. In this set of experiments, two temperatures were chosen which 200ºC were and 240ºC. Three different amounts of catalyst (1%, 2% and 3%) were used to investigate the effect of catalyst loading on the reaction products.

The glycerol conversion and 1,2PD selectivity over the reaction time at different temperatures are shown in Figure 5-8.

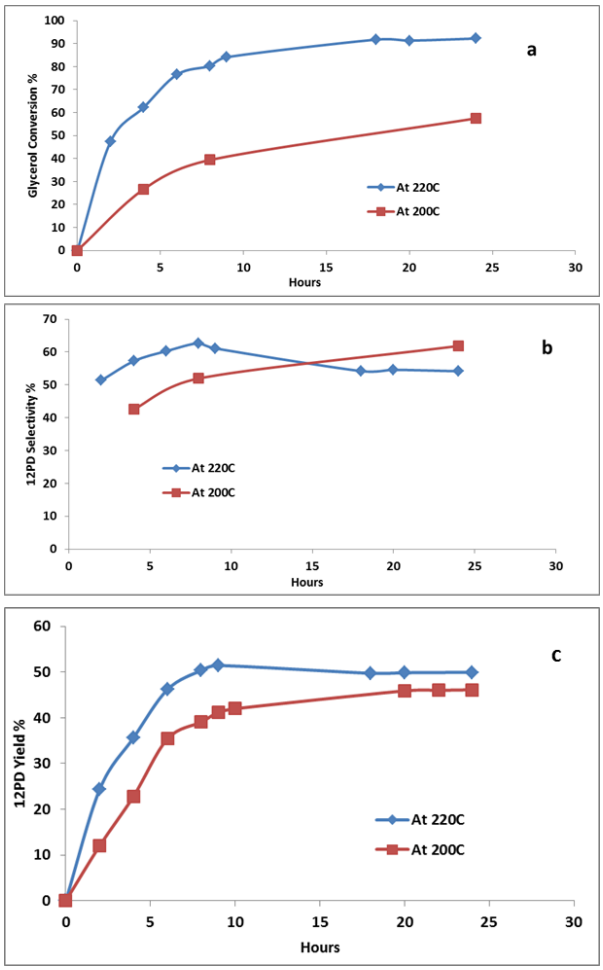

Figure 5-8 Effect of Temperature on: a) Glycerol Conversion; b) 1,2PD Selectivity; c) 1,2PD Yield. Conditions: 15bar N_2, 20wt% Glycerol, Water/Methanol=1.2, 3wt% catalyst, 500RPM, Cu/Zn/Al=45/45/10 oxalate gel-coprecipitation.

From Figure 5-8a, it can be seen that at high temperature (220ºC), the glycerol conversion is higher over the reaction time, but the 1,2PD selectivity is slightly lower than that when the temperature is lower (200ºC) (Figure 5-8b). The same behavior has been observed for glycerol hydrogenolysis via molecular hydrogen as reported in Chapter 4. At higher temperature, the solubility of hydrogen in the reaction mixture becomes lower, therefore, more by-products might be formed due to side reactions with acetol. It is found previously in Chapter 4 that the glycerol hydrogenolysis reaction is highly temperature dependent, so when the temperature is higher, the rate of glycerol dehydration would be increased and more

acetol is produced. Figure 5-8c shows the 1,2PD yield over the reaction time at different temperatures; since the glycerol conversion at 220ºC is significantly higher than that at 200ºC, the 1,2PD yield at 220ºC during the reaction is higher than that at 200ºC.

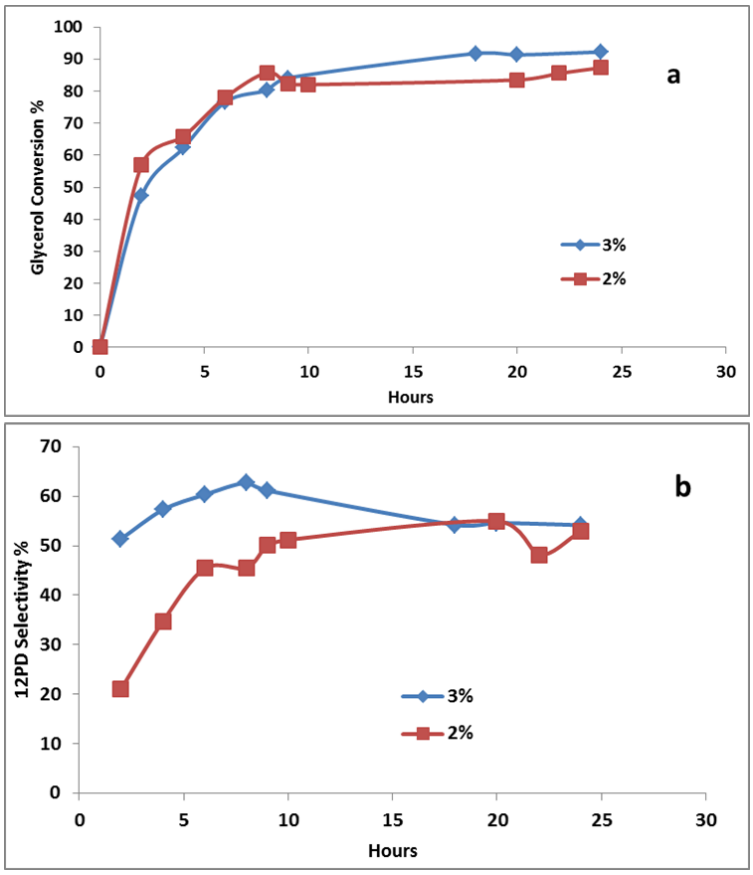

Figure 5-9 Effect of Catalyst Amount on: a) Glycerol Conversion; b) 1,2PD Selectivity. Conditions: 15bar N_2, 20wt% Glycerol, Water/Methanol=1.2, 220 ºC catalyst, 500RPM Cu/Zn/Al=45/45/10 OA co-precipitation.

Figure 5-9a shows that at 220ºC, when the catalyst amount is increased from 2wt% to 3wt%, the conversion of glycerol is increased from 87.3% to 92.2%. From Figure 5-9b, it can be seen that the selectivity to 1,2PD is slightly increased when the catalyst loading is increased from 2wt% to 3wt%. Detailed product distributions using different amounts of catalyst at different temperatures are shown in Table 5-3 and Figure 5-10.

Table 5-3 Effect of Catalyst Loading and Temperature on Product Distribution[a]

	Glycerol Conversion	1,2PD Selectivity	1,2PD Yield	Acetol Yield	EG Yield	PrOH Yield	Others Yield
3g 220˚C	92.2	54.2	49.9	5.0	2.8	1.1	33.4
2g 220˚C	87.3	52.9	46.1	4.3	3.3	1.0	33.6
1g 220˚C	71.5	48.6	34.7	4.7	2.8	1.1	28.2
3g 200˚C	57.5	61.9	35.5	5.8	1.8	1.3	12.9
2g 200˚C	45.6	64.0	29.2	5.5	1.6	0.0	9.3
1g 200˚C	31.7	55.8	17.7	7.4	0.0	0.0	6.6

[a]Conditions: 15bar N_2, 20wt% Glycerol, Water/Methanol=1.2, 500RPM, Cu/Zn/Al=45/45/50, oxalate gel-coprecipitation, 8 hours.

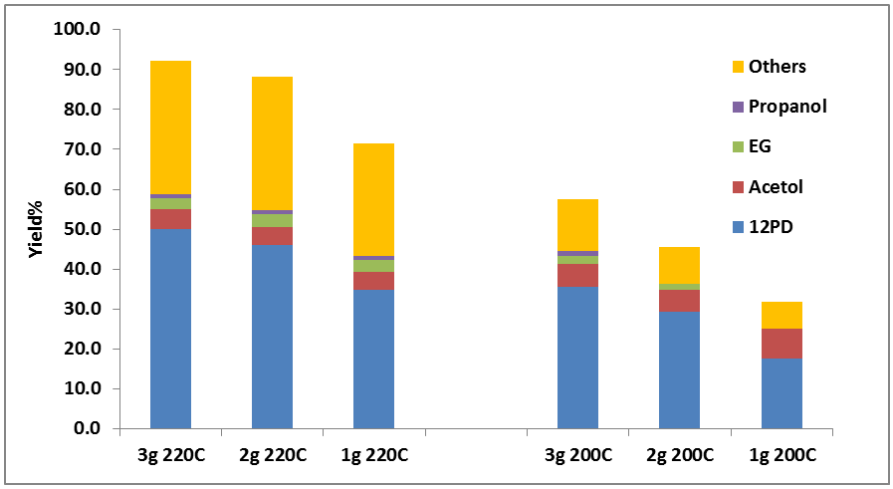

Figure 5-10 Effects of Catalyst Loading and Temperature on Product Distribution. Conditions: 15bar N_2, 20wt% Glycerol, Water/Methanol=1.2, 500RPM, Cu/Zn/Al=45/45/50, Oxalate gel-coprecipitation, 8 hours.

Figure 5-11 and Table 5-3 show the effect of catalyst loading and temperature on the reaction products. It can be seen that glycerol conversion is higher at higher temperature up to 220 ºC and when the catalyst loading is higher up to 3wt%. However, the selectivity to 1,2PD is slightly lower at 220 ºC than at 200 ºC and it is not affected by catalyst loading up to 3wt%. At high glycerol conversion, the yield of 1,2PD is still high at 220 ºC and 3wt% catalyst loading.

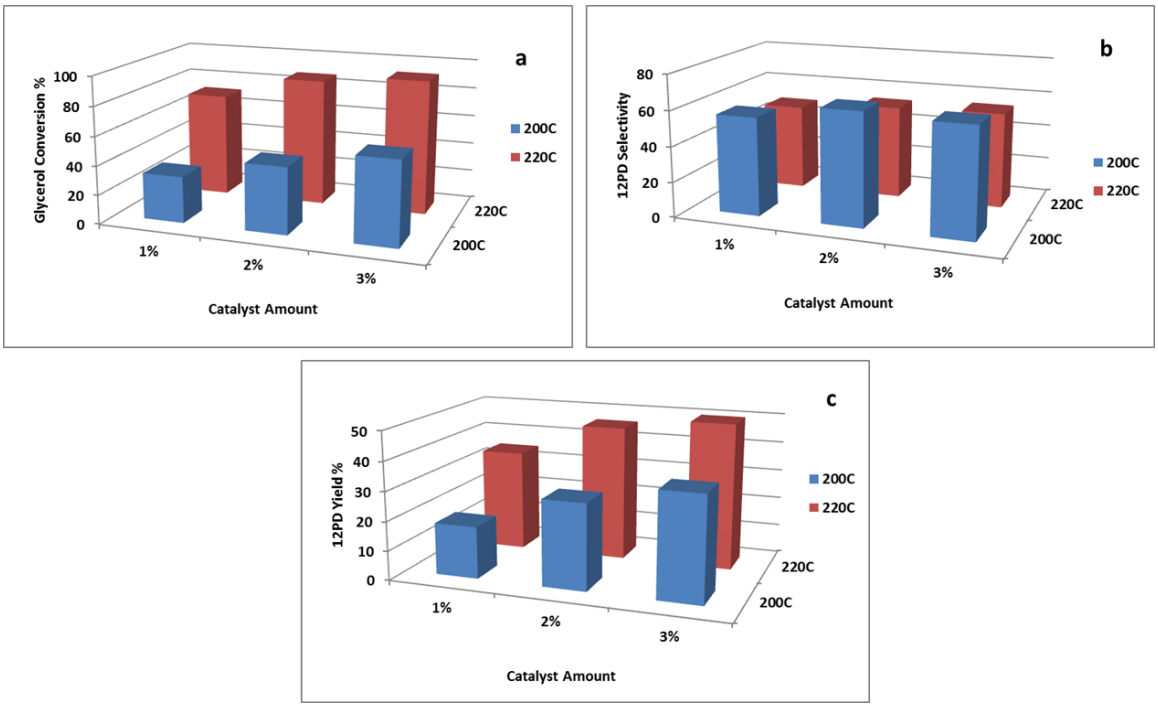

Figure 5-11 Effects of Catalyst Loading and Temperature on: a) Glycerol Conversion; b) 1,2PD Selectivity c) 1,2PD Yield. Conditions: 15bar N_2, 20wt% Glycerol, Water/Methanol=1.2, 500RPM, Cu/Zn/Al=45/45/10, OA co-precipitation, 8 hours.

5.1.4 Effect of Cu/Zn/Al Composition

For a $Cu/ZnO/Al_2O_3$ catalyst, the molar ratio of Cu/Zn is usually reported to be 1 for both methanol steam reforming [138, 146] and glycerol hdyrogenolysis [47, 67, 76]. In 2010, Wang *et al.* [76] specifically investigated the effect of Cu/Zn ratio; four ratios were examined (0.4/1, 1/1, 2/1 and no Zn), and the catalyst with a Cu/Zn molar ratio of 1:1 was shown to have the highest Cu surface area, therefore, giving the highest 1,2PD selectivity and fastest reaction rate. In this section, the ratio of Cu/Zn was kept at 1 and the effect of aluminum content was investigated. The experimental results are shown in Figure 5-12.

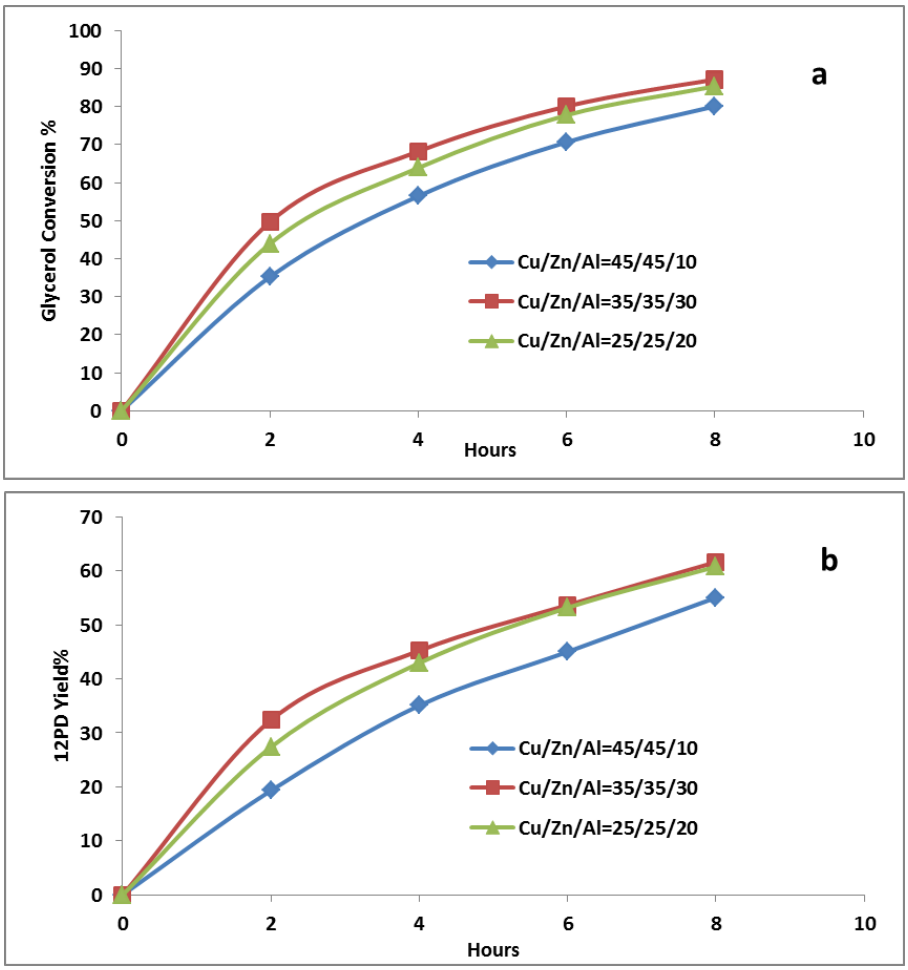

Figure 5-12 Effect of Aluminum Content on: a) Glycerol Conversion; b) 1,2PD Yield. Conditions: 220ºC, 15bar N_2, 20wt% Glycerol, Water/Methanol=1.2, 3wt% catalyst, 500RPM.

It can be seen from Figure 5-12 that when the aluminum molar content is increased from 10% to 30%, the glycerol conversion (Figure 5-12a) and the 1,2PD yield (Figure 5-12b) are significantly increased. However, if the aluminum molar content is further increased to 50%, the glycerol conversion and 1,2PD yield is slightly lower than when the aluminum molar content is 30%. The detailed products distributions are shown in Figure 5-13 as well as in Table 5-4.

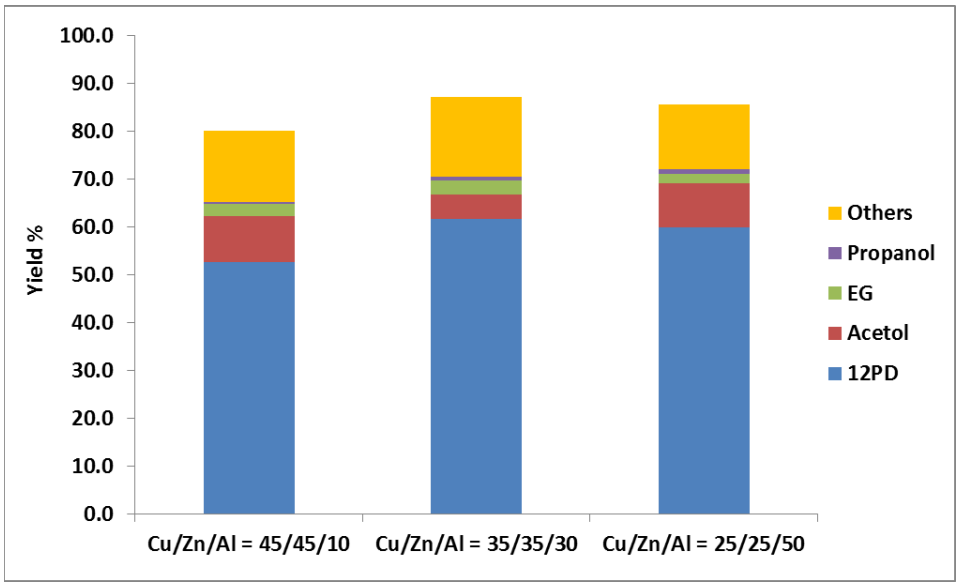

Figure 5-13 Effect of Aluminum Content on Products Distribution. Conditions: 220ºC, 15bar N_2, 20wt% Glycerol, Water/Methanol=1.2, 3wt% catalyst, 500RPM, 8 hours.

Table 5-4 Effect of Aluminum Molar Content on Products Distribution[a].

	Glycerol Conversion	1,2PD Selectivity	1,2PD Yield	Act Yield	EG Yield	PrOH Yield	Others Yield
Cu/Zn/Al = 45/45/10	80.2	65.7	52.7	9.5	2.6	0.5	14.9
Cu/Zn/Al = 35/35/30	87.1	70.7	61.6	5.2	2.9	0.7	16.7
Cu/Zn/Al = 25/25/50	85.7	69.9	59.9	9.2	2.0	0.9	13.7

[a]Conditions: 220ºC, 15bar N_2, 20wt% Glycerol, Water/Methanol=1.2, 3wt% catalyst, 500RPM, 8 hours.

Therefore, the catalyst with a Cu/Zn/Al molar ratio of 35/35/30 was chosen as the optimum ratio for further study. It has been reported that the presence of alumina improved the dispersion of Cu particles in the catalyst [79]. Also the presence of alumina was reported to be able to significantly prevent Cu/ZnO catalyst deactivation by isolating the individual metal particles to prevent sintering [80, 134, 150]. Ga_2O_3, ZrO_2 and Al_2O_3 are most frequently reported to be added to the supported Cu/ZnO catalyst. Considering the economics of this process, Al_2O_3 is a very good choice since it is much cheaper.

5.2 Study of Ni as a Promoter for the $Cu/ZnO/Al_2O_3$ Catalyst

Nickel (Ni) based catalysts are normally useful catalysts for hydrogenation and they are less costly compared to precious metal hydrogenation catalysts such as platinum, palladium and ruthenium; it is also often used as a catalyst in various hydrocarbon reforming processes. It has been reported to be used for both glycerol hydrogenolysis [55, 151-154] and methanol steam reforming [155-159]. In this section, the promotion effect of Ni addition on glycerol hydrogenolysis using *in situ* hydrogen produced by methanol steam reforming is reported.

5.2.1 Effect of Ni and $Ni/Cu/ZnO/Al_2O_3$: Composition Study

$Ni/Cu/ZnO/Al_2O_3$ catalysts were prepared by oxalate gel-coprecipitation method as described in Section 3.1.1. The aluminum molar content was kept at 30% and the molar ratio of Cu/Zn was kept at 1. Four different Ni loadings (molar%), i.e. 0, 1, 3 and 5, were tested to study the effect of Ni on the reaction products. The experimental results are shown in Figure 5-14.

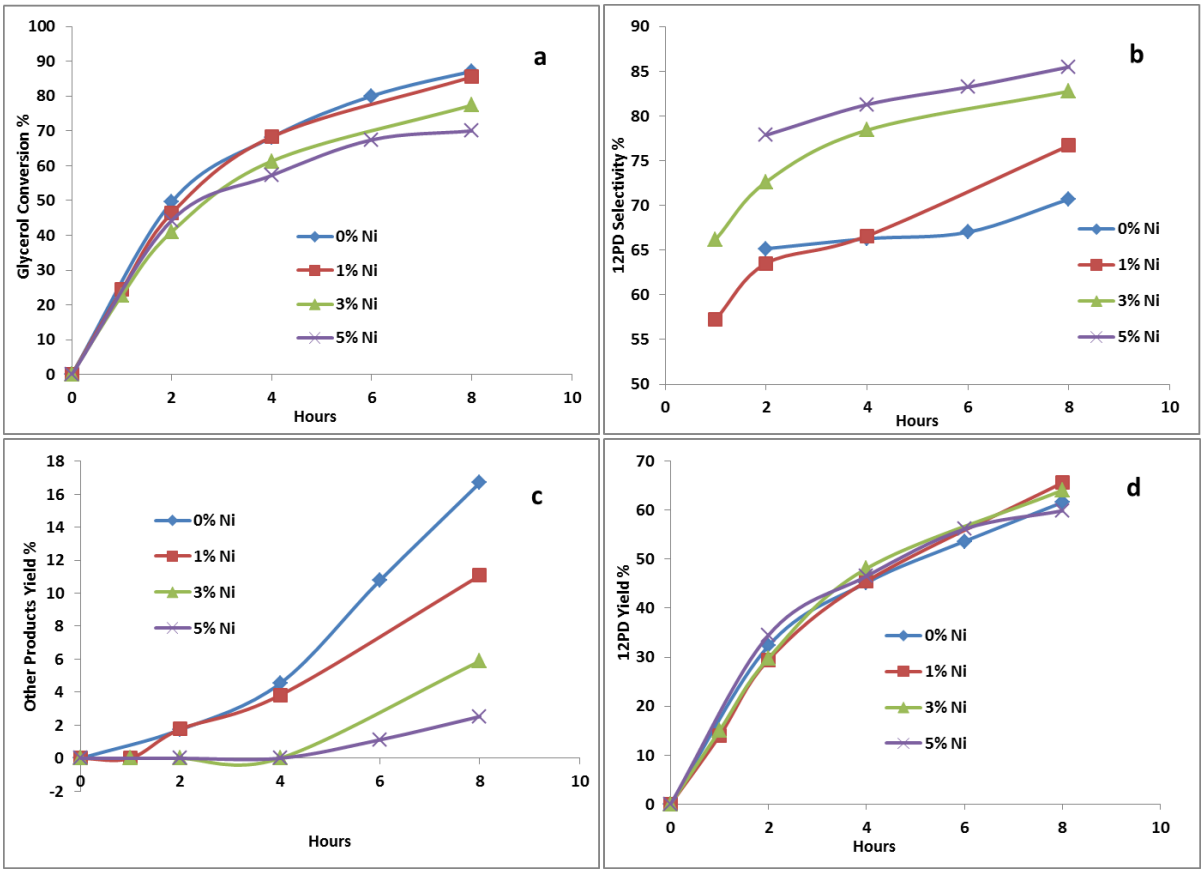

Figure 5-14 Effect of Ni Content on: a) Glycerol Conversion; b) 1,2PD Selectivity; c) Others Yield; d) 1,2PD Yield. Conditions: 220ºC, 15bar N_2, 20wt% Glycerol, Water/Methanol=1.2, 3wt% catalyst, 500RPM, 30mole% Al content, Cu/Zn=1.

From 5-14a, it can be seen that by adding Ni to the Cu/ZnO/Al_2O_3 catalyst, the glycerol conversion during the reaction time is lower compared with that without added Ni; the higher the amount of Ni loaded, the lower the glycerol conversion becomes. This might be because as Ni is loaded, the amount of strong acidic sites are reduced resulting in some loss of activity for the glycerol dehydration process. A detailed explanation will be provided in the NH_3 TPD analysis provided in Section 6.1. However, from Figure 5-14b, it can be seen that the selectivity to 1,2PD is increased as the amount of Ni loaded is increased. This is due to the improved hydrogenation activity provided by Ni addition as discussed in Section 4.8. Without Ni loading, the yield of by-products grows much faster than with Ni loading as

shown in Figure 5-14c and becomes 16.7% at the end of the reaction (8^{th}. hour). As the molar content of Ni is increased from 1% to 5%, the yield of other by-products over the reaction time becomes lower. When the Ni loading is 5mole%, the yield of other by-products is only 2.5% at the end of the reaction. Since the high selectivity to 1,2PD on Ni addition, even though the glycerol conversion is lower, the yields of 1,2PD for these four catalysts are not much different as shown in Figure 5-14d. Detailed product distributions for these four catalysts are shown in Figure 5-15 and Table 5-5. The catalyst with 1mole% Ni gives the highest 1,2PD yield which is about 65.6%; without added Ni the 1,2PD yield is 61.6%. With 5mole% Ni added, the yield of 1,2PD is slightly lower, being about 60%; however, the selectivity to 1,2PD is very high and the yield of other by-products is only 2.5%.

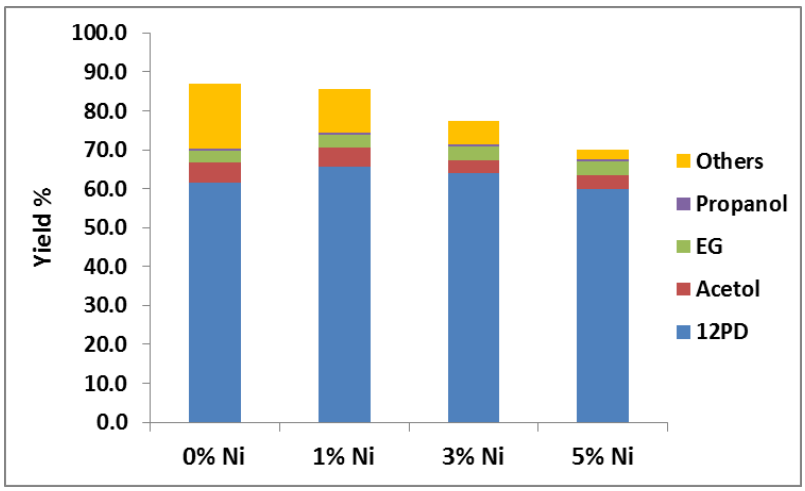

Figure 5-15 Effect of Ni Content on Products Distributions. Conditions: 220 ºC, 15bar N_2, 20wt% Glycerol, Water/Methanol=1.2, 3wt% catalyst, 500RPM, 30mole% Al content, Cu/Zn=1, 8hours.

Table 5-5 Effect of Ni Molar Content on Product Distributions[a]

	Glycerol Conversion	1,2PD Selectivity	1,2PD Yield	Act Yield	EG Yield	PrOH Yield	Others Yield
0% Ni	87.1	70.7	61.6	5.2	2.9	0.7	16.7
1% Ni	85.5	76.7	65.6	4.9	3.4	0.6	11.1
3% Ni	77.4	82.8	64.1	3.3	3.6	0.5	5.9
5% Ni	70.0	85.5	59.9	3.5	3.5	0.6	2.5

[a]Conditions: 220 ºC, 15bar N_2, 20wt% Glycerol, Water/Methanol=1.2, 3wt% catalyst, 500RPM, 30mole% Al content, Cu/Zn=1, 8hours.

It has been discussed in Chapter 4 that the 1,2PD selectivity is strongly dependent on hydrogen pressure since the major by-products are due to side reactions with acetol [99]. Therefore, one reason why Ni can improve the 1,2PD selectivity might be due to the improved activity for the methanol steam reforming reaction to produce more hydrogen. In order to study the effect of Ni on methanol steam reforming, experiments have been carried out without taking any sample during the reaction for 24 hours. The initial mass of methanol fed was weighed and recorded as m_{in}, and the final mass of methanol left over in the products was analyzed by GC and recorded as m_f, and the methanol conversion can then be calculated using Equation 5-2.

$$Conversion = \frac{m_i - m_f}{m_i} \times 100\% \qquad \textbf{Equation 5-2}$$

It has also been reported that Ni can be used for glycerol steam reforming to produce hydrogen [160-162]. Since in this set of experiments, no samples were taken during the reaction, the glycerol mass balance was also calculated using Equation 5-3.

$$Glycerol\_Balance = \frac{\sum mol(carbonaceous\_products + glycerol_f)}{mol(glycerol_i)} \times 100\% \qquad \textbf{Equation 5-3}$$

The experimental results are shown in Figure 5-16 and Table 5-6.

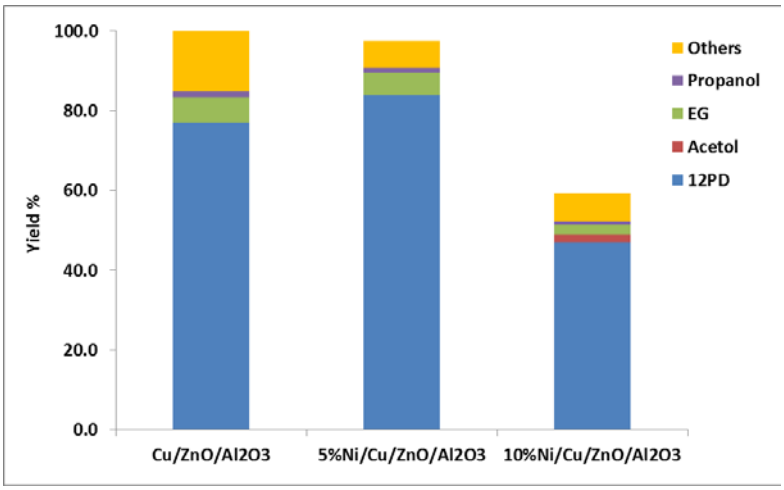

Figure 5-16 Effect of Ni Content on Products Distributions (No sample was taken during the reaction time). Conditions: 220 ºC, 15bar N_2, 20wt% Glycerol, Water/Methanol=1.2, 3wt% catalyst, 500RPM, 30mole% Al content, Cu/Zn=1, 24hours.

Table 5-6 Effect of Ni Content on Products Distributions and Mass Balance[a].

	Glycerol Conversion	1,2PD Selectivity	1,2PD Yield	Acetol Yield	EG Yield	PrOH Yield	Others Yield	Methanol Conversion	Mass Balance
$Cu/ZnO/Al_2O_3$	100.0	77.0	77.0	0.0	6.4	1.6	15.1	17.7	96.5
$5\%Ni/Cu/ZnO/Al_2O_3$	97.4	86.0	83.8	0.0	5.8	1.2	6.7	21.6	100.4
$10\%Ni/Cu/ZnO/Al_2O_3$	59.4	78.9	46.9	2.1	2.5	0.7	7.2	22.6	99.8

[a]Conditions: 220ºC, 15bar N_2, 20wt% Glycerol, Water/Methanol=1.2, 3wt% catalyst, 500RPM, 30mole% Al content, Cu/Zn=1, 24hours.

From Table 5-6, it can be seen that with 5mole% Ni added onto the $Cu/ZnO/Al_2O_3$ catalyst, the methanol conversion is increased from 17.7% to 21.6% compared with that without Ni added. When Ni loading is further increased from 5mole% to 10mole%, the methanol conversion is slightly increased from 21.6% to 22.6%; however, the glycerol conversion is significantly decreased from 97.4% to 59.4% as shown in Figure 5-16. Therefore, the addition of Ni can improve methanol conversion to produce more hydrogen to hydrogenate the acetol; hence the 1,2PD selectivity is improved. From the calculated glycerol mass balance shown in Table 5-6, it is found that the glycerol balance for all the three experiments

are closed to 100% (the deviation might be due to some experimental error). This suggests that glycerol is not consumed by the steam reforming reaction under the current reaction conditions. The chromatograms of the final samples obtained from the reaction with the $Cu/ZnO/Al_2O_3$ catalyst and with 10mole% Ni added are compared as shown in Figure 5-17.

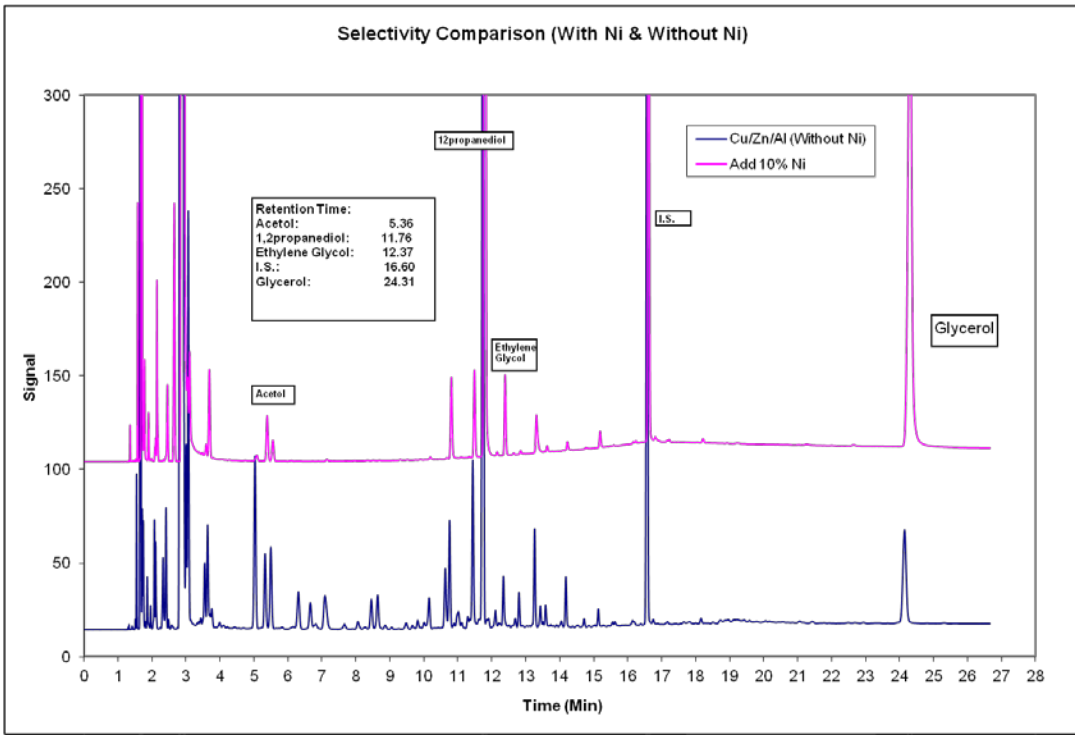

Figure 5-17 Chromatograms of the Final Sample of: (Blue) $Cu/ZnO/Al_2O_3$ catalyst, (Pink) $Ni/Cu/ZnO/Al_2O_3$ catalyst.

From the GC results shown in Figure 5-17, it can be seen that with Ni added, the signal is much less complex compared with the one without Ni added showing that much less by-products are formed. The retention times of all the products for these two samples match each other very well suggesting that the addition of Ni does not cause formation of any new by-product.

It has been discussed in Chapter 4 that the loading of Ni will inhibit the glycerol dehydration process. Since it has been reported that Cu is active for glycerol dehydration [106, 143, 149], a $Ni/ZnO/Al_2O_3$ catalyst without Cu loading was used to study the effect of Cu on the

glycerol hydrogenolysis process. The experimental results are shown in Figure 5-18 and Table 5-7.

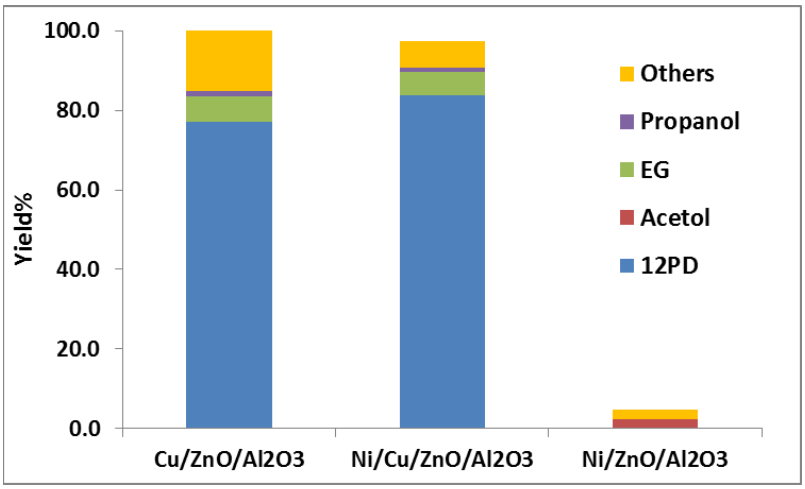

Figure 5-18 Effect of Ni and Cu on Products Distributions. Conditions: 220 ºC, 15bar N_2, 20wt% Glycerol, Water/Methanol=1.2, 3wt% catalyst, 500RPM, Cu/Zn/Al=35/35/30, Ni/Cu/Zn/Al=5/32.5/32.5/30, Ni/Zn/Al=10/60/30, 24 hours.

Table 5-7 Effect of Ni Content on Products Distributions[a]

	Glycerol Conversion	1,2PD Selectivity	1,2PD Yield	Acetol Yield	EG Yield	PrOH Yield	Others Yield	Methanol Conversion	mass balance
$Cu/ZnO/Al_2O_3$	100.0	77.0	77.0	0.0	6.4	1.6	15.1	17.7	96.5
$Ni/Cu/ZnO/Al_2O_3$	97.4	86.0	83.8	0.0	5.8	1.2	6.7	21.6	100.4
$Ni/ZnO/Al_2O_3$	4.8	0.0	0.0	2.3	0.0	0.0	2.5	23.3	94.6

[a]Conditions: 220 ºC, 15bar N_2, 20wt% Glycerol, Water/Methanol=1.2, 3wt% catalyst, 500RPM, Cu/Zn/Al=35/35/30, Ni/Cu/Zn/Al=5/32.5/32.5/30, Ni/Zn/Al=10/60/30, 24 hours.

From Figure 5-18 as well as Table 5-7, it can be seen that without Cu added, the $Ni/ZnO/Al_2O_3$ catalyst is completely inactive for the reaction. However, the methanol conversion for the methanol steam reforming reaction is 23.3%. Therefore, it can be understood that when Ni is added to the $Cu/ZnO/Al_2O_3$ catalyst by co-precipitation, the glycerol conversion is lowered because Ni is not active for the glycerol dehydration step.

Because of its activity for methanol steam reforming and acetol hydrogenation, the 1,2PD selectivity is increased when Ni is added.

Figure 5-19 shows the activity of the Ni/Cu/ZnO/Al_2O_3 catalyst with different metal composition. It can be more clearly seen that as the Ni content is increased, the glycerol conversion decreases (Figure 5-19a), however, the 1,2PD selectivity is increased (Figure 5-19b). The yields of 1,2PD are the highest when the aluminum molar content is 30% with the Ni molar content between 1% and 3% (Figure 5-19c). The numerical data is shown in Table B-1 in Appendix B.

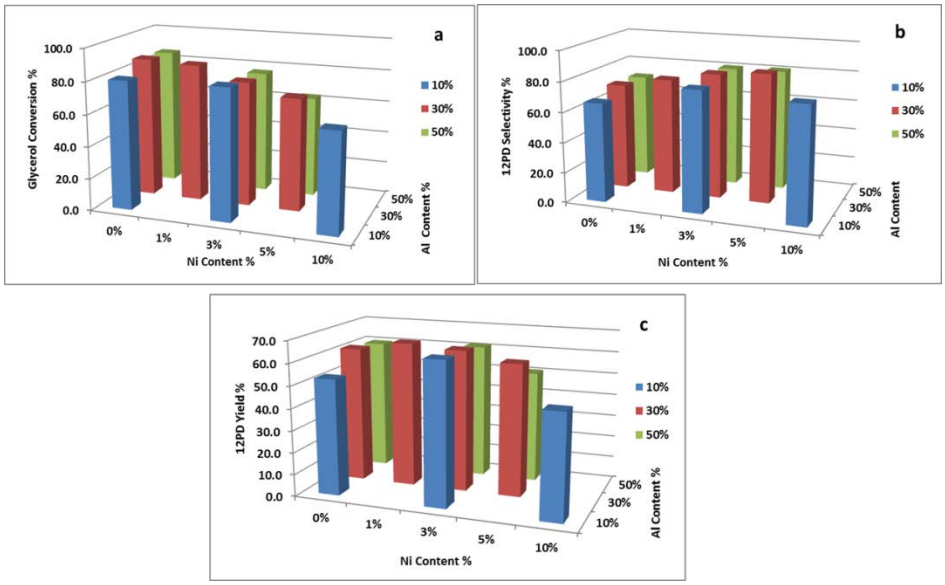

Figure 5-19 Ni/Cu/Zn/Al Composition Study: a) Glycerol Conversion; b) 1,2PD Selectivity; c) 12PD Yield. Conditions: 220ºC, 15bar N_2, 20wt% Glycerol, Water/Methanol=1.2, 3wt% catalyst, 500RPM, 8 Hours.

5.2.2 The activity of a Cu/ZnO/Al_2O_3 Catalyst Physically Mixed with Ni

It has been previously discussed that the glycerol hydrogenolysis reaction rate is lowered by Ni addition via the coprecipitation preparation method. An experiment with the Cu/ZnO/Al_2O_3 catalyst physically mixed with Ni was carried out to investigate the effect of Ni interactions with the Cu/ZnO/Al_2O_3 catalyst. In the reaction, 5mole% NiO was mixed

with the $Cu/ZnO/Al_2O_3$ catalyst (Cu/Zn/Al = 35/35/30). The particle mixture was reduced at 300 ºC before reaction, and the experimental results are shown in Figure 5-20.

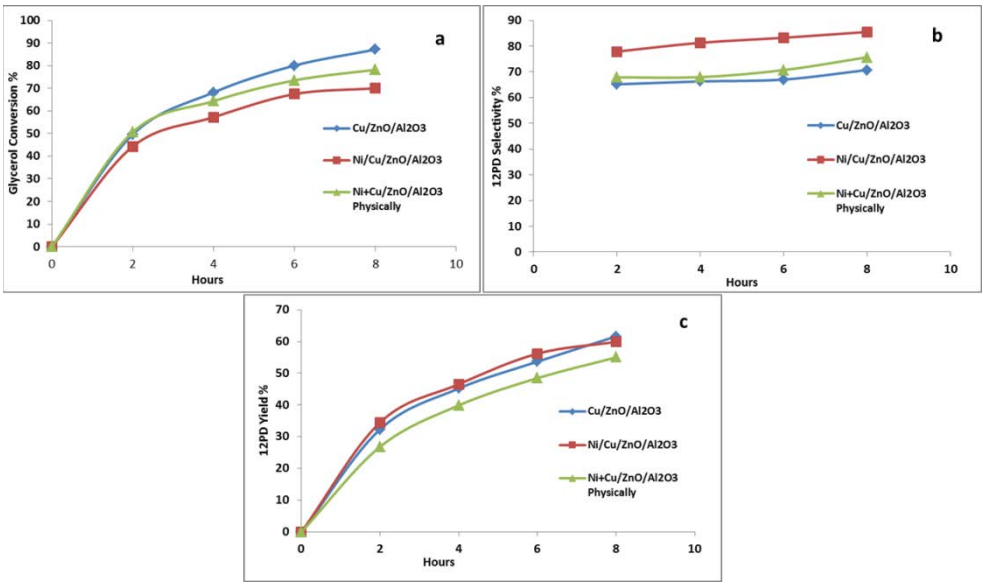

Figure 5-20 $Cu/ZnO/Al_2O_3$ Catalyst Physically Mixed with Ni: a) Glycerol Conversion; b) 1,2PD Selectivity; c) 1,2PD Yield. Conditions: 220 ºC, 15bar N_2, 20wt% Glycerol, Water/Methanol=1.2, 3wt% catalyst, 500RPM.

From Figure 5-20, it can be seen that when Ni is physically mixed with $Cu/ZnO/Al_2O_3$, the glycerol conversion is improved compared with the $Ni/Cu/ZnO/Al_2O_3$ catalyst prepared via a coprecipitation method; however, it is still lower than the glycerol conversion when using the $Cu/ZnO/Al_2O_3$ catalyst as shown in Figure 5-20a. The selectivity to 1,2PD is slightly higher compared with the $Cu/ZnO/Al_2O_3$ catalyst, but much lower than that using the $Ni/Cu/ZnO/Al_2O_3$ catalyst prepared via coprecipitation as shown in Figure 5-20b. This suggests that the glycerol dehydration step is also inhibited by the physical addition of Ni. Therefore, the yield of this catalyst is the lowest compared with the other two catalysts. Detailed product distributions using these three catalysts are shown in Table 5-8.

Table 5-8 Products Distributions by Physically Mixing Ni with $Cu/ZnO/Al_2O_3$ Catalyst[a].

	Glycerol Conversion	1,2PD Selectivity	1,2PD Yield	Acetol Yield	EG Yield	PrOH Yield	Others Yield
$Cu/ZnO/Al_2O_3$	87.1	70.7	61.6	5.2	2.9	0.7	16.7
$Ni/Cu/ZnO/Al_2O_3$	70.0	85.5	59.9	3.5	3.5	0.6	2.5
$Ni+Cu/ZnO/Al_2O_3$ Physically	78.2	75.7	59.2	5.2	3.1	0.6	10.1

[a]Conditions: 220 ºC, 15bar N_2, 20wt% Glycerol, Water/Methanol=1.2, 3wt% catalyst, 8 hours, 500RPM.

It has been reported in Section 5.1.2 that the reduction of the $Cu/ZnO/Al_2O_3$ catalyst plays an important role on the catalytic activity. To study the effect of the reduction on a $Ni/Cn/ZnO/Al_2O_3$ catalyst temperature programmed reduction experiments were carried out to find out the optimal reduction temperature. The experimental results are shown in Figure 5-21. More detailed analysis is provided in the TPR analysis provided in Section 6.2.

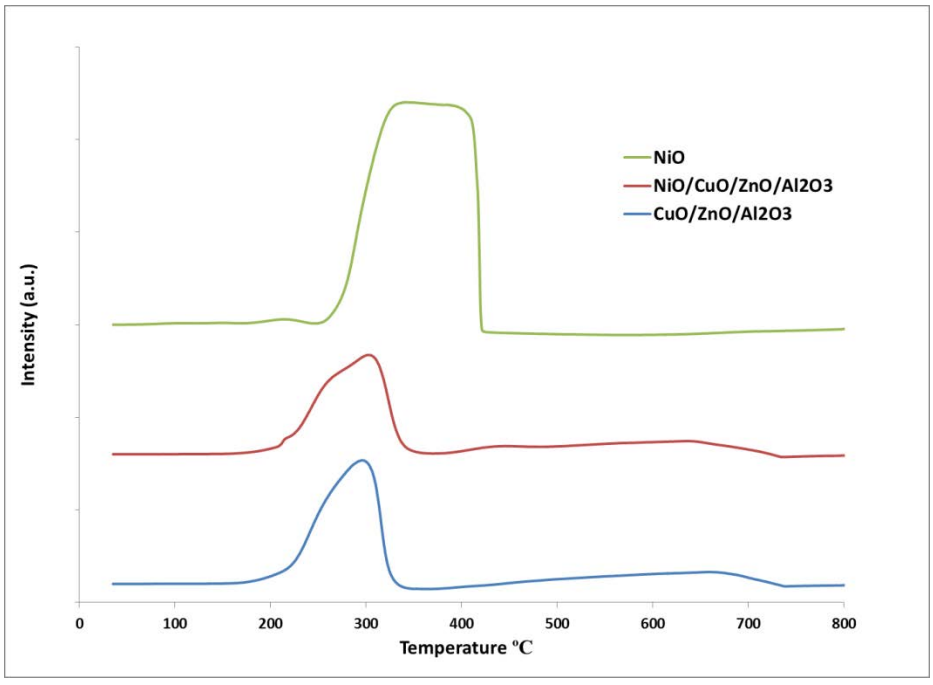

Figure 5-21 TPR Profile for $NiO/CuO/ZnO/Al_2O_3$, $CuO/ZnO/Al_2O_3$ and NiO: Ni/Cu/Zn/Al=5/32.5/32.5/30, Cu/Zn/Al=35/35/30.

From Figure 5-21, it can be seen that the reduction peaks for the $CuO/ZnO/Al_2O_3$ catalyst and $NiO/CuO/ZnO/Al_2O_3$ catalyst prepared by oxalate gel-coprecipitation are almost at the same temperature (255 ºC) and only one peak is found for the $NiO/CuO/ZnO/Al_2O_3$ catalyst. For NiO, the reduction started at 250ºC and a peak occurred at 330ºC, which is much higher than for the $NiO/CuO/ZnO/Al_2O_3$ catalyst prepared by oxalate gel-coprecipitation. This indicates that NiO and CuO are well mixed when using the coprecipitation method, which can facilitate catalyst reduction at a significantly lower temperature. Since the reduction peak for NiO occurred at a higher temperature than for the $NiO/CuO/ZnO/Al_2O_3$ catalyst, a reaction using a reduction temperature of 360ºC was carried out for the $CuO/ZnO/Al_2O_3$ catalyst physically mixed with NiO. The experimental results are shown in Figure 5-22.

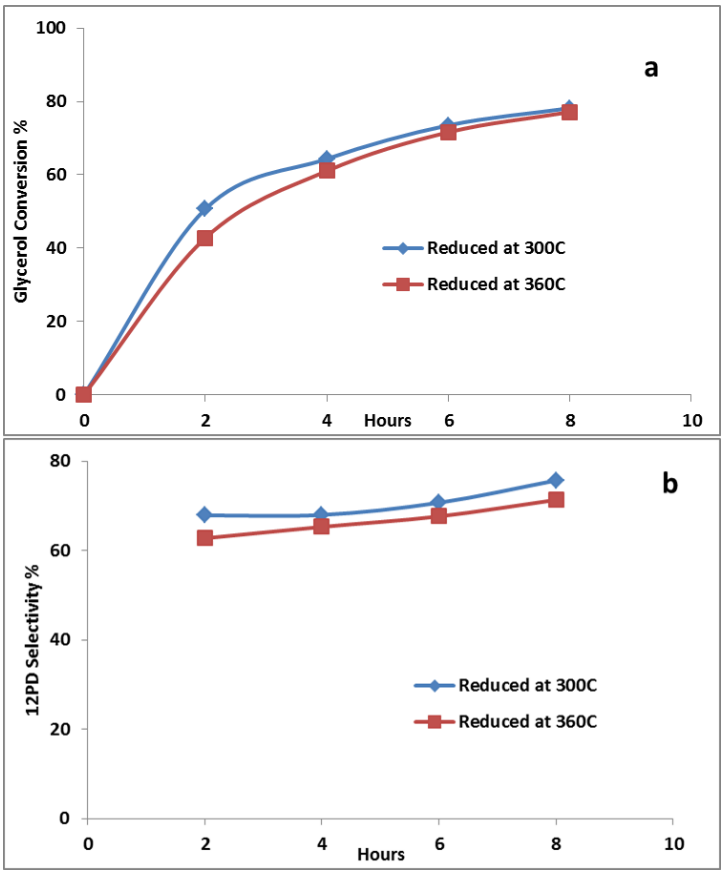

Figure 5-22 Effect of Reduction Temperature on: a) Glycerol Conversion; b) 1,2PD Selectivity. Conditions: 220ºC, 15bar N_2, 20wt% Glycerol, Water/Methanol=1.2, 3wt% catalyst, 500RPM, Catalyst: 5wt% Ni Physically Mixed with $Cu/ZnO/Al_2O_3$.

It can be seen from Figure 5-22a that the glycerol conversions are not significantly changed by increasing the reduction temperature from 300ºC to 360ºC. Figure 5-21b shows that the selectivity to 1,2PD using the catalysts at these two reduction temperatures are also similar. The 1,2PD selectivity for the reduction temperature of 300ºC is even slightly higher than that at 360ºC. It appears that the $Cu/ZnO/Al_2O_3$ catalyst physically mixed with Ni can be reduced efficiently at 300 ºC. The slightly higher 1,2PD selectivity at the lower reduction temperature is possibly due to experimental error or possibly catalyst sintering occurs at the higher reduction temperature.

5.3 $Cu/MgO/Al_2O_3$ Catalyst

Recently, magnesium based catalysts have been frequently reported to be active for glycerol hydrogenolysis [64, 81-83]. A $Cu/Mg/Al_2O_3$ catalyst has also been used for methanol steam reforming [163, 164]. In this section, the reactivity of a $Cu/MgO/Al_2O_3$ catalyst will be investigated and the effect of Pd and Ni as promoters will be discussed.

5.3.1 Catalysts Screening

Cu, Zn, Al, Mg, Zr, and La have all been reported to be active for glycerol hydrogenolysis. In this section, catalysts with different combinations of these metals have been prepared by the oxalate gel-coprecipitation method and investigated to identify the most active catalyst. The combinations are shown in Table 5-9, and the experimental results are shown in Figure 5-23.

Table 5-9 Catalysts Screening: Different Metal Combinations.

Catalyst #	Combination	Molar Ratio	Ref.
1	Cu/Zn/Zr	45/45/10	[165, 166]
2	Cu/Zr/Al	52.5/17.5/30	[145, 166]
3	Cu/Mg/Al	35/35/30	[64, 81]
4	Cu/Zn/Al	35/35/30	[47, 138]
5	Cu/La/Al	20/50/30	

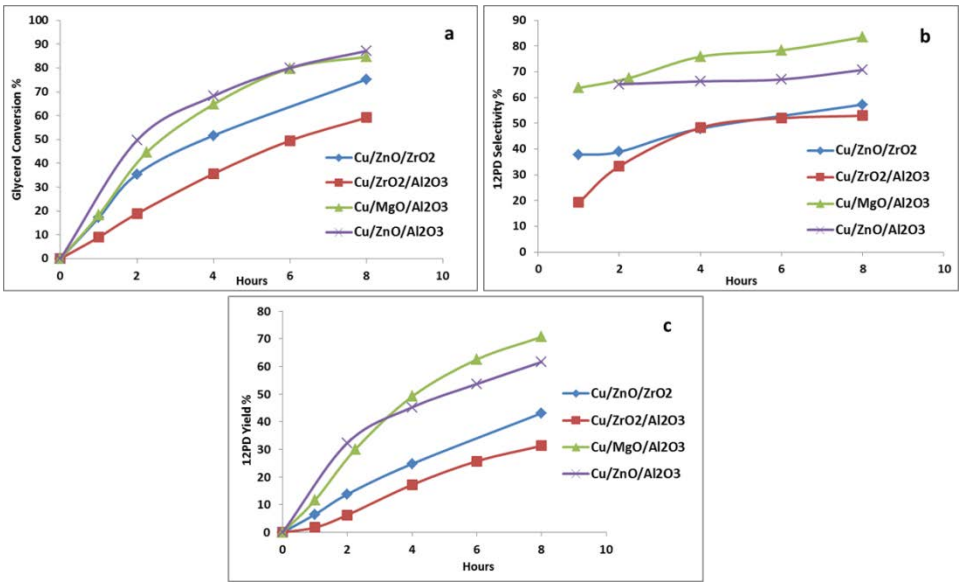

Figure 5-23 Different Metal Combinations: a) Glycerol Conversion; b) 1,2PD Selectivity; c) 1,2PD Yield. Conditions: 220 ºC, 15bar N_2, 20wt% Glycerol, Water/Methanol=1.2, 3wt% catalyst, 500RPM, 8 hours.

It can be seen that the Cu/MgO/Al_2O_3 and Cu/ZnO/Al_2O_3 catalysts show similar glycerol conversions, which are much higher than those of the Cu/ZnO/ZrO_2 and Cu/ZrO_2/Al_2O_3 catalysts (Figure 5-23a). Cu/MgO/Al_2O_3 shows distinctly higher selectivity to 1,2PD compared with the other three catalysts as shown in Figure 5-23b. Therefore, the yield of 1,2PD using the Cu/MgO/Al_2O_3 catalyst is the highest among all the catalysts. The high selectivity for the Cu/MgO/Al_2O_3 catalyst compared with other metal selections also results in a lower yield of other by-products as shown in Figure 5-24 and Table 5-10.

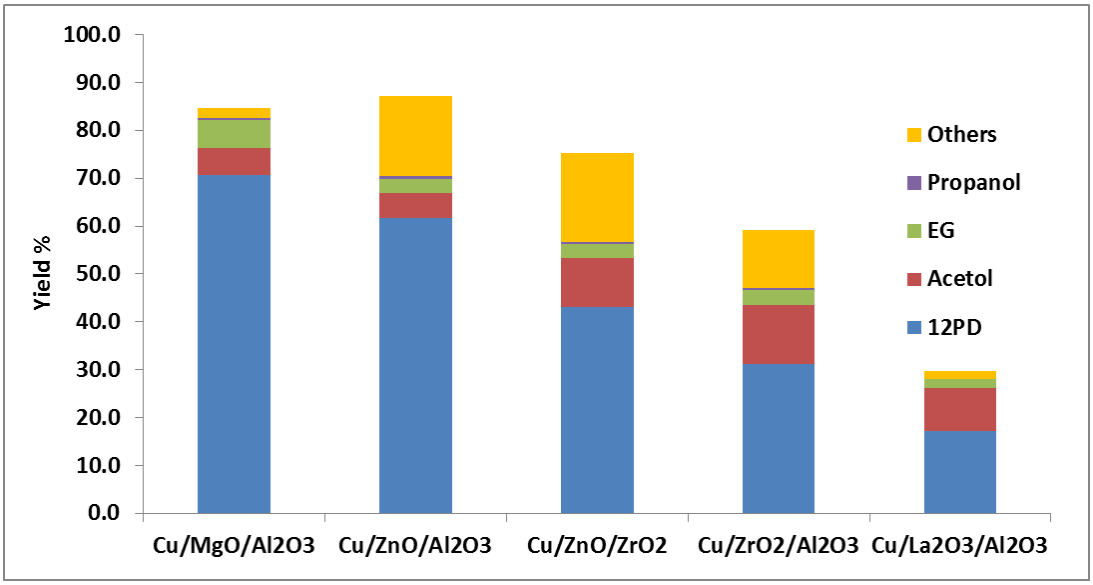

Figure 5-24 Products Distributions for the Catalysts with Different Metal Combinations. Conditions: 220 ºC, 15bar N_2, 20wt% Glycerol, Water/Methanol=1.2, 3wt% catalyst, 500RPM, 8 hours.

Table 5-10 Product Distributions for the Catalysts with Different Metal Combinations[a]

	Glycerol Conversion	1,2PD Selectivity	1,2PD Yield	Acetol Yield	EG Yield	PrOH Yield	Others Yield
$Cu/MgO/Al_2O_3$	84.7	83.4	70.7	5.6	5.9	0.4	2.2
$Cu/ZnO/Al_2O_3$	87.1	70.7	61.6	5.2	2.9	0.7	16.7
$Cu/ZnO/ZrO_2$	75.2	57.3	43.1	10.3	2.8	0.5	18.5
$Cu/ZrO_2/Al_2O_3$	59.1	52.9	31.3	12.2	3.1	0.5	12.1
$Cu/La_2O_3/Al_2O_3$	29.7	58.0	17.2	8.9	1.8	0.0	1.7

[a]Conditions: 220 ºC, 15bar N_2, 20wt% Glycerol, Water/Methanol=1.2, 3wt% catalyst, 500RPM, 8 hours.

It can be seen that by using the $Cu/MgO/Al_2O_3$ catalyst, the yield of other by-products is only 2.2% which is noticeably lower than for the other catalysts. However, the ethylene glycol yield is higher being about 6%. Table 5-10 also shows that $Cu/La_2O_3/Al_2O_3$ does not exhibit a very high activity.

5.3.2 Effect of Cu/Mg/Al Composition.

Since it has been discussed that the Cu/MgO/Al_2O_3 catalyst shows promising activity for glycerol hydrogenolysis using *in situ* hydrogen produced from methanol steam reforming, the composition of Cu/Mg/Al has been optimized. A 3x3 factorial design was carried out. Three Cu/Zn molar ratios (1/1, 1/3 and 1/5) and three alumina molar content (0%, 10% and 30%) have been picked for the optimization study of the compositions as shown in Table 5-11. The experimental results are shown in Figure 5-25 and Table 5-12**.**

Table 5-11 Composition Study of Cu/MgO/Al_2O_3 Catalysts.

	Aluminum Content %		
Cu/Mg	0%	10%	30%
1/1	1/1	45/45/10	35/35/30
1/3	1/3	22.5/67.5/10	17.5/52.5/30
1/5	1/5	15/75/10	11.7/58.3/30

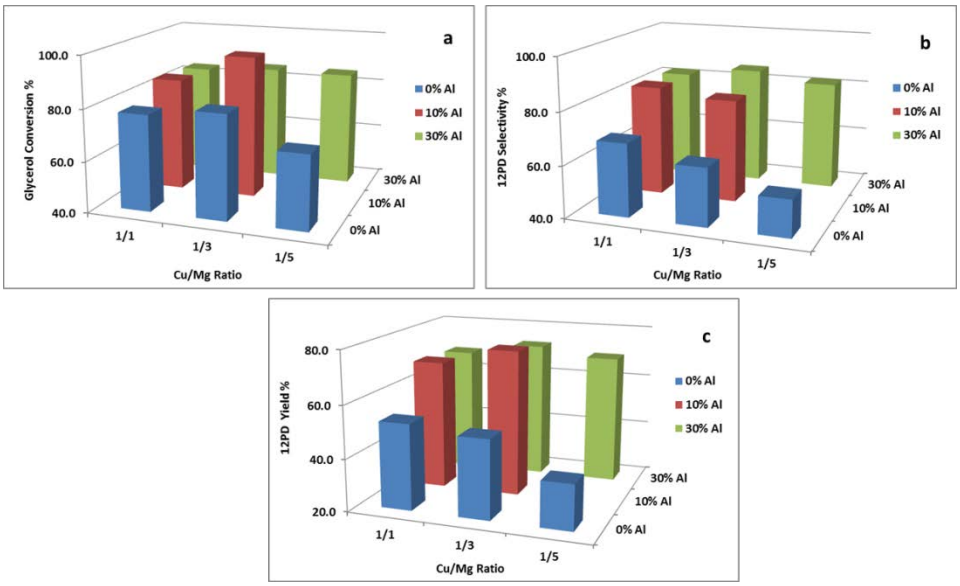

Figure 5-25 Cu/Mg/Al Composition Optimization Study: a) Glycerol Conversion; b) 1,2PD Selectivity; c) 1,2PD Yield. Conditions: 220 ºC, 15bar N_2, 20wt% Glycerol, Water/Methanol=1.2, 3wt% catalyst, 500RPM, 8 hours.

Table 5-12 Cu/Mg/Al Composition Optimization Study[a].

Composition	Glycerol Conversion	1,2PD Selectivity	1,2PD Yield	Acetol Yield	EG Yield	PrOH Yield	Others Yield
1/1	77.6	68.1	52.9	1.8	7.3	0.6	15.0
1/3	80.6	62.3	50.2	2.2	5.7	0.9	21.5
1/5	68.8	54.2	37.3	2.6	4.7	1.1	23.1
45/45/10	84.5	82.3	69.5	1.5	8.3	0.6	4.6
22.5/67.5/10	95.6	79.5	75.9	1.0	7.7	0.8	10.1
35/35/30	83.4	81.9	68.4	6.7	5.6	0.4	2.3
17.5/52.5/30	85.2	85.3	72.7	5.0	6.3	0.4	0.8
11.7/58.3/30	84.9	81.9	69.5	2.6	6.8	0.6	5.4

[a]Conditions: 220 ºC, 15bar N_2, 20wt% Glycerol, Water/Methanol=1.2, 3wt% catalyst, 500RPM, 8 hours.

From Figure 5-25a and Table 5-12, it can be seen that for all the aluminum contents, a Cu/Mg molar ratio of 1/3 always shows the highest glycerol conversion. When the Cu/Mg molar ratio is 1/3 and the aluminum content is 10 mole%, the glycerol conversion is remarkably higher than for the others, being 95.6%. Figure 5-25b shows that the 1,2PD selectivity increases when the aluminum content is increased. Because of the high conversion of glycerol when the molar ratio of Cu/Mg/Al is 22.5/67.5/10, the yield of 1,2PD is the highest using a catalyst with this composition as shown in Figure 5-25c, being 75.9%. This is higher than that using a catalyst with 30mole% aluminum content (72.7% selectivity to 1,2PD).

A repeatability study of the catalyst with a Cu/Mg/Al ratio of 22.5/67.5/10 has been carried out using 95% confidence interval to ensure that the high apparent yield of 1,2PD is not due to experimental error. Three experiments with this catalyst were conducted under the same experimental conditions. The 95% confidence interval is calculated using Equation 5-4 and Equation 5-5 and the results are shown in Table 5-13.

$$95\%C.I. = \left[\overline{X} - 1.96 \times SD, \overline{X} + 1.96 \times SD\right] \qquad \textbf{Equation 5-4}$$

$$SD = \frac{S}{\sqrt{n}} = \frac{1}{\sqrt{n}}\left(\sqrt{\frac{\sum\left(x_i - \bar{x}\right)^2}{n}}\right)$$ **Equation 5-5**

Table 5-13 Repeatability Study on $Cu/MgO/Al_2O_3$ Catalyst[a].

	Glycerol Conversion	1,2PD Selectivity	1,2PD Yield	Acetol Yield	EG Yield	PrOH Yield	Others Yield
Run 1	96.4	78.6	75.8	0.9	7.9	0.7	11.2
Run 2	94.2	79.4	74.8	1.3	7.5	0.8	9.8
Run 3	96.2	80.3	77.3	0.9	7.8	0.8	9.4
Mean	95.6	79.4	75.9	1.0	7.7	0.8	10.1
SD	0.72	0.50	0.73	0.12	0.10	0.02	0.55
95% C.I.	**95.6±1.4**	**79.4±0.98**	**75.9±1.43**	**1.0±0.12**	**7.7±0.20**	**0.8±0.05**	**10.1±0.55**

aConditions: 220 ºC, 15bar N_2, 20wt% Glycerol, Water/Methanol=1.2, 3wt% catalyst, 500RPM, 8 hours, Cu/Mg/Al = 22.5/67.5/10.

As shown in Table 5-13, the 95% confidence interval for the 1,2PD yield using a catalyst with a Cu/Mg/Al ratio of 22.5/67.5/10 is [77.33%, 74.47%]. The yield of 1,2PD by using the catalyst with a Cu/Mg/Al molar ratio of 17.5/52.5/30 catalyst is 72.7%, which is below the lower bound of the interval. Therefore, it can be stated with 95% confidence that the $Cu/MgO/Al_2O_3$ catalyst with a Cu/Mg/Al molar ratio of 22.5/67.5/10 gives a higher 1,2PD yield than that with a Cu/Mg/Al molar ratio of 17.5/52.5/30.

In order to study the effect of the calcination environment, the $Cu/MgO/Al_2O_3$ catalyst was calcined under helium and the activity was tested. The experimental results are shown in Figure 5-26.

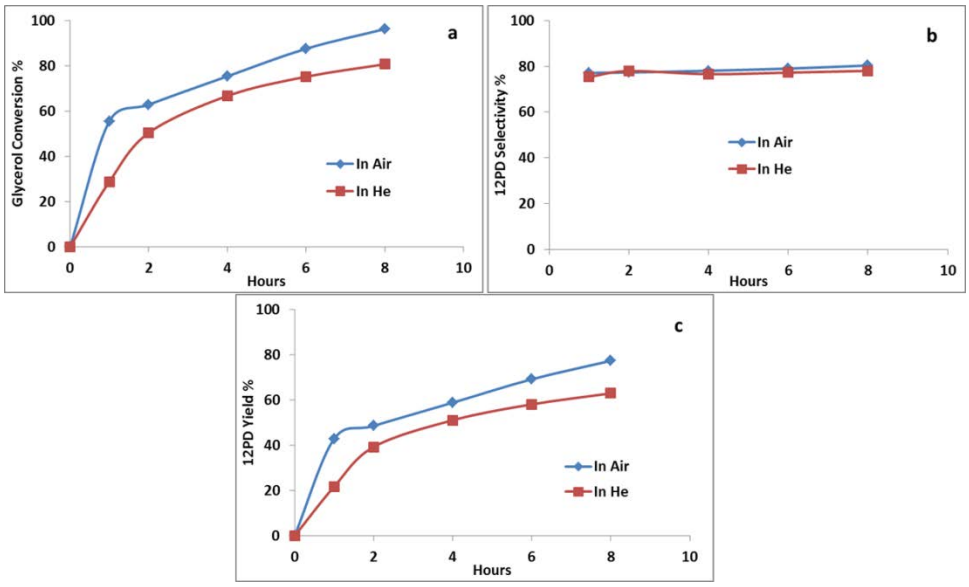

Figure 5-26 Effect of Calcination Environment: a) Glycerol Conversion; b) 1,2PD Selectivity; c) 1,2PD Yield. Conditions: 220 ºC, 15bar N_2, 20wt% Glycerol, Water/Methanol=1.2, 3wt% catalyst, 500RPM, Cu/Mg/Al = 22.5/67.5/10.

From Figure 5-26a, it can be observed that when using the catalyst calcined in helium, the glycerol conversion is significantly lower than that calcined in air. The 1,2PD selectivity for the catalysts calcined in these two environments are similar as shown in Figure 5-26b, therefore, the yield of 1,2PD using the catalyst calcined in air is higher than that calcined in helium. It suggests that the decarboxylation process is more complete under air than helium at 360 ºC for 4 hours.

5.3.3 Recyclability of Cu/MgO/Al_2O_3 Catalyst

The life time of the Cu/MgO/Al_2O_3 and Cu/ZnO/Al_2O_3 catalysts have also been investigated and the experimental results are compared. The catalyst was recycled and reused. The experimental results for the Cu/MgO/Al_2O_3 catalyst recycling study are shown in Figure 5-27 and Table 5-14.

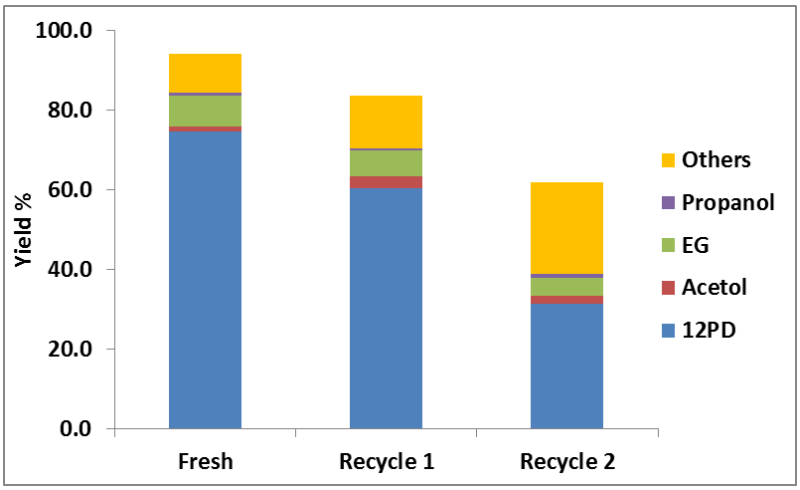

Figure 5-27 Cu/MgO/Al_2O_3 Catalyst Recycling Study. Conditions: 220 ºC, 15bar N_2, 20wt% Glycerol, Water/Methanol=1.2, 3wt% catalyst, 500RPM, 8 hours, Cu/Mg/Al = 22.5/67.5/10.

Table 5-14 Cu/MgO/Al_2O_3 Catalyst Recycling Study[a].

	Glycerol Conversion	1,2PD Selectivity	1,2PD Yield	Acetol Yield	EG Yield	PrOH Yield	Others Yield
Fresh	94.2	79.4	74.8	1.3	7.5	0.8	9.8
Recycle 1	83.7	72.3	60.5	3.0	6.4	0.6	13.1
Recycle 2	61.9	50.9	31.5	1.9	4.6	0.9	23.0

[a]Conditions: 220 ºC, 15bar N_2, 20wt% Glycerol, Water/Methanol=1.2, 3wt% catalyst, 500RPM, 8 hours, Cu/Mg/Al = 22.5/67.5/10.

It can be seen that the Cu/MgO/Al_2O_3 catalyst loses its activity when it is recycled and reused. The glycerol conversion drops from 94.2% using a fresh catalyst down to 83.7% for first recycle and is lowered to 61.9% for the second recycle.

It has been discussed in Section 4.6 that the Cu/ZnO/Al_2O_3 catalyst has an outstanding life time for the glycerol hydrogenolysis process with added molecular hydrogen. Therefore, the life time of the Cu/ZnO/Al_2O_3 catalyst was also investigated for the glycerol hydrogenolysis process using *in situ* hydrogen produced by methanol steam reforming. The Cu/ZnO/Al_2O_3 catalyst with different molar composition were used (Cu/Zn/Al = 35/35/30 and Cu/Zn/Al = 25/25/50). The experimental results are shown in Figure 5-28 and Table 5-15.

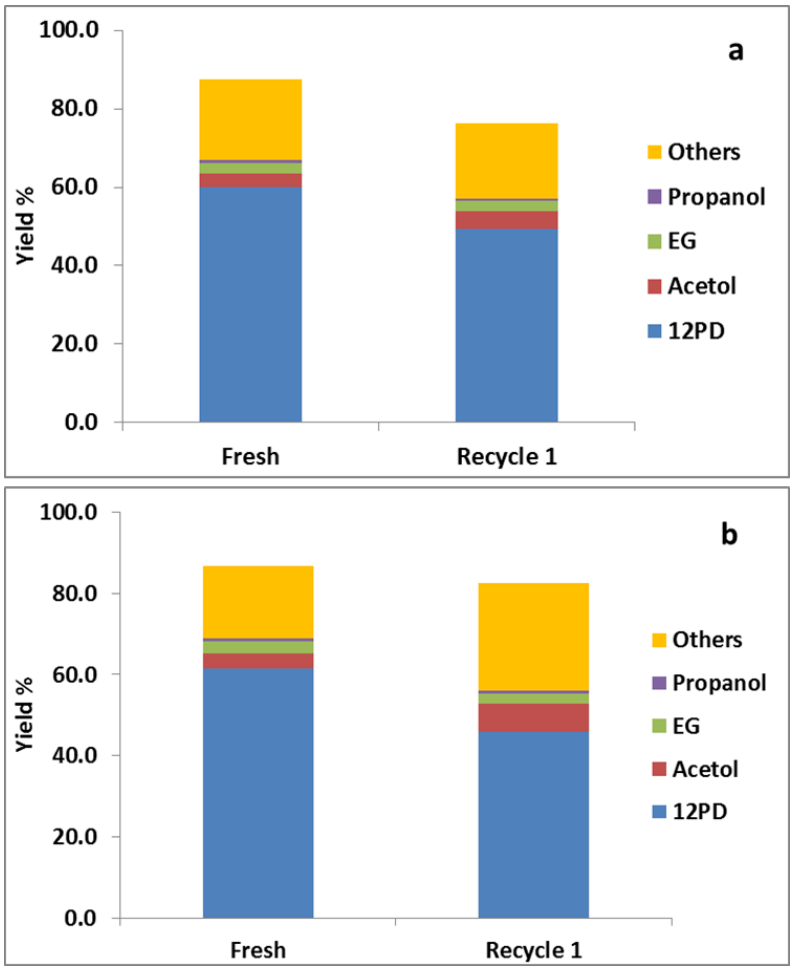

Figure 5-28 $Cu/ZnO/Al_2O_3$ Catalyst Recycling Study. Conditions: 220 ºC, 15bar N_2, 20wt% Glycerol, Water/Methanol=1.2, 3wt% catalyst, 500RPM, 8 hours. a) Cu/Zn/Al = 35/35/30; b) Cu/Zn/Al = 25/25/50.

Table 5-15 $Cu/ZnO/Al_2O_3$ Catalyst Recycling Study[a].

35/35/30	Glycerol Conversion	1,2PD Selectivity	1,2PD Yield	Acetol Yield	EG Yield	PrOH Yield	Others Yield
Fresh	87.4	68.7	60.0	3.4	2.8	0.7	20.5
Recycle 1	76.4	64.6	49.3	4.5	2.6	0.7	19.2
25/25/50	Glycerol Conversion	1,2PD Selectivity	1,2PD Yield	Acetol Yield	EG Yield	PrOH Yield	Others Yield
Fresh	86.7	70.9	61.5	3.6	2.9	0.7	18.0
Recycle 1	82.6	55.5	45.8	7.0	2.6	0.7	26.5

[a]Conditions: 220 ºC, 15bar N_2, 20wt% Glycerol, Water/Methanol=1.2, 3wt% catalyst, 500RPM, 8 hours, Cu/Mg/Al = 22.5/67.5/10.

From Figure 5-28 and Table 5-15, it can be seen that both catalysts show deactivation after the first recycle. The glycerol conversion and 1,2PD selectivity drop significantly. It was reported in Section 4.6 that when using the $Cu/ZnO/Al_2O_3$ catalyst with a Cu/Zn/Al molar ratio of 25/25/50, after 5 recycles, the catalyst did not show any significant activity loss. Therefore, there might be several reasons causing this activity loss for the process when using *in situ* hydrogen produced via methanol steam reforming. First of all, CO_2 is produced as the by-product of methanol steam reforming as shown in Equation 5-1. The dissolved CO_2 gas might interact with the metals, i.e. Cu, Zn and Mg, to produce metal carbonates; therefore, some active sites might be lost. Another reason is possibly due to some carbonaceous compound, which is formed via side reactions when insufficient hydrogen is produced, and deposited on the catalyst surface.

5.3.4 Effect of KOH

It has been widely reported that when some base is present in the reactant i.e. KOH or NaOH, the catalytic activity can be improved [81, 167, 168]; also K^+ and Na^+ were also found to improve the activity of methanol steam reforming [169]. Currently, most biodiesel plants in the world are using KOH or NaOH as the catalyst, therefore, there is always KOH or NaOH residues remaining in the crude glycerol, which is reported to be about 1% [129]. In order to investigate the effect of KOH on the catalyst life time as well as catalytic activity, experiments have been carried out with 0.5g KOH added (2.5wt% with respect to glycerol weight), and then the catalysts were recycled and re-used under the same conditions. The experimental results are shown in Figure 5-29 and Table 5-16.

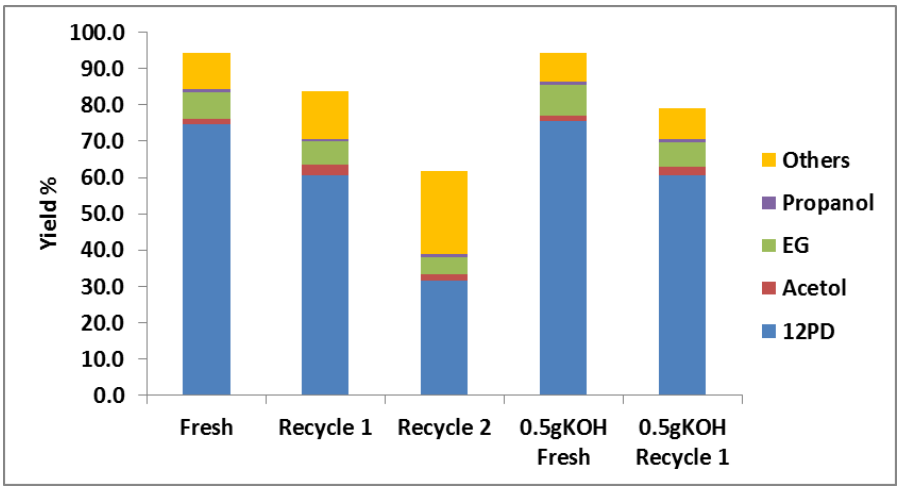

Figure 5-29 Effect of KOH on the Lifetime of $Cu/MgO/Al_2O_3$ catalyst. Conditions: 220 ºC, 15bar N_2, 20wt% Glycerol, Water/Methanol=1.2, 3wt% catalyst, 500RPM, 8 hours, Cu/Mg/Al = 22.5/67.5/10.

Table 5-16 Effect of KOH on the Lifetime of $Cu/MgO/Al_2O_3$ catalyst[a].

	Glycerol Conversion	1,2PD Selectivity	1,2PD Yield	Acetol Yield	EG Yield	PrOH Yield	Others Yield
Fresh	94.2	79.4	74.8	1.3	7.5	0.8	9.8
Recycle 1	83.7	72.3	60.5	3.0	6.4	0.6	13.1
Recycle 2	61.9	50.9	31.5	1.9	4.6	0.9	23.0
0.5gKOH Fresh	94.2	80.3	75.6	1.3	8.7	0.9	7.8
0.5gKOH Recycle 1	79.2	76.5	60.6	2.3	6.9	0.9	8.6

[a]Conditions: 220 ºC, 15bar N_2, 20wt% Glycerol, Water/Methanol=1.2, 3wt% catalyst, 500RPM, 8 hours, Cu/Mg/Al = 22.5/67.5/10

From Figure 5-29 as well as Table 5-16, it can be seen that the product distributions for the reactions without adding KOH are similar to those when adding 0.5g KOH. Without adding KOH, when the catalyst was recycled and reused, the 1,2PD yield drops from 74.8% to 60.5%; when 0.5g KOH is added, and when the catalyst is recycled and reused, the 1,2PD yield drops from 75.6% to 60.6%. Hence by adding 0.5g KOH, catalyst deactivation is also observed.

To further investigate the effect of KOH, 10g of KOH was added into the reactant system. The experimental results are shown in Figure 5-30.

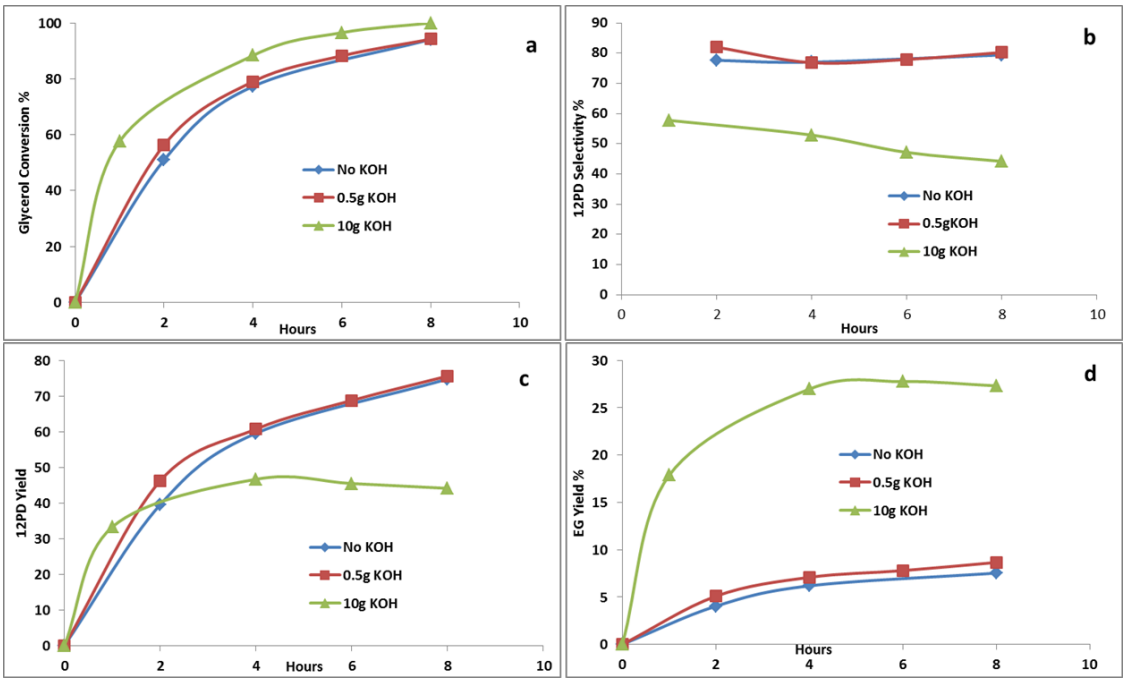

Figure 5-30 Effect of KOH on the Cu/MgO/Al2O3 activity: a) Glycerol Conversion; b) 1,2PD Selectivity; c)1,2PD Yield; d) EG Yield. Conditions: 220 ºC, 15bar N_2, 20wt% Glycerol, Water/Methanol=1.2, 3wt% catalyst, 500RPM, 8 hours, Cu/Mg/Al = 22.5/67.5/10.

From Figure 5-30, it can be seen that by adding a significant amount of KOH (10g in this case, 50wt% with respect to glycerol weight), the glycerol is converted much faster than for the glycerol conversion when no KOH is added over the reaction time as shown in Figure 5-30a. However, the selectivity to 1,2PD is much lower when 10g KOH is added as shown in Figure 5-30b, therefore, the yield of 1,2PD is significantly lower (Figure 5-30c). This is not only caused by the formation of other by-products, but also a significant amount of EG is formed which as shown in Figure 5-30d, Figure 5-31 and Table 5-17. Therefore, it is apparent that the basicity of the reaction environment can promote C-C bond cleavage resulting in a high EG yield.

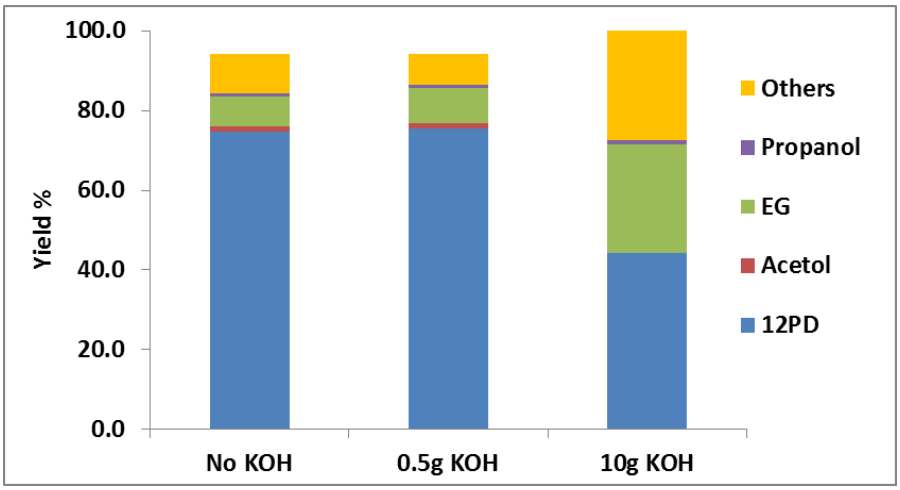

Figure 5-31 Effect of KOH on the Products Distribution. Conditions: 220 ºC, 15bar N_2, 20wt% Glycerol, Water/Methanol=1.2, 3wt% catalyst, 500RPM, 8 hours, Cu/Mg/Al = 22.5/67.5/10.

Table 5-17 Effect of KOH on Product Distribution[a].

	Glycerol Conversion	1,2PD Sel.	1,2PD Yield	Act Yield	EG Yield	PrOH Yield	Others Yield
No KOH	94.2	79.4	74.8	1.3	7.5	0.8	9.8
0.5g KOH	94.2	80.3	75.6	1.3	8.7	0.9	7.8
10g KOH	100.0	44.2	44.2	0.0	27.3	1.0	27.6

[a]Conditions: 220 ºC, 15bar N_2, 20wt% Glycerol, Water/Methanol=1.2, 3wt% catalyst, 500RPM, 8 hours, Cu/Mg/Al = 22.5/67.5/10.

5.3.5 Effect of Glycerol Feed Concentration

An experiment with a higher glycerol concentration (30%) was carried out to study the effect of glycerol concentration on the 1,2PD selectivity. A higher glycerol concentration is desired in industry since the operational cost will be lower by running fewer batch reactions and smaller reactors are required. However, it can be expected that for a higher glycerol concentration, the concentration of methanol and water will be lower; hence less hydrogen will be produced. In this case the selectivity to 1,2PD will be affected. The experimental results obtained are shown in Figure 5-32.

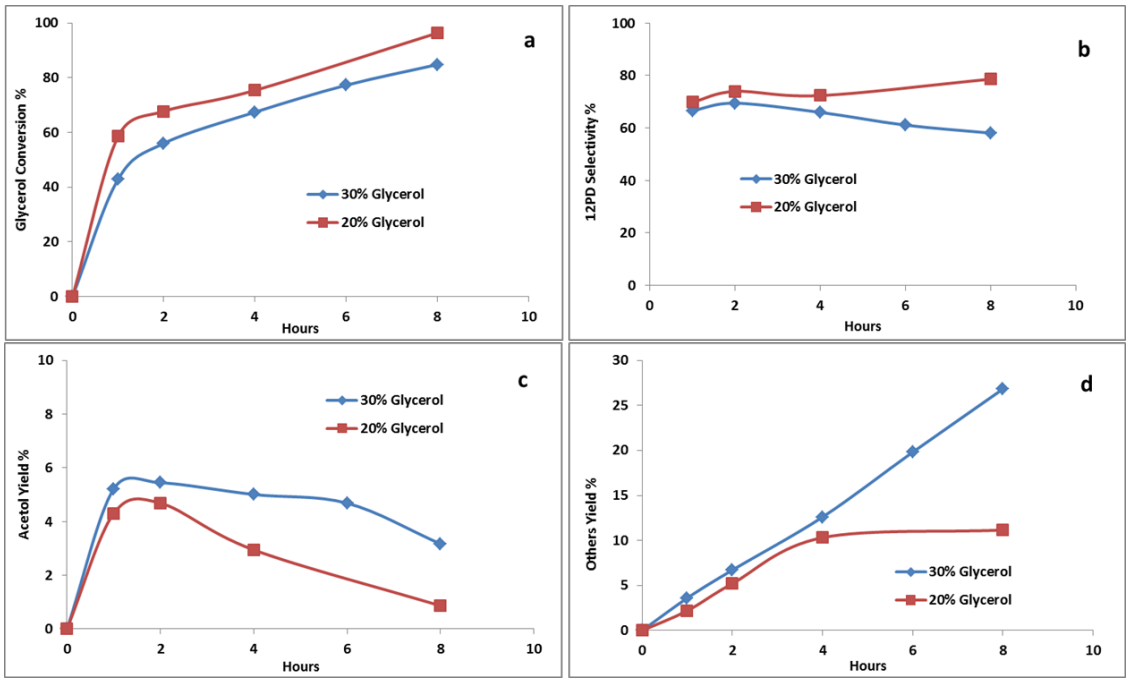

Figure 5- 32 Effect of Glycerol Concentration on: a) Glycerol Conversion; b) 1,2PD Selectivity; c) Acetol Yield; d) Others Yield. Conditions: 220 ºC, 15bar N_2, Water/Methanol=1.2, 3wt% catalyst, 500RPM, 8 hours, Cu/Mg/Al = 22.5/67.5/10.

It can be seen that when the glycerol concentration is increased from 20% to 30%, the glycerol conversion over the reaction time becomes lower as shown in Figure 5-32a. This is because with the same amount of catalyst, when the glycerol concentration is higher, the catalyst concentration with respect to glycerol load is lower. When the glycerol concentration is higher, the selectivity to 1,2PD is much lower than that when the glycerol concentration is 20% (Figure 5-32b**)**, since when the glycerol concentration is higher, the concentration of methanol and water will be lower and less hydrogen will be produced for acetol hydrogenation. As Figure 5-23c shows, the yield of acetol at higher glycerol concentration is higher resulting in a higher yield of by-products due to side reactions with acetol, as shown in Figure 5-23d. The detailed final product distributions for these two glycerol initial concentration experiments are shown in Figure 5-33 as well as in Table 5-18.

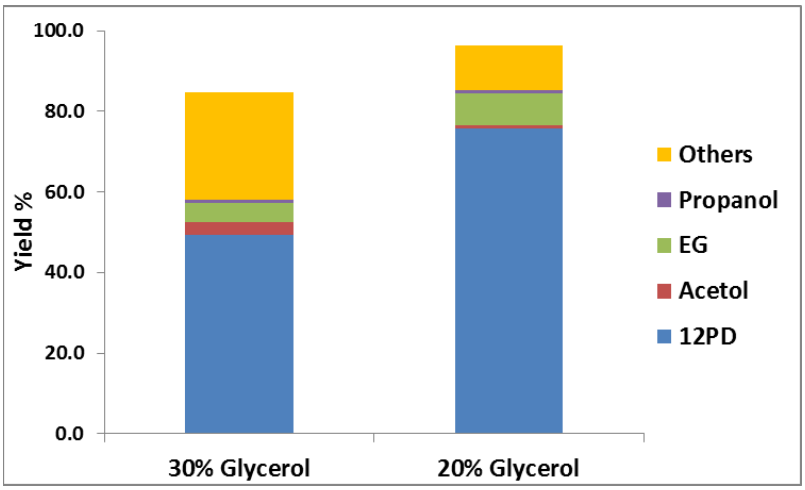

Figure 5-33 Effect of Glycerol Concentration on the Products Distribution. Conditions: 220 ºC, 15bar N_2, Water/Methanol=1.2, 3wt% catalyst, 500RPM, 8 hours, Cu/Mg/Al = 22.5/67.5/10.

Table 5-18 Effect of Glycerol Concentration on Product Distribution[a]

	Glycerol Conversion	1,2PD Selectivity	1,2PD Yield	Acetol Yield	EG Yield	PrOH Yield	Others Yield
30% Glycerol	84.8	58.1	49.2	3.2	5.0	0.6	26.8
20% Glycerol	95.6	79.5	75.9	1.0	7.7	0.8	10.1

[a]Conditions: 220 ºC, 15bar N_2, Water/Methanol=1.2, 3wt% catalyst, 500RPM, 8 hours, Cu/Mg/Al = 22.5/67.5/10.

Therefore, a more active catalyst for methanol steam reforming or acetol hydrogenation is required if a higher concentration of glycerol is to be used as the feedstock.

5.4 Study of Pd as a Promoter for the $Cu/MgO/Al_2O_3$ and $Cu/ZnO/Al_2O_3$ Catalysts

Palladium has been used for many hydrogenation process. Recently it has been reported that adding Pd to a Cu based catalyst [60, 82, 106] can improve the catalytic acitivity for the glycerol hydrogenolysis process.

5.4.1 Effect of Pd Precursors and Preparation Methods

It has been reported that palladium acetate can be reduced to palladium nano-particles by some reducing agents such as ethanol, $NaBH_4$ or hydrazine [170, 171]. A similar method was used to prepare a palladium supported on $Cu/ZnO/Al_2O_3$ catalyst. A pre-calculated amount of $Pd(Ac)_2$ in acetone was added drop wise into a slurry containing 20g of calcined $CuO/ZnO/Al_2O_3$ catalyst and 350ml ethanol with vigorous stirring for 4 hours. The palladium acetate was reduced to metallic palladium as the ethanol acted as a reducing agent [172]. The solid was filtered and dried in air at 110 ºC for 12 hours. The particles were calcined in air at 360 ºC for 4 hours (PdAc Red.). For comparison, a catalyst was prepared by a conventional impregnation method (PdAc Imp.). The detailed procedures are provided in Section 3.1. In order to study the effect of the palladium precursor, a palladium nitrate $Pd(NO_3)_2$ precursor was also used for impregnation. The procedure was similar to the method described previously when palladium acetate was used as the precursor except water was used as the solvent and the solvent was evaporated on an oil bath at 110 ºC, the catalyst was referred to as $Pd(NO_3)_2$ Imp.

Gopinath *et al.* in 2008 reported that the supported palladium catalyst prepared by deposition precipitation had a higher activity [173] compared with the catalyst prepared by impregnation. Therefore, a Pd supported on $Cu/ZnO/Al_2O_3$ catalyst prepared by $Pd(NO_3)_2$ deposition precipitation was prepared. 20 gram of calcined $CuO/ZnO/Al_2O_3$ catalyst was first dispersed

into a 350ml aqueous solution of $Pd(NO_3)_2$. 0.5M $(NH_4)_2CO_3$ was slowly added to the palladium solution until the pH value of the mixture reached 10. The suspension was stirred for 1h. The solid was filtered and washed with deionized water until the pH of the filtrate became 7.0. The catalyst was then dried in air at 110 ºC for 12 hours and calcined in air at 360 ºC for 4 hours. The catalyst was referred to as $Pd(NO_3)_2$ D.P.. The experimental results are shown in Figure 5-34 and Table 5-19.

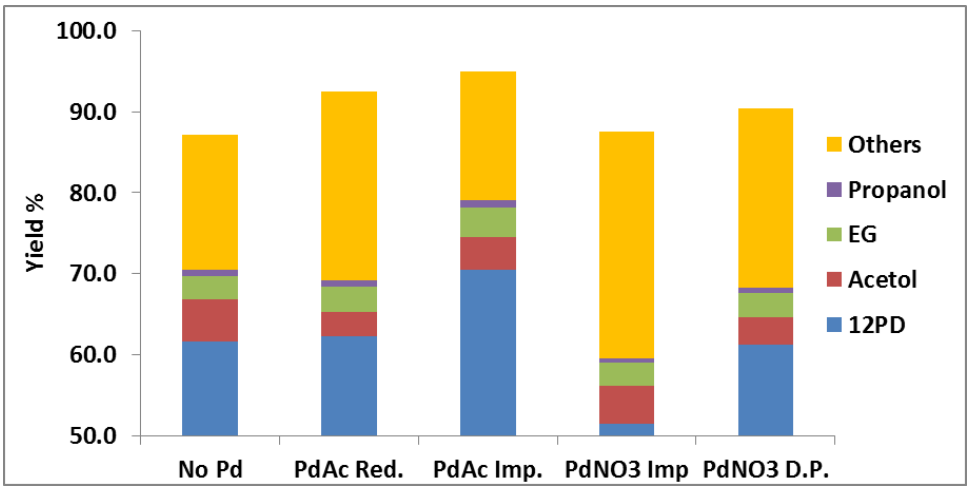

Figure 5-34 Effect of Preparation Method of Pd Supported on $Cu/ZnO/Al_2O_3$ on the Products Distribution. Conditions: 220 ºC, 15bar N_2, 20wt% Glycerol, Water/Methanol=1.2, 3wt% catalyst, 500RPM, 8 hours, Cu/Zn/Al = 35/35/30, 1wt% Pd Loading.

Table 5-19 Effect of Preparation Method of Pd Supported on $Cu/ZnO/Al_2O_3$ on Product Distribution[a].

Catalyts	Glycerol Conversion	1,2PD Selectivity	1,2PD Yield	Acetol Yield	EG Yield	PrOH Yield	Others Yield
No Pd	87.1	70.7	61.6	5.2	2.9	0.7	16.7
PdAc Red.	92.4	67.4	62.3	3.0	3.2	0.7	23.2
PdAc Imp.	94.9	74.3	70.5	3.9	3.7	0.8	15.9
$Pd(NO_3)_2$ Imp	87.6	58.8	51.5	4.6	2.8	0.6	28.0
$Pd(NO_3)_2$ D.P.	90.4	67.7	61.2	3.4	2.9	0.6	22.2

[a]Conditions: 220 ºC, 15bar N_2, 20wt% Glycerol, Water/Methanol=1.2, 3wt% catalyst, 500RPM, 8 hours, Cu/Mg/Al = 22.5/67.5/10, 1wt% Pd Loading.

From Figure 5-34 as well as Table 5-19, it can be seen that only the impregnation method using palladium acetate as the precursor has a positive effect on the catalyst activity. With 1wt% loading, the glycerol conversion increases from 87.1% to 94.9% compared with a $Cu/ZnO/Al_2O_3$ catalyst without loading Pd; the 1,2PD selectivity also increases from 70.7% to 74.3%. The other three preparation methods (PdAc Red., $Pd(NO_3)_2$ Imp. and $Pd(NO_3)_2$ D.P.) all have negative effects on the catalytic activity.

Knowing that the addition of Pd via an impregnation method can promote the activity of the catalyst, two different catalysts, which are $Cu/ZnO/Al_2O_3$ and $Cu/MgO/Al_2O_3$, were used. The experimental results are shown in Table 5-20.

Table 5-20 Effect of Support for Pd on Product Distribution[a]

Catalysts	Glycerol Conversion	1,2PD Selectivity	1,2PD Yield	Acetol Yield	EG Yield	PrOH Yield	Others Yield
$Cu/ZnO/Al_2O_3$	87.1	70.7	61.6	5.2	2.9	0.7	16.7
1wt%Pd-$Cu/ZnO/Al_2O_3$	94.9	74.3	70.5	3.9	3.7	0.8	15.9
$Cu/MgO/Al_2O_3$	95.6	79.5	75.9	1.0	7.7	0.8	10.1
1wt%Pd-$Cu/MgO/Al_2O_3$	97.2	83.4	81.0	0.0	9.2	0.7	6.2

[a]Conditions: 220 ºC, 15bar N_2, 20wt% Glycerol, Water/Methanol=1.2, 3wt% catalyst, 500RPM, 8 hours, Cu/Zn/Al = 35/35/30, Cu/Mg/Al = 22.5/67.5/10, 1wt% Pd Loading.

It has been discussed in Section 5.3.1 that $Cu/MgO/Al_2O_3$ gave a higher activity than the $Cu/ZnO/Al_2O_3$ catalyst for glycerol hydrogenolysis using *in situ* hydrogen produced by methanol steam reforming. It can be seen from Table 5-20 that 1wt% addition of Pd can improve the activities of both the $Cu/ZnO/Al_2O_3$ and $Cu/MgO/Al_2O_3$ catalysts; the Pd supported on $Cu/MgO/Al_2O_3$ catalyst has a higher activity than that of Pd supported on $Cu/ZnO/Al_2O_3$. The promoting effect of Pd is possibly due to a greater suppy of surface hydrogen by Pd as shown in the H_2 TPD results shown in Section 6.4 and the promoting effect on the methanol steam reforming reaction as has been frequently reported [174, 175].

5.4.2 Effect of Pd Loading

It has been discussed in Section 5.3.5 that the 1,2PD selectivity was lower when the glycerol concentration was higher. Therefore, to further investigate if the small improvement (glycerol conversion 95.6% to 97.2% and 1,2PD selectivity 79.5% to 83.7%) when 20% aqueous glycerol was used as the feedstock was due to the addition of Pd or experimental errors, a higher glycerol concentration (40%) was used in the experiment. The catalyst with different amount of Pd loading (wt%) (0, 1, 2, 3) were used and the experimental results are shown in Figure 5-35.

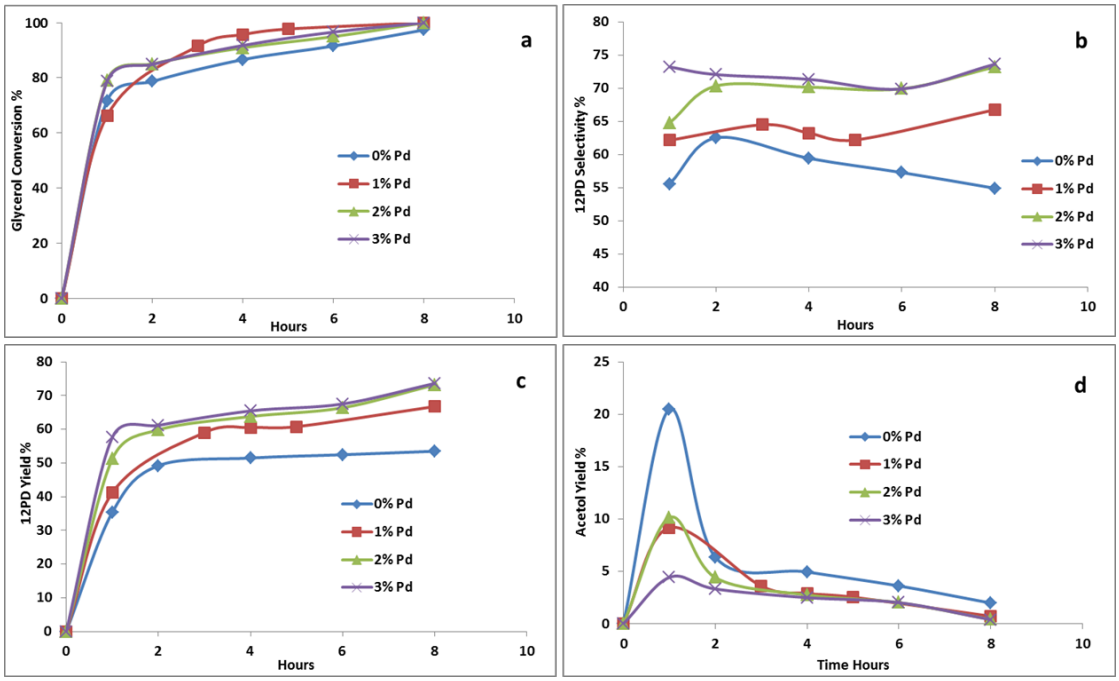

Figure 5-35 Effect of Pd Loading on: a) Glycerol Conversion; b) 1,2PD Selectivity; c) 1,2PD Yield; d) Acetol Yield. Conditions: 220 ºC, 15bar N_2, Water/Methanol=1.2, Glycerol Concentration=40wt%, 7wt% catalyst, 500RPM, 8 hours, Cu/Mg/Al = 22.5/67.5/10.

As shown in Figure 5-35a, the glycerol conversions for these four catalysts are not very different since they all reach 100% glycerol conversion after 8 hours. This suggests that 7wt% of catalyst is enough to provide 100% glycerol conversion in 8 hours when 40% aqueous

glycerol is used as the feedstock. From Figure 5-35b, it can be seen that as the Pd loading is increased from 0wt% to 2wt%, the 1,2PD selectivity increases significantly from 53.5% to 73.2% as shown in Figure 5-36 and Table 5-20. When the Pd loading is further increased from 2wt% to 3wt%, the selectivity of 1,2PD does not change significantly (73.2% to 73.6%). Therefore, 2wt% of Pd loading is selected as the optimum amount. The yield of other by-products decreases from 35.5% (no Pd loaded) to 18.4% when 2wt% Pd is loaded. Figure 5-36d shows that when the Pd loading is increased, the concentration of acetol in the mixture becomes lower, which is the main cause for the formation of by-products.

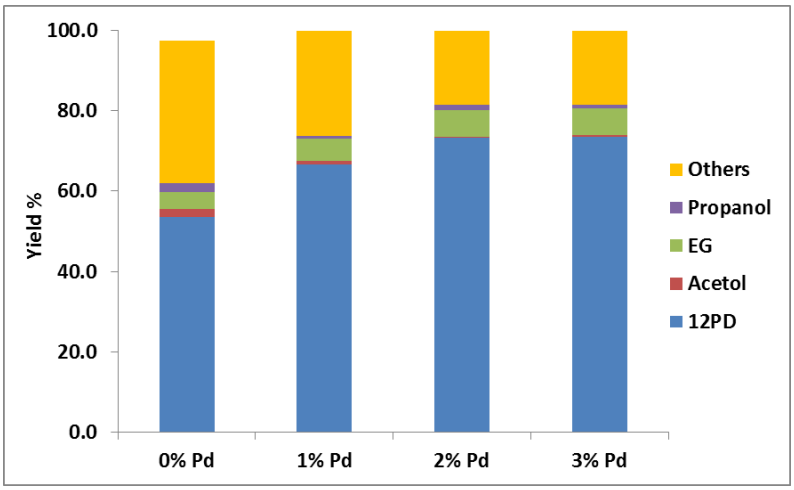

Figure 5-36 Effect of Pd Loading on $Cu/MgO/Al_2O_3$ on the Products Distribution. Conditions: 220 ºC, 15bar N_2, 40wt% Glycerol, Water/Methanol=1.2, 7wt% catalyst, 500RPM, 8 hours, Support: Cu/Mg/Al = 22.5/67.5/10, 40wt% Glycerol.

Table 5-21 Effect of Pd Loading on $Cu/MgO/Al_2O_3$ on Product Distribution[a]

	Glycerol Conversion	1,2PD Selectivity	1,2PD Yield	Acetol Yield	EG Yield	PrOH Yield	Others Yield
0% Pd	97.4	54.9	53.5	2.0	4.4	2.1	35.5
1% Pd	100.0	66.8	66.8	0.7	5.5	0.7	26.3
2% Pd	100.0	73.2	73.2	0.4	6.6	1.4	18.4
3% Pd	100.0	73.6	73.6	0.4	6.6	0.8	18.6

[a]Conditions: 220 ºC, 15bar N_2, 40wt% Glycerol, Water/Methanol=1.2, 7wt% catalyst, 500RPM, 8 hours, Support: Cu/Mg/Al = 22.5/67.5/10, 40wt% Glycerol.

5.4.3 Effect of Pd-Cu/MgO/Al_2O_3 Catalyst Amount

Experiments with different amounts of 2wt%Pd-Cu/MgO/Al_2O_3 catalyst loading were also carried out to study the effect of catalyst amount on the reaction products. Three amounts (3wt%, 5wt% and 7wt%) were selected and the experimental results are shown in Figure 5-37.

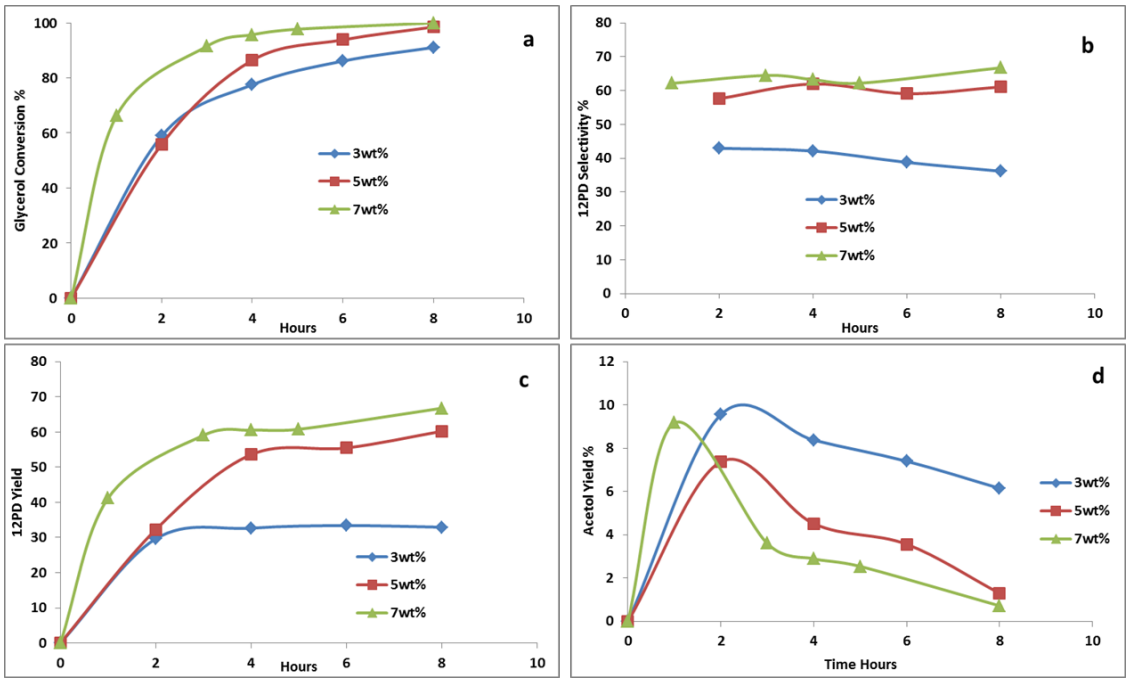

Figure 5-37 Effect of Catalyst Amount on: a) Glycerol Conversion; b)1,2PD Selectivity; c) 1,2PD Yield d) Acetol Yield. Conditions: 220 ºC, 15bar N_2, Water/Methanol=1.2, 7wt% catalyst, 500RPM, 8 hours, Catalyst: 1% Pd on Cu/Mg/Al = 22.5/67.5/10 40wt% Glycerol.

Figure 5-37a shows that when the catalyst amount is increased, the glycerol conversion over the reaction time is higher. When 7wt% of catalyst is loaded, the conversion of glycerol reaches 100% in 5 hours while when 5wt% of catalyst is loaded, the conversion is 100% in 8 hours. Figure 5-37b shows that when the catalyst amount is increased from 3wt% to 5wt%, the selectivity to 1,2PD is improved significantly from 36.2% to 61.1%; the detailed product distribution is shown in Figure 5-38 and Table 5-22. When the catalyst amount is further increased from 5wt% to 7wt%, the selectivity to 1,2PD is only improved from 61.1% to

66.8%. Figure 5-38d shows that the concentration of acetol is lower when the catalyst loading is higher; therefore, the selectivity to 1,2PD is higher when more catalyst is loaded. When more catalyst is loaded, apparently more active sites will be available for methanol steam reforming; therefore, more hydrogen will be produced for acetol hydrogenation resulting in a lower yield of by-products.

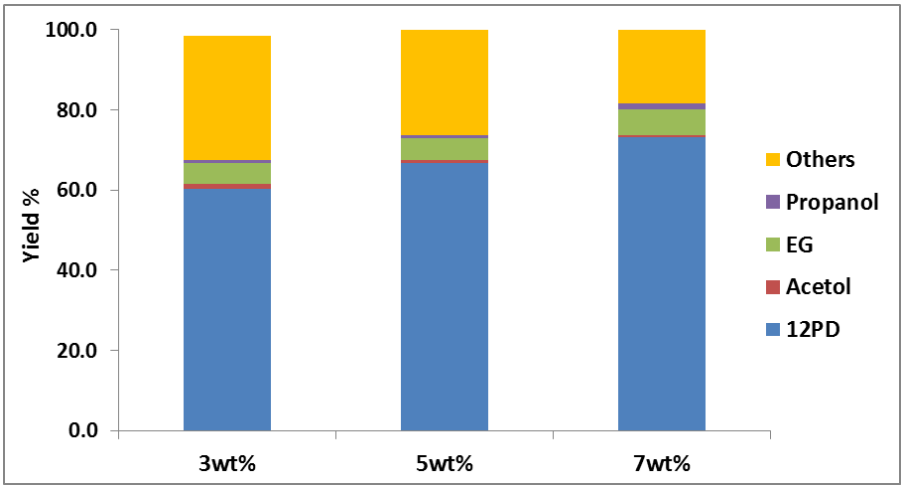

Figure 5-38 Effect of Pd on Cu/MgO/Al_2O_3 Catalyst Amount on the Products Distribution. Conditions: 220 ºC, 15bar N_2, 20wt% Glycerol, Water/Methanol=1.2, 7wt% catalyst, 500RPM, 8 hours, Catalyst: 1wt% Pd on Cu/Mg/Al = 22.5/67.5/10, 40wt% Glycerol.

Table 5-22 Effect of Pd on Cu/MgO/Al_2O_3 Catalyst Amount on the Product Distribution[a]

	Glycerol Conversion	1,2PD Selectivity	1,2PD Yield	Acetol Yield	EG Yield	PrOH Yield	Others Yield
3wt%	91.1	36.2	32.9	6.2	2.9	1.3	47.7
5wt%	98.5	61.1	60.2	1.3	5.1	0.9	31.0
7wt%	100.0	66.8	66.8	0.7	5.5	0.7	26.3

[a]Conditions: 220 ºC, 15bar N_2, 20wt% Glycerol, Water/Methanol=1.2, 7wt% catalyst, 500RPM, 8 hours, Catalyst: 1wt% Pd on Cu/Mg/Al = 22.5/67.5/10 40wt% Glycerol.

5.4.4 Methanol Steam Reforming Using 2wt% Pd-Cu/MgO/Al_2O_3

Experiments of methanol steam reforming to produce hydrogen have been carried out using 2wt% Pd on the Cu/MgO/Al_2O_3 catalyst. Two temperatures were used to study the temperature effect on the reaction products, which were 220ºC and 240ºC. The reaction conditions were: 3wt% catalyst, 500RPM, 6 hours reaction time, water to methanol molar ratio of 1.2; 25bar (363 psi) of nitrogen was used to keep the reactant in liquid phase. The experimental results are shown in Figure 5-39 and Figure 5-40.

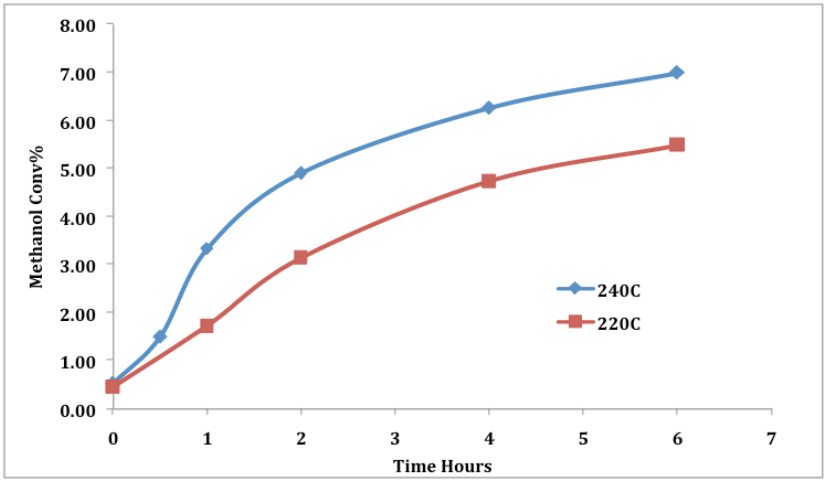

Figure 5-39 Methanol Conversions for Methanol Steam Reforming Using Pd on Cu/MgO/Al_2O_3 Catalyst. Conditions: 3wt% catalyst, 500RPM, 25bar N_2, water to methanol molar ratio is 1.2, catalyst 2% Pd on Cu/Mg/Al=22.5/67.5/10.

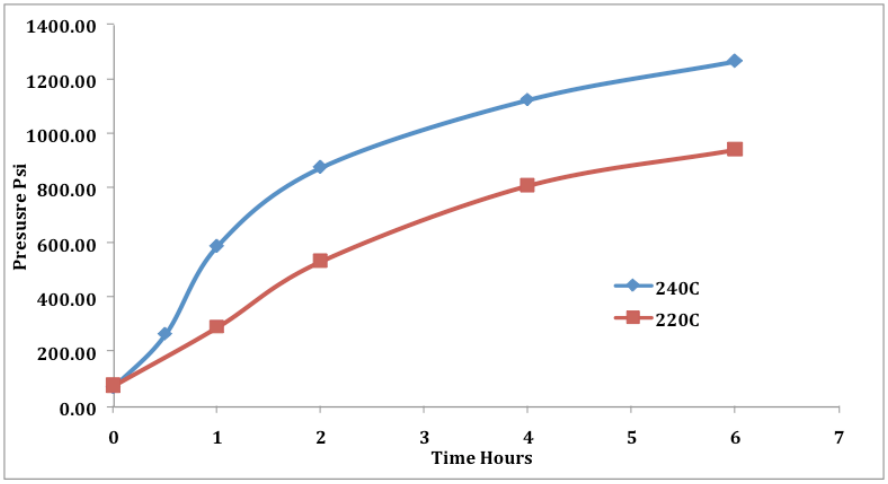

Figure 5-40 Hydrogen Pressure During the Reaction Time for Methanol Steam Reforming Using Pd on Cu/MgO/Al_2O_3 Catalyst. Conditions: 3wt% catalyst, 500RPM, 25bar N_2, water to methanol molar ratio is 1.2, catalyst 2% Pd on Cu/Mg/Al=22.5/67.5/10.

From Figure 5-39 and Figure 5-40, it can be seen that when the temperature is at 240ºC, the methanol conversion after 6 hours is about 7% and at 220ºC, only 5.5% of methanol is converted; accordingly the hydrogen pressure at 240ºC is higher than that at 220ºC. All the results of the gas phase were calculated based on the van der Waal's Equations as shown by Equation 5-6 and Equation 5-7. The results are shown in Table 5-22.

$$(p_i + \frac{n_i^2 a}{V^2})(V - n_i b) = n_i RT \qquad \textbf{Equation 5-6}$$

where n is calculated by an online calculator provided V, p_i, a, b, T and R

$$p_i = p_{total} \times x_i \qquad \textbf{Equation 5-7}$$

where x_i is provided by RGA

Table 5-22 RGA Data for Methanol Steam Reforming.

		%					Psi					mmol	Meth Conv
220˚C	Psi total	H2	N2	CO	CO2	CH4	H2	N2	CO	CO2	CH4	H2	%
0	1103	7.00	91.53	0.31	1.17	0.00	77.16	1009.56	3.38	12.89	0.00	25.88	0.46
1	1435	20.29	75.74	0.03	3.94	0.00	291.18	1086.86	0.48	56.48	0.00	96.95	1.73
2	1594	33.41	61.60	0.08	4.92	0.00	532.51	981.84	1.20	78.45	0.00	175.82	3.15
4	1824	44.43	48.88	0.12	6.55	0.03	810.32	891.55	2.11	119.42	0.60	264.96	4.74
6	1860	50.64	41.93	0.18	7.15	0.10	941.97	779.96	3.31	132.97	1.79	306.60	5.48

240˚C		%					Psi					mmol	Meth Conv
	Psi total	H2	N2	CO	CO2	CH4	H2	N2	CO	CO2	CH4	H2	%
0	1050	6.90	91.89	0.06	1.15	0.00	72.41	964.88	0.68	12.03	0.00	30.00	0.54
0.5	1786	14.97	79.59	0.06	5.38	0.00	267.36	1421.39	1.15	96.09	0.00	84.51	1.51
1	1893	31.15	62.78	0.15	5.92	0.00	589.71	1188.41	2.88	112.01	0.00	186.47	3.34
2	2020	43.42	48.56	0.17	7.83	0.02	877.03	980.94	3.44	158.23	0.36	274.41	4.91
4	2112	53.26	37.43	0.27	8.85	0.18	1124.92	790.56	5.80	186.92	3.80	350.04	6.26
6	2242	56.47	29.35	0.31	13.50	0.38	1266.04	658.01	6.94	302.59	8.41	390.58	6.99

It can also be observed that the Pd supported on $Cu/MgO/Al_2O_3$ catalyst has a very high selectivity towards CO_2 since there is only 0.18% of CO present in the gas mixture at 220ºC and only 0.31% CO at 240ºC. The selectivity to hydrogen is calculated using Equation 5-8, which is 98.94% at 220ºC and 99.05% at 240ºC.

$$Selectivity = \frac{H_2\% \div 3}{H_2\% \div 3 + CO\%} \times 100 \qquad \textbf{Equation 5-8}$$

An experiment of glycerol hydrogenolysis using *in situ* hydrogen produced from methanol steam reforming has been carried out. The gas samples were analyzed by RGA and the experimental results were compared with the methanol steam reforming results as shown in Figure 5-41 and Figure 5-42.

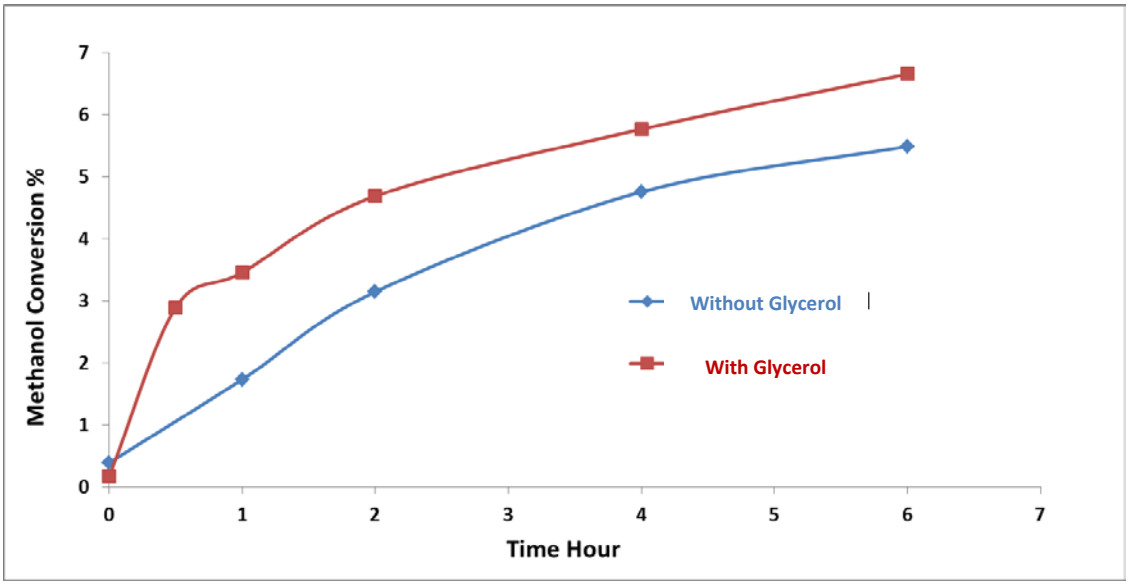

Figure 5-41 Methanol Conversion Comparison Between the Feedstock with Glycerol Added and without Glycerol Added: (Red) With Glycerol Added Conditions: 220 ºC, 25bar N_2, 30wt% Glycerol, Water/Methanol=1.2, 3wt% catalyst, 500RPM, 8 hours, Catalyst: 2wt% Pd on Cu/Mg/Al = 22.5/67.5/10; (Blue) Without Glycerol Added Conditions: 3wt% catalyst, 500RPM, 25bar N_2, water to methanol molar ratio is 1.2, catalyst 2% Pd on Cu/Zn/Al=22.5/67.5/10.

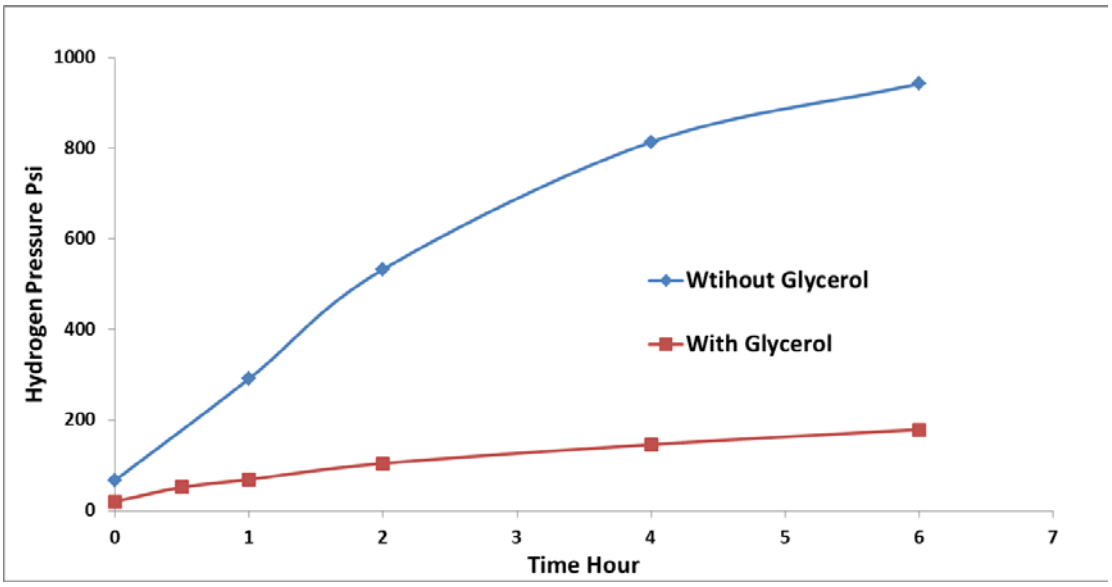

Figure 5-42 Hydrogen Pressure Comparison Between the Feedstock with Glycerol Added and without Glycerol Added: (Red) With Glycerol Added Conditions: 220 ºC, 25bar N_2, 30wt% Glycerol, Water/Methanol=1.2, 3wt% catalyst, 500RPM, 8 hours, Catalyst: 2wt% Pd on Cu/Mg/Al = 22.5/67.5/10; (Blue) Without Glycerol Added Conditions: 3wt% catalyst, 500RPM, 25bar N_2, water to methanol molar ratio is 1.2, catalyst 2% Pd on Cu/Zn/Al=22.5/67.5/10.

From Figure 5-41, it can be seen that with glycerol added, the methanol conversion is higher than without glycerol added. It is possibly because that when hydrogen is consumed the lower hydrogen pressure will drive the equilibrium of methanol steam reforming towards the products. From Figure 5-42, it can be seen that because of the hydrogen consumption, the hydrogen pressure with glycerol added is much lower than that when no glycerol is added. The hydrogen pressure stays below 200psi during the reaction. At the beginning of the reaction (first two hours), the hydrogen pressure is below 100 psi. Based on the discussion in Chapter 4, the minimum hydrogen pressure required to avoid the formation of other by-products is 400psi. So the low hydrogen pressure is possibly one of the reasons for the low selectivity to 1,2PD when the glycerol concentration is high.

The hydrogen consumption is calculated using Equation 5-9 to determine the portion of hydrogen used for glycerol hydrogenolysis from the hydrogen produced via

methanol steam reforming and the results are shown in Table 5-23 as well as in Figure 5-43.

$$Consumption\% = \frac{mol\_of\_1,2-propanediol}{total\_mol\_of\_hydrogen} \times 100\%$$

Equation 5-9

Table 5-23 Hydrogen Consumption[a].

Time	H_2 consumed	Methanol Conversion
Hours	%	%
0	0.0	0.2
0.5	84.7	2.9
1	82.9	3.5
2	81.0	4.7
4	78.4	5.8
6	77.1	6.7

[a]Conditions: 220 ºC, 25bar N_2, 30wt% Glycerol, Water/Methanol=1.2, 3wt% catalyst, 500RPM, 8 hours, Catalyst: 2wt% Pd on Cu/Mg/Al = 22.5/67.5/10 40wt% Glycerol.

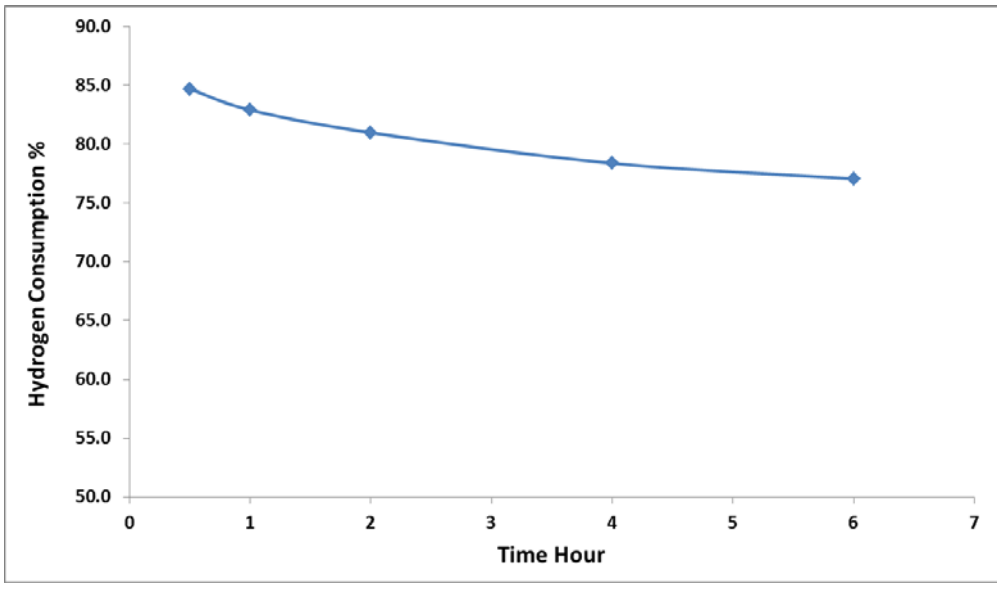

Figure 5-43 Hydrogen Consumption. Conditions: 220 ºC, 3wt% Catalyst, 500RPM, 6 hours reaction time, water to methanol molar ratio is 1.2, 30wt% of glycerol added.

From Figure 5-43 and Table 5-23, it can be seen that around 77% to 85% of the hydrogen is consumed by hydrogenation. The H_2 consumption decreases along the reaction from 85% to 77%, since at the beginning of the reaction, the concentration of acetol is higher, and hence the hydrogenation rate is higher. As the reaction proceeds, the acetol concentration decreases, therefore, the hydrogen consumption becomes lower.

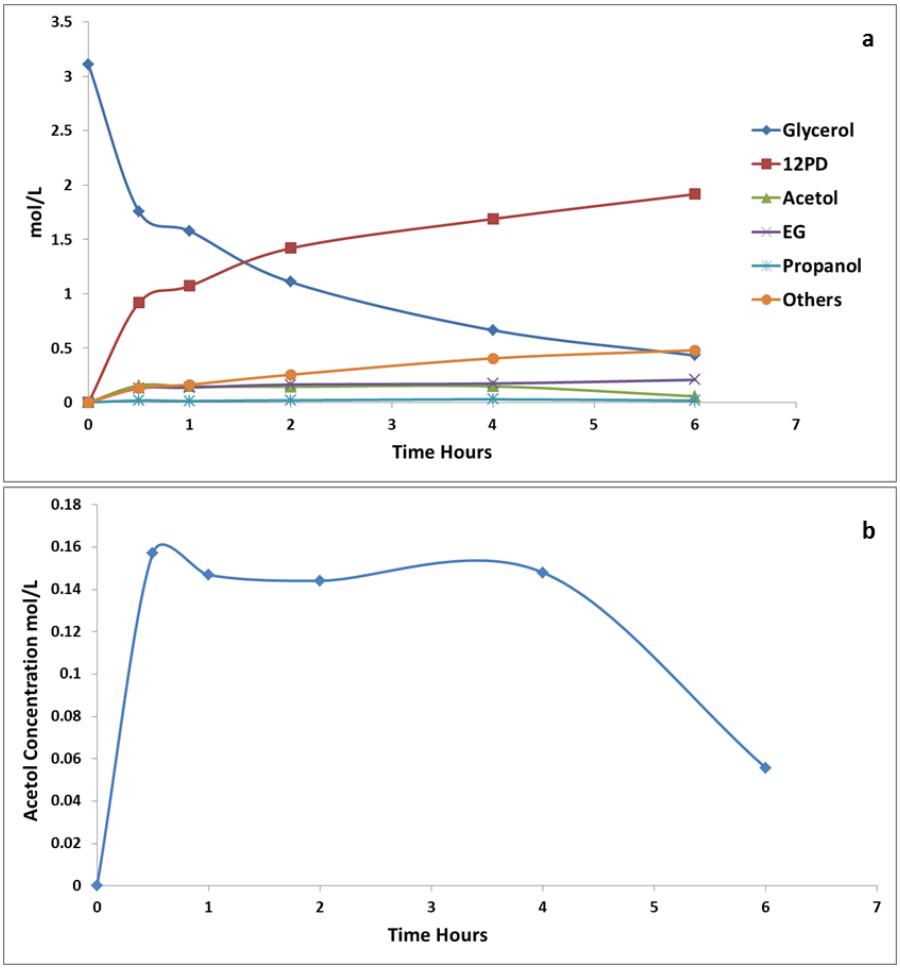

Figure 5-44 Concentration Profile of Each Product for Glycerol Hydrogenolysis Using the H_2 Produced by Methanol Steam Reforming: a) All the Products; b) Acetol. Conditions: 220ºC, 3wt% catalyst, 500RPM, 6 hours, water to methanol molar ratio is 1.2, 30wt% of Glycerol Added.

Figure 5-44 shows the concentration profile of each product over the reaction time, it can be observed that the concentration of acetol increases first and then slowly

decreases; the decreasing acetol concentration decreases the hydrogen consumption rate.

5.4.5 Glycerol Hydrogenolysis Using *in situ* Hydrogen Produced via Methanol Steam Reforming with Molecular Hydrogen Initially Added

It has been discussed that a lower hydrogen production rate is one of the reasons for the low 1,2PD selectivity especially during the early stages of the reaction. An experiment with hydrogen added initially with methanol steam reforming was carried out to investigate the improvement in the 1,2PD selectivity. The experimental procedure was: hydrogen was used to flush the air out of the reactor, and then at room temperature, 25bar of hydrogen was charged into the reactor. The reaction conditions were: 220ºC, 7wt% catalyst loaded, 500RPM, 6 hours reaction time, with a water to methanol molar ratio of 1.2, and with 40wt% of aqueous glycerol added. Figure 5-45 and Table 5-24 show the experimental results and the comparison with those when molecular hydrogen was continuous fed at the same temperature without methanol steam reforming in Section 4.11.

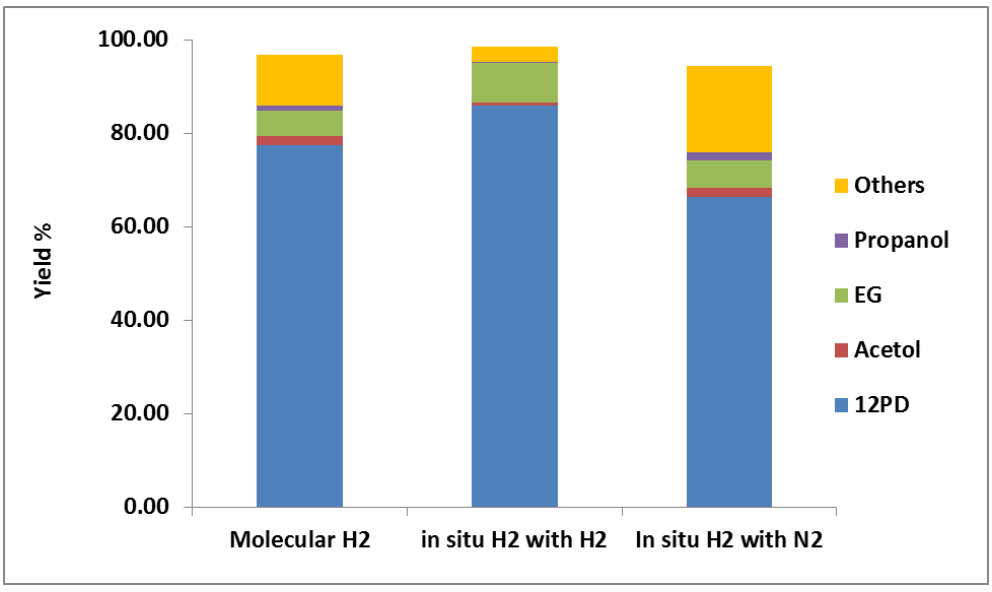

Figure 5-45 Comparison between Molecular Hydrogen and in situ Hydrogen. Molecular H_2: 220**ºC,** 400psi H_2, 500RPM, 5wt% catalyst with respect to glycerol weight, 50% aqueous glycerol, 24 hours; in situ H_2: 7wt% Catalyst, 40wt% Glycerol, W/M = 1.2, 6 hours 25bar H_2 initially; Catalyst: 2wt% Pd on $Cu/MgO/Al_2O_3$

Table 5-24 Effect of Initial Hydrogen Gas on Product Distribution[a]

	Glycerol Conversion	1,2PD Selectivity	1,2PD Yield	Acetol Yield	EG Yield	PrOH Yield	Others Yield
Molecular H_2	96.87	80.03	77.52	1.83	5.52	1.11	10.88
In situ H_2 with H_2	98.64	87.18	85.99	0.58	8.47	0.36	3.24
In situ H_2 with N_2	94.98	69.91	66.40	2.02	5.82	1.76	18.98

[a]Conditions: Molecular H_2: 220**°C,** 400psi H_2, 500RPM, 5wt% catalyst with respect to glycerol weight, 50% aqueous glycerol, 24 hours; in situ H_2: 7wt% Catalyst, 40wt% Glycerol, W/M = 1.2, 6 hours, 25bar H_2 initially; Catalyst: 2wt% Pd on $Cu/MgO/Al_2O_3$

From Table 5-24 and Figure 5-45, it can be seen that at the same temperature, when molecular hydrogen is used, the 1,2PD selectivity (80.03%) is lower than that when in situ hydrogen is used with molecular hydrogen initially added (87.18%). It also can be seen that with molecular hydrogen at 220°**C**, around 10.88% of byproducts was formed but with in situ hydrogen, the yield of byproducts was only 3.2%. This is possibly because the in situ hydrogen generated from methanol steam reforming can exist in the form of adsorbed hydrogen atom facilitating the acetol hydrogenation step. Therefore, it can more effectively hydrogenate the acetol avoiding side reactions occure.

5.5 Effect of Ni on $Cu/MgO/Al_2O_3$ Catalyst

It was discussed in Section 5.2 that when Ni was added onto a $Cu/ZnO/Al_2O_3$ catalyst, the 1,2PD selectivity was improved but the glycerol conversion was lower. In this section, different amounts of Ni were added into a $Cu/MgO/Al_2O_3$ catalyst (1mole% and 5mole%), the results are shown in Figure 5-46 and Table 5-25.

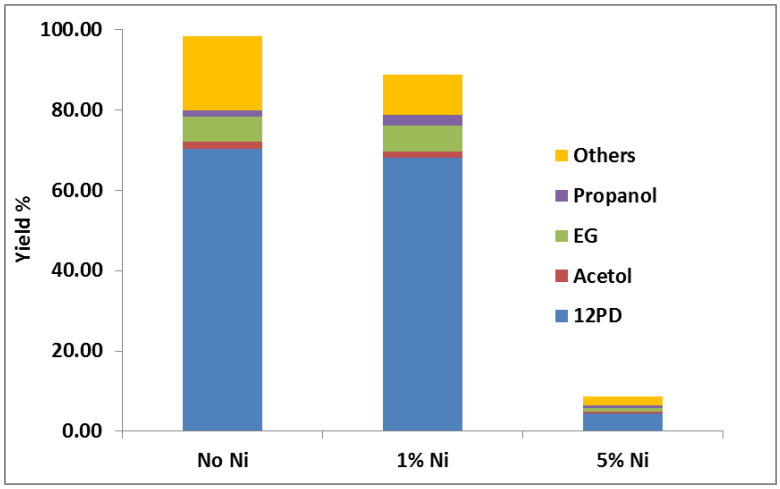

Figure 5-46 Effect of Ni on Cu/MgO/Al_2O_3 Catalyst on Product Distribution. Conditions: 220ºC, 5wt% catalyst, 500RPM, 6 hours, water to methanol molar ratio is 1.2, 30wt% of glycerol added. Catalyst: 10mole% Aluminum, Cu/Mg = 1/3, 25bar N_2.

Table 5-25 Effect of Ni on Cu/MgO/Al_2O_3 Catalyst on Product Distribution[a]

	Glycerol Conversion	1,2PD Selectivity	1,2PD Yield	Acetol Yield	EG Yield	PrOH Yield	Others Yield
No Ni	97.29	72.26	70.30	1.70	6.27	1.69	18.33
1mole% Ni	88.73	76.73	68.08	1.49	6.46	2.80	9.91
5mole% Ni	8.70	50.48	4.39	0.48	0.82	0.73	2.27

[a]Conditions: 220ºC, 5wt% catalyst, 500RPM, 6 hours, water to methanol molar ratio is 1.2, 30wt% of glycerol added. Catalyst: 10mole% Aluminum, Cu/Mg = 1/3, 25bar N_2.

It is noticed that the same trend to that observed when Ni/Cu/ZnO/Al_2O_3 is used when 1mole% Ni is loaded, and the 1,2PD selectivity is improved from 72.3% to 76.7%, but the glycerol conversion drops from 97.3% to 88.7% and the glycerol conversion over the reaction time is always lower than that without Ni loaded (Figure 5-47a). The yield of un-desired by-products is also reduced from 18.3% to 9.9% and the acetol yield is also lower with 1mole% Ni loaded (Figure 5-47d). However, when the Ni amount is increased to 5mole%, the glycerol conversion is only 8.7% and the selectivity to 1,2PD is 50.5%; the catalyst is almost completely deactivated by adding 5mole% Ni. It is found from the NH_3 TPD results that by adding Ni, the number of

acidic sites is reduced; when 5mole% Ni is added, and the acidic sites are completely eliminated. A detailed acidity analysis will be provided in Section 6.1. Since the acidic sites are important for glycerol dehydration, the addition of Ni might result in a lower glycerol conversion.

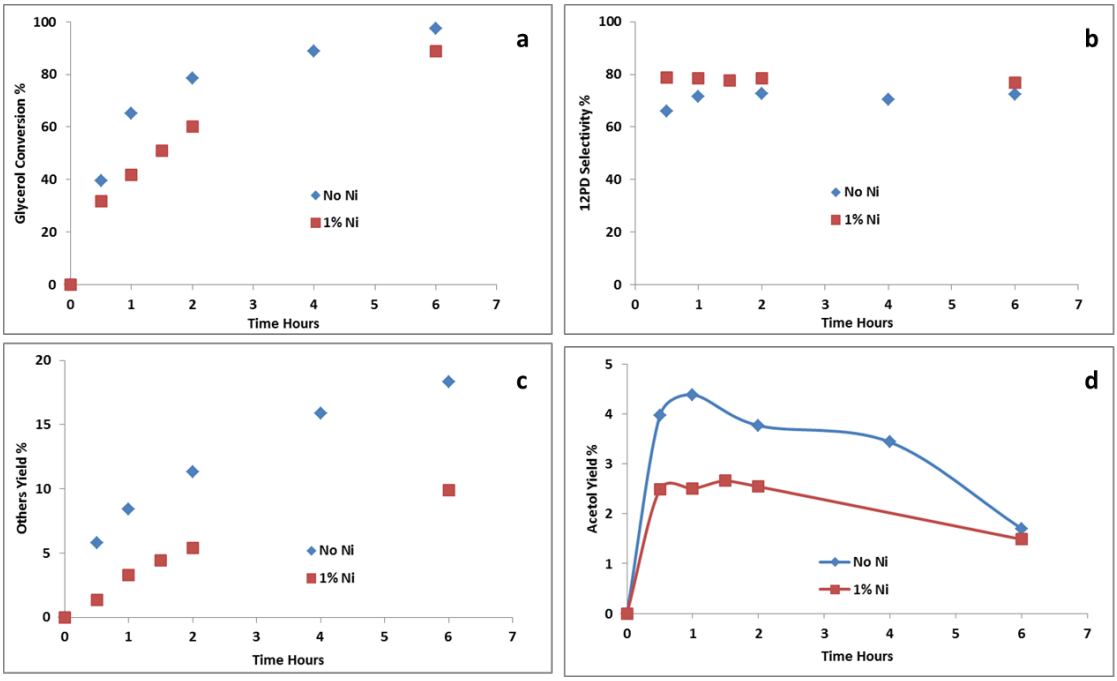

Figure 5-47 Effect of Ni on Cu/MgO/Al_2O_3 Catalyst Activity: a) Glycerol Conversion; b)1,2PD Selectivity; c) Others Yield d) Acetol Yield. Conditions: 220ºC, 25bar N_2, 30wt% Glycerol, Water/Methanol=1.2, 5wt% catalyst, 500RPM, 6 hours, Catalyst: 10mole% Aluminum, Cu/Mg = 1/3.

5.6 Cu/MgO/Ga_2O_3 Catalyst

It was reported by Bienholz *et al.* in 2010 that Ga can prevent Cu/ZnO catalyst deactivation [80]; and also it was reported that Ga could improve the Cu/ZnO catalyst stability in a methanol steam reforming process [176]; therefore, in this section Ga was loaded onto a Cu/MgO catalyst to investigate the effect on the catalytic activity and stability.

5.6.1 Activity Comparison between $Cu/MgO/Al_2O_3$ and $Cu/MgO/Ga_2O_3$

10 mole% of gallium was loaded onto the Cu/MgO catalyst to replace Al. The preparation procedures were described in Section 3.1. The experimental results are shown in Figure 5-48.

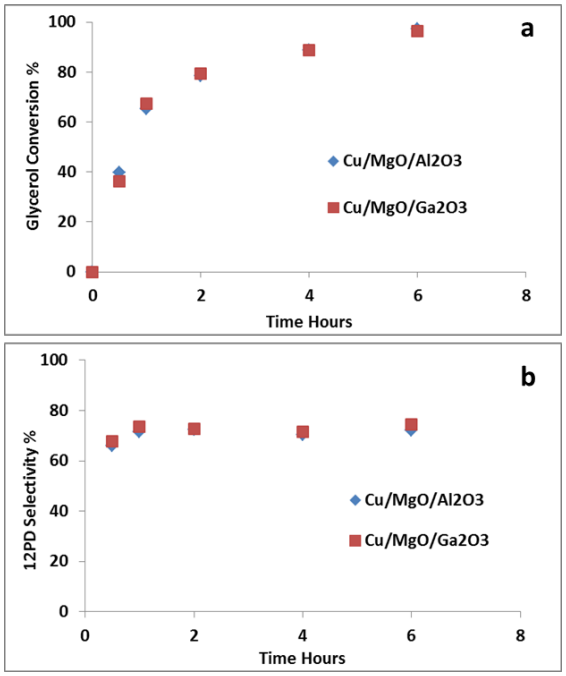

Figure 5-48 Effect of Ga on Cu/MgO Catalyst Activity. Conditions: 220ºC, 25bar N_2, 30wt% Glycerol, Water/Methanol=1.2, 5wt% catalyst, 500RPM, 6 hours, Catalyst: Cu/Mg/Al = 22.5/67.5/10, Cu/Mg/Ga = 22.5/67.5/10.

As shown in Figure 5-48, no obvious difference is observed on glycerol conversion and 1,2PD selectivity ove the reaction time. The final glycerol conversion and 1,2PD selectivity using $Cu/MgO/Al_2O_3$ after 6 hours are 97.3% and 72.3 respectively, and the final glycerol conversion and 1,2PD selectivity using $Cu/MgO/Ga_2O_3$ are 96.5% and 74.5% respectively; the yields of all the other by-products using both catalysts are very similar as listed in Table 5-26. Therefore, no significant improvement of catalytic activity is observed by replacing Al by Ga.

Table 5-26 Product Distribution Comparison between $Cu/MgO/Al_2O_3$ and $Cu/MgO/Ga_2O_3$[a].

	Glycerol Conversion	1,2PD Selectivity	1,2PD Yield	Acetol Yield	EG Yield	PrOH Yield	Others Yield
$Cu/MgO/Al_2O_3$	97.29	72.26	70.30	1.70	6.27	0.69	18.33
$Cu/MgO/Ga_2O_3$	96.49	74.51	71.90	1.77	6.39	0.00	16.43

[a]Conditions: 220ºC, 25bar N_2, 30wt% Glycerol, Water/Methanol=1.2, 5wt% catalyst, 500RPM, 6 hours, Catalyst: Cu/Mg/Al = 22.5/67.5/10 and Cu/Mg/Ga = 22.5/67.5/10.

5.6.2 Effect of Ga on Cu/MgO Catalyst Stability

The $Cu/MgO/Ga_2O_3$ catalyst was recycled and reused to investigate the stability of the catalyst. The glycerol conversion and 1,2PD selectivity during the reaction time are shown in Figure 5-49. It can be seen from Figure 5-49a that the glycerol conversion is lower when the catalyst is recycled, as shown in Table 5-27, with about a 7% to 9% glycerol conversion drop every time the catalyst is recycled. The 1,2PD selectivity during the reaction time drops significantly from 74.5% to 57.1% when the catalyst is recycled the first time; as the catalyst is further recycled, the decrease in 1,2PD selectivity is only about 3% to 4% every time the catalyst is recycled as shown in Figure 5-49b and Table 5-27. It is found that fresh catalyst is significantly deactivated during the first cycle of reaction, and when the catalyst is further recycled and reused, the deactivation becomes less significant.

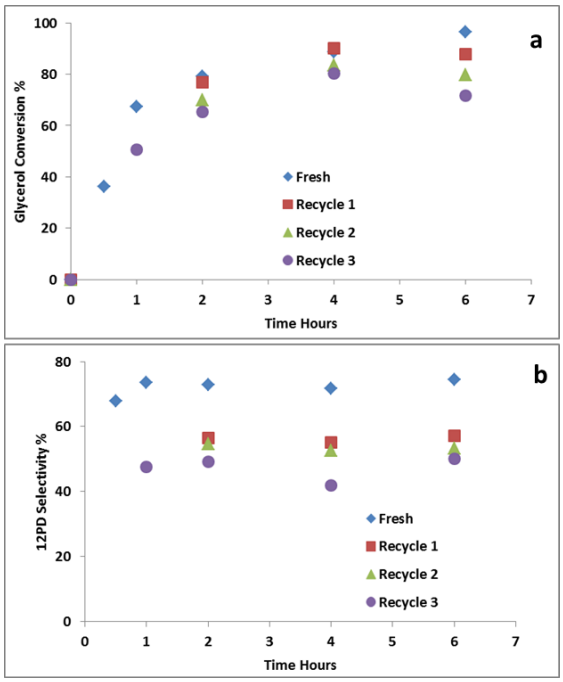

Figure 5-49 Study of Cu/MgO/Ga_2O_3 Catalyst Stability. Conditions: 220ºC, 25bar N_2, 30wt% Glycerol, Water/Methanol=1.2, 5wt% catalyst, 500RPM, 6 hours, Catalyst: Cu/Mg/Ga = 22.5/67.5/10.

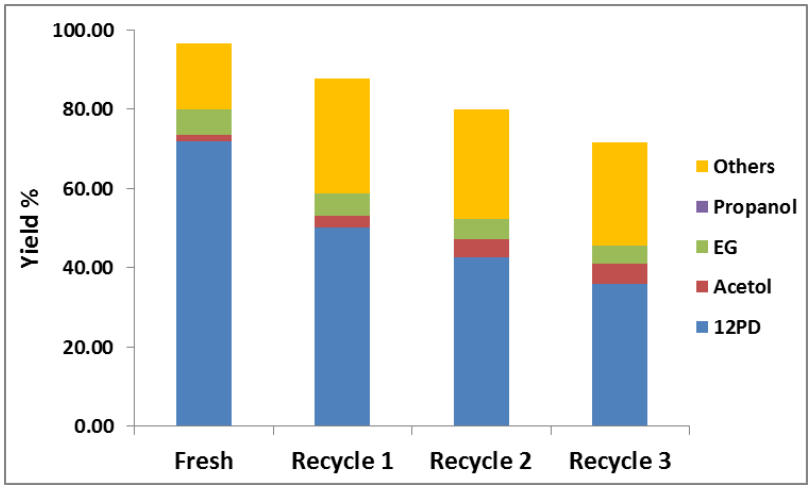

Figure 5-50 Products Yield Using the Fresh and Recycled Cu/MgO/Ga_2O_3 Catalyst. Conditions: 220ºC, 25bar N_2, 30wt% Glycerol, Water/Methanol=1.2, 5wt% catalyst, 500RPM, 6 hours, Catalyst: Cu/Mg/Ga = 22.5/67.5/10.

Table 5- 27 Product Yield Using the Fresh and Recycled Cu/MgO/Ga_2O_3 Catalyst[a].

	Glycerol Conversion	1,2PD Selectivity	1,2PD Yield	Acetol Yield	EG Yield	PrOH Yield	Others Yield
Fresh	96.44	74.49	71.84	1.76	6.40	0.00	16.45
Recycle 1	87.66	57.13	50.08	2.85	5.67	0.00	29.05
Recycle 2	80.00	53.18	42.54	4.65	5.06	0.00	27.75
Recycle 3	71.63	50.08	35.87	5.15	4.41	0.00	26.20

[a]Conditions: 220ºC, 25bar N_2, 30wt% Glycerol, Water/Methanol=1.2, 5wt% catalyst, 500RPM, 6 hours, Catalyst: Cu/Mg/Ga = 22.5/67.5/10.

5.7 Effect of Pd on Cu/MgO/Ga_2O_3

2wt% Pd was also loaded onto the Cu/MgO/Ga_2O_3 catalyst to investigate the selectivity promoting effect of Pd on the reaction products; the results are compared with the Pd loaded onto Cu/MgO/Al_2O_3 catalyst. The glycerol conversion and 1,2PD are shown in Figure 5-51.

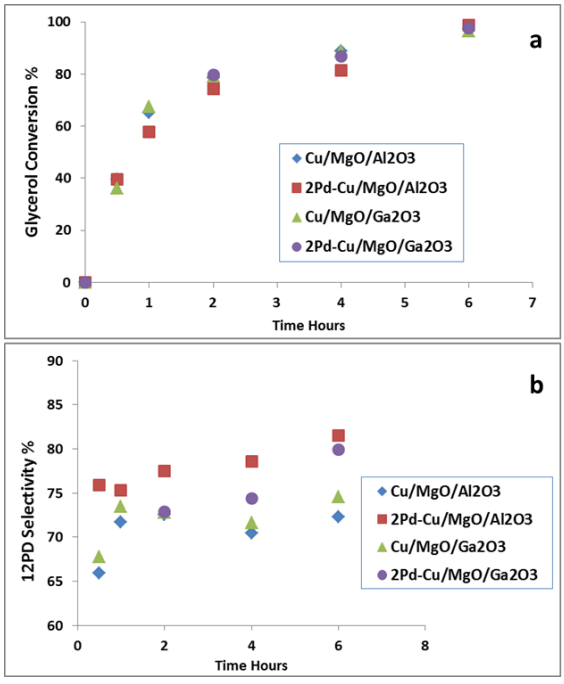

Figure 5-51 Effect of Pd on Cu/MgO/Al_2O_3 and Cu/MgO/Ga_2O_3 Catalyst Activity: a) Glycerol Conversion; b) 1,2PD Selectivity. Conditions: 220ºC, 25bar N_2, 30wt% Glycerol, Water/Methanol=1.2, 5wt% catalyst, 500RPM.

It can be seen that Pd loading does not significantly improve the glycerol conversion during the reaction (Figure 5-51a); the 1,2PD selectivity can be improved by loading 2wt% Pd on both Cu/MgO/Al_2O_3 and Cu/MgO/Ga_2O_3 catalysts as shown in Figure 5-51b. By comparing the Cu/MgO/Al_2O_3 and Cu/MgO/Ga2O3 with 2wt% Pd loaded, no obvious activity improvement is observed (Table 5-28).

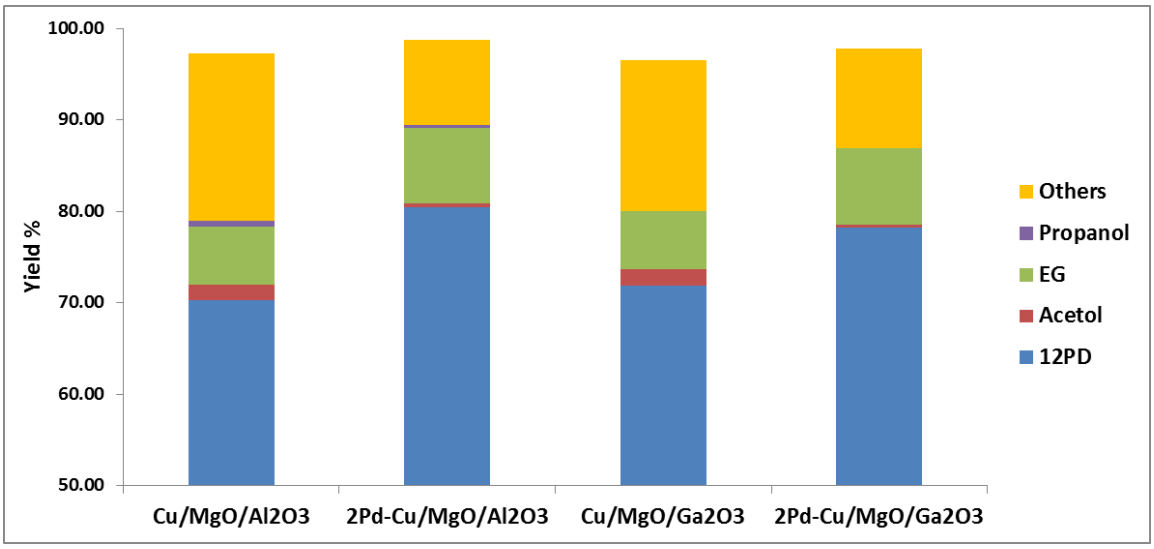

Figure 5-52 Effect of Pd on the Products Yield Using Cu/MgO/Al_2O_3 and Cu/MgO/Ga_2O_3 Catalysts. Conditions: 220ºC, 25bar N_2, 30wt% Glycerol, Water/Methanol=1.2, 5wt% catalyst, 500RPM, 6 hours reaction time.

Table 5-28 Effect of Pd on Product Yield Using Cu/MgO/Al_2O_3 and Cu/MgO/Al_2O_3 as Supports[a].

	Glycerol Conversion	1,2PD Selectivity	1,2PD Yield	Acetol Yield	EG Yield	PrOH Yield	Others Yield
Cu/MgO/Al_2O_3	97.29	72.26	70.30	1.70	6.27	0.69	18.33
2Pd-Cu/MgO/Al_2O_3	98.74	81.50	80.47	0.43	8.18	0.32	9.34
Cu/MgO/Ga_2O_3	96.49	74.51	71.90	1.77	6.39	0.00	16.43
2Pd-Cu/MgO/Ga_2O_3	97.79	79.93	78.17	0.39	8.34	0.00	10.90

[a]Conditions: 220ºC, 25bar N_2, 30wt% Glycerol, Water/Methanol=1.2, 5wt% catalyst, 500RPM, 6 hours reaction time.

5.8 Investigation of the Effects of Experimental Conditions by Factorial Design Using a Pd-Cu/MgO/Al_2O_3 Catalyst

A series of factorial designed experiments were carried out and a statistical analysis was conducted in this section to investigate the effect of different factors on the experimental results and the interactions between two factors.

5.8.1 Advantages of Factorial Design

It is believed that many factors can possibly affect the catalyst activity; nevertheless, only a limited number of experiments can be carried out. A factorial design is a powerful technique to investigate the effect of different factors on the experimental system. Generally in a factorial experimental design, experimental trials are carried out at all combination of factor levels. Therefore, it can efficiently examine a number of factors which may possibly affect the catalyst activity by a reduced number of experiments. Compared to the unvariate (one factor at a time) method in which only one experimental factor is changed while the remaining ones are held constant, the factorial experiments combine all levels of one factor with all levels of another factor and can detect both single factor effects and multi-factor-interactions.

5.8.2 Experimental Methods

In this section, seven factors are investigated which are: reaction temperature, catalyst loading, glycerol concentration, Pd loading, stirring speed, nitrogen pressure and water to methanol molar ratio. Two levels of each factor were used which were coded as +1 (high) and -1 (low); the reaction conditions for high level and low level are shown in Table 5-29. A full factorial design for seven factors requires 2^7 experiments which are 128 experiments. To make an efficient fractional factorial design, the concept of design resolution is a useful way to catalog fractional factorial design.

Since only two factor interaction study is necessary in this case a resolution IV design was used which no main effect was aliased with any other main effect or two-factor interactions, but two-factor interactions were aliased with each other. To investigate the two-factor interactions, only main effect interactions were investigated. The criteria for the fractional experimental design are listed in Table 5-30 [177].

Table 5-29 Experimental Conditions for High Level (-1) Middle Level (0) and Low Level (-1) for a Fractional Factorial Design.

Conditions	-1	0	1
Temperature (°C)	200	220	240
Catalyst wt%	3	5	7
Glycerol Concentration	20	30	40
Pd Loading wt%	0	1	2
Stirring Speed RPM	400	500	600
Nitrogen Pressure bar	15	25	35
Water to Methanol Molar Ratio	1	1.2	1.4

A 1/8 2^7 fractional design was carried out in this study which included 16 experiments. 4 factors were chosen as the main factors for a 2^4 full factorial design which were reaction temperature (A), catalyst loading (B), glycerol concentration (C) and Pd loading (D). The other 3 factors were generated by: E (stirring speed) = ABC, F (N_2 pressure) = BCD and G (water to methanol molar ratio) = (ACD). Five responses were investigated, which were glycerol conversion, 1,2PD selectivity, 1,2PD yield, EG yield, and yield of other by-products. The experiments at 0 conditions (middle level) were repeated 3 times to test the repeatability of the experiment and to estimate some statistical parameters such as standard deviation, variance, sum of square and mean square. The two-factor interactions were also estimated by simply multiplying the codings of the two factors. Only two-factor interactions among the main factors were investigated which were AB, AC, AD, BC, BD, CD interactions. The full factorial design and the experimental results are shown in Table 5-31.

Table 5-30 Criteria for a Fractional Factorial Design [177]*

Number of Factors k	Fraction	Number of Runs	Design Generators	Number of Factors k	Fraction	Number of Runs	Design Generators
3	2_{III}^{3-1}	4	$C = \pm AB$	10			$H = \pm ABCG$
4	2_{IV}^{4-1}	8	$D = \pm ABC$				$J = \pm ACDE$
5	2_{V}^{5-1}	16	$E = \pm ABCD$		2_{V}^{10-3}	128	$K = \pm ACDF$
	2_{III}^{5-2}	8	$D = \pm AB$				$G = \pm BCDF$
			$E = \pm AC$				$H = \pm ACDF$
6	2_{VI}^{6-1}	32	$F = \pm ABCDE$				$J = \pm ABDE$
	2_{IV}^{6-2}	16	$E = \pm ABC$		2_{IV}^{10-4}	64	$K = \pm ABCE$
			$F = \pm BCD$				$F = \pm ABCD$
	2_{III}^{6-3}	8	$D = \pm AB$				$G = \pm ABCE$
			$E = \pm AC$				$H = \pm ABDE$
			$F = \pm BC$				$J = \pm ACDE$
7	2_{VII}^{7-1}	64	$G = \pm ABCDEF$		2_{IV}^{10-5}	32	$K = \pm BCDE$
	2_{IV}^{7-2}	32	$E = \pm ABC$				$E = \pm ABC$
			$G = \pm ABDE$				$F = \pm BCD$
	2_{IV}^{7-3}	16	$E = \pm ABC$				$G = \pm ACD$
			$F = \pm BCD$				$H = \pm ABD$
			$G = \pm ACD$				$J = \pm ABCD$
	2_{III}^{7-4}	8	$D = \pm AB$		2_{III}^{10-6}	16	$K = \pm AB$
			$E = \pm AC$	11			$G = \pm CDE$
			$F = \pm BC$				$H = \pm ABCD$
			$G = \pm ABC$				$J = \pm ABF$
8	2_{V}^{8-2}	64	$G = \pm ABCD$				$K = \pm BDEF$
			$H = \pm ABEF$		2_{IV}^{11-5}	64	$L = \pm ADEF$
	2_{IV}^{8-3}	32	$F = \pm ABC$				$F = \pm ABC$
			$G = \pm ABD$				$G = \pm BCD$
			$H = \pm BCDE$				$H = \pm CDE$
	2_{IV}^{8-4}	16	$E = \pm BCD$				$J = \pm ACD$
			$F = \pm ACD$				$K = \pm ADE$
			$G = \pm ABC$		2_{IV}^{11-6}	32	$L = \pm BDE$
			$H = \pm ABD$				$E = \pm ABC$
9	2_{VI}^{9-2}	128	$H = \pm ACDFG$				$F = \pm BCD$
			$J = \pm BCEFG$				$G = \pm ACD$
	2_{IV}^{9-3}	64	$G = \pm ABCD$				$H = \pm ABD$
			$H = \pm ACEF$				$J = \pm ABCD$
			$J = \pm CDEF$				$K = \pm AB$
	2_{IV}^{9-4}	32	$F = \pm BCDE$		2_{III}^{11-7}	16	$L = \pm AC$
			$G = \pm ACDE$				
			$H = \pm ABDE$				
			$J = \pm ABCE$				
	2_{III}^{9-5}	16	$E = \pm ABC$				
			$F = \pm BCD$				
			$G = \pm ACD$				
			$H = \pm ABD$				
			$J = \pm ABCD$				

*Reprinted Montgomery and Runger, Applied Statistics and Probability for Engineers, 3rd ed., pp. 560, 2003 with permission from the John Wiley & Sons, Inc.

Table 5-31 Experimental Results for the 1/8 2^7 Factorial Design.

A	B	C	D	E=ABC	F=BCD	G=ACD					
Temp	Cat wt	GL%	Pd	Stirring	P	W/M	Conv	1,2PD Sel.	1,2PD Yield	EG Yield	Others Yield
1	1	1	1	1	1	1	99.2	74.0	73.5	9.8	13.9
1	1	1	-1	1	-1	-1	100.0	39.6	39.6	4.3	52.7
1	1	-1	1	-1	-1	-1	100.0	79.7	79.7	14.2	3.8
1	1	-1	-1	-1	1	1	100.0	79.8	79.8	14.4	4.0
1	-1	1	1	-1	-1	1	93.0	44.3	41.2	5.3	43.5
1	-1	1	-1	-1	1	-1	86.2	30.5	26.3	4.0	51.8
1	-1	-1	1	1	1	-1	99.0	82.0	81.1	11.7	4.3
1	-1	-1	-1	1	-1	1	100.0	73.4	73.4	9.0	15.2
-1	1	1	1	-1	1	-1	82.1	78.8	64.7	5.9	9.9
-1	1	1	-1	-1	-1	1	78.1	67.7	52.8	3.9	18.7
-1	1	-1	1	1	-1	1	88.7	85.8	76.1	11.4	0.5
-1	1	-1	-1	1	1	-1	79.8	85.1	68.0	7.9	2.2
-1	-1	1	1	1	-1	-1	98.6	41.2	40.6	5.4	49.6
-1	-1	1	-1	1	1	1	51.9	51.1	26.5	2.4	17.7
-1	-1	-1	1	-1	1	1	69.0	85.4	59.0	7.2	2.4
-1	-1	-1	-1	-1	-1	-1	61.3	79.4	48.7	5.2	5.5
0	0	0	0	0	0	0	96.2	81.7	78.7	8.2	8.0
0	0	0	0	0	0	0	98.2	82.1	80.6	9.1	7.7
0	0	0	0	0	0	0	98.8	81.5	80.5	8.2	9.4

5.8.3 Main Effect by Each Factor

The main effect of one factor is the difference between the average response at the high level of this factor and the average response at the low level of this factor. For instance, the main effect of temperature on glycerol conversion is calculated to be the average value of the glycerol conversions at high temperature (8 trials when the temperature is high) minus the average value of the glycerol conversion at low temperature as shown in Equation 5-10.

$$Temperature\_Effect\_GL-Conversion=\frac{\sum Conv.\_at\_high\_temp}{8}-\frac{\sum Conv.\_at\_low\_temp}{8}$$

$$=\frac{99.2+100+100+100+93+86.2+99+100}{8}-\frac{82.1+78.1+88.7+79.8+98.6+51.9+69+61.3}{8}=21.0$$

Equation 5-10

The main effects of all factors are listed in Table 5-32.

Table 5-32 Main Effects by All Factors and Two Factor-Interactions.

	Effect		Conversion	1,2PD Selectivity	1,2PD Yield	EG Yield	Others Yield
A	Temperature	240	97.2	62.9	61.8	9.1	23.6
		200	76.2	71.8	54.6	6.2	13.3
		Effect	21.0	-8.9	7.3	2.9	10.4
B	Catalyst Weight	7%	91.0	73.8	66.8	9.0	13.2
		3%	82.4	60.9	49.6	6.3	23.7
		Effect	8.6	12.9	17.2	2.7	-10.5
C	GL%	40%	86.1	53.4	45.7	5.1	32.2
		20%	87.2	81.3	70.7	10.1	4.7
		Effect	-1.1	-27.9	-25.1	-5.0	27.5
D	Pd Loading	With	91.2	71.4	64.5	8.9	16.0
		Without	82.2	63.3	51.9	6.4	21.0
		Effect	9.0	8.1	12.6	2.5	-5.0
E	Stirring	600	89.7	66.5	59.9	7.8	19.5
		400	83.7	68.2	56.5	7.5	17.4
		Effect	5.9	-1.7	3.3	0.3	2.1
F	Pressure	35 bar	83.4	70.9	59.9	7.9	13.3
		25 bar	90.0	63.9	56.5	7.3	23.7
		Effect	-6.6	7.0	3.3	0.6	-10.4
G	W/M	1.4	85.0	70.2	60.3	7.9	14.5
		1	88.4	64.5	56.1	7.3	22.5
		Effect	-3.4	5.7	4.2	0.6	-8.0
AB	Temp/Cat weight	+1	85.0	66.3	55.9	7.9	18.7
		-1	88.4	68.5	60.5	7.4	18.2

		Effect	-3.3	-2.2	-4.5	0.5	0.4
AC	Temp/GL%	+1	84.7	65.5	54.0	6.9	21.6
		-1	88.7	69.2	62.3	8.4	15.4
		Effect	-4.0	-3.7	-8.3	-1.5	6.2
AD	Temp/Pd	+1	82.8	70.4	58.9	7.6	13.7
		-1	90.6	64.3	57.4	7.7	23.2
		Effect	-7.8	6.1	1.5	-0.2	-9.6
BC	Cat weight/GL%	+1	86.1	72.5	61.6	7.1	15.3
		-1	87.3	62.2	54.8	8.1	21.6
		Effect	-1.2	10.4	6.8	-1.0	-6.3
BD	Cat weight/Pd	+1	83.7	69.1	58.6	7.7	14.8
		-1	89.7	65.6	57.8	7.5	22.2
		Effect	-6.0	3.5	0.9	0.2	-7.4
CD	GL%/Pd	+1	89.3	69.5	61.2	7.9	18.0
		-1	84.1	65.2	55.1	7.4	19.0
		Effect	5.2	4.3	6.1	0.5	-1.0

To investigate which factor(s) has (have) significant effect(s) on each response, normal probability plots of the effects was used. The expected normal value (y-axis) was obtained based on the normal probability of each effect given by the relationship $\frac{(i-0.5)}{n}$ where i was the order of each factor and n was the total number of effects. The effects that are not significant will fall along a line; on the other hand, the significant effects will deviate from the straight line. Figure 5-53 illustrates the normal plot of all the effects for all the responses.

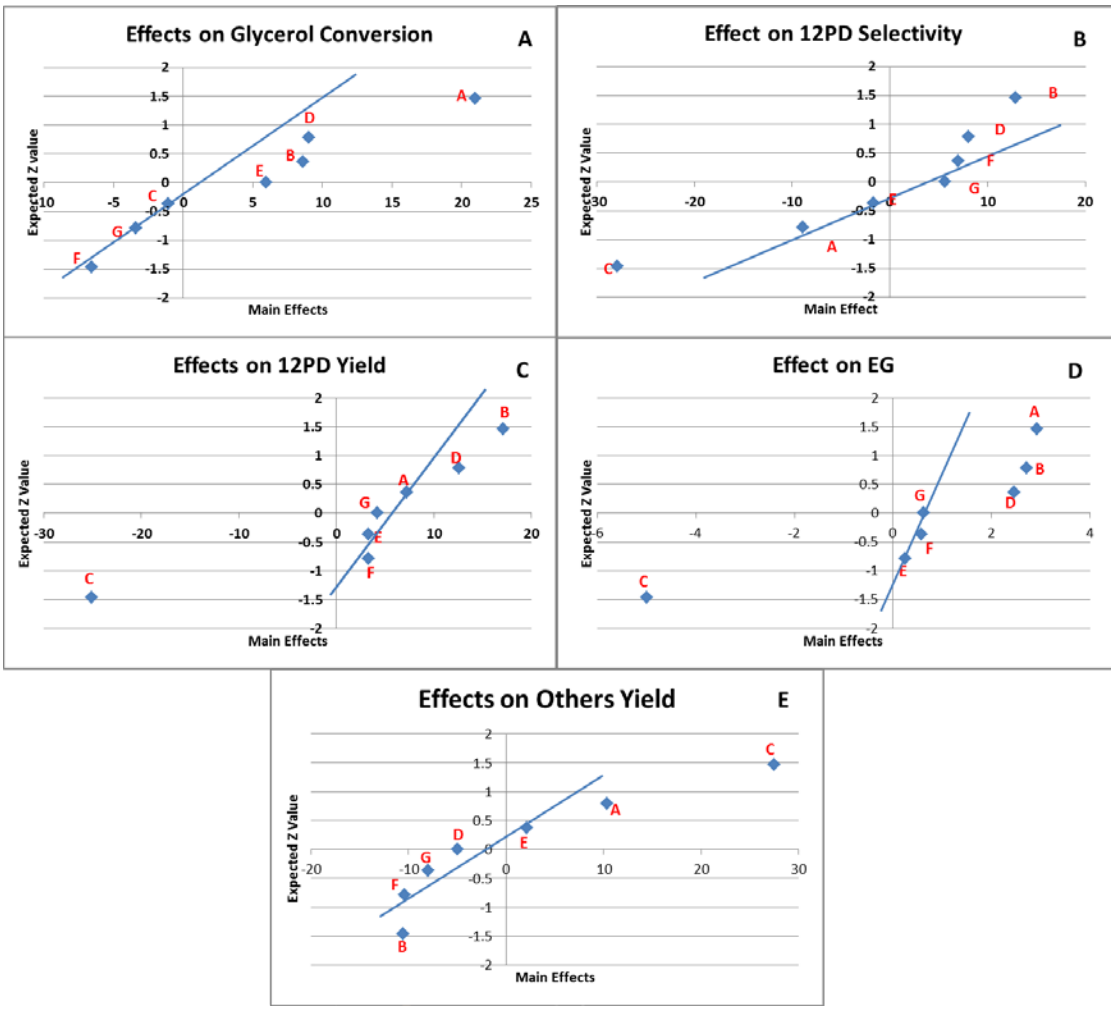

Figure 5-53 The Normal Plot of Effects: A) Effects on Glycerol Conversion, B) Effects on 1,2PD Selectivity, C) Effects on 1,2PD Yield, D) Effects on EG Yield and E) Effects on Others Yield.

In Figure 5-53A, the main effects of A, B, D, E are significant for glycerol conversion which are temperature, catalyst weight, palladium loading and stirring. Among them, temperature (A) has the most significant effect on glycerol conversion. When the temperature is increased from 200°C to 240°C, the average glycerol conversion increases significantly. The palladium loading (D) also has an important effect on glycerol conversion; this is possibly because palladium can increase the methanol steam reforming conversion to more effectively hydrogenate acetol. The effect of catalyst loading on glycerol conversion is also expected since more catalyst loading will provide more active sites; therefore, the reaction rate might be higher.

Figure 5-53B and Figure 5-53C show that B, D and C have significant effects on 1,2PD selectivity and yield, which are catalyst weight, palladium loading and glycerol concentration. Glycerol concentration has the most significant effect on 1,2PD selectivity and yield and it has a negative effect. When glycerol concentration is higher, the rate of glycerol dehydration is faster and the acetol concentration will be higher; also when the glycerol concentration is high the concentration of water and methanol will be lower and the amount of hydrogen produced via methanol steam reforming will be possibly lower; thus, the insufficient amount of hydrogen and higher acetol concentration will cause lower 1,2PD selectivity and 1,2PD yield. The catalyst weight also has a significant effect on 1,2PD selectivity and yield. The reason might be that when more catalyst is loaded, more active sites will be available for methanol steam reforming; therefore, more hydrogen can be produced to rapidly hydrogenate the acetol. Pd loading has a positive effect on 1,2PD selectivity and yield since Pd can promote methanol steam reforming to produce more hydrogen and also improve the catalysts activity for acetol hydrogenation as discussed in Section 5.4.

Figure 5-53D shows that A, B, D and C have significant effects on EG yield, which are temperature, catalyst weight, palladium loading and glycerol concentration. Higher temperature (A), higher catalyst weight (B) and palladium loading (D) can improve the activity of the catalyst for methanol steam reforming reactions; more hydrogen will be produced to facilitate the C-C bond cleavage, therefore, possibly causing a higher EG yield. Glycerol concentration (A) has a negative effect on EG yield, possibly since the rate of a side reaction between acetol and ethylene glycol is high when the glycerol concentration is high [99].

Figure 5-53E shows that B (catalyst weight) and C (glycerol concentration) have significant effects on the yield of other by-products. This can be explained in an opposite way to the main effect on 1,2PD selectivity. When 1,2PD selectivity is lower, the yield of the other by-products will be higher.

5.8.4 Two Factor Interactions

A two-factor interaction indicates whether the effect of one factor on a response depends upon the level of another factor. The interaction effect can be calculated as the difference between the

average effect of one factor at the high level of the other factor and the average effect of one factor at the low level of the other factor. Therefore, if the lines of two factors are parallel, there is no interaction. On the contrary, when the lines significantly deviate from being parallel, there is an interaction between these two factors. The results of the two-factor interactions are shown in Figure 5-54 to Figure 5-58.

From Figure 5-54, it can be observed that temperature x palladium loading and glycerol feed concentration x palladium loading have significant interactions on glycerol conversion. In Figure 5-54C, when the temperature is increased from 200°C to 240°C, the increase of glycerol conversion for the catalyst without palladium is must faster than that with palladium. At 240°C the average glycerol conversion is over 96% for both catalysts and at 200°C the average glycerol conversion for the catalyst with Pd loading is much higher than that without Pd loading. Therefore, the increase of glycerol conversion for the catalyst with Pd loading is not as fast as the one without Pd loading. If glycerol conversion is the only response being considered, at high temperature, the loading of Pd becomes less necessary since it is an expensive metal. In Figure 5-54F, a significant interaction between glycerol feed concentration and palladium loading on glycerol conversion is observed. With palladium loading, when the glycerol concentration is increased from 20wt% to 40wt%, the glycerol conversion does not change significantly since the glycerol concentration does not affect the glycerol conversion significantly as observed in Figure 5-53A. Without palladium loading, a significant drop of glycerol conversion occurs. This is possibly because Pd can promote methanol steam reforming to produce more hydrogen to rapidly hydrogenate the acetol; hence the equilibrium of the glycerol dehydration reaction will be shifted in the forward direction. Therefore, for lower glycerol concentration, Pd loading is not essential to obtain a higher glycerol conversion. However, when the glycerol concentration is increased, the improvement of glycerol conversion by loading palladium will become more significant.

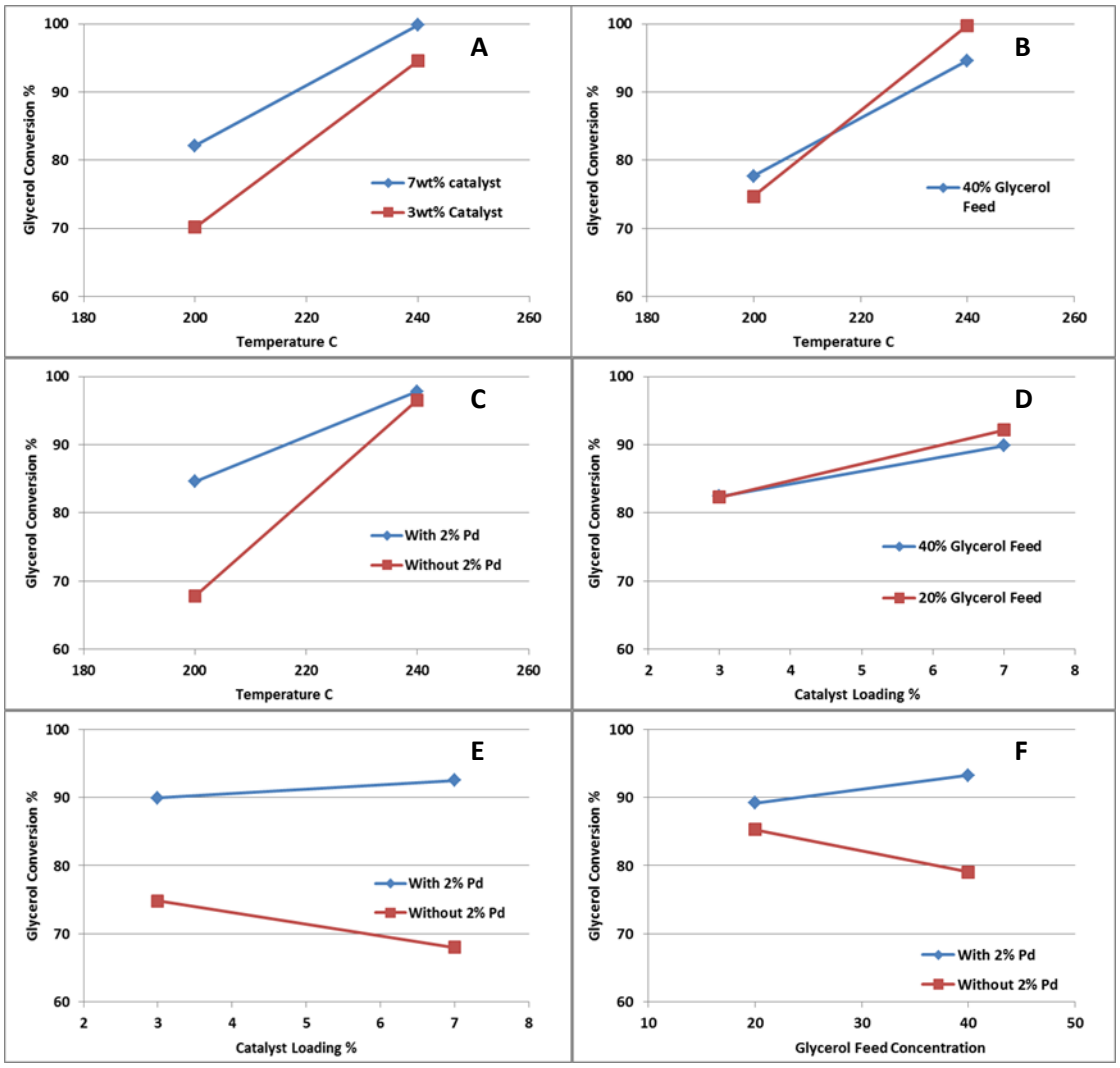

Figure 5-54 Two-Factor Interactions on Glycerol Conversion: A) Catalyst Weight x Temperature, B) Temperature x Glycerol Concentration, C) Temperature x Palladium Loading, D) Catalyst Weight x Glycerol Concentration, E) Catalyst Weight x Palladium Loading, F) Glycerol Concentration x Palladium Loading.

Figure 5-55 illustrates the two-factor interactions on 1,2PD selectivity, which is a very important response for the glycerol hydrogenolysis process. It can be observed that palladium loading x temperature (Figure 5-55C), catalyst weight x glycerol feed concentration (Figure 5-55D) and catalyst weight x palladium loading (Figure 5-55E) have significant interactions on 1,2PD selectivity. As shown in Figure 5-55C, with Pd loading, when the temperature is increased from 200°C to 240°C, the 1,2PD selectivity does not change significantly; without Pd loading, the 1,2PD selectivity is significantly lower when the temperature is higher. As shown in Table 5-32, temperature has a negative effect on 1,2PD selectivity; therefore, at high temperature Pd needs to be loaded if high selectivity to 1,2PD is desired; this is because at higher temperature, more hydrogen is needed to obtain a high 1,2PD selectivity as discussed in Section 4.11. Figure 5-55D shows that the glycerol feed concentration and catalyst weight have a significant interaction for 1,2PD selectivity. When only 20wt% glycerol is fed, the 1,2PD selectivity does not change significantly when the catalyst loading is increased from 3% to 7%; the selectivity to 1,2PD is over 80%. When 40wt% glycerol is fed, the selectivity to 1,2PD is significantly lower since the glycerol feed concentration is the main effect on 1,2PD selectivity as discussed in Section 5.8.3. However, more catalyst weight can significantly improve the 1,2PD selectivity when the glycerol feed concentration is high. In Figure 5-55E, it can be observed that the palladium loading and catalyst weight also have a significant interact on 1,2PD selectivity. When no palladium is loaded, the selectivity to 1,2PD does not change significantly when the catalyst weight is increased from 3wt% to 7wt% and they were all very low; when palladium is loaded; the more catalyst loaded, the higher selectivity to 1,2PD.

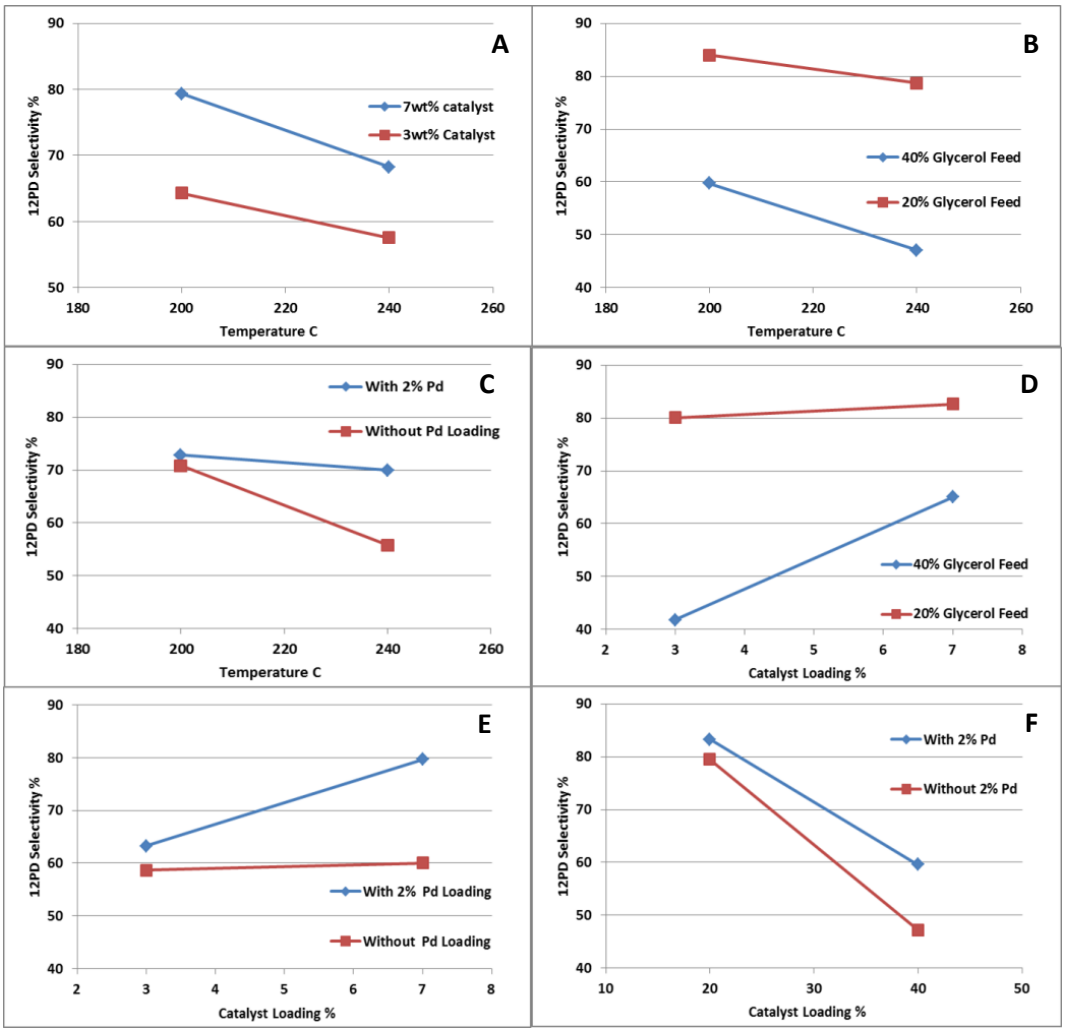

Figure 5-55 Two-Factor Interactions on 1,2PD Selectivity: A) Catalyst Weight x Temperature, B) Temperature x Glycerol Concentration, C) Temperature x Palladium Loading, D) Catalyst Weight x Glycerol Concentration, E) Catalyst Weight x Palladium Loading, F) Glycerol Concentration x Palladium Loading.

Figure 5-56 shows the 2-factor interactions on 1,2PD yield. Figure 5-56A shows that the catalyst weight and temperature have a significant interaction on 1,2PD yield. When the temperature is increased from 200°C to 240°C, if 3wt% catalyst is used, the increase of 1,2PD yield is much higher than when 7wt% catalyst is used. In Figure 5-56B, it can be observed that temperature and glycerol feed concentration also have a significant interaction on 1,2PD yield. When the temperature is increased from 200°C to 240°C, the 1,2PD yield increases much more when 20wt% of glycerol is fed than that when 40wt% glycerol is fed, however when the glycerol feed concentration is high, high temperature does not improve the yield of 1,2PD.

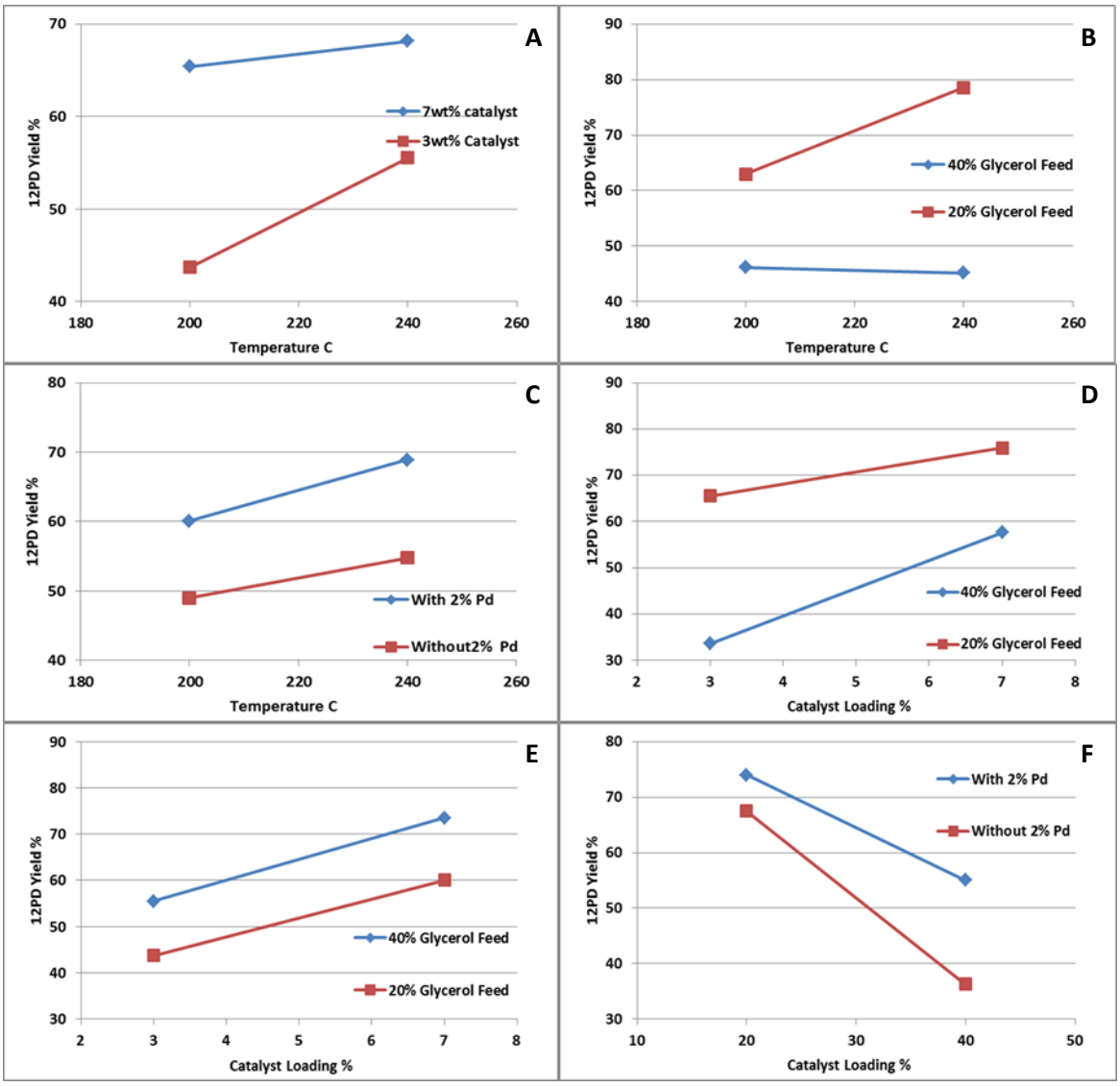

Figure 5-56 Two-Factor Interactions on 1,2PD Yield: A) Catalyst Weight x Temperature, B) Temperature x Glycerol Concentration, C) Temperature x Palladium Loading, D) Catalyst Weight x Glycerol Concentration, E) Catalyst Weight x Palladium Loading, F) Glycerol Concentration x Palladium Loading.

From Figure 5-57, only catalyst weight and glycerol feed concentration have a significant interaction on EG yield. It can be observed that when the glycerol concentration is low (20wt%), as catalyst weight is increased from 3wt% to 7wt%, and the EG yield increases much faster than that when the glycerol concentration is high (40%). This is possibly because at a lower glycerol concentration, more active sites can be provided for C-C cleavage to produce more EG.

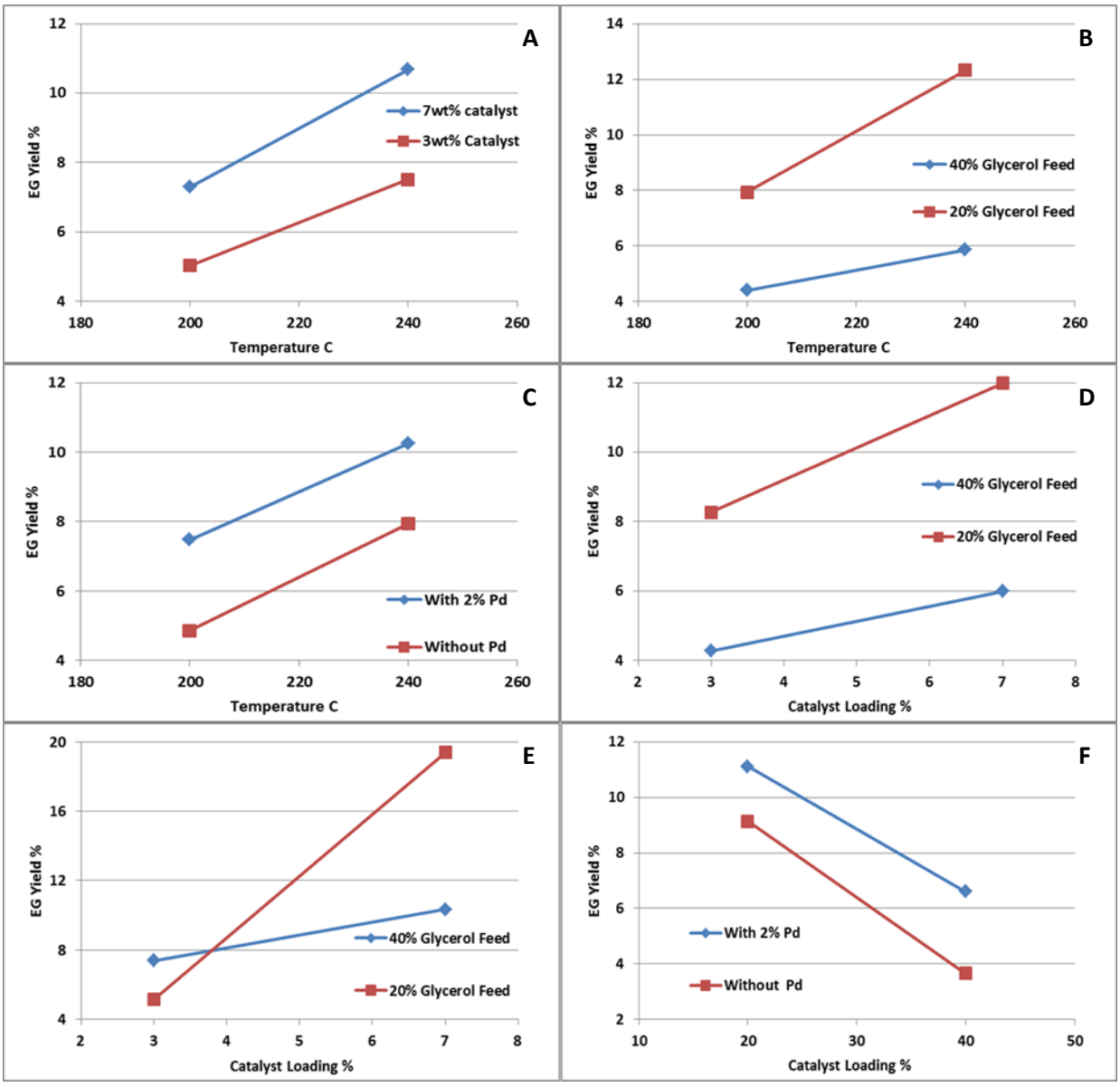

Figure 5-57 Two-Factor Interactions on EG Yield: A) Catalyst Weight x Temperature, B) Temperature x Glycerol Concentration, C) Temperature x Palladium Loading, D) Catalyst Weight x Glycerol Concentration, E) Catalyst Weight x Palladium Loading, F) Glycerol Concentration x Palladium Loading.

Figure 5-58 shows the two-factor interactions on the yield of other undesired by-products. In Figure 5-58B, it can be observed that the temperature and glycerol feed concentration interaction has a significant effect on the yield of other by-products. Temperature has a negative effect on 1,2PD selectivity as discussed in Section 5.8.3; therefore, more by-products will be formed when the temperature is increased. When the glycerol feed concentration is 40%, if the temperature is

increased from 200°C to 240°C, the increase in yield of other by-products was much more than that when the glycerol feed concentration is 20%. Therefore, temperature has more effect on the by-product yield when the glycerol feed concentration is high. Figure 5-58C shows that the palladium loading and temperature interaction also have a significant effect on by-products yield. When no Pd is loaded, if the temperature is increased from 200°C to 240°C, the other by-products increases more rapidly than with Pd loaded. It can be observed that with Pd loaded, the yield of other by-products stays stable at a very low level. Therefore, Pd can provide high selectivity even at high temperature.

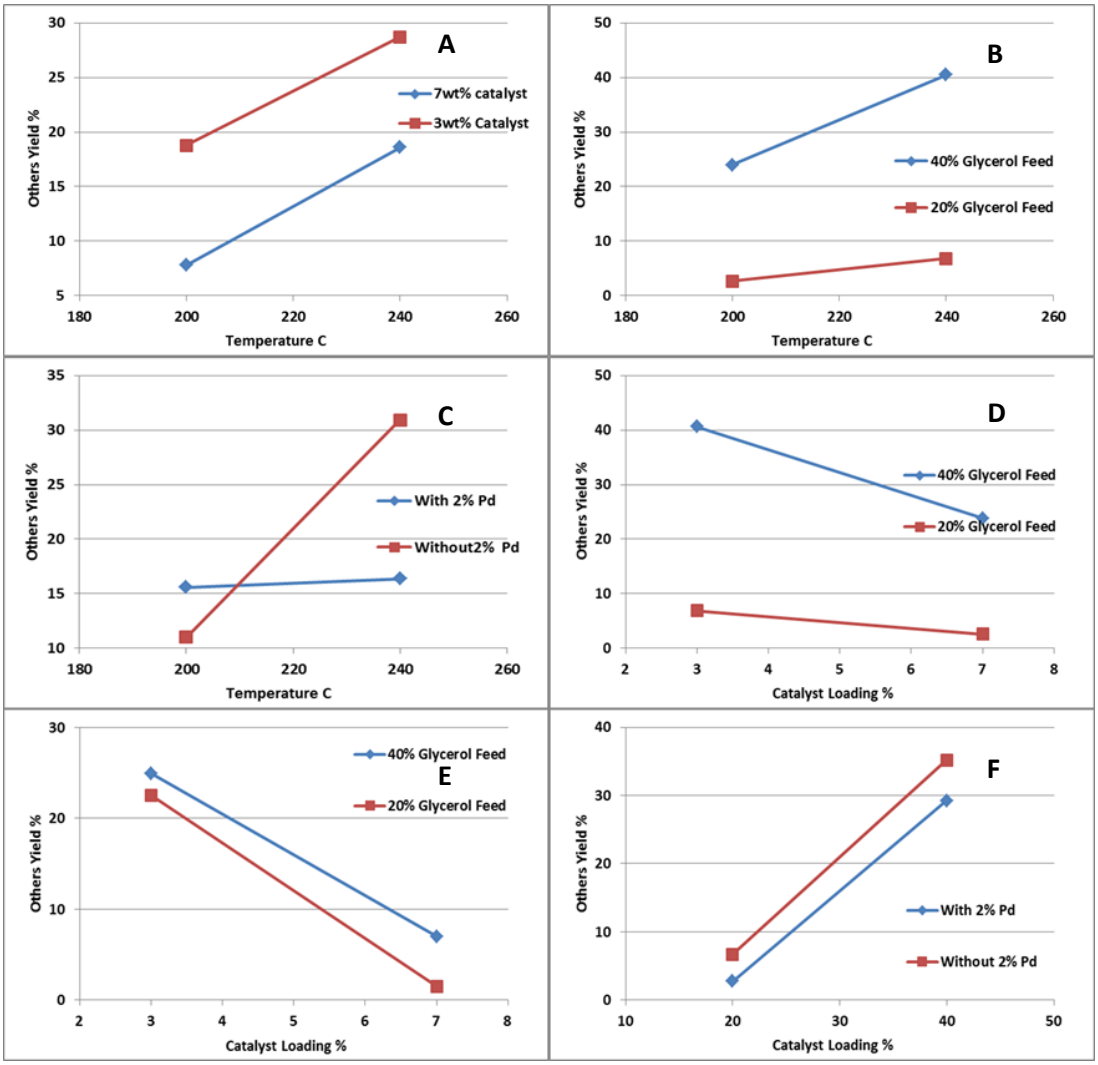

Figure 5-58 Two-Factor Interactions on others Yield: A) Catalyst Weight x Temperature, B) Temperature x Glycerol Concentration, C) Temperature x Palladium Loading, D) Catalyst Weight x Glycerol Concentration, E) Catalyst Weight x Palladium Loading, F) Glycerol Concentration x Palladium Loading.

5.9 Conclusion

In this Chapter, experiments of glycerol hydrogenolysis using *in situ* hydrogen produced via methanol steam reforming have been reported.

The activities of the $Cu/ZnO/Al_2O_3$ catalysts prepared by different methods were determined using a batch autoclave. The experimental results showed that the catalyst prepared by oxalate gel-coprecipitation had the best catalytic activity for glycerol conversion and 1,2PD selectivity. Different Cu/Zn/Al molar ratios have been investigated to determine the optimum composition of the catalyst; it was found that the best metal molar ratio was Cu/Zn/Al = 35/35/30.

Ni was added onto a $Cu/ZnO/Al_2O_3$ catalyst to investigate its promoting effect on catalytic activity. From the experimental results, it was seen that with Ni loaded, the 1,2PD selectivity was improved and the glycerol conversion was lower than that without Ni loaded. It was found that by adding Ni, more hydrogen was produced via methanol steam reforming to improve the 1,2PD selectivity; on the other hand, the addition of Ni had a negative effect on the glycerol dehydration reaction resulting in a lower glycerol conversion. From the experimental results using the $Ni/ZnO/Al_2O_3$ catalyst without Cu added, no glycerol conversion was observed suggesting that Ni was not active for glycerol dehydration. Hence Cu was the active site for the glycerol dehydration reaction.

$Cu/MgO/Al_2O_3$ catalysts prepared by oxalate gel-coprecipitation were also studied for glycerol hydrogenolysis using *in situ* hydrogen produced via methanol steam reforming. A composition study has been conducted and the optimum metal molar ratio was determined to be 22.5/67.5/10, which corresponded to Cu/Mg = 1/3 (molar) and 10mole% aluminum. Compared with the $Cu/ZnO/Al_2O_3$, $Cu/MgO/Al_2O_3$ catalysts this catalyst gave a higher glycerol conversion and a better 1,2PD selectivity under the same experimental conditions. It was also found that the glycerol concentration significantly affected the 1,2PD selectivity; when the glycerol concentration was higher, the 1,2PD selectivity was lower due to less hydrogen being produced via methanol steam reforming.

Ni was added onto a $Cu/MgO/Al_2O_3$ catalyst to investigate the promoting effect on the catalytic activity. With only 1mole% Ni loaded, the glycerol conversion was lower than that without Ni

loaded and 1,2PD selectivity was slightly improved; it was interesting to note that when the Ni loading was increased to 5mole%, the catalyst was almost completely inactive.

Pd was added onto a $Cu/MgO/Al_2O_3$ catalyst to investigate the promoting effect on the catalytic activity. It was found that Pd significantly improved the 1,2PD selectivity especially when the glycerol concentration was high.

Ga was added to a Cu/MgO catalyst and the experimental results were compared with those using a $Cu/MgO/Al_2O_3$ catalyst. No obvious improvement on the catalytic activity was observed. Since Ga is more expensive than Al, no further studies were carried out to study the effects of different parameters on the catalyst with Ga loading.

$Cu/ZnO/Al_2O_3$, $Cu/MgO/Al_2O_3$ and $Cu/MgO/Ga_2O_3$ catalysts were recycled and reused to investigate the stability of the catalysts. All the catalysts deactivated after they were recycled and reused. This might be due to the formation of carbonates when the metals were contacted with CO_2 which was formed via methanol steam reforming.

Chapter Six
Catalyst Characterization

In this chapter, the results of catalyst characterization are reported. The experiments were carried out to study the relationship between the catalyst physicochemical properties and the catalytic activities. The characterization techniques included NH_3 temperature programmed desorption (TPD), CO_2 TPD, temperature programmed reduction (TPR), H_2 TPD, **t**hermogravimetric analysis (TGA), differential thermal analysis (DTA), X-Ray diffraction (XRD), transmission electron microscopy (TEM) and Brunauer–Emmett–Teller (BET) surface area analysis.

6.1 NH_3 Temperature Programmed Desorption (TPD)

NH_3 TPD is a very useful technique to study the acidity of a catalyst. The catalyst is firstly saturated with NH_3 and then heated based on a designated thermal profile. The peaks as a function of a temperature profile can provide information on acid strength and the number of acidic sites. The number of acidic sites can be calculated based on the area of the peak and the temperature at which the desorption peaks are and they can be used to determine the acid strength of the catalyst, i.e. NH_3 can be desorbed from a stronger acidic site at a higher temperature. The detailed experimental method used was described in Section 3.5.1.

6.1.1 Effect of Catalyst Preparation Method on Catalyst Acidity

It has been shown that the catalyst preparation method plays an important role on the catalyst activity for a $Cu/ZnO/Al_2O_3$ catalyst. NH_3 TPD experiments on $Cu/ZnO/Al_2O_3$ catalysts prepared by three different methods were carried out, and the TPD profiles are shown in Figure 6-1. Based on the NH_3 desorption behavior of each catalyst as shown in Figure 6-1, the acidic sites are classified into two types, which are weak to moderate acidic sites (80ºC-420ºC) and

strong acidic sites (400ºC-790ºC). The acidic sites over different temperature ranges are listed in Table 6-1. In Figure 6-1, it can be observed that the catalyst prepared by the Na_2CO_3 coprecipitation method shows a weak desorption peak at 194ºC, which represents some weak acidic sites. The catalyst prepared by oxalate gel-coprecipitation with alumina present shows both medium acidic sites (363ºC) and strong acidic sites (676ºC); the strong acidic sites are a majority, which can improve the catalyst activity by facilitating glycerol dehydration. Similar results have been reported by Yang *et al*. in 2010 [178], and in that report it was found that for a $Cu/ZnO/Al_2O_3$ catalyst prepared by the oxalate gel-coprecipitation method two peaks at around 300ºC and 600ºC were observed; the total number of acidic sites was reported to be $0.14 mmol NH_3/g_{cat}$, which is also similar to the number of acidic sites for the $Cu/ZnO/Al_2O_3$ catalyst prepared by oxalate gel-coprecipitation method listed in Table 6-1. Without adding alumina, a desorption peak is observed at 326ºC, which is lower than the catalyst with alumina added. The large peak shown at 205ºC for the catalyst prepared by the impregnation method is mainly due to the high amount of acidic alumina used for the catalyst preparation; it has been widely reported that for an acidic alumina, the NH_3 desorption peaks are normally observed between 150ºC to 250ºC depending on the methods used [84, 179-182], which agrees with the desorption peak temperature for the $Cu/ZnO/Al_2O_3$ catalyst by impregnation as observed in Figure 6-1. According to the results, the oxalate gel-coprecipitation method can significantly improve the number of acidic sites and acidic strength; furthermore, the addition of alumina can generate a high amount of strong acidic sites.

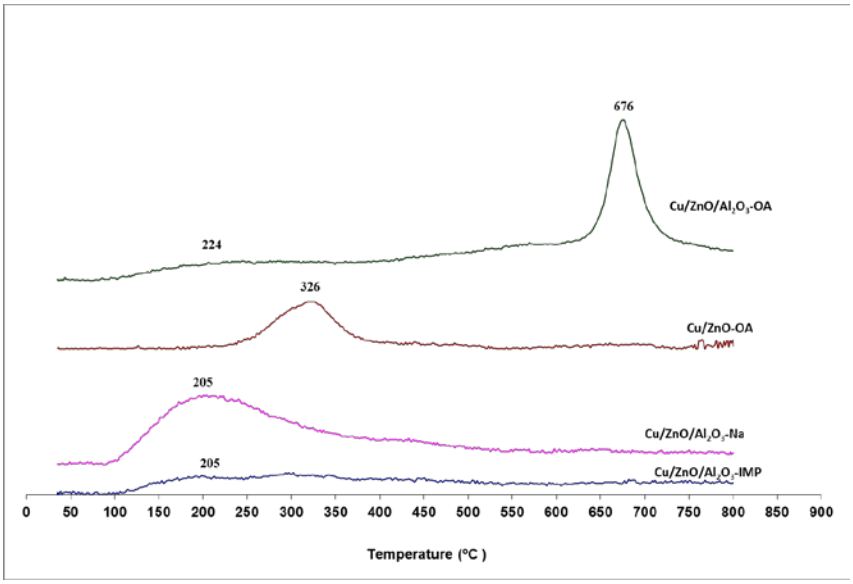

Figure 6-1 NH_3 TPD Profile for the $Cu/ZnO/Al_2O_3$ Catalyst Prepared by Different Methods.

Table 6-1 NH_3 Uptake by the $Cu/ZnO/Al_2O_3$ Catalysts Prepared by Different Methods.

Catalysts	Acidic Strength $mmmolNH_3/g_{cat}$	Total acidic sites $mmmolNH_3/g_{cat}$
$Cu/ZnO/Al_2O_3$-OA-25/25/50	0.031 (89.2-359.1°C) 0.18 (599.5-787.4°C)	0.21
Cu/ZnO-OA-50/50	0.08 (222.9-426.3°C)	0.08
$Cu/ZnO/Al_2O_3$-Na-25/25/50	0.04 (107.04-392.0°C)	0.04
$Cu/ZnO/Al_2O_3$-IMP	0.27 (94.3-542.2°C)	0.27

6.1.2 Effect of Ni on the Acidity of $Cu/ZnO/Al_2O_3$ Catalysts

In Chapter 4 and Chapter 5, it was found that with Ni added into a $Cu/ZnO/Al_2O_3$ catalyst, the glycerol conversion rate was negatively affected. NH_3 TPD experiments have been carried out using $Cu/ZnO/Al_2O_3$ (Cu/Zn/Al=35/35/30), $Ni/Cu/ZnO/Al_2O_3$ (Ni/Cu/Zn/Al=1/34.5/34.5/30) and $Ni/Cu/ZnO/Al_2O_3$ (Ni/Cu/Zn/Al=5/32.5/32.5/30) catalysts to study the effect of Ni on the acidity of $Cu/ZnO/Al_2O_3$ catalysts. As Figure 6-2 shows, three distinct peaks are observed between 51.3°C and 289.7°C, 281.7°C and 468.8°C, 589.9°C and 760.3°C, denoted as low, medium and high strength acidic sites. It can be observed that as more Ni is loaded, the number of strong acidic sites is reduced. When 1mole% of Ni is loaded, the number of strong acidic sites is about the same; if 5mole% Ni is loaded, the number of strong acidic sites is reduced from 0.075mmol/g-cat to 0.030mmol/g-cat (Table 6-2). It is apparent that when Ni is added into the

$Cu/ZnO/Al_2O_3$ mixed oxides, some acidic sites are blocked. This behavior has been reported in some reports of NH_3 TPD analysis when Ni is loaded [183]. Since the rate determining step of glycerol hydrogenolysis is the glycerol dehydration, so the loading of Ni may cause a slower reaction rate resulting in a lower glycerol conversion. According to the results discussed in Section 4.9 for the glycerol hydrogenolysis process using molecular hydrogen, when 5mole% Ni was loaded, the pseudo-first-order rate constant decreased from $2.54s^{-1}$ to $1.80s^{-1}$ which was about a 30% decrease; from the results discussed in Section 5.2.1, the glycerol conversion shows a positive relationship with the total number of strong acidic sites as shown in Figure 6-3.

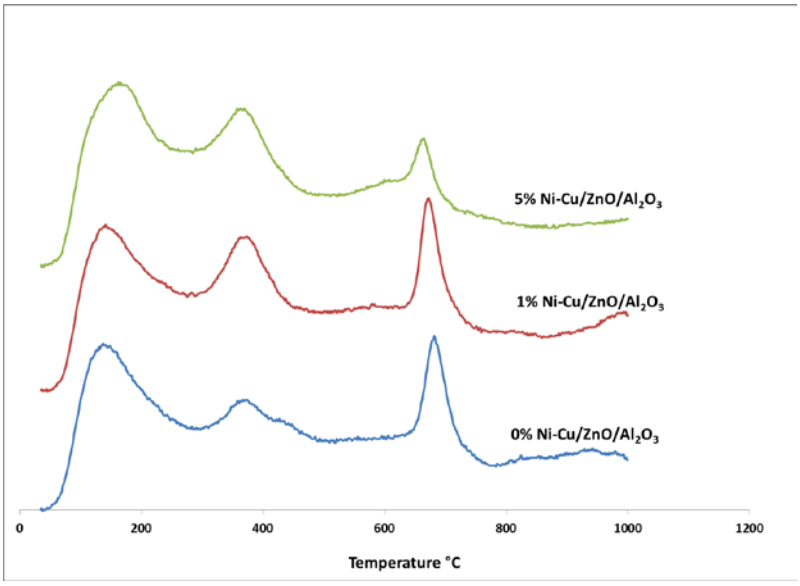

Figure 6-2 NH_3 TPD Profile for the $Cu/ZnO/Al_2O_3$ Catalyst with Different Amount of Ni Loading. Cu/Zn=1/1, 30% Al.

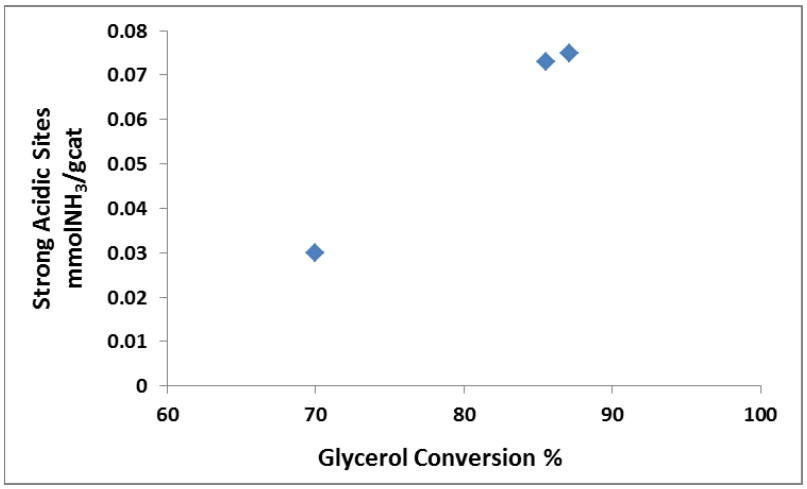

Figure 6-3 The Relationship between the Glycerol Conversion and Number of Strong Acidic Sites. Conditions: Conditions: 220 ºC, 25bar N_2, 20wt% Glycerol, Water/Methanol=1.2, 3wt% catalyst, 500RPM, 30% Al content, Cu/Zn=1, 8hours.

Table 6-2 Effect of Ni and Pd on the Acidity of a $Cu/ZnO/Al_2O_3$.

Catalysts	Desorption Temperature ℃			Total Acidic Sites	Glycerol Conversion
	$mmolNH_3/gcat$			$mmolNH_3/gcat$	%
0% $Ni-Cu/ZnO/Al_2O_3$[a]	51.3-289.7	294.9-435.1		589.9-749.3	
Uptake (mmol/gcat)	0.226	0.020	0.321	0.075	87.1
1% $Ni-Cu/ZnO/Al_2O_3$[b]	58.9-269.6	281.7-468.8		630-760.3	
Uptake (mmol/gcat)	0.198	0.076	0.347	0.073	85.5
5% $Ni-Cu/ZnO/Al_2O_3$[c]	60.2-247.8	295.4-466.2		617.3-712.0	
Uptake (mmol/gcat)	0.197	0.071	0.298	0.030	70.0
2% $Pd-Cu/ZnO/Al_2O_3$[a]	51.2-249.2	271.2-455.4		629.5-741.9	
Uptake (mmol/gcat)	0.167	0.066	0.292	0.059	94.9

[a] Cu/Zn/Al=35/35/30
[b]Ni/Cu/Zn/Al=1/34.5/34.5/30
[c]Ni/Cu/Zn/Al=5/32.5/32.5/30

6.1.3 Effect of Pd on the Acidity of $Cu/ZnO/Al_2O_3$ Catalysts

The effect of Pd loading on the acidity of Cu/ZnO/Al2O3 catalysts has been investigated as shown in Figure 6-4 and the quantification of NH_3 uptake is listed in Table 6-2. It can be observed that when 2wt% Pd is loaded, the number of strong acidic sites is reduced from 0.075mmol/g-cat to 0.059mmol/g-cat. This suggests that Pd may cover some strong acidic sites.

A desorption peak is interestingly observed between 751.9°C and 1001.6°C; however, no literature has reported that Pd can generate super acidic sites, thus it is possibly due to either an experimental error or the decomposition of a $Pd(NH_3)_x$ complex. Therefore, the promoting effect of Pd on glycerol hydrogenolysis reaction is mainly due to the improvements of the catalyst activity for methanol steam reforming and acetol hydrogenation.

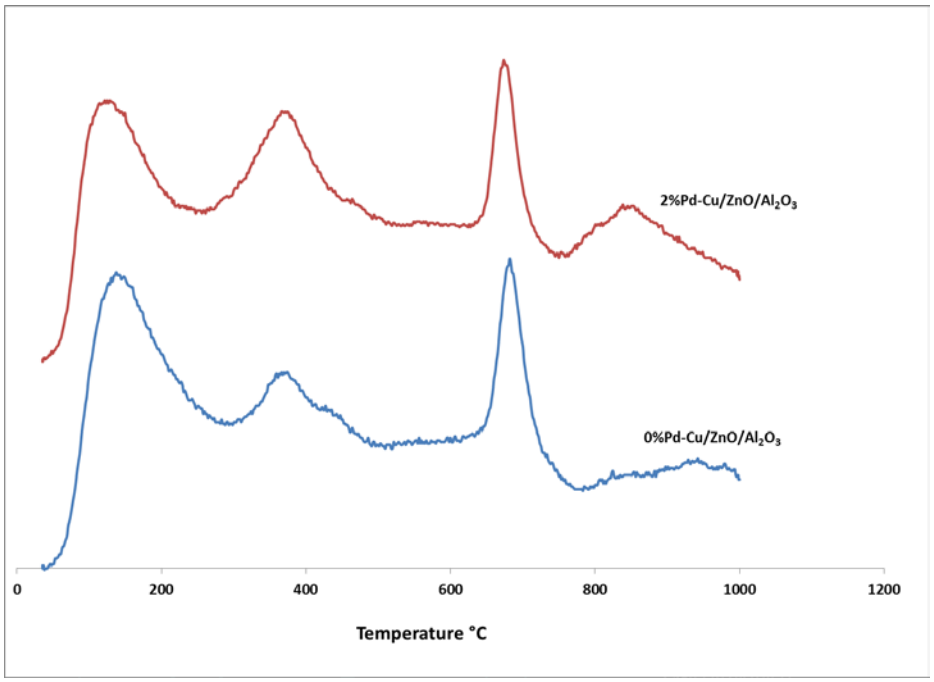

Figure 6-4 NH_3 TPD Profile for $Cu/ZnO/Al_2O_3$ and $Pd/Cu/ZnO/Al_2O_3$ Catalysts. Cu/Zn/Al=35/35/30.

6.1.4 NH_3 TPD for a $Cu/MgO/Al_2O_3$ Catalyst: Effect of Al on the Catalyst Acidity

The acidity analysis has been conducted for $Cu/MgO/Al_2O_3$ catalysts with different Al content. The experimental results are shown in Figure 6-5 and Table 6-3. If no Al is added, two peaks are observed between 314.7°C and 517.2°C representing medium acidity and strong acidity. With 10mole% alumina added, only one large peak is observed between 312.8°C and 526.9°C. This suggests that the addition of alumina can improve the mixing of Cu and Mg oxides. Also if 10mole% alumina is added, the total number of acidic sites (3.341mmol/g-cat) is higher than that when no alumina is added (2.967mmol/g-cat). However, if 30mole% alumina is added, the acidity is significantly reduced resulting in only 1.12mmol/g-cat. The reason for this might be because the medium and strong acidic sites are due to Cu; if a high amount of alumina is added,

it might block the acidic sites of Cu. As discussed in Section 5.3.2, when 10mole% Al is added, the catalyst shows the best activity among different Al contents suggesting the number of acidic sites play an important role on the catalyst activity.

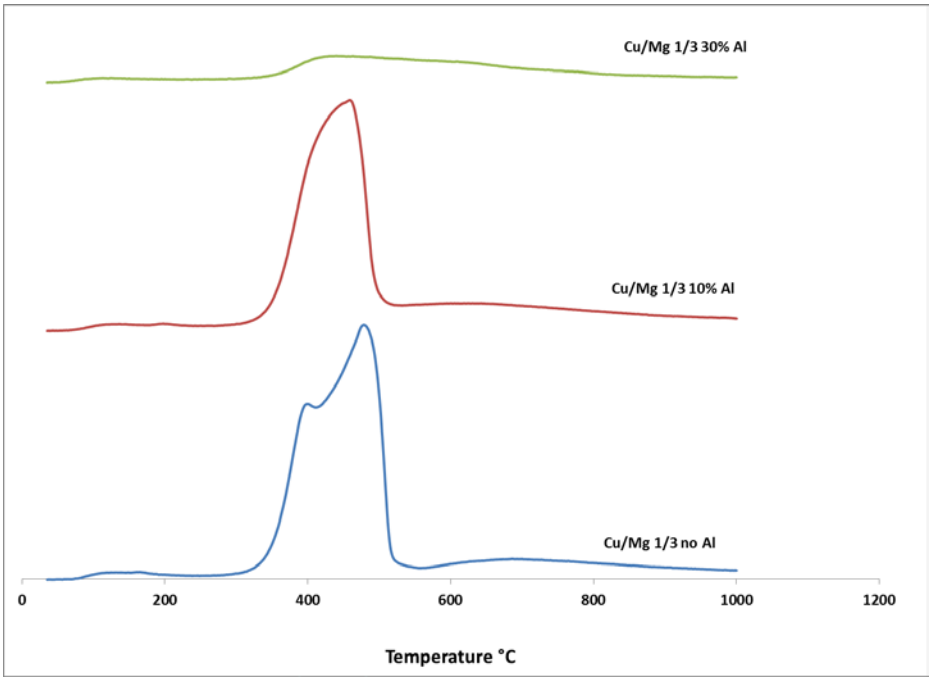

Figure 6-5 NH_3 TPD Profile for $Cu/MgO/Al_2O_3$, Effect of Al Content.

Table 6-3 Number of Acidic Site for $Cu/MgO/Al_2O_3$ Catalysts with Different Al Molar Contents.

Catalysts	Desorption Temperature °C mmolNH_3/gcat		Total Acidic Sites mmolNH_3/gcat
Cu/Mg 1/3	72.2-210.6	347.7-415.1	
Uptake (mmol/gcat)	0.065	2.902	2.967
Cu/Mg 1/3 10% Al	73.5-253.4	312.8-526.9	
Uptake (mmol/gcat)	0.070	3.270	3.341
Cu/Mg 1/3 30% Al	46.2-282.2	283.8-1001.1	
Uptake (mmol/gcat)	0.047	1.076	1.123

6.1.5 Effect of Pd on the Acidity of $Cu/MgO/Al_2O_3$ Catalysts

A NH_3 TPD experiment was carried out using 2wt% Pd supported on $Cu/MgO/Al_2O_3$ with a Cu/Mg/Al molar ratio of 22.5/67.5/10. The results are shown in Figure 6-6. It can be observed that the Pd blocks some medium acidic sites. A broad peak is observed between 270.7°C and 1003.3°C and the total acidic sites (3.89mmol/g-cat) is slightly more than that of $Cu/MgO/Al_2O_3$

(3.48mmol/g-cat) as shown in Table 6-4. The peak area at high temperature agrees with the observation of Pd loaded on $Cu/ZnO/Al_2O_3$ explained in Section 6.1.3; the NH_3 desorption at high temperature is possibly due to the formation of a $Pd(NH_3)_x$ complex which is decomposed at high temperature.

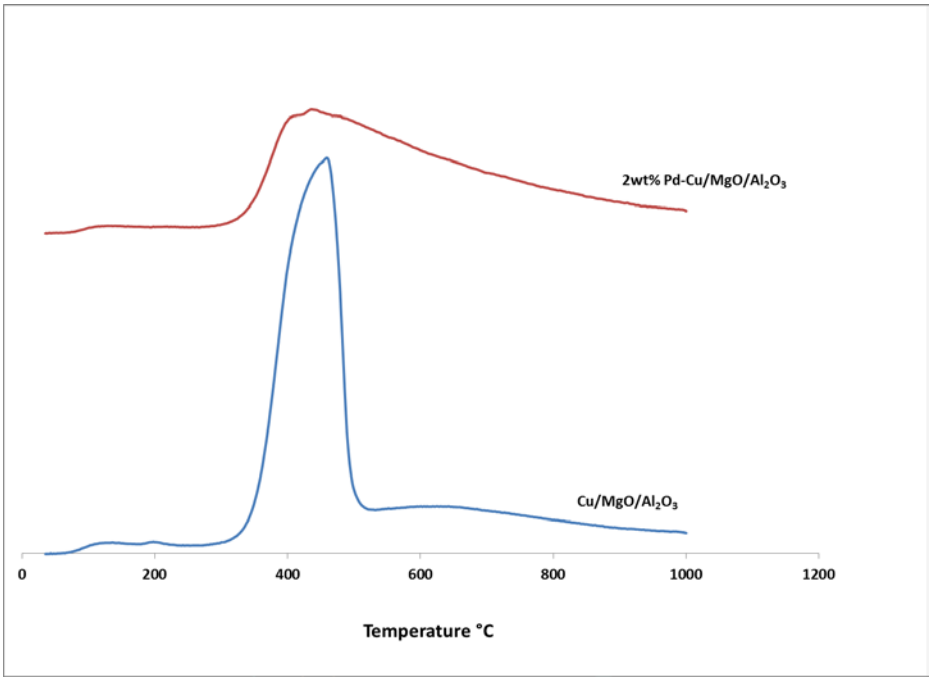

Figure 6-6 Effect of Pd on the Acidity of a $Cu/MgO/Al_2O_3$: Cu/Mg/Al = 22.5/67.5/10

Table 6-4 Effect of Pd on Number of Acidic Site for a $Cu/MgO/Al_2O_3$ Catalyst[a].

Catalysts	Desorption Temperature °C	mmolNH_3/gcat	Total Acidic Sites mmolNH_3/gcat
$Cu/MgO/Al_2O_3$	73.5-253.4	312.8-526.9	
Uptake (mmol/gcat)	0.070	3.270	3.341
2%Pd-$Cu/MgO/Al_2O_3$	69.2-284.1	270.7-1003.3	
Uptake (mmol/gcat)	0.044	3.848	3.892

[a]Cu/Mg/Al = 22.5/67.5/10

6.1.6 Effect of Ni on the Acidity of the $Cu/MgO/Al_2O_3$ Catalyst

The effect of Ni on the acidity of the $Cu/MgO/Al_2O_3$ catalyst has been investigated. As Figure 6-6 shows, when 1mole% Ni is loaded, the number of acidic sites is slightly reduced. If the Ni

loading is increased to 5mole%, the acidic sites between 356.6°C and 483.1°C are significantly reduced from 3.270mmol/g-cat to only 0.116mmol/g-cat as shown in Table 6-5. This possibly can be explained in that if Ni loading is high, it will block the acidic sites provided by Cu resulting in a low glycerol conversion as discussed in Section 5.5. When the Ni loading is increased from 0mole% to 5mole%, the glycerol conversion using the Ni/Cu/MgO/Al_2O_3 catalyst is significantly decreased from 97.3% to only 8.7%. A positive relationship between the glycerol conversion and the total number of the strong acidic sites can be observed from Figure 6-8.

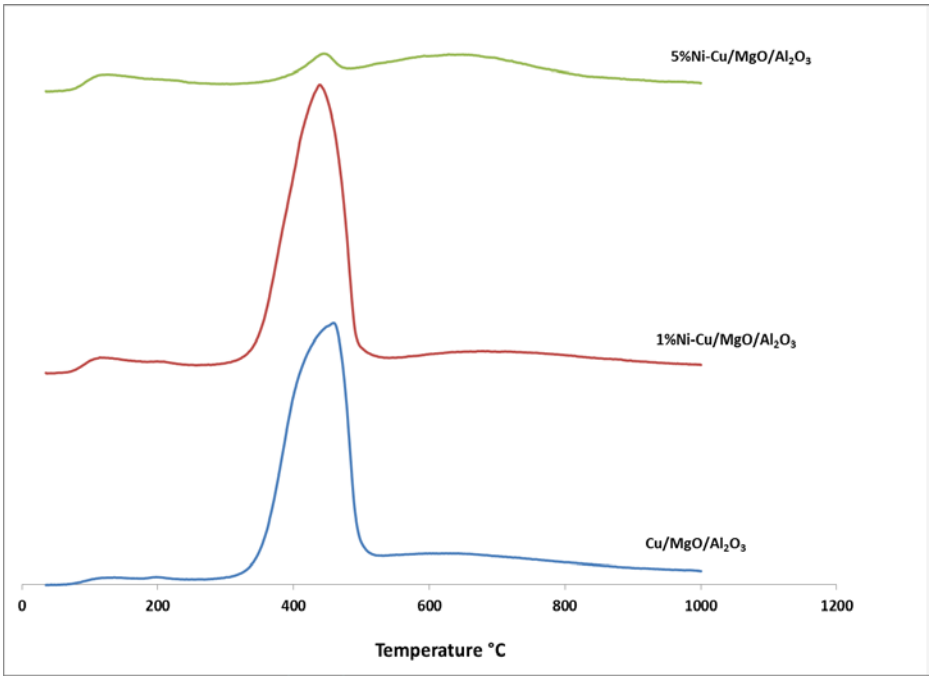

Figure 6-7 NH3 TPD Profile for Ni/Cu/MgO/Al_2O_3 Catalysts with Different Ni Content: Cu/Mg = 1/3, 10% Al

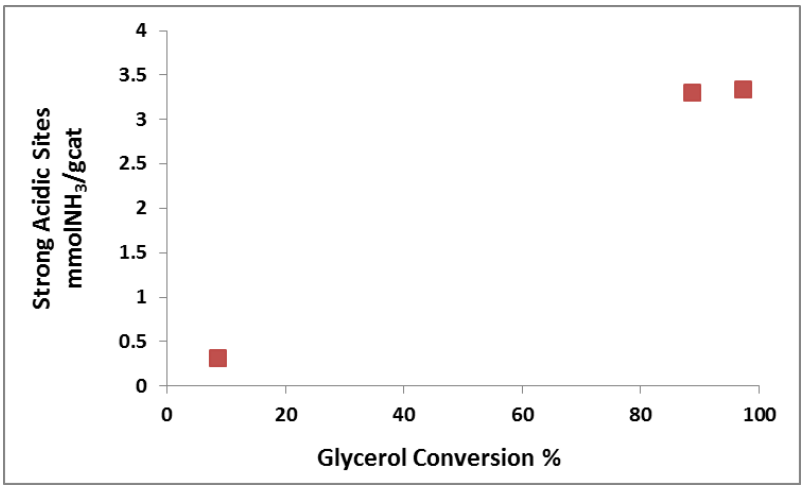

Figure 6-8 The Relationship between the Glycerol Conversion and Number of Strong Acidic Sites. Conditions: 220ºC, 25bar N_2, 20wt% Glycerol, Water/Methanol=1.2, 3wt% catalyst, 500RPM, Cu/Mg=1/3, 10mole% Al, 6hours.

Table 6-5 Number of Acidic Site for Ni/Cu/MgO/Al_2O_3 Catalysts with Different Ni Molar Contents.

Catalysts	Desorption Temperature		Total Acidic Sites	Glycerol Conversion[c]
	mmolNH3/gcat		mmolNH3/gcat	%
Cu/MgO/Al_2O_3[a]	73.5-253.4	312.8-526.9		
Uptake (mmol/gcat)	0.070	3.270	3.341	97.3
1%Ni/Cu/MgO/Al_2O_3[b]	65.1-258.3	286.9-541.5		
Uptake (mmol/gcat)	0.151	3.150	3.301	88.7
5%Ni/Cu/MgO/Al_2O_3[b]	45.4-295.7	356.6-483.1		
Uptake (mmol/gcat)	0.208	0.116	0.324	8.7

[a]Cu/Mg/Al = 22.5/67.5/10
[b]Cu/Mg=1/3, 10% Al
[c]Conditions: 220ºC, 15bar N2, 20wt% Glycerol, Water/Methanol=1.2, 3wt% catalyst, 500RPM, Cu/Mg=1/3, 10mole% Al, 6hours

6.1.7 Acidity Comparison between Cu/ZnO/Al_2O_3 and Cu/MgO/Al_2O_3

Figure 6-9 compares the acidity between Cu/ZnO/Al_2O_3 (Cu/Zn/Al=35/35/30) catalyst and Cu/MgO/Al_2O_3 (22.5/67.5/10) catalyst. A large medium desorption peak is observed between 312.8°C and 526.9°C for the Cu/MgO/Al_2O_3 catalyst. For the Cu/ZnO/Al_2O_3 catalyst, a strong desorption peak is observed between 589.9°C and 749.3°C, but the amount of acidic sites are significantly reduced compared with the Cu/MgO/Al_2O_3 catalyst. The total number of acidic

sites for the $Cu/MgO/Al_2O_3$ catalyst (3.34mmol/g-cat) is about 10 times higher than that for the $Cu/ZnO/Al_2O_3$ catalyst (0.32mmol/g-cat) as shown in Table 6-6. As discussed in Section 4.10, when molecular hydrogen is used the rate constant is only increased from $1.456s^{-1}$ using a $Cu/ZnO/Al_2O_3$ catalyst to $2.254s^{-1}$ using a $Cu/MgO/Al_2O_3$ catalyst. The activities are not different by a factor of 10 as the total number of acidic sites shows. This is possibly because both the strength of the acidity and number of acidic sites play important roles on the catalyst activity, as even the $Cu/MgO/Al_2O_3$ catalyst can provide about 10 times more acidic sites than the $Cu/ZnO/Al_2O_3$ catalyst, with the majority of them being medium acidic sites, while the major acidic sites provided by $Cu/ZnO/Al_2O_3$ catalyst are stronger according to a higher desorption temperature.

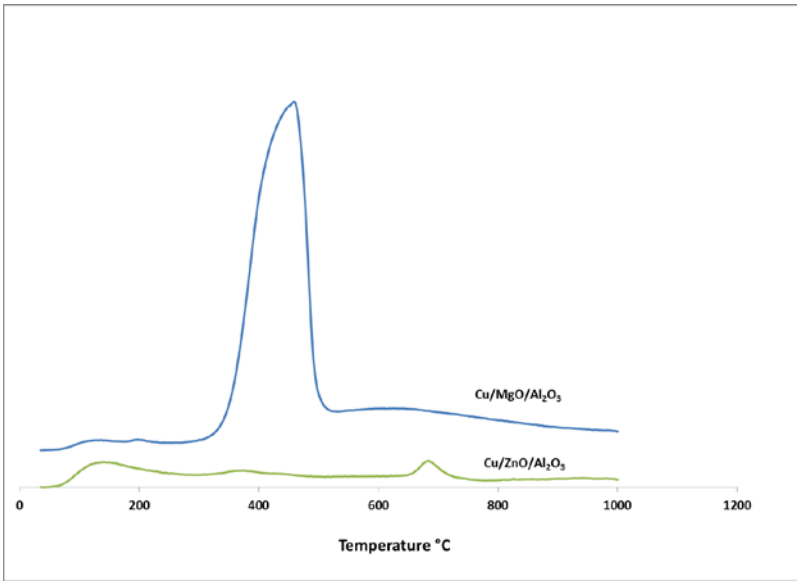

Figure 6-9 NH_3 TPD Profile Comparison between $Cu/ZnO/Al_2O_3$ and $Cu/MgO/Al_2O_3$

Table 6-6 Number of Acidic Sites Comparison between $Cu/MgO/Al_2O_3$ and $Cu/ZnO/Al_2O_3$.

Catalysts	Desorption Temperature $mmolNH_3/gcat$			Total Acidic Sites $mmolNH_3/gcat$
$Cu/MgO/Al_2O_3$[a]	73.5-253.4	312.8-526.9		
Uptake (mmol/gcat)	0.070	3.270		3.341
$Cu/ZnO/Al_2O_3$[b]	51.3-289.7	294.9-435.1	589.9-749.3	
Uptake (mmol/gcat)	0.23	0.02	0.07	0.321

[a]Cu/Mg/Al=22.5/67.5/10
[b]Cu/Zn/Al=35/35/30

6.2 H_2 Temperature Programmed Reduction (TPR)

H_2 TPR is a technique used to investigate the optimum reduction temperature of a catalyst since it has been reported that metallic Cu^0 is the active site of the catalyst, the catalyst reduction plays a very important role on the catalytic activity. The catalyst is heated based on a pre-designed thermal profile while the catalyst is exposed to a flowing stream of high purity hydrogen gas. The peaks as a function of temperature can provide the information of the hydrogen consumption for the catalyst reduction. The detailed experimental method was described in Section 3.5.4.

6.2.1 TPR Data for the $CuO/ZnO/Al_2O_3$ Catalysts by Different Preparation Methods.

Figure 6-10 illustrates the TPR profile for the catalysts prepared by different methods. All the profiles indicate that the reduction of the catalysts can be completed below 300ºC suggesting that a 300ºC reduction temperature is sufficient to reduce the CuO to metallic Cu^0. For the $Cu/ZnO/Al_2O_3$ catalyst prepared by Na_2CO_3 precipitation, a pronounced shoulder peak at 177ºC is observed beside the dominant peak which is at 230ºC. This is possibly due to the formation of two types of CuO species which are bulk CuO and well dispersed CuO in the catalyst as reported by Fierro *et al* [184]; also it might be due to the reduction of CuO to Cu^+ at lower temperature as suggested by Bienholz *et al*. [80]; while for the $Cu/ZnO/Al_2O_3$ catalyst prepared by the oxalate gel-coprecipitation method, the shoulder peak at 201ºC beside the dominant peak (253ºC) is much less intense indicating that this preparation method could generate well dispersed CuO particles and the interactions between CuO and Al_2O_3 can facilitate the direct reduction of CuO to metallic Cu^0. For Cu/ZnO prepared by the oxalate gel-coprecipitation method without alumina added, the reduction peak is observed at 225ºC, which is lower than those for the $Cu/ZnO/Al_2O_3$ catalysts prepared by Na_2CO_3 coprecipitation (230ºC), oxalate gel-coprecipitation (253ºC) and impregnation (263ºC) indicating that the addition of alumina could generate interactions between Al_2O_3 and CuO to make the reduction temperature higher as reported by Panyad *et al*. [185].

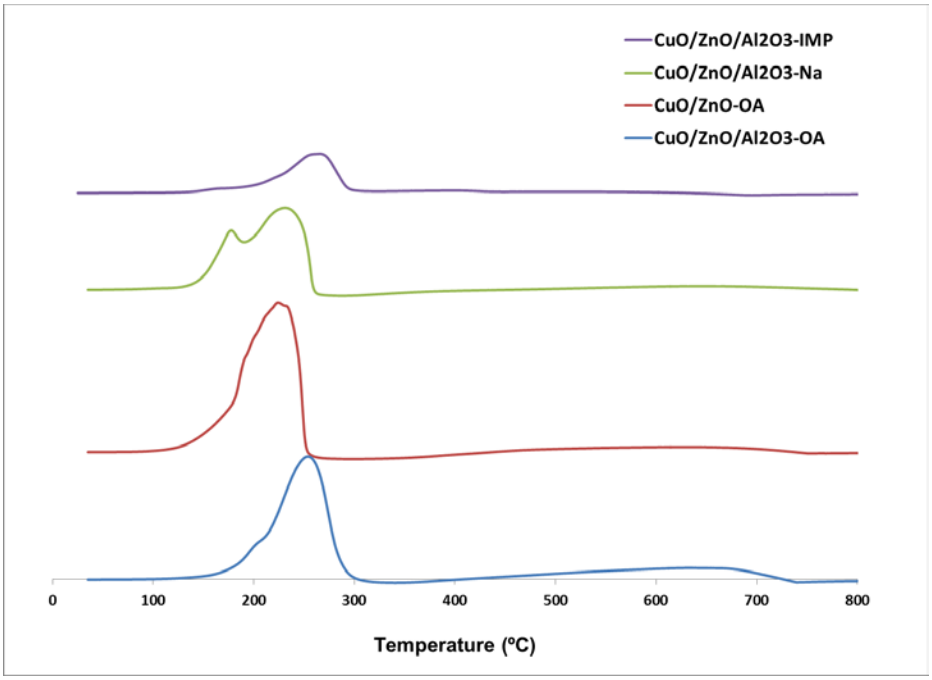

Figure 6-10 TPR Profile for the $CuO/ZnO/Al_2O_3$ by Different Preparation Methods: Cu/Zn/Al=25/25/50 for Na and OA; Cu/Zn=50/50 for CuO/ZnO-OA; Cu/Zn/Al=15/15/70 for IMP.

6.2.2 TPR Data Comparison between $CuO/ZnO/Al_2O_3$ and $NiO/CuO/ZnO/Al_2O_3$ Catalysts

Figure 6-11 shows the TPR profiles of $NiO/CuO/ZnO/Al_2O_3$ (Ni/Cu/Zn/Al = 5/32.5/32.5/30), $CuO/ZnO/Al_2O_3$ (Cu/Zn/Al = 35/35/30) catalyst, and NiO only. From the graph it can be observed that both $NiO/CuO/ZnO/Al_2O_3$ and $CuO/ZnO/Al_2O_3$ catalyst shows the reduction peak at around 300°C. A very broad peak is observed for the NiO profile starting from 330°C to 400°C. However, no distinctive peak is observed in the $NiO/CuO/ZnO/Al_2O_3$ profile between 330°C and 400°C. This suggests that NiO and CuO are well mixed and can be effectively reduced at 300°C [186].

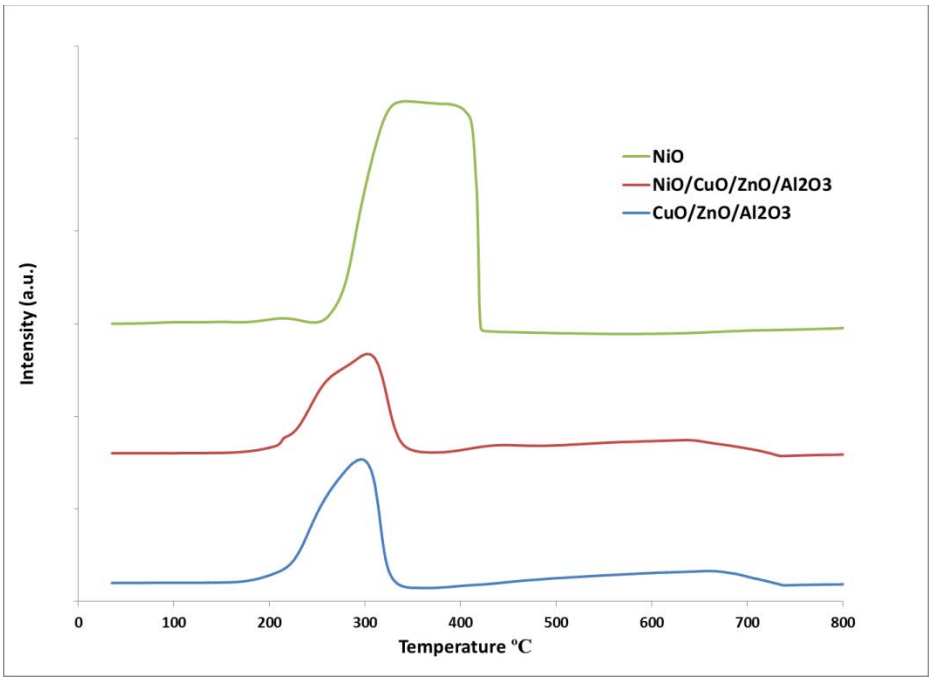

Figure 6-11 TPR Profile for NiO/CuO/ZnO/Al_2O_3, CuO/ZnO/Al_2O_3 and NiO: Ni/Cu/Zn/Al=5/32.5/32.5/30, Cu/Zn/Al=35/35/30.

6.2.3 TPR Data Comparison between CuO/MgO/Al_2O_3 and NiO/CuO/MgO/Al_2O_3 Catalysts

Figure 6-12 shows the TPR profile of NiO/CuO/MgO/Al_2O_3 (Ni/Cu/Mg/Al = 5/21.25/63.75/10), CuO/MgO/Al_2O_3 (Cu/Mg/Al = 22.5/67.5/10) catalyst and NiO only. It can be observed that for the CuO/MgO/Al_2O_3 catalyst, the reduction peak appears at 280°C, which is much lower than that for CuO/ZnO/Al_2O_3; when 5mole% NiO is added, the reduction peak appears at even a lower temperature being around 247°C and also no distinctive reduction peak is observed for NiO. Therefore, when 300°C was chosen as the reduction temperature for the CuO/MgO/Al_2O_3 and NiO/CuO/MgO/Al_2O_3, the catalysts can be effectively reduced.

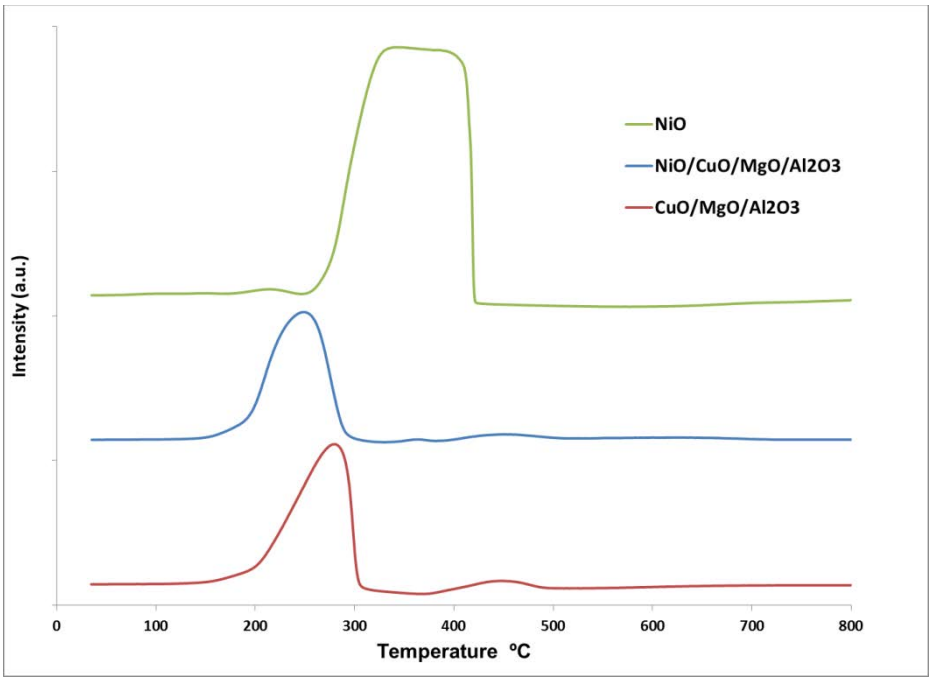

Figure 6-12 TPR Profile for NiO/CuO/MgO/Al_2O_3, CuO/MgO/Al_2O_3 and NiO: Ni/Cu/Mg/Al=5/21.5/63.75/10, Cu/Mg/Al=22.5/67.5/10

6.2.4 TPR Data Comparison between CuO/MgO/Al_2O_3 and PdO/CuO/MgO/Al_2O_3 Catalysts

Figure 6-13 shows the TPR profile of PdO/CuO/MgO/Al_2O_3 (2wt% Pd, Cu/Mg/Al = 22.5/67.5/10) catalyst and CuO/MgO/Al_2O_3 (Cu/Mg/Al = 22.5/67.5/10) catalyst. It can be observed that as 2wt% Pd is loaded, the reduction peak is shifted to a lower temperature from 280°C to 180°C. This suggests that Pd is very fine and well mixed with CuO, and hence Pd can reduce Cu in situ [186].

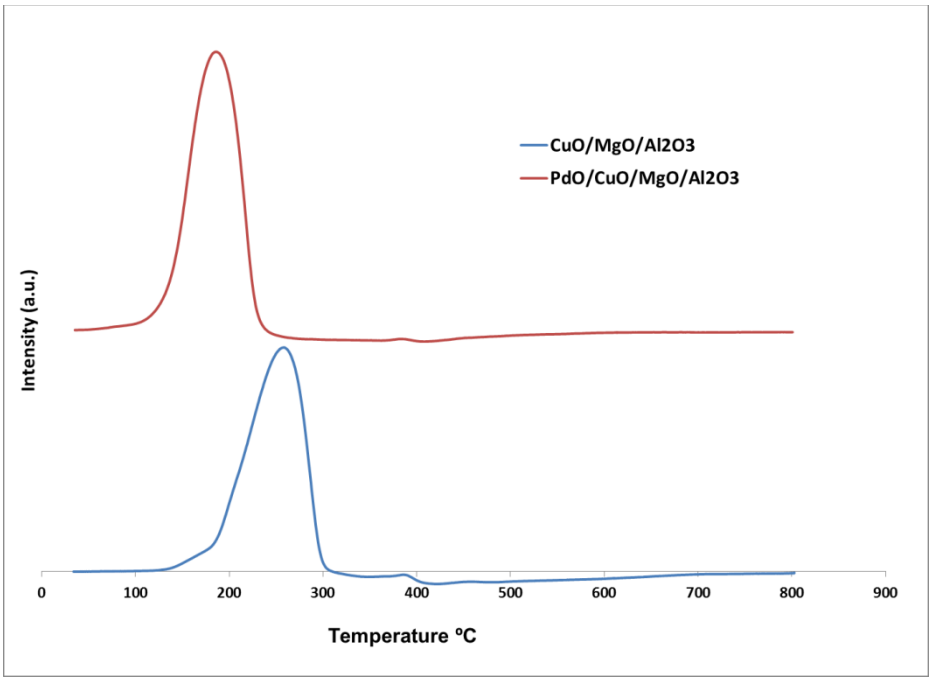

Figure 6-13 TPR Profile for $PdO/CuO/MgO/Al_2O_3$ and $CuO/MgO/Al_2O_3$: 2wt%Pd, Cu/Mg/Al=22.5/67.5/10.

6.3 CO_2 TPD

CO_2 TPD is a technique to study the basicity of a catalyst. The catalyst is first saturated with CO_2 and then heated based on a designated thermal profile. The peaks as a function of a temperature profile can provide the information of basic strength and number of basic sites. The number of acidic sites can be calculated based on the area of the peak and the temperature at which the desorption peaks are can be used to determine the basic strength of the catalyst. The detailed experimental method was described in Section 3.5.2.

6.3.1 Effect of Cu/Mg ratio and Al content on the Basicity of the $Cu/MgO/Al_2O_3$ Catalysts

The Cu/Mg molar ratios of 1/1, 1/3 and 1/5 were tested for the glycerol hydrogenolysis reactions using *in situ* hydrogen produced from methanol steam reforming in order to find the optimum Cu/Mg ratio; also 10%, 20% and 30% Al (molar) were added into the Cu/MgO catalyst to study

the effect of Al on the catalytic activity as discussed in Section 5.3.2. CO_2 TPD experiments have been carried out using the Cu/MgO/Al_2O_3 catalysts to study the effect of the metals molar ratio on the catalyst basicity. From Figure 6-14 it can be observed that as the Cu/Mg molar ratio is changed from 1/1 to 1/3 and further to 1/5, the number of basic sites is increased as Mg content increases. This is expected since Mg is known to be a basic metal. The numbers of basic sites for the catalysts with different metal molar ratios are listed in Table 6-7. Al can also affect the basicity of the catalysts. From Figure 6-14 as well as Figure 6-15, it can be observed for all the Cu/Mg molar ratios when no Al is added, the catalysts always shows the largest amount of basic sites; the addition of Al does not change the strength of the catalysts' basicity. When the Al content is increased to 10mole%, the amount of basic sites is reduced significantly especially when Cu/Mg molar ratios are 1/1 and 1/3; when Al molar content is further increased to 30%, all the catalysts show essentially no basic sites (Figure 6-15A). Based on the experimental results provided in Chapter 5, the catalyst with a Cu/Mg molar ratio of 1/3 and 10mole% Al content gave the best catalytic activity for the glycerol hydrogenolysis reactions. No direct relationship is observed between the basicity and the catalyst activity as shown in Table 6-7 and Figure 6-16.

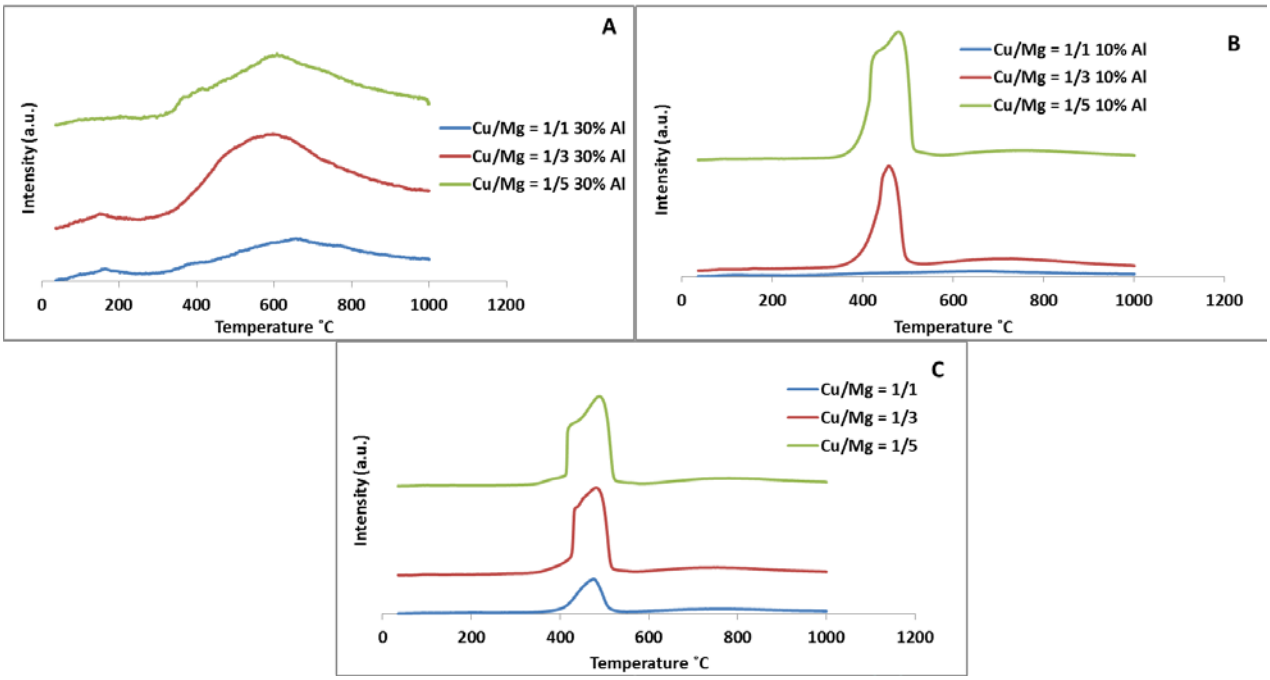

Figure 6-14 Effect of Cu/Mg Molar Ratio on the Basicity of Catalysts: A) 30mole% Al; B) 10mole% Al; C) no Al

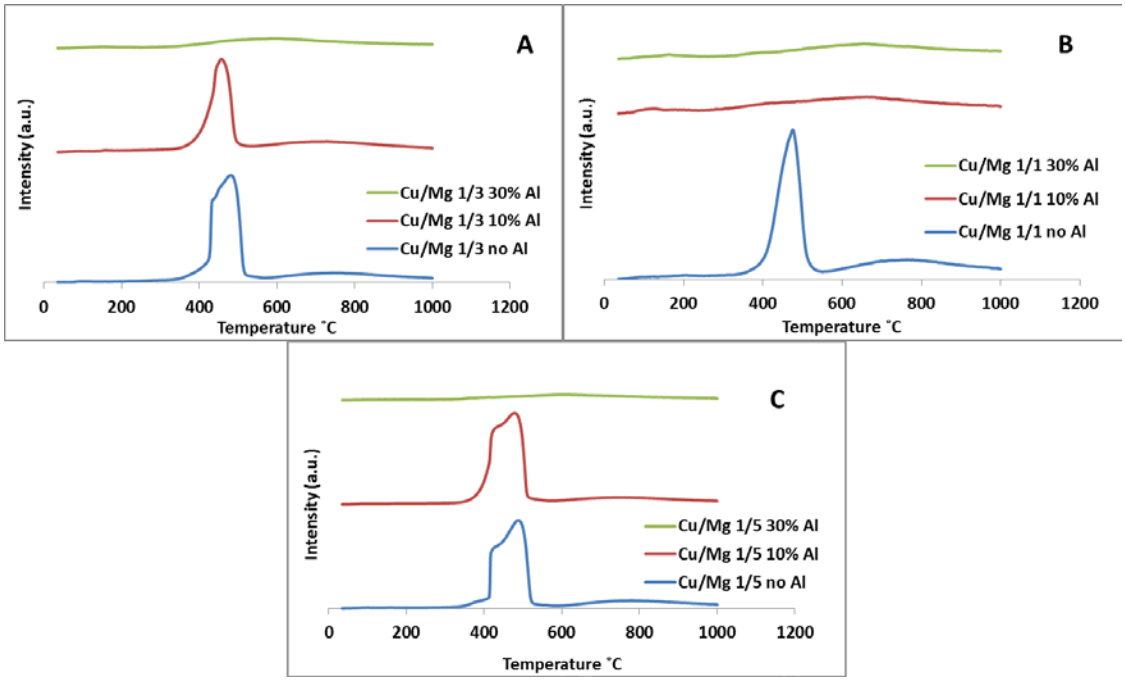

Figure 6-15 Effect of Al molar Content on the Basicity of Catalysts: A) Cu/Mg = 1/1; B) Cu/Mg = 1/3; C) Cu/Mg = 1/5

Table 6-7 CO_2 Uptake for Cu/MgO/Al_2O_3 Catalysts with Different Metals Molar Ratio

Catalysts	Desorption Temperature		Total Basic Sites	Glycerol Conversion
	mmolCO_2/gcat		mmolCO_2/gcat	%
Cu/Mg = 1/1	337.0-546.3	559.6-1003.4	Total Basic Sites	
	5.19	1.73	6.91	77.6
Cu/Mg = 1/3	321.6-570.5	582.3-997.7		
	15.27	2.18	17.45	80.6
Cu/Mg = 1/5	302.2-584.5	604.4-994.5		
	17.45	2.33	19.78	68.8
Cu/Mg = 1/1 10% Al	36.2-255.8	271.5-1002.8		
	0.15	2.27	2.42	84.5
Cu/Mg = 1/3 10% Al	334.5-535.4	537.1-1002.7		
	10.13	2.83	12.96	95.6
Cu/Mg = 1/5 10% Al	330.8-591.3	594.6-1002.8		
	18.88	2.03	20.91	
Cu/Mg = 1/1 30% Al		287.2.3-1003.1		
		1.96	1.96	83.4
Cu/Mg = 1/3 30% Al		264.6-1003.3		
		5.13	5.13	85.2
Cu/Mg = 1/5 30% Al		248.1-999.7		
		4.39	4.39	84.9

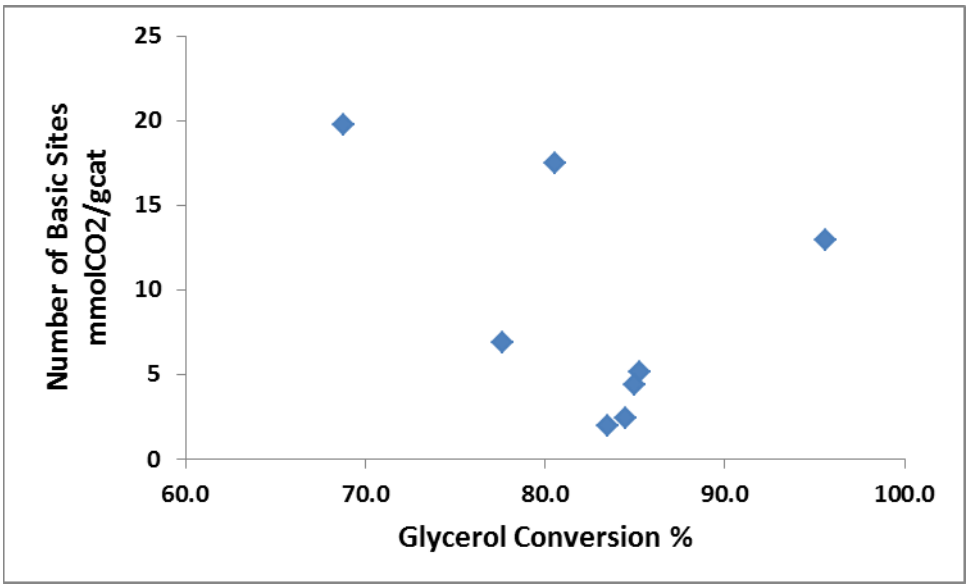

Figure 6-16 The Relationship between the Glycerol Conversion and Number of Basic Sites. Conditions: Conditions: 220ºC, 15bar N_2, 20wt% Glycerol, Water/Methanol=1.2, 3wt% catalyst, 500RPM, 8hours.

6.4 H_2 TPD for the Effect of Pd on $Cu/MgO/Al_2O_3$ Catalysts

It has been reported that the amount of surface hydrogen provided plays an important role in hydrogenation and hydrogenolysis reactions [106]. A series of H_2 TPD experiments have been carried out to investigate the amount of adsorbed hydrogen species on the catalysts. The detailed experimental method was described in Section 3.5.3. It can be seen from Figure 6-17 that a distinct hydrogen desorption peak ocurrs between 180°C and 800°C and the highest point of the peak is at 400°C. This suggests that when the reaction temperature is between 180°C and 220°C, a major amount of the hydrogen species will not be desorbed from the catalyst surface. From Figure 6-17 as well as Table 6-8, it can be seen that when Pd is loaded, the amount of desorbed hydrogen is increased. The amount of hydrogen desorbed for a $Cu/MgO/Al_2O_3$ catalyst without Pd loading is calculated to be 0.39mmol/g-cat, when 1wt% Pd is loaded the amount of hydrogen desorbed is increased to 0.57mmol/g-cat, and when the Pd loading is increased from 1wt% to 2wt%, the desorbed hydrogen amount is increased to 0.86mmol/g-cat, and when 3wt% Pd is loaded, the desorbed hydrogen amount is only increased from 0.86mmol/g-cat to 0.88mmol/g-cat. Therefore, it is known that when Pd is loaded on the $Cu/MgO/Al_2O_3$ catalyst surface, the hydrogen storage capacity is improved since Pd is a very active metal for hydrogen transfer [37,

187]. When the loading of hydrogen is increased, the Pd may cover some Cu surface and also Pd can overlap each other; therefore, the amount of adsorbed hydrogen is not significantly improved when the Pd loading is very high.

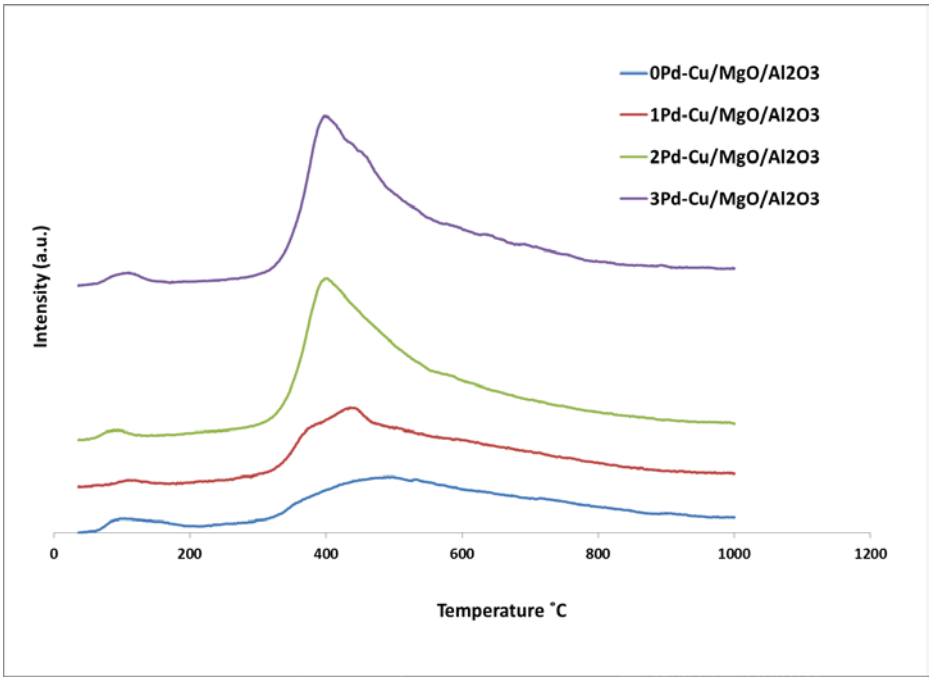

Figure 6-17 H_2 TPD Profile for the Cu/Mg/Al Catalysts with Different Pd Loading. Cu/Mg/Al=22.5/67.5/10.

Table 6-8 The H_2 Uptake for the $Cu/MgO/Al_2O_3$ Catalysts with Different Pd Loading[a].

Catalysts	Desorption Temperature mmolH_2/gcat		Total H_2 Desorbed mmolH_2/gcat	Glycerol Conversion[b] %
$Cu/MgO/Al_2O_3$	66.5-177.4	186.8-967.9	Total	
Uptake (mmol/gcat)	0.02	0.37	0.39	54.9
1%Pd- $Cu/MgO/Al_2O_3$	36-206.8	212.6-900.9	Total	
Uptake (mmol/gcat)	0.01	0.57	0.57	66.8
2%Pd- $Cu/MgO/Al_2O_3$	56-143	164.9-1001.9	Total	
Uptake (mmol/gcat)	0.01	0.85	0.86	73.2
3%Pd- $Cu/MgO/Al_2O_3$	51.8-175.3	253.4-945.2	Total	
Uptake (mmol/gcat)	0.02	0.86	0.88	73.6

[a]Cu/Mg/Al=22.5/67.5/10

[b]Conditions: 220 ºC, 15bar N2, 40wt% Glycerol, Water/Methanol=1.2, 7wt% catalyst, 500RPM, 8 hours, Support: Cu/Mg/Al = 22.5/67.5/10 40wt% Glycerol

Since it has been discussed that the 1,2PD selectivity strongly depends on the amount of H_2 supplied for the acetol hydrogenation reaction, the relationship between the 1,2PD selectivity and the total amount of desorbed H_2 was investigated based on the results discussed in Section 5.4.2. In Figure 6-18 it can be observed that the 1,2PD selectivity has a strong linear relationship with the total amount of desorbed H_2. Therefore, it is known that one of the promotion effects of Pd on the $Cu/MgO/Al_2O_3$ catalyst is that it can effectively catalyze the transfer hydrogenation reaction by providing more surface hydrogen.

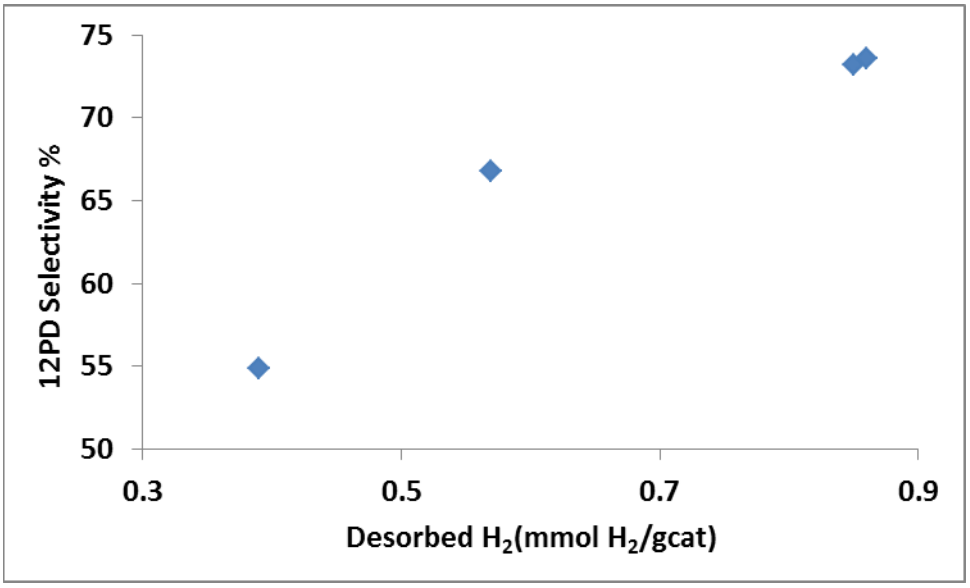

Figure 6-18 Relationship between the Amount of Desorbed H_2 and 1,2PD Selectivity. Conditions: 220 ºC, 15bar N_2, 40wt% Glycerol, Water/Methanol=1.2, 7wt% catalyst, 500RPM, 8 hours, Support: Cu/Mg/Al = 22.5/67.5/10 40wt% Glycerol.

6.5 Thermogravimetric Analysis (TGA) and Differential Thermal Analysis (DTA)

The thermal treatment of the catalysts is a very important parameter affecting the catalyst activity. Therefore, thermo analysis experiments have been carried out using a TGA equipment (SDT Q600) integrated with DTA analysis. The detailed experimental method was described in Section 3.5.6.

6.5.1 Thermo Analysis for Cu/ZnO/Al_2O_3 Catalyst Prepared by Oxalate Gel-coprecipitation

The experiments on Cu-oxalate and Zn-oxalate have been carried out for reference. Figure 6-19A and Figure 6-19B shows the TGA and DTA profile for Cu-oxalate and Zn-oxalate respectively. The decarboxylation for Cu-oxalate started at around 200ºC and is completed at around 300ºC; whereas, Zn-oxalate starts to decompose at around 320ºC and continues until it is complete at 400ºC. The exothermic peaks (upward temperature difference peak if exothermic) at 305ºC and 390ºC represent the fastest decarboxylation temperatures for Cu-oxalate and Zn-oxalate respectively.

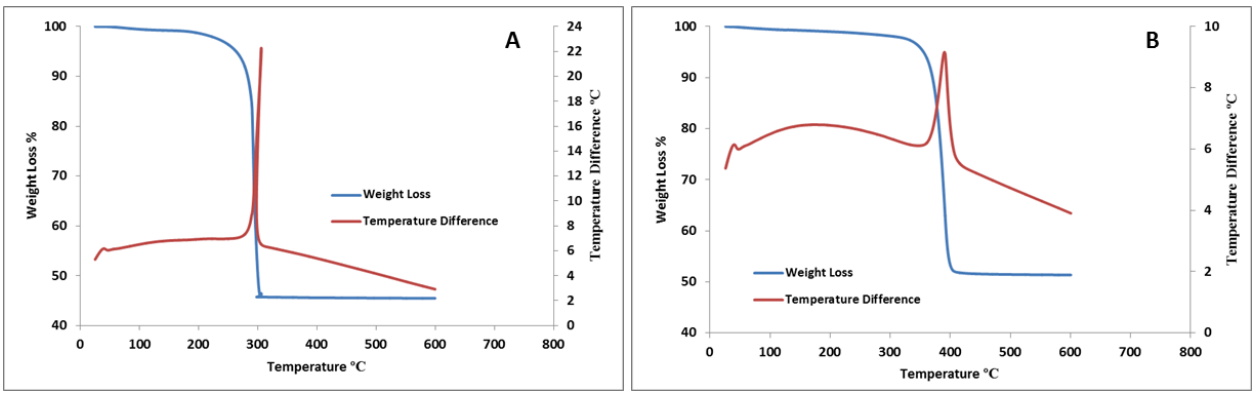

Figure 6-19 TGA and DTA Profile for: A) Cu-oxalate; B) Zn-oxalate.

Figure 6-20 and Figure 6-21 illustrate the TGA and DTA profile for Cu/ZnO (Cu/Zn = 1/1) and Cu/ZnO/Al_2O_3 (Cu/Zn/Al = 25/25/50) catalysts prepared by oxalic acid co-precipitation. When the alumina is present in Figure 6-20, only one peak is observed between 220ºC and 325ºC indicating that the Cu and Zn oxalates are in a very well mixed phase, while in absence of alumina in Figure 6-21, a small peak is observed between 215ºC and 250ºC and a large peak appeares between 290ºC and 350ºC indicating higher Zn content within this temperature range. It is known that that with Al added the metals are well mixed, which suggests that the mixing of metals plays an important role on the catalytic activity since with Al added the activity of the catalyst was improved as introduced in Chapter 4. For both catalysts, the decomposition can be completed before 350ºC, so 360ºC as the calcination temperature is sufficient for both catalysts.

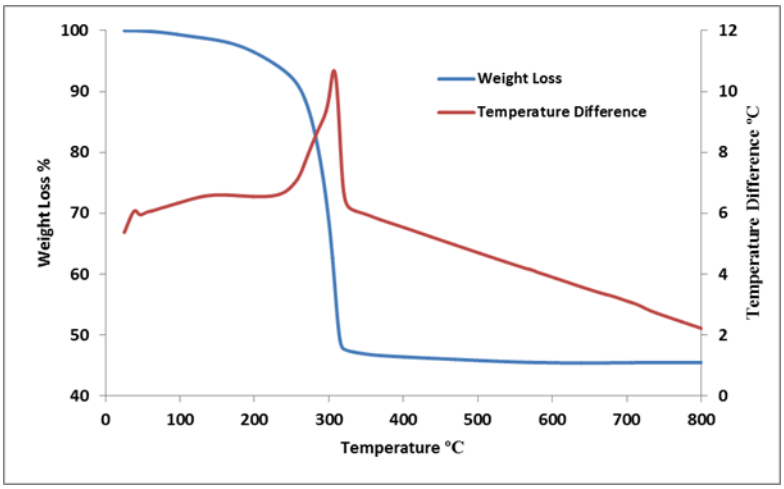

Figure 6-20 TGA and DTA Profile for Cu/ZnO/Al_2O_3 Catalyst Prepared via Oxalate Gel-coprecipitation.

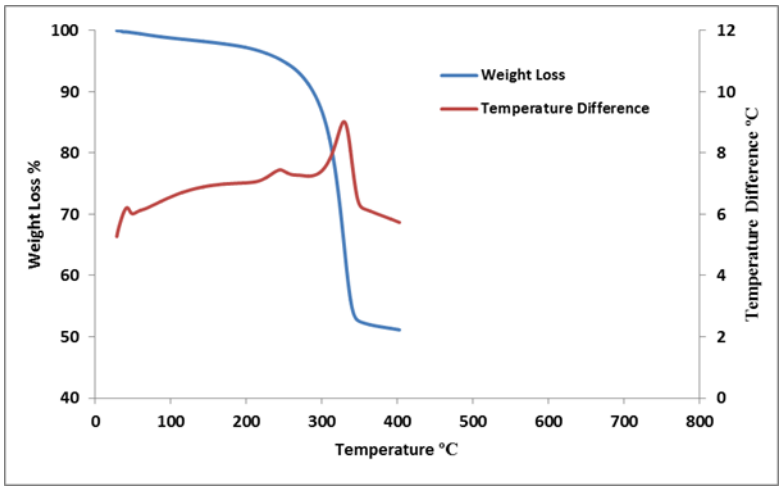

Figure 6-21 TGA and DTA Profile for Cu/ZnO Catalyst Prepared via Oxalate Gel-coprecipitation.

6.5.2 Thermo Analysis for Cu/ZnO/Al_2O_3 Catalysts Prepared by Na_2CO_3 Coprecipitation and Impregnation

For the Cu/ZnO/Al_2O_3 catalyst prepared by Na_2CO_3 co-precipitation (Cu/Zn/Al = 25/25/50) as shown in Figure 6-22, a slow decarboxylation occurs from 195ºC up to 400ºC followed by a small amount of mass loss between 550ºC and 630ºC, which was also reported by Zhang *et al.* [188]. Therefore, the calcination temperature is designed to be 600ºC. The high calcination temperature can cause sintering of Cu resulting in larger Cu size particles, which is observed in

the XRD pattern in Section 6.7. The profile shown in Figure 6-23 is for $Cu/ZnO/Al_2O_3$ prepared via the impregnation method (Cu/Zn/Al = 15/15/70). From 220ºC to 260ºC and from 260ºC to 305ºC, two endothermic peaks are observed corresponding to the decomposition of $Cu(NO_3)_2$ and $Zn(NO_3)_2$ respectively [189]. So 400ºC is used as the calcination temperature for this catalyst. Therefore, oxalate gel-coprecipitation with alumina present favors a chemical homogenous phase of Cu and Zn, which is in a good agreement with the XRD analysis presented in Section 6.7.

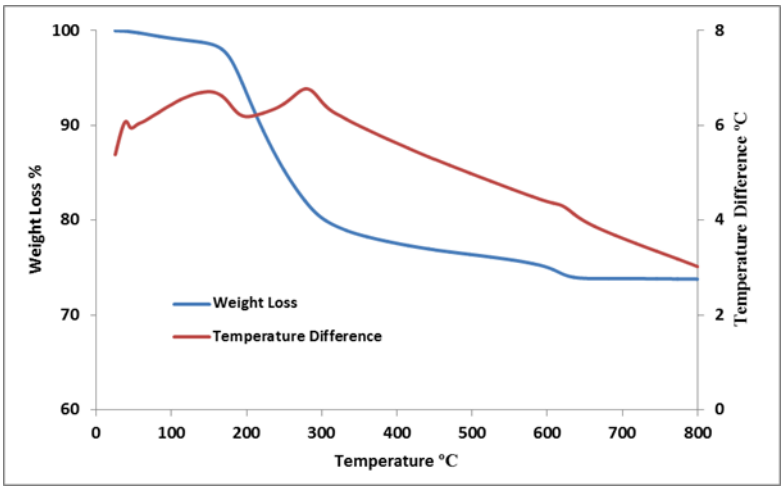

Figure 6-22 TGA and DTA Profile for $Cu/ZnO/Al_2O_3$ Catalyst Prepared via Na_2CO_3 Coprecipitation

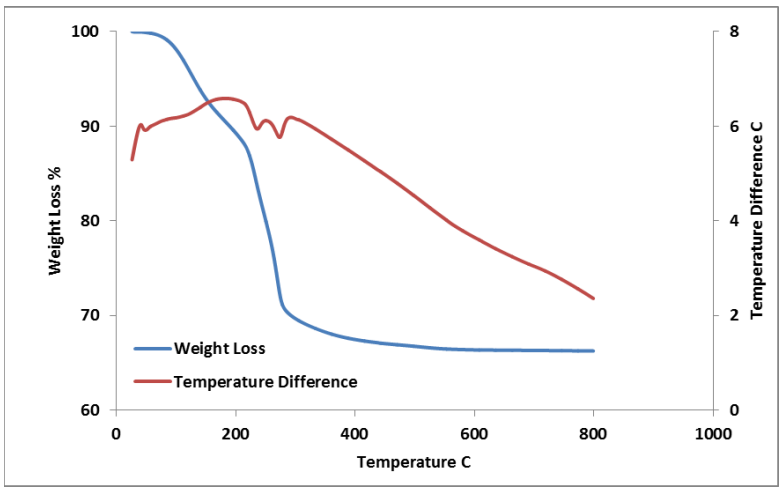

Figure 6-23 TGA and DTA Profile for $Cu/ZnO/Al_2O_3$ Catalyst Prepared via Impregnation

6.5.3 Thermo Analysis for $Cu/MgO/Al_2O_3$ Catalyst Prepared by Oxalate Gel-coprecipitation

Figure 6-24 shows the decomposition profile for a $Cu/MgO/Al_2O_3$ catalyst prepared by oxalic acid co-precipitation (Cu/Mg/Al = 22.5/67.5/10). A small exothermic peak between 218ºC and 260ºC is observed on the shoulder of the main peak which is between 218ºC and 340ºC. The decomposition of this catalyst is completed after 340ºC. Therefore, 360ºC is used as the calcination temperature for this catalyst.

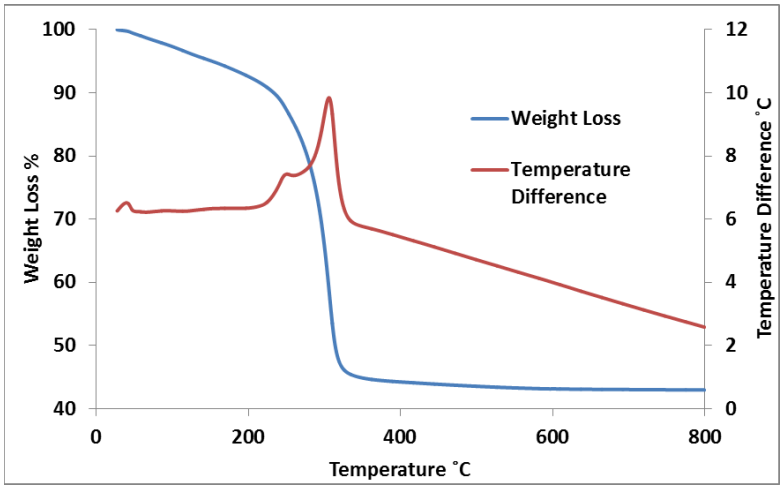

Figure 6-24 TGA and DTA Profile for $Cu/MgO/Al_2O_3$ Catalyst Prepared via Oxalate Gel-coprecipitation

6.5.4 Thermo Analysis for 2wt% Pd Supported on $Cu/ZnO/Al_2O_3$ and $Cu/MgO/Al_2O_3$ Catalysts

Figure 6-25 and Figure 6-26 illustrate the thermal decomposition profiles of 2wt% Pd supported on $Cu/ZnO/Al_2O_3$ (Cu/Zn/Al = 25/25/50) and 2wt% Pd supported on $Cu/MgO/Al_2O_3$ (Cu/Mg/Al = 22.5/67.5/10) catalysts using palladium acetate as the palladium precursor. Both profiles show an exothermic peak between 230ºC and 250ºC indicating the decomposition temperature of palladium acetate. The weight loss stops at 275 ºC for Pd-$Cu/ZnO/Al_2O_3$ and at 350ºC for Pd-$Cu/MgO/Al_2O_3$. Therefore, 360ºC is used for the calcination temperature for these catalysts.

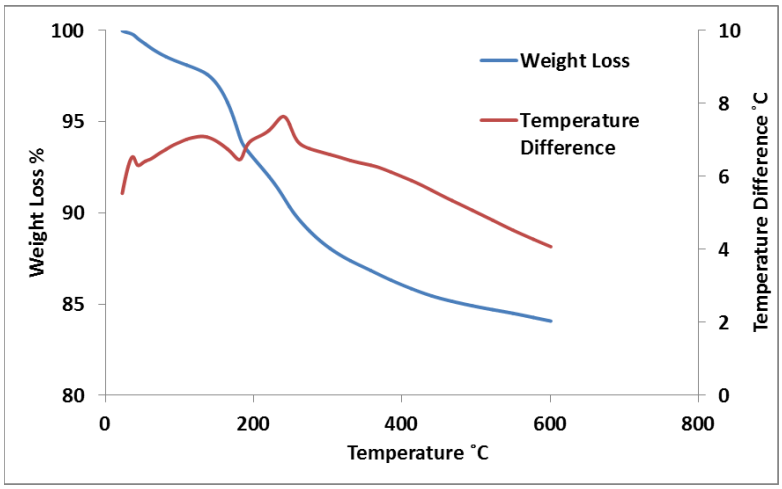

Figure 6-25 TGA and DTA Profile for 2wt% Pd on Cu/ZnO/Al_2O_3 Catalyst.

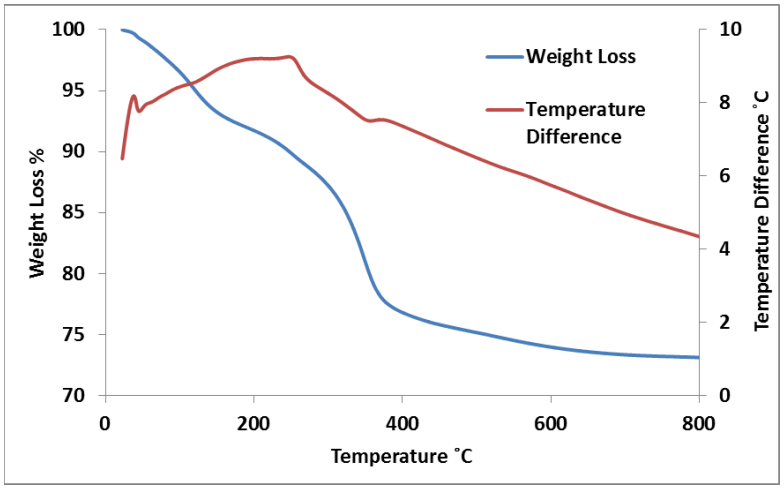

Figure 6-26 TGA and DTA Profile for 2wt% Pd on Cu/MgO/Al_2O_3 Catalyst.

6.6 Transmission Electron Microscopy (TEM)

TEM experiments have been carried out to investigate the catalyst particle size, particle shapes and crystal structures. Fresh and spent catalysts have been used to investigate the morphology change before and after the reaction.

6.6.1 Effect of Al on Cu/ZnO Catalysts Prepared via Oxalate Gel-coprecipitation

Figure 6-27 shows TEM pictures of Cu/ZnO (Cu/Zn = 50/50) catalyst and Cu/ZnO/Al_2O_3 (Cu/Zn/Al = 25/25/50) catalyst. It can be observed that particles of both catalysts are well dispersed and no aggregation is observed. With Al added, the particle shape is more regular and much smaller; also the particle size is more uniformly distributed. The particle size for the catalyst with Al added is calculated to be 10.41nm with a standard deviation of 2.04nm as shown in Figure 6-28 and Table 6-9. If Al is not added, it can be observed that the particles are formed very irregularly. The particle size is much larger compared with that when Al is added; the particle size is calculated as 14.96nm with a much larger standard deviation. As discussed in Section 4.2, adding alumina can significantly improve the catalyst activity for a glycerol hydrogenolysis process; therefore, the particle size is an important factor affecting the catalyst activity and smaller particle size can give a higher catalytic activity.

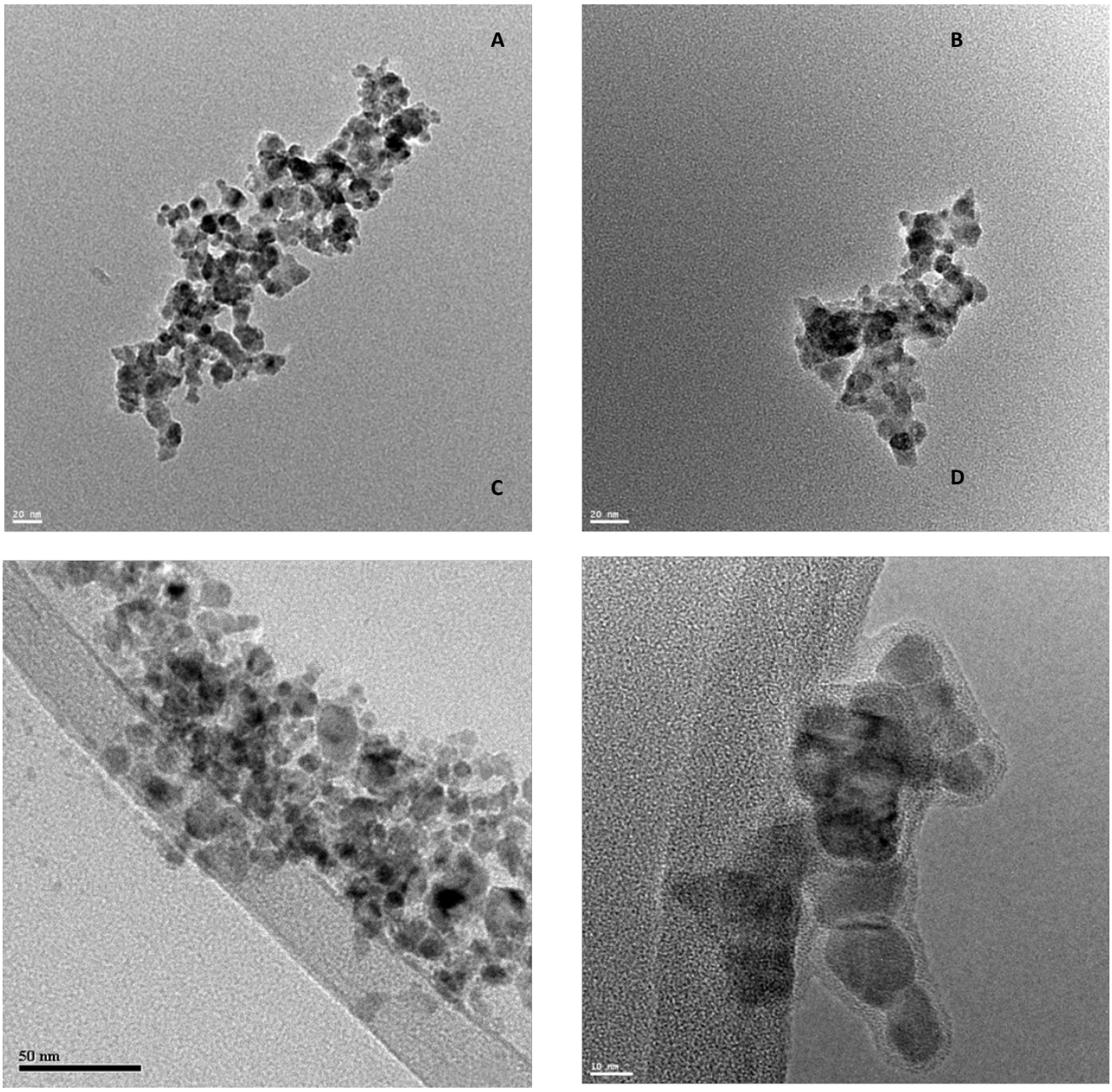

Figure 6-27 TEM Images of: A&B) $Cu/ZnO/Al_2O_3$ Catalyst; C&D) Cu/ZnO Catalysts.

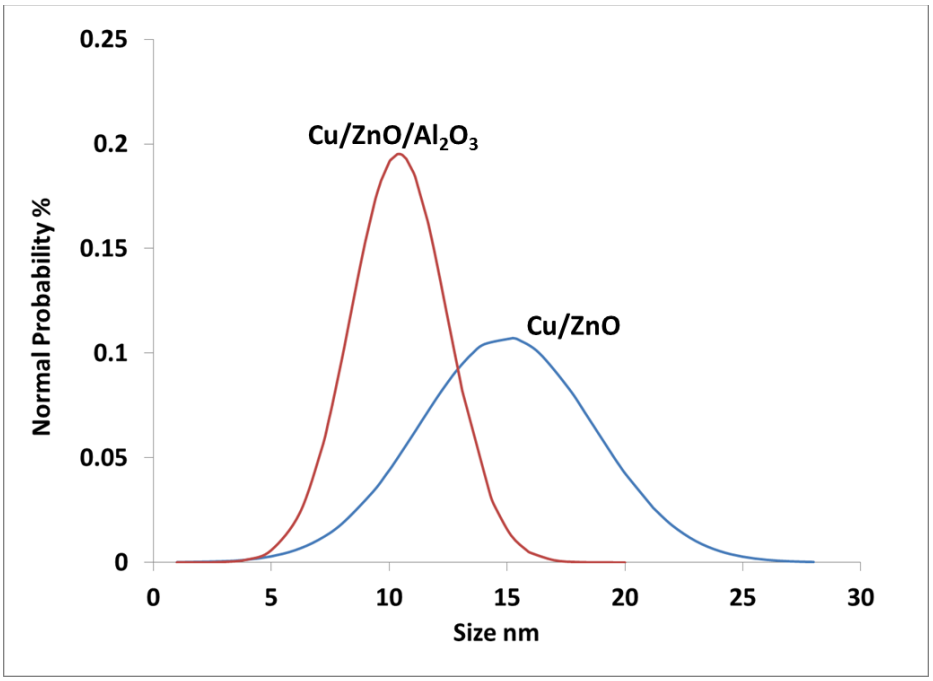

Figure 6-28 Effect of Al on Cu/ZnO Particle Size Distribution.

Table 6-9 Effect of Al on Cu/ZnO Particle Size Distribution.

	Mean	SD
$Cu/ZnO/Al_2O_3$	10.41	2.04
Cu/ZnO	14.96	3.71

6.6.2 Effect of Preparation Method

Figure 6-29 shows TEM pictures of $Cu/ZnO/Al_2O_3$ catalysts from different preparation methods. From Figure 6-29C and Figure 6-29D, it can be observed that for the catalyst prepared by Na_2CO_3 precipitation, the particle shape is elliptical while with oxalic acid precipitation, the particles are spherical as shown in Figure 6-29A and Figure 6-29B. For the elliptical particles the average size of the major axis is calculated to be 18.83nm which is much larger than that of the catalyst prepared by oxalic acid precipitation as shown in Table 6-10 and Figure 6-30, and the distribution of the particle size is also wider since the calculated standard deviation is larger. It has been discussed in Section 4.1 that the $Cu/ZnO/Al_2O_3$ catalyst prepared by oxalage gel-coprecipitation has a higher activity for the glycerol hydrogenolysis than the catalyst prepared by Na_2CO_3 coprecipitation; one of the reasons being that this preparation method can provide a

smaller particle size. This is in a good agreement with some literature reporting this preparation method [78, 120, 122].

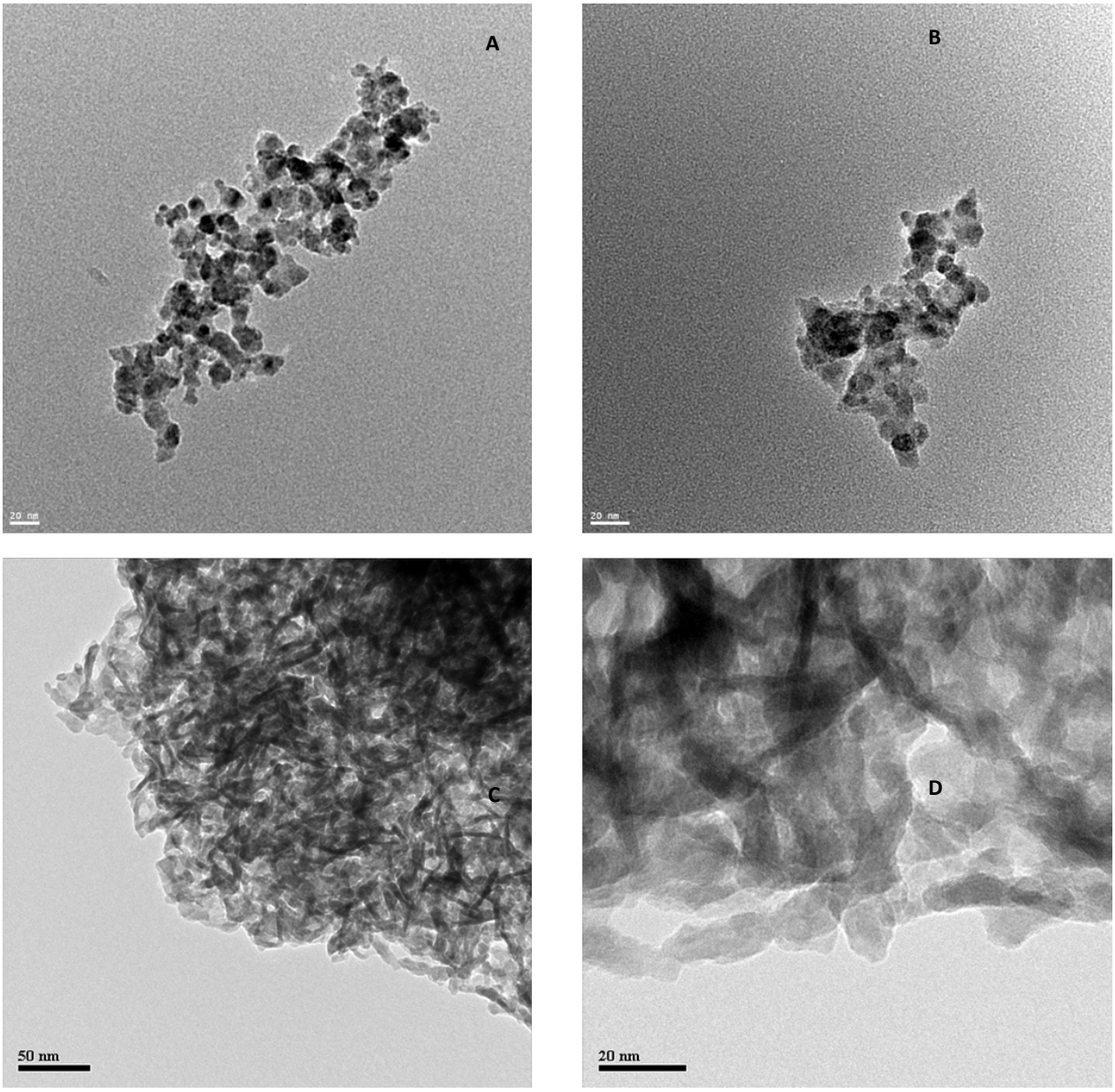

Figure 6-29 TEM Images of: A&B) $Cu/ZnO/Al_2O_3$ Catalyst Prepared via Oxalic Acid Co-Precipitation; C&D) $Cu/ZnO/Al_2O_3$ Catalysts Prepared via Na_2CO_3 Co-Precipitation.

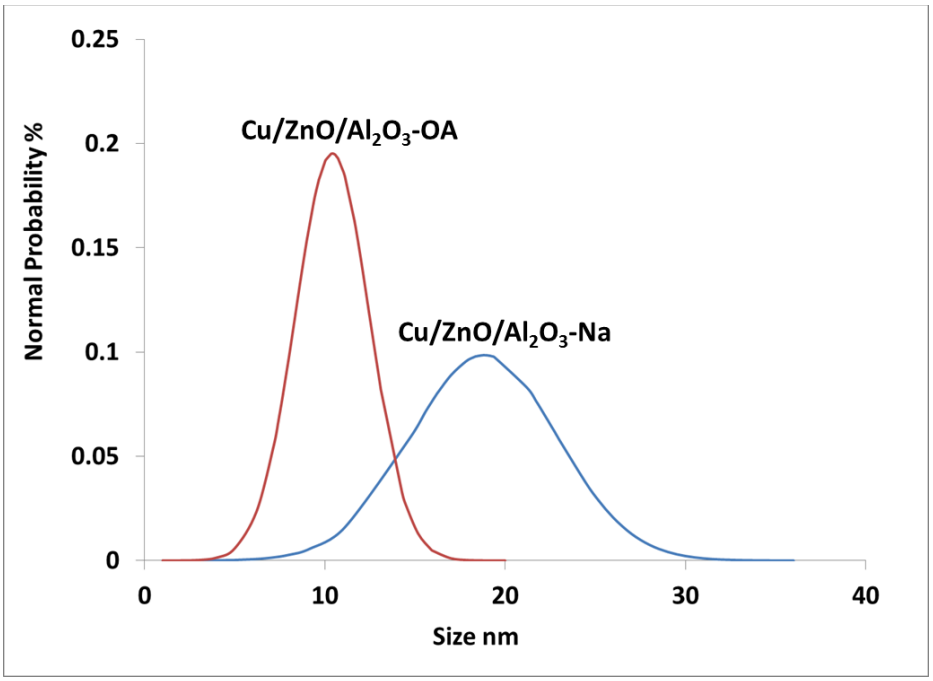

Figure 6-30 Effect of Preparation Method on $Cu/ZnO/Al_2O_3$ Catalyst Particle Size Distribution.

Table 6-10 Effect of Preparation Method on $Cu/ZnO/Al_2O_3$ Catalyst Particle Size Distribution.

	Mean	SD
$Cu/ZnO/Al_2O_3$-OA	10.41	2.04
$Cu/ZnO/Al_2O_3$-Na	18.83	4.05

6.6.3 Analysis of Fresh and Spent Catalysts

Figure 6-31 and Figure 6-32 show a comparison of the morphology of the catalysts between the fresh catalyst and the spent catalyst used for the glycerol hydrogenolysis reaction with molecular hydrogen added as discussed in Section 4.6. Both fresh $Cu/ZnO/Al_2O_3$ Cu/ZnO catalysts particles disperse very well. Both spent catalysts undergo a certain level of agglomeration. However, by comparing Figure 6-31C and Figure 6-31D with Figure 6-32C and Figure 6-32D, it can be observed that the agglomeration for spent Cu/ZnO catalyst is more serious than that of the $Cu/ZnO/Al_2O_3$ catalyst since the particles of the spent Cu/ZnO catalyst is more irregular and only large particles are observed. From Figure 6-32 and Table 6-11, it can clearly be seen that the particle size distribution of the spent $Cu/ZnO/Al_2O_3$ catalyst is not significantly changed

compared with the fresh catalyst. The average particle size of the Cu/ZnO catalyst grew remarkably from 14.96nm to 24.29nm after it was recycled and the distribution was much wider as seen by a larger standard deviation. This result indicates that the presence of Al can not only reduce the particle size of the catalyst but also can prevent catalyst aggregation during the reactions, therefore, improving the life time of the catalyst. This is in a very good agreement with what was discussed in Section 4.6 that with Al added, the Cu/ZnO/Al_2O_3 catalyst could be recycled and reused for 5 times with no significant deactivation being observed. When Cu/ZnO was used without Al added, the catalyst was deactivated when it was recycled and reused for the first time.

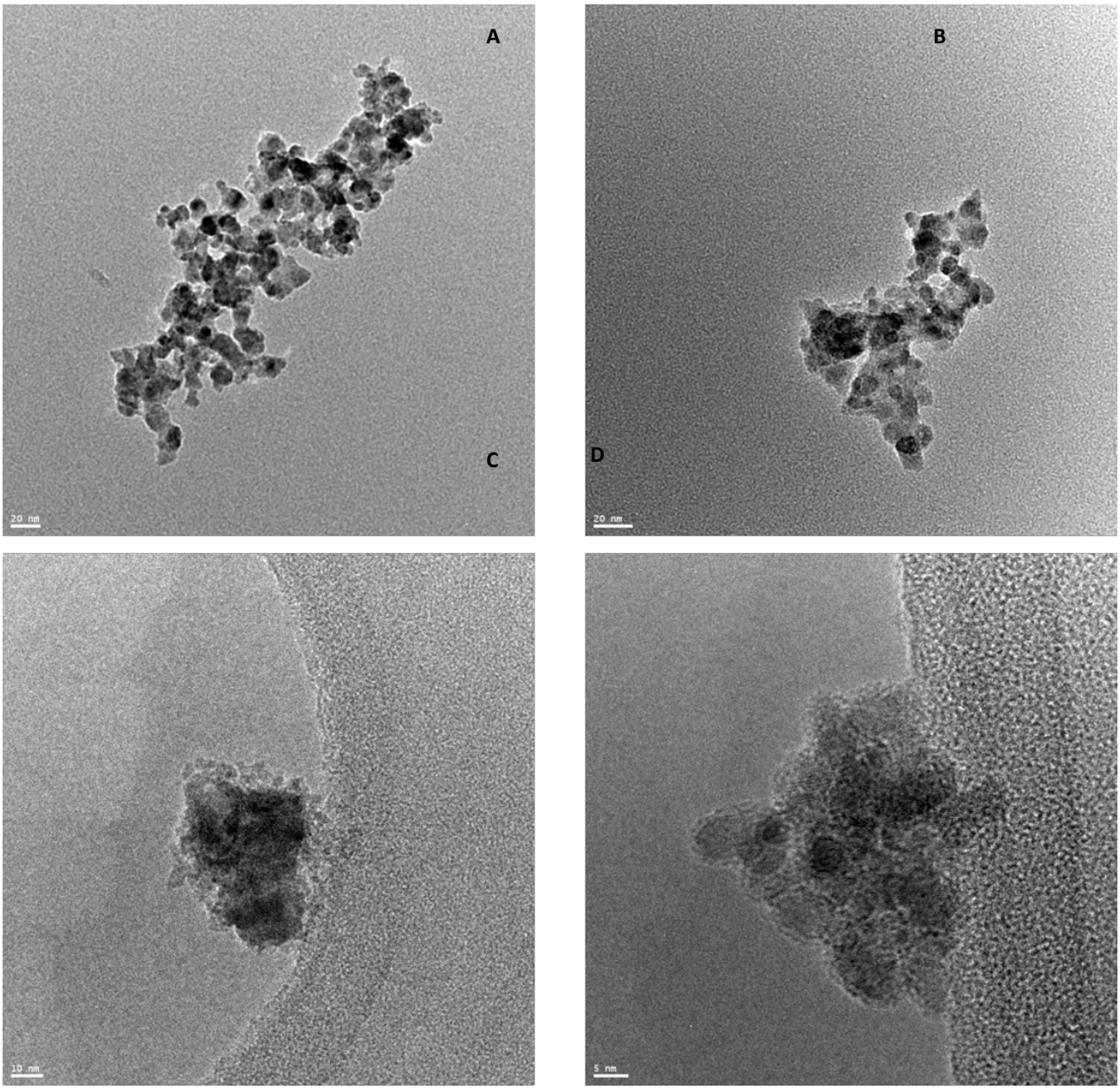

Figure 6-31 TEM Images of: A&B) $Cu/ZnO/Al_2O_3$ Fresh Catalyst Prepared by Oxalic Acid Co-Precipitation; C&D) $Cu/ZnO/Al_2O_3$ Spent Catalysts Prepared by Oxalic Acid Co-Precipitation.

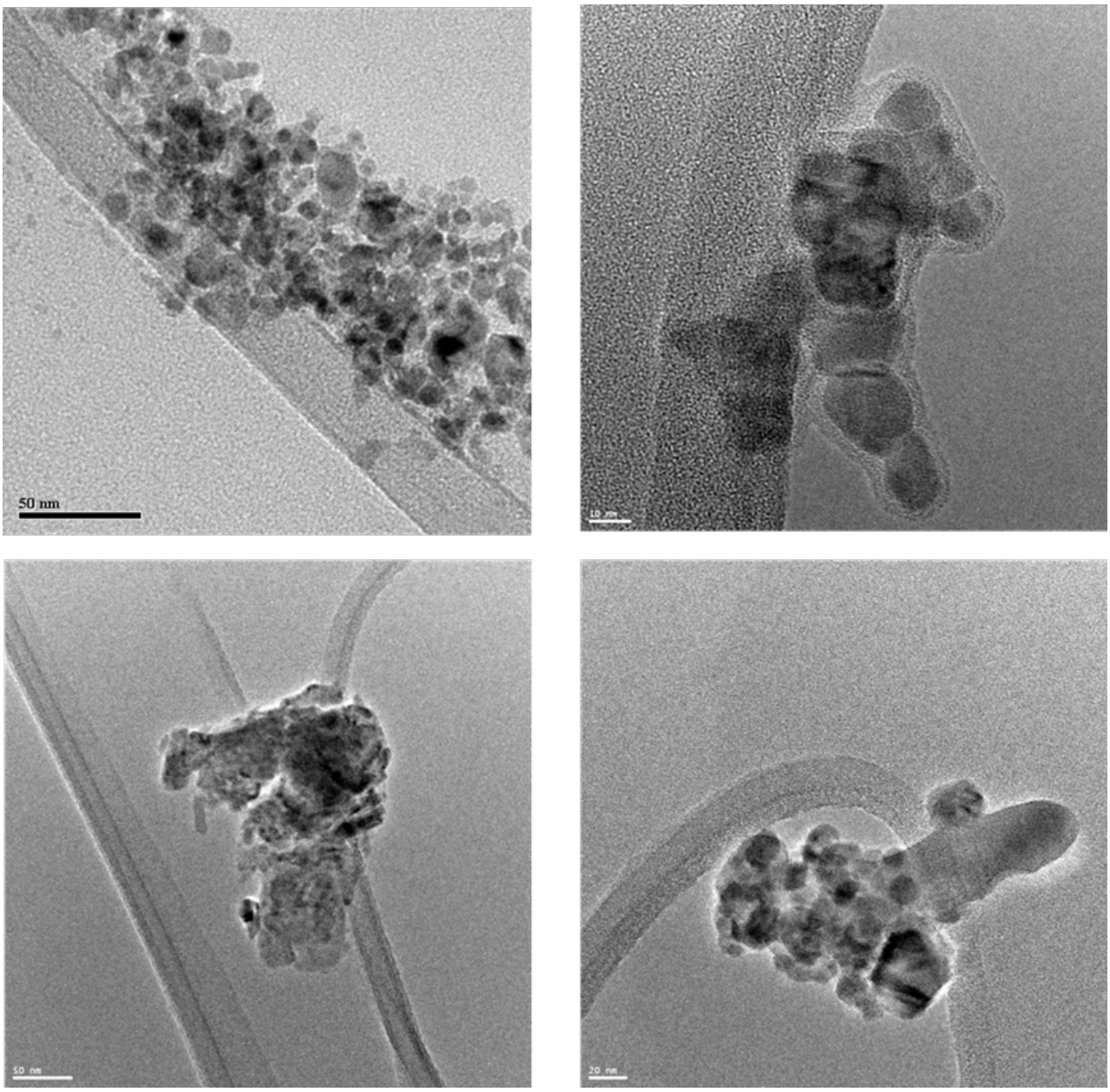

Figure 6-32 TEM Images of: A&B) Cu/ZnO Fresh Catalyst Prepared by Oxalic Acid Co-Precipitation; C&D) Cu/ZnO Spent Catalysts Prepared by Oxalic Acid Co-Precipitation.

Table 6-11 Catalyst Particle Size Distribution Comparison between Fresh Catalysts and Spent Catalysts.

	$Cu/ZnO/Al_2O_3$ Fresh	$Cu/ZnO/Al_2O_3$ Spent	Cu/ZnO Fresh	Cu/ZnO Spent
Mean	10.41	11.24	14.96	24.29
STDEV	2.04	2.04	3.71	8.14

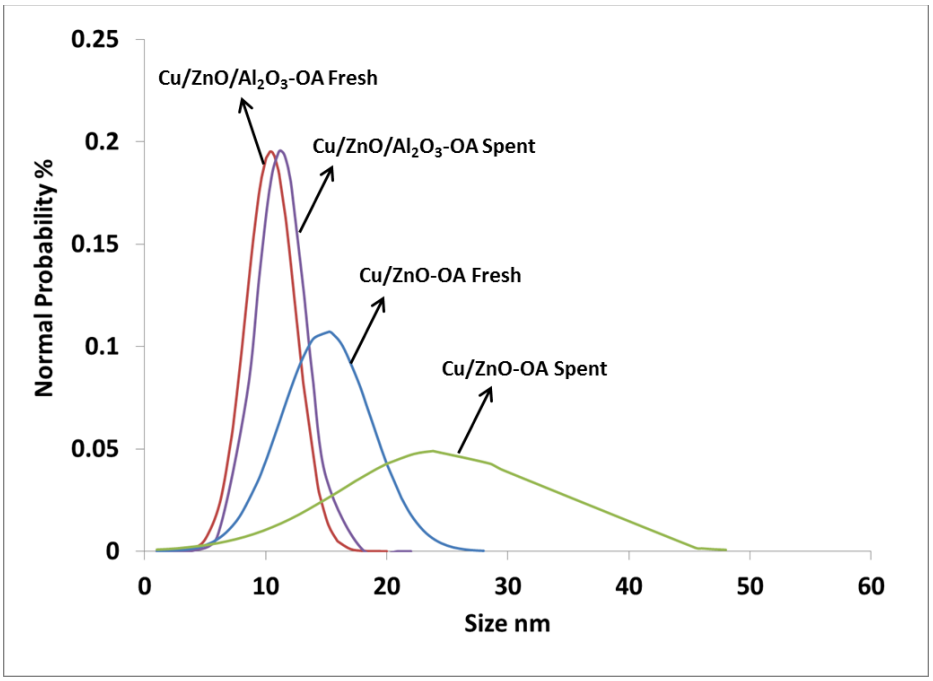

Figure 6-33 Catalyst Particle Size Distribution Comparison between Fresh Catalysts and Spent Catalysts.

6.6.4 TEM Analysis of $Cu/MgO/Al_2O_3$ Catalyst and Comparison with $Cu/ZnO/Al_2O_3$ Catalyst

In Figure 6-34C and Figure 6-34D, it can be observed that the $Cu/MgO/Al_2O_3$ (Cu/Mg/Al = 22.5/67.5/10) catalyst particles also has a spherical shape and dispersed very well. The average particle size of $Cu/MgO/Al_2O_3$ catalyst is measured to be 9.87nm, which is slightly smaller than that of the $Cu/ZnO/Al_2O_3$ catalyst and the size distribution of $Cu/MgO/Al_2O_3$ catalyst is narrower as shown in Table 6-12.

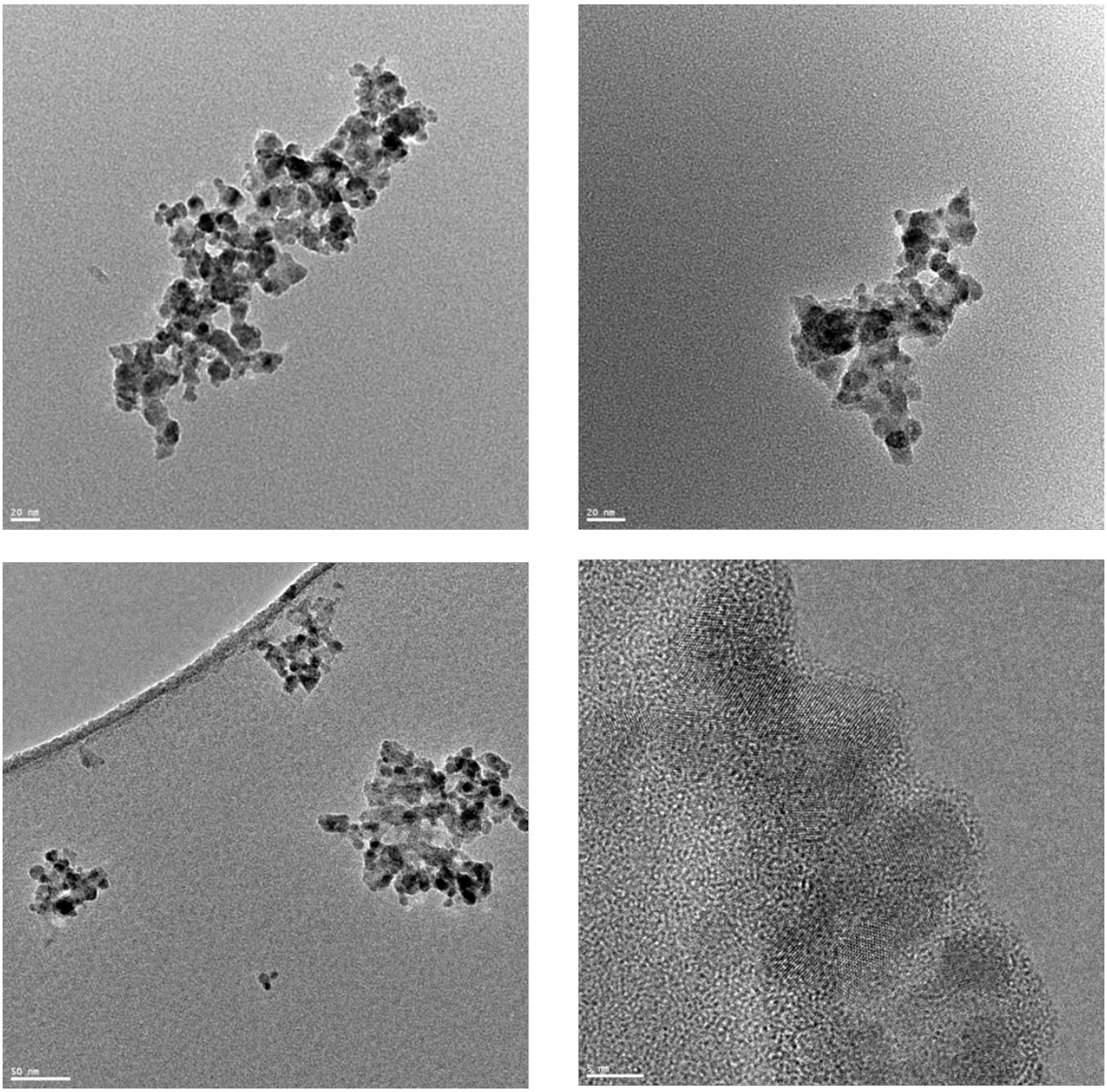

Figure 6-34 TEM Images of: A&B) $Cu/ZnO/Al_2O_3$ Catalyst Prepared via Oxalate Gel-coprecipitation; C&D) $Cu/MgO/Al_2O_3$ Catalysts Prepared via Oxalate Gel-coprecipitation

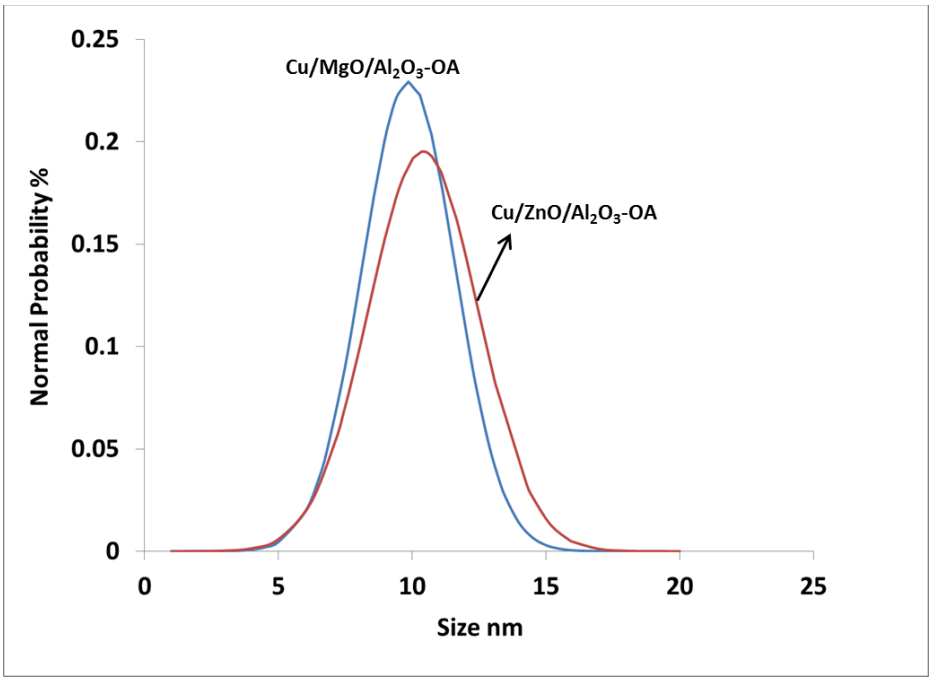

Figure 6-35 Particle Distribution Comparison between $Cu/MgO/Al_2O_3$ and $Cu/ZnO/Al_2O_3$.

Table 6-12 Particle Distribution Comparison between $Cu/MgO/Al_2O_3$ and $Cu/ZnO/Al_2O_3$.

	$Cu/ZnO/Al_2O_3$	$Cu/MgO/Al_2O_3$
Mean	10.41	9.87
STDEV	2.04	1.74

Table 6-13 and Figure 6-36 illustrate the relationship between the particle sizes of different catalysts and the rate constants for glycerol hydrogenolysis reactions using molecular hydrogen as reported in Chapter 4. It can be seen that the rate constant is higher when the particle size of the catalyst is smaller. Therefore, the particle size can significantly affect the catalyst activity and a smaller particle size is always desired for higher catalytic activity.

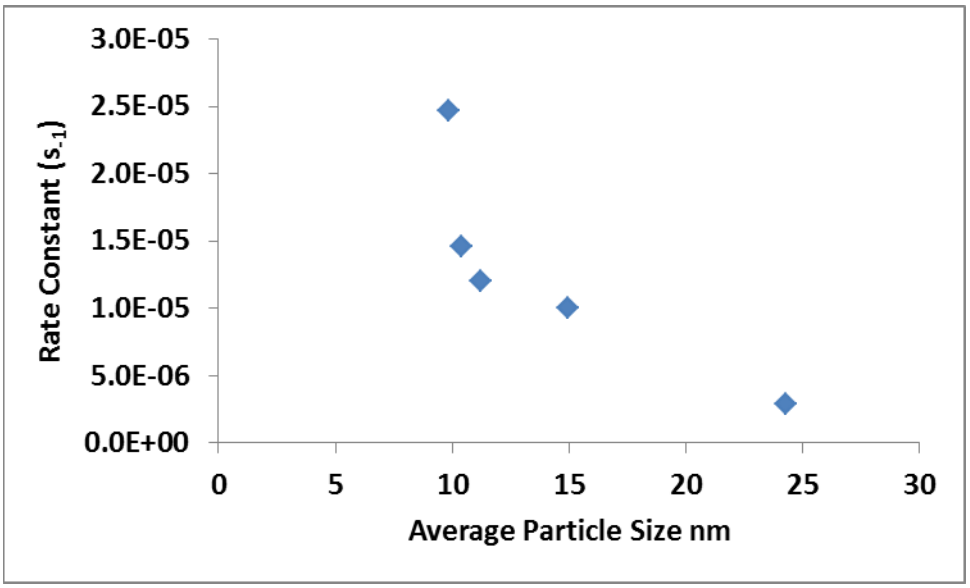

Figure 6-36 Relationship between the Catalyst Particle Size and the Rate Constant. Experimental Condition: 200ºC, 500RPM, 5wt% catalyst with respect to glycerol weight, 50wt% aqueous glycerol.

Table 6-13 Relationship between the Catalyst Particle Size and the Rate Constant[a]

Catalysts	Average Particle Size nm	Rate Constant s^{-1}
$Cu/MgO/Al_2O_3$ Fresh	9.87	2.469E-05
$Cu/ZnO/Al_2O_3$ Fresh	10.41	1.456E-05
$Cu/ZnO/Al_2O_3$ Spent	11.24	1.201E-05
Cu/ZnO Fresh	14.96	9.984E-06
Cu/ZnO Spent	24.29	2.885E-06

[a]Experimental Condition: 200ºC, 500RPM, 5wt% catalyst with respect to glycerol weight, 50wt% aqueous glycerol, 400psi H_2.

6.7 X-Ray Diffraction (XRD)

XRD experiments have been carried out using different catalysts to study the crystal structure of different catalysts. The detailed experimental method was described in Section 3.5.7.

6.7.1 XRD Parterns for Cu/ZnO/Al_2O_3 Catalysts Prepared by Different Methods

Figure 6-37 shows the XRD patterns for metal oxalates before calcination. The profile for Cu-oxalate and Zn-oxalate are shown for reference. Zn-oxalate peaks are observed at 2θ angles of 19.1°, 23.9° and 25.2° and a Cu-oxalate peak is observed at a 2θ angle of 22.8°, which is consistent with the data reported by Deng *et al*. in 1996 [78]. Both Cu/Zn/Al and Cu/Zn oxalate particles only show one broad peak at 2θ angles of 23.0° indicating that Cu and Zn are well mixed resulting in the overlaping of the peaks.

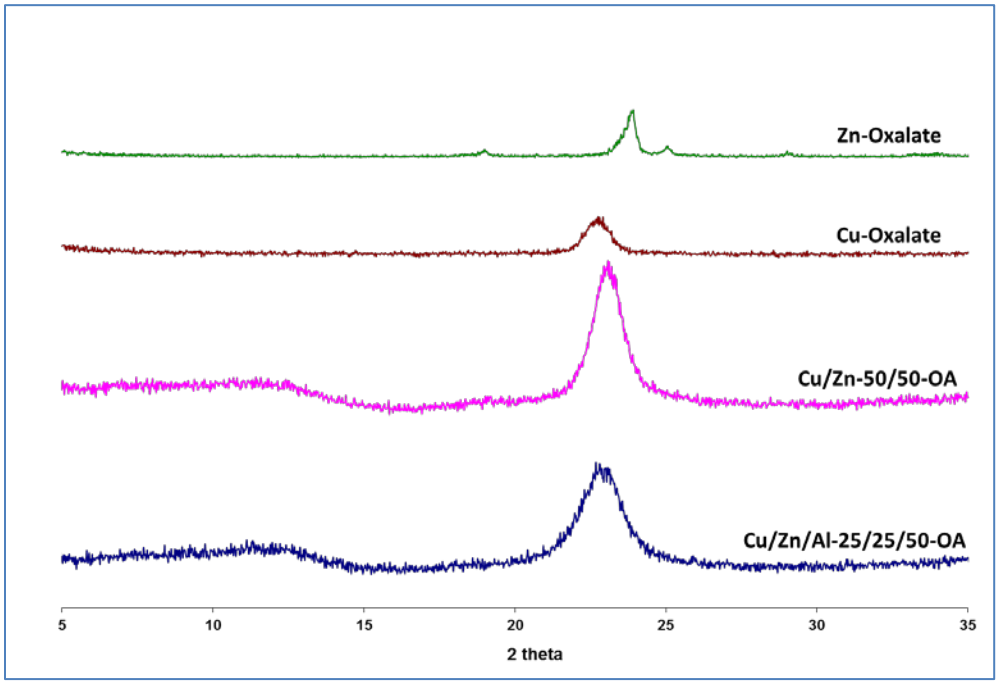

Figure 6- 37 XRD Patterns for Different Metal Oxalates.

Figure 6-38 illustrates the XRD patterns for calcined CuO/ZnO/Al_2O_3 catalysts prepared by different preparation methods. The calcined CuO and ZnO prepared by oxalic acid are shown for reference. CuO peaks are observed at 2θ angles of 35.4° and 38.6°, ZnO peaks show 2θ angles of 31.8°, 34.4° and 36.3°. For the CuO/ZnO/Al_2O_3-IMP catalyst, sharp CuO and ZnO peaks are observed representing high crystallization. The CuO/ZnO/Al_2O_3-Na and CuO/ZnO-OA show much more broaden peaks and some overlapping is shown in the 2θ region at 33.8º and 37.6º. In the pattern of the CuO/ZnO/Al_2O_3-OA catalyst, the peaks are even more broadened and the CuO

and ZnO peaks totally overlap each other and no Al_2O_3 peak is observed, which suggests that the particles are very well mixed and homogeneously distributed through the catalyst [79, 122].

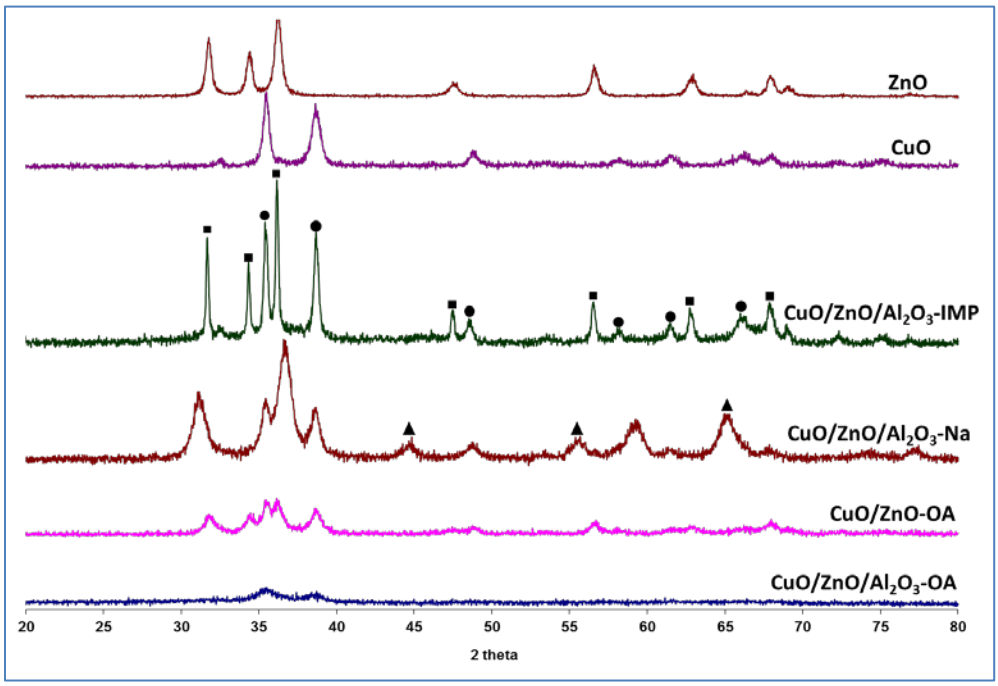

Figure 6-38 XRD Patterns for the Calcined Catalysts Prepared by Different Preparation Methods: (●) CuO, (■) ZnO, (▲) Al_2O_3. Cu/Zn/Al=25/25/50 for CuO/ZnO/Al_2O_3-OA and CuO/ZnO/Al_2O_3-Na, Cu/Zn=50/50 for CuO/ZnO-OA, Cu/Zn/Al=15/15/70 for CuO/ZnO/Al_2O_3-IMP.

Figure 6-39 shows the XRD patterns of the reduced catalysts. No CuO peaks are observed suggesting that CuO is completely reduced to Cu^0 under the reduction temperature of 300°C. Similarly to Figure 6-38, no ZnO and Al_2O_3 peaks are observed in the pattern for the catalyst Cu/ZnO/Al_2O_3-OA and the Cu^0 peak is much broader compared to the catalysts prepared by other methods. The Cu^0 particle size calculated by Scherre equation is the smallest (7.28nm shown in Table 6-14), which is important for glycerol hydrogenolysis, this observation is in good agreement with the discussion for the TEM images in Section 6.6. Therefore, the oxalate gel-coprecipitation with aluminum present has a significant effect on the particle dispersion and the catalyst structure.

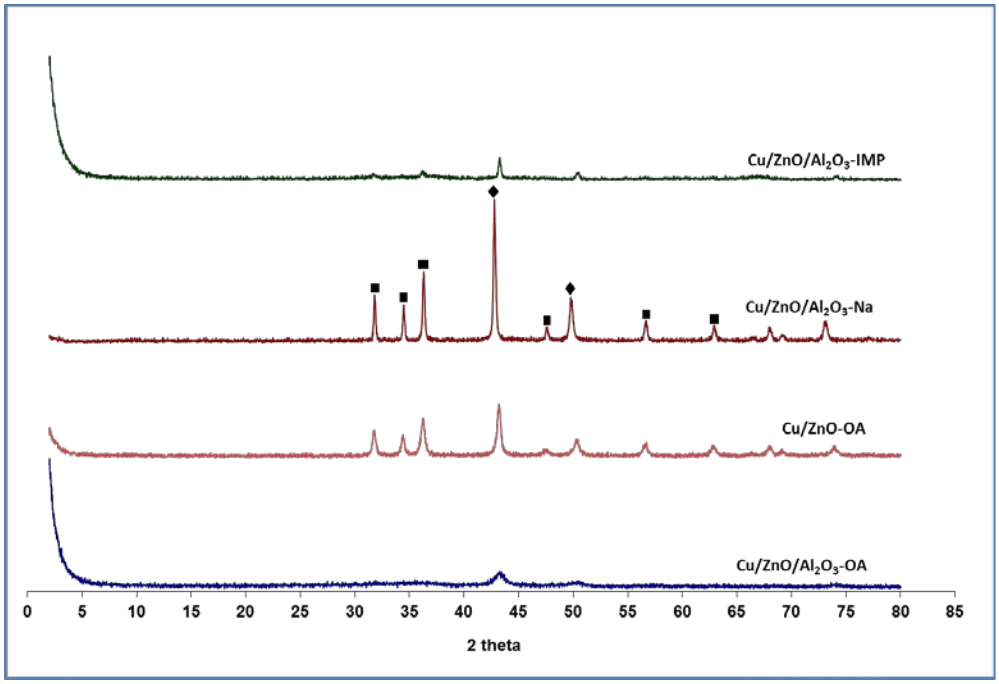

Figure 6-39 XRD Patterns for the Reduced Catalysts Prepared by Different Preparation Method: (♦) Cu, (■) ZnO. Cu/Zn/Al=25/25/50 for $Cu/ZnO/Al_2O_3$-OA and $Cu/ZnO/Al_2O_3$-Na, Cu/Zn=50/50 for Cu/ZnO-OA, Cu/Zn/Al=15/15/70 for $Cu/ZnO/Al_2O_3$-IMP

Table 6-14 Physical Chemical Properties of the Catalysts Prepared by Different Methods

Catalysts (Molar Feed Composition)[a]	Specific Surface Area [b]	Crystallite Size of Cu^0 [c]	Acidic Strength[d]	Total Acidic Sites[d]	Observed Metal Content (Cu; Zn; Al)[e]
	m^2/g	nm	$mmolNH_3/g_{cat}$	$mmolNH_3/g_{cat}$	wt%
Cu/Zn/Al-OA (25/25/50)	113.92	7.28	0.03 (89.2-359.0℃) 0.18 (399.5-787.4℃)	0.21	(30.78; 24.91; 11.56)
Cu/Zn-OA (50/50)	34.06	22.78	0.08 (222.9-426.3℃)	0.08	(44.02; 44.97; 0)
Cu/Zn/Al-Na (25/25/50)	53.09	35.99	0.04 (107.04-511.0℃)	0.04	(23.15; 23.32; 19.63)
Cu/Zn/Al-IMP (16.7/16.7/66.6)	95.58	32.36	0.27 (94.3-542.2℃)	0.27	(17.30; 17.79; 28.12)

[a.] Molar feed composition used to make the catalysts
[b] Measured by BET Surface Area Experiments
[c.] Calculated by Scherrer Equation from XRD Patterns
[d.] Measured by NH_3 TPD Experiments
[e.] Measured by ICP Experiments

6.7.2 XRD Patterns for $Cu/MgO/Al_2O_3$ Catalysts with Different Cu/Mg Molar Ratios

Figure 6-40 illustrates the calcined $Cu/MgO/Al_2O_3$ catalysts with different Cu/Mg ratio. It can be observed that as the Cu/Mg molar ratio increases, the CuO peaks at 2θ angles of 35.4° and 38.6° are getting sharper and the intensity is much higher suggesting that highly crystallized phases formed when the copper content is high. When the Cu/Mg molar ratio is 1/5, the peaks for CuO are less intense and no MgO peak is observed suggesting that Cu is in a highly dispersed form and well mixed with Mg. The particle size is calculated to be smaller when the copper content is lower as listed in Table 6-15. It has been discussed in Section 6.7 and Chapter 4 that the catalysts with smaller particle sizes can give higher activities for the glycerol hydrogenolysis reactions; however, based on the experimental results in Section 5.3.2, the catalyst is more active when the Cu/Mg molar ratio is 1/3. This is possibly because when the Cu content is very low, there will be less Cu sites on the catalyst surface resulting in a lower catalytic activity since it has been reported by Bienholz *et al*. in 2011 that the catalyst activity strongly depends on the copper surface area [190].

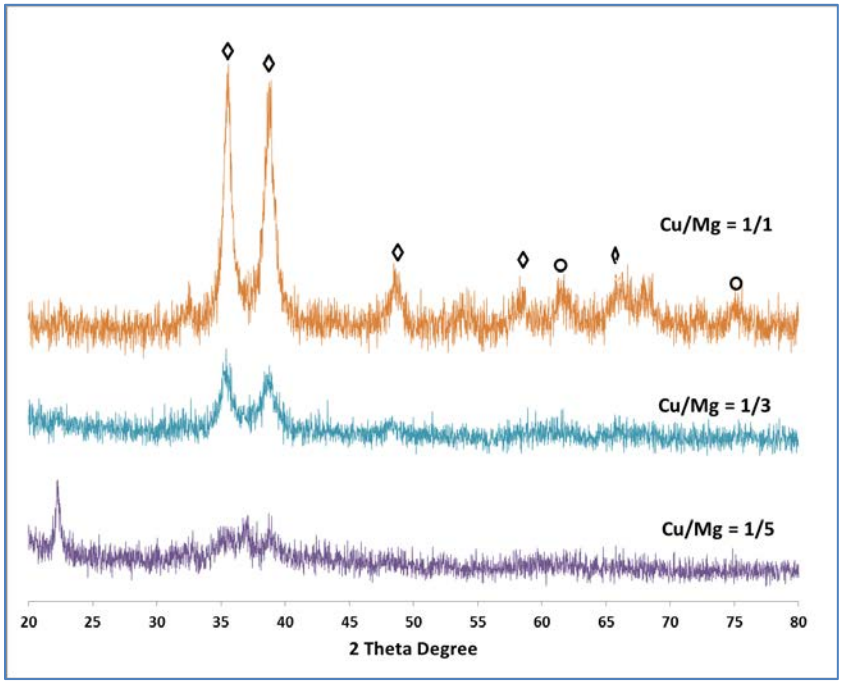

Figure 6-40 XRD Patters for $Cu/MgO/Al_2O_3$ Catalysts with Different Cu/Mg Ratio: ◊ CuO, ○ MgO.

Table 6-15 Crystal Sizes of $Cu/MgO/Al_2O_3$ Catalysts with Different Cu/Mg Ratios[a].

	Crystal Sizes	
	CuO	MgO
Cu/Mg=1/1	13.21	7.50
Cu/Mg=1/3	9.48	6.55
Cu/Mg=1/5	8.66	

[a]Calculated by Scherrer Equation

6.7.3 XRD Patterns for Pd Supported on $Cu/MgO/Al_2O_3$ Catalysts

Figure 6-41 illustrates the XRD patterns for the calcined Pd supported on $Cu/MgO/Al_2O_3$ catalysts with different Pd loading. It can be observed that no PdO diffraction peak was observed suggesting a high dispersion of Pd up to 3wt% loading. The crystal structures of CuO and MgO are not affected by Pd impregnation and the particle sizes of CuO and MgO are not significantly changed as listed in Table 6-16.

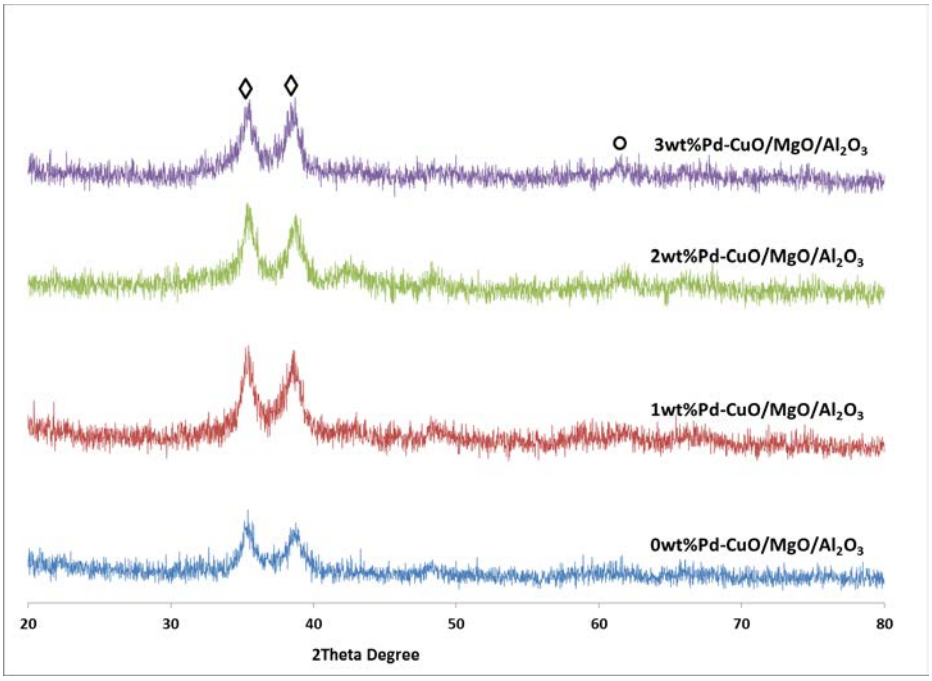

Figure 6-41 XRD Patters for Pd Supported on $Cu/MgO/Al_2O_3$ Catalysts: Cu/Mg/Al=22.5/67.5/10.

Table 6-16 Particle Sizes for Pd Supported on $Cu/MgO/Al_2O_3$ Catalysts[a].

	Crystal Sizes	
	CuO	MgO
0%Pd	9.475	6.55
1%Pd	10.81	8.89
2%Pd	10.735	8.33
3%Pd	9.965	7.11

[a]Cu/Mg/Al=22.5/67.5/10

6.7.4 XRD Patterns for the Recycled $Cu/MgO/Al_2O_3$ Catalysts

Figure 6-42 demonstrates the XRD patterns for fresh $CuO/MgO/Al_2O_3$ catalyst and spent $CuO/MgO/Al_2O_3$ catalyst. It can be clearly observed that both CuO and MgO peaks for the recycled catalyst are much sharper compared with the fresh catalyst; the CuO and ZnO particle sizes for the fresh catalyst are calculated to be 9.48nm and 6.55nm respectively and CuO and MgO particle sizes for the spent catalyst are significantly larger than that of a fresh catalyst which are 23.80nm and 12.43nm respectively as shown in Table 6-17. This suggests that severe catalyst sintering occurred during the reaction leading to an increase in the particle size and therefore, a decrease in the active surface area and hence a loss of activity. This observation is in a good agreement with what has been discussed in Section 5.3.4 in that the $Cu/MgO/Al_2O_3$ catalyst was significantly deactivated after it was recycled and in agreement with some literature reporting on such catalyst deactivation [68, 80].

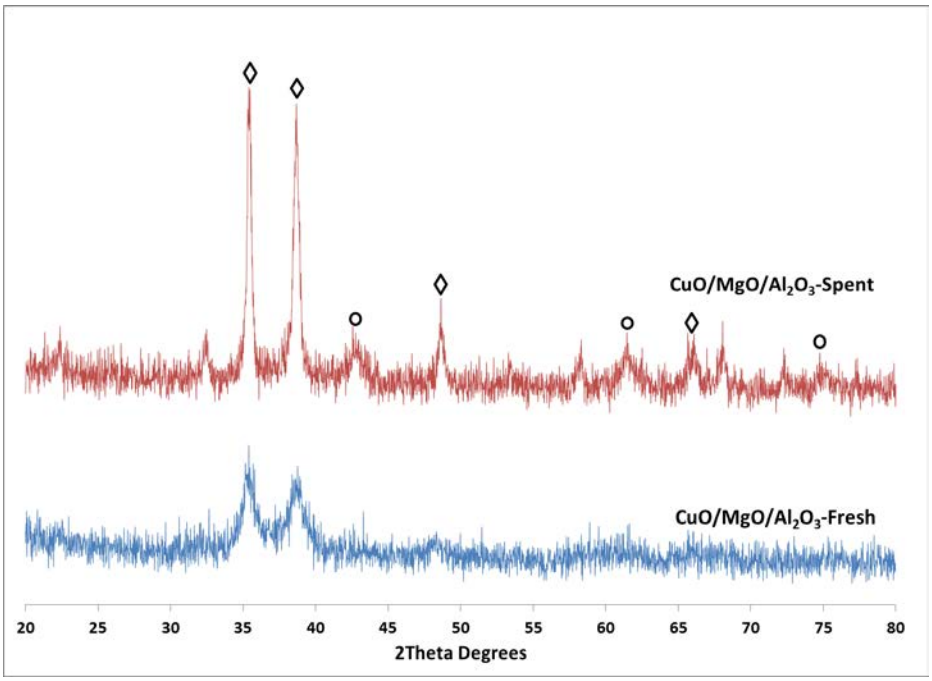

Figure 6-42 XRD Patterns for Fresh $CuO/MgO/Al_2O_3$ and Recycled $CuO/MgO/Al_2O_3$ Catalysts: ◊ CuO, ○ MgO.

Figure 6-43 illustrates the XRD patterns for fresh and spent 2wt%Pd-$CuO/MgO/Al_2O_3$ catalysts. The peaks for CuO and MgO changed in a similar way as described in the XRD patterns for the recycled $CuO/MgO/Al_2O_3$ catalyst. As listed in Table 6-17, the CuO and ZnO particle sizes for the fresh catalyst are calculated to be 10.74nm and 8.33nm respectively and CuO and MgO particle sizes for the spent catalyst are 16.67nm and 17.40nm respectively. As shown in the pattern for the fresh catalyst, no PdO peak is observed due to a high dispersion of palladium on the catalyst; when the catalyst is recycled, a PdO peak is observed at a 2θ angle of 34.2° suggesting that Pd is also sintered during the reaction resulting in a larger particle size which is calculated to be 15.43nm. Therefore, the catalyst is deactivated after it was recycled and reused as discussed in Section 4.10.

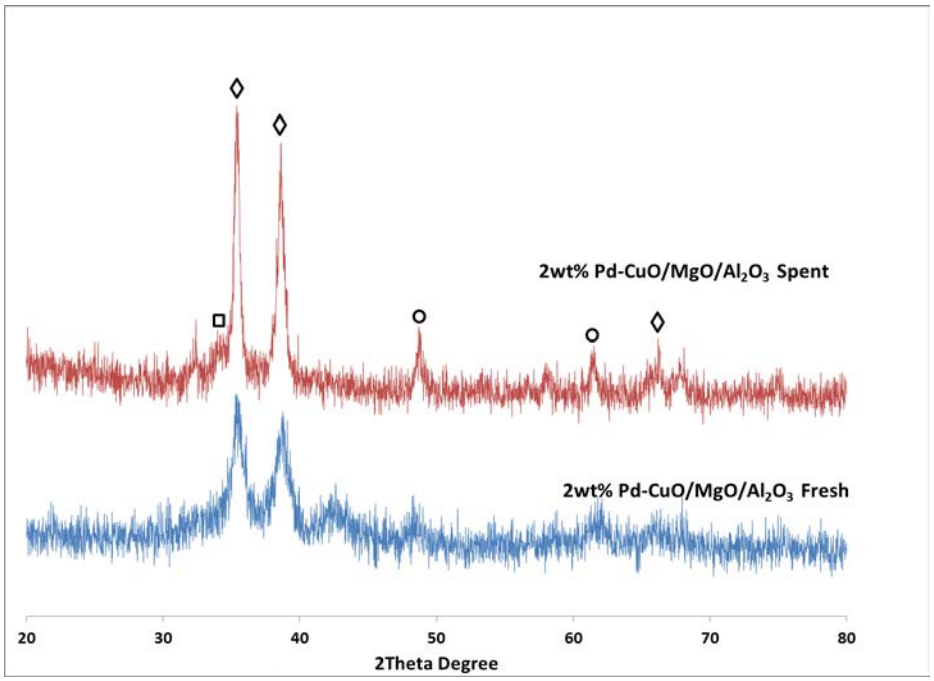

Figure 6-43 XRD Patterns for Fresh and Recycled 2%Pd Supported on $CuO/MgO/Al_2O_3$ Catalysts: ◊ CuO, ○ MgO, ▫ PdO.

Table 6-17 Particle Size for Fresh and Recycled Catalysts[a].

	Crystal Sizes		
	CuO	MgO	PdO
Fresh Cu/MgO/Al2O3	9.48	6.55	
Recycled Cu/MgO/Al2O3	23.80	12.43	
Fresh 2%Pd-Cu/MgO/Al2O3	10.74	8.33	
Recycled 2%Pd-Cu/MgO/Al2O3	16.67	17.40	15.43

[a]Cu/Mg/Al=22.5/67.5/10

6.8 Conclusions

In this chapter, catalysts have been characterized by different catalyst characterization techniques to study the relationship between the catalyst structure and the catalytic activity.

NH_3 TPD experiments have been conducted to investigate the acidity of the different types of catalysts. From the results, it was seen that the $Cu/ZnO/Al_2O_3$ catalyst prepared via oxalate gel-coprecipitation had stronger acidic sites compared with the ones prepared via Na_2CO_3 coprecipitation and impregnation; therefore, the $Cu/ZnO/Al_2O_3$ catalyst exhibited the highest activity for the glycerol hydrogenolysis reaction. $Cu/MgO/Al_2O_3$ NH_3 TPD results showed that the major acidic sites were of medium strength and the number of acidic sites was an order of magnitude higher than that for a $Cu/ZnO/Al_2O_3$ catalyst. The effect of Ni on the catalyst acidity has been investigated and it was found that Ni reduced the acidic sites for both the catalysts $Cu/ZnO/Al_2O_3$ and $Cu/MgO/Al_2O_3$. It was found that the catalyst activity was strongly dependent on the number of strong acidic sites [191].

H_2 TPR experiments have been carried out to investigate the reduction behavior of the catalyst and to determine the optimum reduction temperature. It was found that Ni does not affect the reduction temperature of both $Cu/MgO/Al_2O_3$ and $Cu/ZnO/Al_2O_3$; Pd could significantly reduce the reduction temperature of $Cu/MgO/Al_2O_3$.

H_2 TPD experiments were carried out to study the characterization of hydrogen adsorption and hydrogen storage capacity for different catalysts. By adding Pd on $Cu/MgO/Al_2O_3$ up to 2wt%, the amount of hydrogen adsorbed on the catalyst surface increased, if more Pd was loaded, the amount of adsorbed catalyst did not significantly increased. It was found that the 1,2PD selectivity was strongly dependent on the amount of hydrogen adsorbed [106].

CO_2 TPD experiments were carried out using $Cu/MgO/Al_2O_3$ to study the basicity of the catalysts with different metal composition. It was found that when the Cu/Mg ratio was lower, a higher amount of basic sites were observed. The loading of Pd significantly reduced the amount of basic sites. No direct relationship was found between the catalyst basicity and the catalyst activity.

TGA experimental results were used to determine the optimum calcination temperature. It was also observed that for a $Cu/ZnO/Al_2O_3$ catalyst prepared by oxalate gel-coprecipitation, with Al added the metals were mixed better than that without Al added.

The TEM images were used to visualize the catalyst particle shape and analyze the particle size distribution. It was found that the $Cu/ZnO/Al_2O_3$ catalyst prepared via an oxalate gel-coprecipitation had a spherical particle shape and the $Cu/ZnO/Al_2O_3$ catalyst prepared via a Na_2CO_3 coprecipitation had an elliptical shape. The effect of Al on the catalyst stability has been analyzed based on the TEM images of fresh and recycled catalysts. It was seen that with Al added, no significant agglomeration was observed and the average particle size was slightly increased after the catalyst was recycled. When the Cu/ZnO catalyst was recycled without Al, severe sintering occurred and only large particles were observed in the images, which was the main reason for the catalyst deactivation. It was found that the catalyst activity was strongly related to the average particle size of the catalyst.

XRD experiments were carried out to study the crystal structure of different catalysts. The $Cu/ZnO/Al_2O_3$ catalyst prepared by oxalate gel-coprecipitation exhibited a better component dispersion with a smaller particle size compared to the catalysts prepared by the Na_2CO_3 co-precipitation and the impregnation methods. For $Cu/MgO/Al_2O_3$ catalysts, when the Cu/Mg ratio was high, the Cu was in a highly crystallized form resulting in a larger particle size. When $Cu/MgO/Al_2O_3$ catalyst and 2wt% $Pd-Cu/MgO/Al_2O_3$ catalyst were recycled, severe sintering occurred leading to a larger particle size, and hence catalyst deactivation [68, 80].

Chapter Seven
Conclusion and Recommendation

7.1 Conclusions on Glycerol Hydrogenolysis Prcesses Using Molecular Hydrogen

The experiments for glycerol hydrogenolysis process using molecular hydrogen have been carried out in an autoclave batch reactor. The $Cu/ZnO/Al_2O_3$ catalysts were prepared by three different preparation methods, i.e. oxalate gel-coprecipitation, Na_2CO_3 coprecipitation and impregnation. The experimental results showed that the catalyst prepared via oxalate gel-coprecipitation exhibited the highest activity. The results of XRD and TGA/DGA showed better metal mixing for the catalyst prepared by oxalate gel-coprecipitation compared with the catalyst prepared by the other two methods. The NH_3 TPD experimental results suggested that the $Cu/ZnO/Al_2O_3$ prepared by gel-coprecipitation provided stronger acidic sites, and these strong acidic sites could facilitate the glycerol dehydration step, which is the rate limiting step, and thus, improve the catalyst acitivity. From the TEM images and XRD analysis, it was seen that the $Cu/ZnO/Al_2O_3$ catalysts prepared by the oxalate gel-coprecipitation method could provide highly dispersed particles and the particle size was smaller compared with the catalyst prepared by the other two methods; more active sites were provided if the particle size was smaller, and hence the catalyst was more active. Therefore, it can be seen that the catalyst acidity, the metal mixing and the particle size play an important role on the catalytic activity of a $Cu/ZnO/Al_2O_3$ catalyst.

The effect of hydrogen pressure on the reaction products of the glycerol hydrogenolysis processes has been investigated using different hydrogen pressures. The experimental results showed that the 1,2PD selectivity strongly depended on the hydrogen pressure. When the hydrogen pressure was low many un-desired by-products were formed resulting in a low 1,2PD selectivity. The by-product formation was mainly due to side reactions with acetol when the supplied hydrogen was not sufficient to rapidly hydrogenate the acetol to 1,2PD as reported by van Ryneveld *et al.* [99]. Acetol hydrogenation reactions at different hydrogen pressures have

also been carried out. Same by-products were detected by GC confirming that the by-product formation was due to side reactions with acetol. The calculated rate constant of acetol hydrogenation was one order of magnitude higher than that for the glycerol hydrogenolysis process under the same reaction conditions suggesting that acetol hydrogenation is the rate determing step [48].

A composition study of Cu/Zn/Al has been carried out and the optimum molar ratio of Cu/Zn/Al was determined to be 25/25/50. It was also found that the addition of alumina did not only increase the activity of a Cu/ZnO catalyst but also improved the stability of the catalyst. Without Al added, the Cu/ZnO catalyst was significantly deactivated when it was reused for the first time recycle; however, when Al was added, after 4 times recycling no obvious deactivation was observed. The TEM results showed that after recycling, the particle size of the Cu/ZnO catalyst without Al added was larger than that for the fresh catalyst, and the particle size for a $Cu/ZnO/Al_2O_3$ catalyst was not significantly changed suggesting that severe sintering has occurred for the Cu/ZnO catalyst during the reaction. This is in a very good agreement with literature reports on catalyst deactivation [68, 80]. The enhancement of the catalyst stability as a result of Al addition was because alumina could isolate the individual metal particles to prevent their sintering [68, 124].

The promoting effect of Ni was also investigated. The acetol hydrogenation experimental results showed that with Ni added, the hydrogenation rate and the 1,2PD selectivity were higher than when using a $Cu/ZnO/Al_2O_3$ catalyst without Ni added suggesting that the addition of Ni improved the hydrogenation activity of the $Cu/ZnO/Al_2O_3$ catalyst. However, when the $Ni/Cu/ZnO/Al_2O_3$ catalyst was used for the glycerol hydrogenolysis reaction; the reaction rate was lower resulting in a lower glycerol conversion. Based on the NH_3 TPD results, the addition of Ni reduced the number of strong acidic sites, which caused some loss of catalyst activity for the glycerol dehydration step, which is the rate limiting step in the glycerol hydrogenolysis process; therefore, the reaction was slower on adding Ni to a $Cu/ZnO/Al_2O_3$ catalyst.

$Cu/MgO/Al_2O_3$ prepared via oxalate gel-coprecipitation has been used in the glycerol hydrogenolysis process. Compared with the $Cu/ZnO/Al_2O_3$ catalyst, the $Cu/MgO/Al_2O_3$ catalyst showed a higher activity for the glycerol hydrogenolysis process. Based on the TEM images and XRD results the particle size of the $Cu/MgO/Al_2O_3$ catalyst was smaller than the $Cu/ZnO/Al_2O_3$

catalyst. The number of acidic sites of the $Cu/MgO/Al_2O_3$ catalyst was ten times more than that for the $Cu/ZnO/Al_2O_3$ catalyst; however, the strength of the acidic sites for the $Cu/MgO/Al_2O_3$ catalyst was slightly lower, and therefore, the rate constant obtained using the $Cu/MgO/Al_2O_3$ catalyst was not a magnitude higher than that obtained using the $Cu/ZnO/Al_2O_3$ catalyst.

The effect of Pd loading on the $Cu/MgO/Al_2O_3$ catalyst was investigated by impregnating Pd on a $Cu/MgO/Al_2O_3$ catalyst. The enhancement of the catalyst acitivity was due to more surface hydrogen supplied with addition of Pd as observed in the results of the H_2 TPD. The stability of the supported Pd on the $Cu/MgO/Al_2O_3$ catalyst has also been investigated by reusing the catalyst. A significant activity loss was observed when the catalyst was first time recycled and used. The catalyst deactivation was possibly due to sintering during the reaction resulting in a large particle size as observed in XRD results.

The activation energy of the reactions using $Cu/ZnO/Al_2O_3$ catalyst and $Pd/Cu/MgO/Al_2O_3$ were calculated based on the Arrhenius Equation, and were 69.39kJ/mol and 113.62kJ/mol respectively. This suggests that the reactions are chemical kinetically controlled for both catalysts with the process using $Pd/Cu/MgO/Al_2O_3$ being more temperature dependent than when using $Cu/ZnO/Al_2O_3$ catalyst.

7.2 Conclusions on Glycerol Hydrogenolysis Processes Using in situ Hydrogen Produced by Methonal Steam Reforming

Experiments for the glycerol hydrogenolysis process using molecular hydrogen have been carried out in an autoclave batch reactor. The $Cu/ZnO/Al_2O_3$ catalysts prepared by three different preparation methods, i.e. oxalate gel-coprecipitation, Na_2CO_3 coprecipitation and impregnation. The experimental results showed that the catalyst prepared via the oxalate gel-coprecipitation gave the highest activity, i.e. higher glycerol conversion and 1,2PD selectivity, which has also been observed in the results for the glycerol hydrogenolysis process using molecular hydrogen. The promoting effect of Ni has been investigated. Based on the experimental results, the addition of Ni improved the 1,2PD selectivity because Ni could promote the methanol steam reforming to produce more hydrogen; however, due to the reduced amount of strong acidic sites on Ni

addition as observed in NH_3 TPD results, the glycerol conversion was lower. When the $Ni/ZnO/Al_2O_3$ catalyst was used without Cu, no glycerol was converted suggesting that Cu was necessary for the glycerol dehydration step when the $Ni/Cu/ZnO/Al_2O_3$ catalyst was used. Pd was loaded on the $Cu/ZnO/Al_2O_3$ catalyst by different preparation methods, i.e. impregnation, reduction deposition and deposition precipitation, and with different Pd precursors, i.e. palladium acetate and palladium nitrate. The catalyst prepared by the impregnation method with palladium acetate as the Pd precursor showed the highest 1,2PD selectivity. Compared with $Cu/ZnO/Al_2O_3$ catalyst the glycerol conversion by the $Pd/Cu/ZnO/Al_2O_3$ catalyst was slightly lower due to fewer strong acidic sites as shown from the NH_3 TPD results and the 1,2PD selectivity was significantly improved due to more surface hydrogen being supplied by Pd as shown from the H_2 TPD results and the promoting effect on the methanol steam reforming reaction as has frequently been reported [174, 175].

A $Cu/MgO/Al_2O_3$ catalyst was used for the glycerol hydrogenolysis process using *in situ* hydrogen produced by methanol steam reforming; both glycerol conversion and 1,2PD selectivity were significantly improved compared with the $Cu/ZnO/Al_2O_3$ catalyst. A Cu/Mg/Al composition study has been carried out and the optimum Cu/Mg/Al molar ratio was found to be 22.5/67.5/10.

The effect of Pd on the $Cu/MgO/Al_2O_3$ has been investigated, a 2wt% Pd loading was found to be the optimal. The H_2 TPD results suggested that the 1,2PD selectivity was strongly related to the total amount of hydrogen adsorbed on the catalyst surface.

The promoting effect of Ni on the $Cu/MgO/Al_2O_3$ catalyst has been investigated. The experimental results showed that the glycerol conversion was decreased as more Ni was loaded; when 5mole% Ni was loaded the catalyst was completely deactivated. This was because when 5mole% Ni was loaded, most of the acidic sites were eliminated based on the NH_3 TPD results.

Ga_2O_3 was added on the Cu/MgO instead of Al_2O_3 to investigate the enhancement of the catalyst activity and stability. No obvious improvement on the catalytic activity was observed by replacing Al_2O_3 with Ga_2O_3 for the fresh catalysts and both $Cu/MgO/Al_2O_3$ and $Cu/MgO/Ga_2O_3$ catalysts were deactivated when they were recycled and reused. Based on the XRD results, severe sintering occurred during the experiments resulting in a larger particle size.

The glycerol hydrogenolysis reactions using *in situ* hydrogen produced by methanol steam reforming were carried out with molecular hydrogen initially added. The 1,2PD selectivity was significantly improved compared with the experiment with nitrogen initially added. Since it has been discussed that the low 1,2PD selectivity was most likely due to insufficient hydrogen produced via methanol steam reforming especially in the early stage of the reaction, the addition of molecular hydrogen initially could enhance the acetol hydrogenation resulting in a higher 1,2PD selectivity.

7.3 Recommendations

It has been reported that a fixed bed reactor is normally used for a continuous process to convert glycerol into 1,2PD [48, 77, 143, 192, 193]. It has been discussed that the low selectivity for the glycerol hydrogenolysis process using *in situ* hydrogen produced by methanol steam reforming is due to insufficient hydrogen for the acetol hydrogenation reactions. In a fixed bed reactor, all of the reaction can be carried out in a gas phase. The gas phase reaction for glycerol hydrogenolysis can eliminate the limitation of low hydrogen solubility in the liquid, therefore, the formation of by-products caused by insufficient hydrogen supply when a batch reactor is used can be reduced; when the reaction is in the gas phase a high methanol conversion can be achieved for methanol steam reforming [138, 145, 194]. Furthermore, it has been discussed that the catalyst deactivation in a glycerol hydrogenolysis process using *in situ* hydrogen produced by methanol steam reforming is possibly due to the formation of carbonate when the metals or metal oxides contact with CO_2 which is the by-product of the methanol steam reforming reaction; therefore, a continuous process can reduce the contact time between CO_2 and the catalyst surface preventing deactivation of the catalyst.

Catalytic distillation (CD) is a novel technology that combines a catalytic reaction in a distillation process. The CD reactor consists of a packed distillation column, within which heterogeneous catalysts are located. During the reaction the reactants and products are separated *in situ* by distillation. This continuous removal of product from the reaction zone can effectively enhance the conversion for equilibrium-limited reactions, resulting in a much higher conversion than the theoretical equilibrium conversion. In addition, the rapid removal of products from the

reaction zones can improve the selectivity by preventing undesirable consecutive reactions due to the lower contact time of the product and the catalyst surface. For a glycerol hydrogenolysis process, it has been discussed that the glycerol dehydration is the rate limiting step of the whole process and water is the inhibitor for this process. The boiling points of the two products (1,2PD and water) are 188.2˚C and 100˚C respectively and the differences between these two boiling points are very large; therefore, CD is expected to be very suitable for this process because it can eliminate the distillation process of separating water and propylene glycol as Figure 7-1 shows. The *in situ* removal of water from the distillate can also enhance the rate of the reaction.

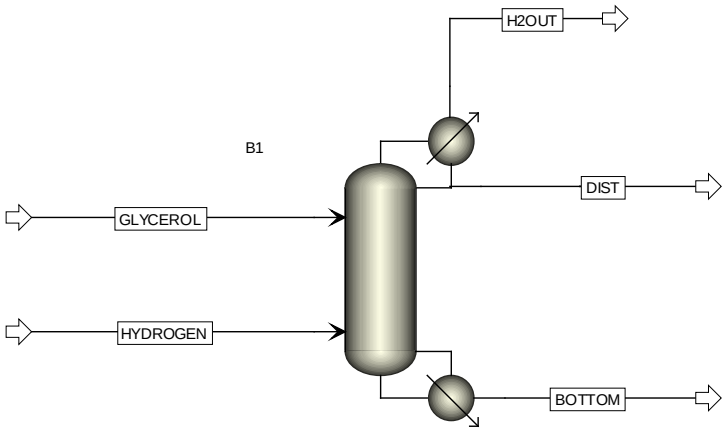

Figure 7-1 Process for Conversion of Glycerol into 1,2-PD via CD.

Appendix A Literature Data

Table A-1 Glycerol Hydrogenolysis to 1,2-Propanediol with Molecular Hydrogen Added.

Catalyst	Catatyst Loading	Glycerol Content	Temperature	Pressure	Reaction Time	Conversion	1,2PD Selectivity	13PD Selectivity	Ref
(Co-Catalyst)	wt%	wt%	C	psi	hr	%	%		
CsPW	4	20	120	73	10	0.0	0.0		alhanash 2008
			180	0		0.0	0.0		
5%Ru/CsPW			120	73		9.8	88.0		
			150			21.0	95.8		
	6					31.0	87.6		
	10					31.0	82.9		
	4		180			23.0	73.6		
			200			27.0	67.7		
5%Rh/CsPW			180			6.3	65.4		
Cu/Zn 40/60	1.2g/100ml	20	200	290	16	30.0	91.0		balaraju 2008
Cu/Zn 50/50						37.0	92.0		
Cu/Zn 60/40						27.0	92.0		
Cu/Zn 70/30						15.0	92.0		
Ru/C (TPA/ZrO2)	3+6	20	180	870	8	44.0	64.3		balaraju 2009
Ru/C (CsTPA)						21.0	60.2		
Ru/C (CsTPA/ZrO2)						25.0	67.0		
IER						25.0	40.9		
Ru/C (Nb2O5)						44.6	60.9		
	0.6g(1.2g)/50ml					62.8	66.5		
Co/SiO2	3	60	200	725	12	8.3	61.7		Huang 2008
Cu/SiO2						5.9	57.5		

Ni/SiO2						8.5	60.5		
Pd/SiO2						2.4	65.3		
Ru/SiO2						24.3	47.8		
Cu/ZnO/Al2O3						20.4	80.1		
Cu/Cr2O3						15.1	73.8		
Ni/Al2O3						32.3	55.1		
Pd/C						2.1	63.2		
30% CuO/SiO2 (PG) 4.5%Na	5	80	180	1305	12	15.4 / 8.6	94.4 / 97.3		Huang 2009
30% CuO/SiO2 (PG) 2.49%Na						21.6	96.7		
30% CuO/SiO2 (PG) 0.54%Na						27.2 / 23.5	98.5 / 97.4		
30% CuO/SiO2 (PG) 0.14%Na						32.7	98.7		
30% CuO/SiO2 (PG) 0.01%Na						28.6 / 21.3	99.0 / 99.2		
30% CuO/SiO2 (PG) 1.9%Na impregnation						24.0	94.3		
Ru/Al2O3	150mg/10ml	40	150	1160	8	18.7	34.5	3.4	Ma 2008
Ru/ZrO2						19.5	36.3	7.2	
Ru/C						29.7	50.9	0.8	
Ru/Al2O3 +Re2(CO)10						53.4	50.1	6.4	
Ru/ZrO2 +Re2(CO)10						27.1	53.1	12.6	
Ru/C +Re2(CO)10						59.4	56.6	7.2	
			160			53.4	50.1	6.4	
			140			29.0	52.8	9.9	
			160	1450		56.3	50.3	8.1	
				870		33.9	46.7	6.1	
Cu/Calcined PG nano 19.6nm	5	80	180	1305	12	52.7	93.1		Huang 2008
Cu/Reduced PG nano 9.0nm						73.4	94.3		
Cu/Calcined IM nano 35.2nm						22.9	94.5		
Cu/Reduced IM nano 31.1nm						25.6	95.2		

Pt/WO3/TiO2	100mg	3mmol/0.2mlDMI	170	1160	18	16.9 (yield)	7.1	6.5	Kurosaka 2008
Pt/WO3/HY						25.9	8.9	7.2	
Pt/WO3/AlMCM-41						27.8	7.0	7.5	
Pt/WO3/SiO2-Al2O3						42.2	11.6	11.0	
Pt/WO3/Al2O3						43.9	11.0	13.2	
Pt/WO3/ZrO2						85.8	12.5	24.2	
Pt/WO3						16.4	7.2	3.0	
WO3/ZrO2						11.5	2.7	2.6	
Pt/ZrO2 + WO3/ZrO2	100+100					21.2	4.6	2.8	
Ru5/C(I) + Amberlyst	150mg + 300mg	2% 20ml	120	1160	10	79.3	74.4		Miyazawa 2008
Ru3/C(I)						2.4	69.6	3.4	
Ru5/C(I)						4.7	59.4	6.7	
Ru3/C(I)-Ar 573K						9.5	75.8	4.6	
Ru5/C(I)-Ar 573K						21.3	76.7	1.5	
Raney Ni	2g/8g	100	150	150	20	12.0	93.0		Perosa 2005
			190		8	32.0	79.0		
					20	63.0	77.0		
					44	97.0	71.0		
Ni/AC-C	0.695g/150g	25	200	725	12	7.4	18.3		Yu 2010
Ni/AC-CB						43.3	76.1		
					24	63.2	77.4		
Ni/AC-H					12	6.3	38.2		
Ni/AC-HB						10.8	63.5		
NiB/AC						16.6	38.3		
Mg/Al	5	80	200	200	24	0.0	0.0		Meher 2009
Zn/Al		100		100					
Ni/Mg/Al						8.7	24.4		
Co/Ni/Mg/Al						9.2	36.2		

Cu/Zn/Al (M2+/M3+=1.5)						58.2	66.2		
Cu/Zn/Al (M2+/M3+=2.13)						67.2	63.0		
Cu/Zn/Al (M2+/M3+=0.5)						47.9	93.8		
Cu/Zn/Al (M2+/M3+=1.0)						55.7	73.8		
Cu/Zn/Al (M2+/M3+=2.0)						62.1	44.5		
Cu/Zn/Al (M2+/M3+=2.5)						66.7	64.0		
Cu/Zn/Al (M2+/M3+=3.0)						69.4	64.5		
Cu/Zn/Al (1:1:4)	3					37.1	78.0		
	7					57.6	89.4		
	10					70.5	75.0		
	5					25.0	50.5		
				300		47.8	90.0		
				200		57.0	59.5		
		50				35.4	75.0		
RuAl(Cl3)	0.9g/120ml	100	240	1160	5	69.0	37.9	0.7	Vasiliadou 2009
RuAl(NO3)						26.7	39.7	0.4	
RuSi(Cl3)						25.2	50.4		
RuSi(NO3)						21.7	60.5		
RuZr(NO3)						40.5	60.5		
Cu-Cr/Ac (100% Cu)	5	40	210	210	10	21.0	98.5		Liang 2009
Cu-Cr/Ac (1:2)						51.0	97.1		
Cu-Cr/Ac (1:5)						50.1	96.2		
Cu-Cr/Ac (5:1)						14.4	99.8		
Cu-Cr/Ac (2:1)						18.8	99.2		
Cu-Cr/Ac (1:1)						24.0	97.8		
Pt/MgO	0.5/20ml	0.2g/ml	220	435	20	50.0	81.2	1.6	Yuan 2009
Pt/HLT						92.1	93.0	0.0	

Pt/Al2O3						39.0	81.2	1.5	
Pt/HZSM5						4.0	19.5	0.0	
Pt/Hbeta						7.0	9.5	0.0	
Pt/C						1.8	43.6	44.3	
Pt/C (pH = 12)						7.3	81.9	11.1	
Pt/HLT	0.5/20ml	0.8g/ml	220	435	20	98.3	91.7	0.2	
Pt/HLT (Rec2)						97.9	98.1	0.4	
Pt/HLT (Rec3)						93.5	92.4	0.3	
Pt/HLT (Rec4)						85.6	93.4	0.5	
Pt/HLT (Rec5)						70.5	94.0	0.4	
Ni/SiO2-Al2O3	5	100	200	218	8	19.0	87.0		Marinoiu 2009
			250			78.0	12.0		
	5.5		200	290		20.0	78.0		
	5		200	362		30.0	100.0		
Cu-ZnO (Cu/Zn =0.6)	7.5mmmol/65ml	20	200	609	12	22.5	20.4	0.0	Wang 2007
Cu-ZnO (Cu/Zn =1.0)						17.2	29.4		
Cu-ZnO (Cu/Zn =2.0)						7.8	51.3		
CuO						4.0	76.8		
ZnO						3.6	0.0		
Cu/Zn =1.0 pH=2						10.4	27.9		
Cu/Zn =1.0 pH=7						21.1	29.4		
Cu/Zn =1.0 pH=12						33.9	77.5		
Ru/C	5	1	200	580	5	40.0	26.0	0.0	Maris 2007
Pt/C	3					13.0	79.0		
Ru/C(0.01M-NaOH)	5					48.0	27.0		
Pt/C(0.01M-NaOH)	3					25.0	55.0		
Ru/C(0.8M-NaOH)	5					100.0	19.0		
Pt/C(0.8M-NaOH)	3					92.0	46.0		
Ru/C(0.01M-CaO)	5					16.0	46.0		

Pt/C(0.01M-CaO)	3					40.0	71.0		
Ru/C(0.8M-CaO)	5					85.0	36.0		
Pt/C(0.01M-CaO)	3					100.0	36.0		
10%Pd/Fe2O3	600mg/50ml	12 (2-propanol)	180	70 N2 (0 H2)	24	100.0	94.0		Musolino 2009
		12 (EtOH)				100.0	90.0		
		12(2-propanol)			12	96.0	84.0		
					8	96.0	87.0		
			150		24	84.0	91.0		
Reduced (H2-2hr 200C)			180		8	100.0	84.0		
					4	87.0	73.0		
acetol Hydrogenation			180		8	100.0	100.0		
14.6%Co/MgO-673K	5	10	200	290	9	5.3	45.3		Guo 2009
15.3%Co/MgO-873K						44.8	42.2		
(3:0)Ru/Cu-Clay	3 (Ru)	5mmol/1ml	195	1450	18	90.7	62.3		Jiang 2009
(3:0.5)Ru/Cu-Clay						71.9	57.6		
(3:1)Ru/Cu-Clay						70.9	71.7		
(3:2)Ru/Cu-Clay						66.1	70.3		
(3:3)Ru/Cu-Clay						64.4	69.5		
(3:4)Ru/Cu-Clay						41.7	72.7		
(3:9)Ru/Cu-Clay						27.0	79.4		
(0:3)Ru/Cu-Clay						26.5	83.1		
(3:1)Ru/Cu-Clay			210	1450		71.4	83.3		
				870		77.4	84.6		
				725		87.6	84.5		
				362		81.6	87.3		
			230	1450		100.0	86.4		
				1160		100.0	83.4		
Ru/CNT-IM (10-60nm)	5 (Ru)	20	200	580	12	42.3	60.2		Wang 2009

Ru/CNT-EG reduction						82.9	30.0		
Ru/AC-IM						51.6	24.4		
Ru/TiO2-IM						81.7	35.2		
Ru/Al2O3-IM						80.8	26.7		
Ru/Graphite-IM						16.0	53.0		
Ru/CNT-IM (10-60nm)	1					11.6	50.7		
	3					27.1	55.1		
	5					42.3	60.2		
	8					75.0	48.3		
	10					56.5	60.3		
Rh-ReOx/SiO2(1/2)	150mg/20ml	20	120	1160	5	79.0	41.5	14.0	Shimao 2009
					2	38.4	46.9	16.1	
Rh-MoOx/SiO2(1/16)					5	45.8	32.1	6.0	
Rh-Wox/SiO2(8/1)						33.7	43.2	11.3	
Rh/SiO2					10	7.2	38.1	7.9	
Ru/C						3.5	26.4	4.9	
Ru/C+Amberlyst	150+300					12.9	55.4	4.9	
Rh-ReOx/SiO2(1/2)	150		160		2	86.2	42.2	10.4	
Rh/SiO2					10	28.2	23.5	3.4	
Rh-ReOx/SiO2(1/2)			120	290	5	42.1	41.1	16.1	
Rh/SiO2					10	1.8	29.7	6.6	
Rh/C + H2WO4	150+180		180	1160	5	5.7	46.8	0.0	
Raney Ni	1500					5.7	36.8	1.5	
Cu-Cr	1500					0.8	53.6	0.0	
Rh-MoOx/SiO2(1/16)	150	100	120			15.0	51.2	28.2	
	50				96	61.3	34.0	19.7	
Ru/SiO2	150mg/10ml	40	160	1160	8	16.8	39.0	6.4	Ma 2009

Ru/SiO2+Re2(CO)10	150mg Ru + equal molar Re					37.0	51.7	10.7	
Ru/ZrO2	150mg/10ml					25.4	31.9	1.8	
Ru/ZrO2 Reduced 450C 4h						19.5	36.3	7.2	
Ru/ZrO2 +Re2(CO)10						37.0	55.7	11.8	
Ru/H-ZSM5						20.5	42.2	6.0	
Ru/H-ZSM5 + Re2(CO)10						30.8	52.2	11.2	
Ru/Al2O3						18.7	34.5	3.4	
Ru/Al2O4 + Re2(CO)10						53.4	53.1	12.6	
Ru/C						29.7	50.9	0.8	
Ru/C + Re2(CO)10						59.4	56.6	7.2	
Ru3(CO)12						15.0	39.4	5.4	
Re2(CO)10						1.2	38.8	11.7	
Ru3(CO)12 + Re2(CO)10						30.2	55.4	10.1	
2.7Pt/NaY	0.22mmol/40ml	20	230	atm	1	18.1	25.0		D'Hondt 2008
2.7Pt/NaY					2	18.4	29.4		
2.7Pt/NaY					4	58.8	41.5		
2.7Pt/NaY					15	85.4	64.0		
2.7Pt/NaY				609	1	98.7	91.3		
3.0Pt/γAl2O3				atm	24	99.9	19.1		
2.7Pt/C					24	94.6	19.1		
2.7Pt/Hbeta					17	12.8	0.0		
Ni/Silica-Alumina	5%	100	200	218	8	20.1	80.5		Marinoiu 2010

Catalyst	Catatyst Loading	Glycerol Content	Temperature	Pressure	Reaction Time	Conversion	1,2PD Selectivity	Acetol Selectivity	EG Selectivity	Others Selectivity	Ref
(Co-Catalyst)	wt%	wt%	C	psi	hr	%	%	%	%	%	
Cu/Cr-1/2 (NaOH)	2	90	220	1160	12	80.3	83.9				Kim 2011
					24	90-92					
Cu/Cr (NH3)	1	20	220	754	5	16	80-82	~9	~3	~7(2-prop)	Mane 2011
Cu/Cr/Ba30						34	85	~3	~5	~8 (2-prop)	
Cu/Zn-1/2 (NaCO3)	1.7	90	220	725	7	84	81		2	17	Bienholz 2011
Cu/Zn/Ga-1/2/4 Unreduced	3.4	50				36	85		3	12	
	1.7	100				60	81		2	17	
	4	100				99	80		2	18	
Cu/Zn/Ga-1/2/4 Reduced	1.6	100				78	80		2	18	
	1.7	80				96	82		2	16	
5Ru/SiO2 (IMP)	0.6	100	240	1160	5	21.7	60.5		28.7	10.8	Vasiliadou 2011
5(Cu-Ru)/SiO2						39.2	85.9		6.9	7.2	
5Cu/HMS(IMP)						28.5	93.2		1.1	5.7	
20Cu/HMS(IMP)						~43	91		1	8	
Cu0.4/Mg5.6/Al2 (NaOH&NaCO3)	10	75	180	435	20	80	98.2		1	0.7	Yuan 2011
Cu0.8/Mg5.2/Al2 (NaOH&NaCO3)						51.8	97.2		2.1	0.7	
Cu1.5/Mg4.5/Al2 (NaOH&NaCO3)						29.6	98.6		0.9	0.5	
Cu0.4/Mg5.6/Al2 (NaOH&NaCO3)	10 (0.5gNaOH)					85	96.2		1.9	1.9	
	10 (1.0gNaOH)					91.2	95.5		2.6	1.9	
Cu0.4/Mg5.6/Al2 (NaOH&NaCO3)	10	75	180	290	10	56.7	97.1		1.1	1.8	Xia 2011
Pd0.024/Cu0.4/Mg5.6/Al2 (NaOH&NaCO3)						70.5	97.9		1.1	1	
Pd0.04/Cu0.4/Mg5.6/Al2 (NaOH&NaCO3)						76.9	97.2		1.6	1.2	
Pd0.08/Cu0.4/Mg5.6/Al2 (NaOH&NaCO3)						66.6	97.5		1.5	1	

Pd0.04/Cu0.4/Mg5.6/Al2 (NaOH&NaCO3)	5					48.7	97.6		1.6	0.8	
Pd0.04/Cu0.4/Mg5.6/Al2 (NaOH&NaCO3)	15					91.2	97		1.7	1.3	
Ru5/Ca/Zn/Mg/Al ((NH4)2CO3)	3	20	180	363	18	58.5	85.5		6.6	7.9	Lee 2011
Ru5/garmaAl2O3						45.6	59.2		22.3	18.5	
Ru5/C	5	20	130	1160	24	49.2	74		5.9	20.1	van Ryneveld 2011
		40				40.3	75.2		7.9	16.9	
		60				34.5	63.1		10.1	26.8	
Ru5/C	5	80	200	580	6	55.7	59.4		15.7	24.9	Wu 2011
Cu(10mol%)MWCNT						31.3	91.1		3.2	5.7	
Ru(5wt%)MWCNT						65.5	72.2		7.6	20.2	
Cu/MWCNT+ Ru/MWCNT						77.2	74.2		9.6	16.2	
CuRu/MWCNT						99.8	86.5		0.1	13.4	
Ru5/SiO2	0.6	100	180	1160	5	7	36	0	64	0	Vasiliadou 2011
			200			15	56	4.0	37.0	3	
			240			21	62	1	30	7	
				870		20	51	23	25	1	
				580		16	41	35	24	0	
				290		11	40	43	17	0	
Ag/Al2O3 (2mmol1gsupport)	2	50	180	522	10	17	91		4	5	Zhou 2011
			200			21	95		3	2	
			220			46	96		2	2	
			240			66	76		6	18	
Ru/bentonite-TiO2 (1:2)	5	20	150	290	7	69.8	80.6		9.9	9.5	Hamzah 2012
Ru/bentonite-TiO2 (1:1)						62.8	83.4		11.2	5.4	
Ru/bentonite+Ru/TiO2						62.3	83.6		11.4	5	
Cu/Zn (1/2) NaOH	2	100	200	725	7	17	87	1	0	12	Bienholz 2009
Cu/Zn (1/2) OA						46	90	1	1	8	
Cu/Zn (1/2) OA Second						10					

Cu/Zn (1/2) OA		50 (water)				5	87	2	9	2	
		50 (1,2-Butanediol)				55	86	1	1	12	
Rh0.02Cu0.4/ Mg5.6Al1.98O8.57	1	75 (methanol)	180	290	10	95.2	98.7		1	0.2	Xia 2012
		75 (ethanol)				91	98.7		1.1	0.2	

Catalyst	Catatyst Loading	Glycerol Content	Temperature	Pressure	Reaction Time	Conversion	1,2PD Selectivity	EG Selectivity	13PD Selectivity	Ref
(Co-Catalyst)	wt%	wt%	C	psi	hr	%	%	%		
CuCr(0.5)	5	100	130	290	4	52.4	99.6			Xiao 2013
Ru-C	5	10	180	1160	24	42	8	30		Gallegos-Suarez 2013
Ru/ZrO2		10	200	870		22.9	45.7	21		Wang 2013
Cu0.4Mg6.46Al1.14O8.17	10	33	200	435	10	86.5	92.5			Xia 2013
Ni/Mg	2	20	200	580	4	67.8	33.7	26		Chen 2013
Ru/Al2O3+HZSM5	4	40	160	1160	8	60.9	12.7	7.3		Li 2013
Cu/Al2O3	5	80	200	580	24	75.7	95.8	0.7		Wolosiak-Hnat 2013
Pt-Ti-W	25	10	180	800	12	55.4	11.8		26.9	Zhang 2013
CuZnAl	3	80	180	580	10	85.8	92.1	2.3		Tan 2013
Pd-Fe2O3	66	1	200	725	12	40	48			Ge 2013
Cu-Al Hydrotalcite	1	1 (1,4-dioxane)	180	145	6	100	99			Mizugaki 2013
CuZr	6	40	200	580	8	12	87.5			Duran-Martin 2013
CuZr 4th						17	3			
CuZr 4th regen						10	90			
CuSiO2(SBA)	0.6	40%(butanol)	240	1160	5	52	96.2	1.8		Vasiliadou 2013
Cu/delaminated hectorite	8	60	200	580	24	61.4	93			Sanchez 2012

CuMgZnAl CuMgZnAl fresh 1st recycle 2nd recycle 3rd recycle 4th recycle	15 7	75	180	290	10	78.2 39.7 34.2 25.6 25.3	99.3 99.6 99.7 99.7 99.6			Xia 2012
CuCr Pd0.5-CuCr	2	90	220	870	12	76 83	79 93			Kim 2012
CuMg(1/4)	6	20	200	580	8	49.3	92.3			Balaraju 2012
CuAl2O3(K2CO3) CuAl2O3(Na2CO3) CuAl2O3(KOH) CuAl2O3(NaOH)	5	20(0.9M NaOH)	220	754	5	38 62 58 51	91 88 88 87	4 10 10 10		Mane 2012
Cu/y Al2O3	2	80	220	348	8	12	78			Vila 2012
Cu/Al2O3 (Citric Acid)	2	100	220	725	12	91	92			Kwak 2012
Raney Nickle	2	30 Cude Glycerol	230	580	9	42 29	28 37			Hosgun 2012
Ru-Cu/ZrO2 Ru/ZrO2 Cu/ZrO2	17	60	180	1450	24	100 100 28	84 47.7 99.6	9.3 26 0.2		Liu 2012
Cu/Cr-1/2 (NaOH)	2	90	220	1160	12 24	80.3 90-92	83.9			Kim 2011
Cu/Cr (NH3)	1	20	220	754	5	16	80-82	~3		Mane 2011
Cu/Cr/Ba30						34	85	~5		
Cu/Zn-1/2 (NaCO3)	1.7	90	220	725	7	84	81	2		Bienholz 2011
Cu/Zn/Ga-1/2/4 Unreduced	3.4	50				36	85	3		
	1.7	100				60	81	2		
	4	100				99	80	2		

Cu/Zn/Ga-1/2/4 Reduced	1.6	100				78	80	2		
	1.7	80				96	82	2		
5Ru/SiO2 (IMP)	0.6	100	240	1160	5	21.7	60.5	28.7		Vasiliadou 2011
5(Cu-Ru)/SiO2						39.2	85.9	6.9		
5Cu/HMS(IMP)						28.5	93.2	1.1		
20Cu/HMS(IMP)						~43	91	1		
Cu0.4/Mg5.6/Al2 (NaOH&NaCO3)	10	75	180	435	20	80	98.2	1		Yuan 2011
Cu0.8/Mg5.2/Al2 (NaOH&NaCO3)						51.8	97.2	2.1		
Cu1.5/Mg4.5/Al2 (NaOH&NaCO3)						29.6	98.6	0.9		
Cu0.4/Mg5.6/Al2 (NaOH&NaCO3)	10 (0.5gNaOH)					85	96.2	1.9		
	10 (1.0gNaOH)					91.2	95.5	2.6		
Cu0.4/Mg5.6/Al2 (NaOH&NaCO3)	10	75	180	290	10	56.7	97.1	1.1		Xia 2011
Pd0.024/Cu0.4/Mg5.6/Al2 (NaOH&NaCO3)						70.5	97.9	1.1		
Pd0.04/Cu0.4/Mg5.6/Al2 (NaOH&NaCO3)						76.9	97.2	1.6		
Pd0.08/Cu0.4/Mg5.6/Al2 (NaOH&NaCO3)						66.6	97.5	1.5		
Pd0.04/Cu0.4/Mg5.6/Al2 (NaOH&NaCO3)	5					48.7	97.6	1.6		
Pd0.04/Cu0.4/Mg5.6/Al2 (NaOH&NaCO3)	15					91.2	97	1.7		
Ru5/Ca/Zn/Mg/Al ((NH4)2CO3)	3	20	180	363	18	58.5	85.5	6.6		Lee 2011
Ru5/garmaAl2O3						45.6	59.2	22.3		
Ru5/C	5	20	130	1160	24	49.2	74	5.9		van Ryneveld 2011
		40				40.3	75.2	7.9		
		60				34.5	63.1	10.1		
Cu/Zn-1/2 OA	1.7	100	200	725	7	46	90	1		Bienholz 2010
	3.4	50 (14Budiol)				55	86	1		
	3.4	50 (Water)				5	87	9		

Table A-2 Glycerol Hydrogenolysis to 1,2-Propanediol without Molecular Hydrogen Added.

Catalysts	Catatyst Loading	Glycerol Content	Hydrogen Source	Temperature	Pressure	Reaction Time	Conversion	1,2PD Selectivity	Acetol Selectivity	EG Selectivity	EthOH	Ref
(Co-Catalyst)	wt%	wt%		C	psi	hr	%	%	%	%	%	
2.7Pt/NaY	0.22mmol pt	20	GL SR	230		1	18.1	25	10		7	D'Hondt 2008
						4	58.8	41.1	4		6.7	
						15	85.4	64	3		9.5	
2.7Pt/Al2O3 (gama)						24	99.9	19.1	1.9		10.6	
Raney Nickle	8.9	50	GL SR	230		15min	91.1	30 (Yield)	4		6	Maglinao 2011
						45min	98.6	28	3		8	
						75min	99.6	23	2		9	
						105min	99.9	18	0		10	
Pt(1wt%)/SiO2	300mg /12ml GL	10	GL SR	200	58	2	1	50	32	0	11	Barbelli 2012
				225			3	42	16	19	7	
			H2	200			0.6	56	23	0	10	
Pt(1wt%)Sn0.2 /SiO2			GL SR				54	59	25	11	2	
			H2				16	84	3	8	2	
Pd(10%)/Fe3O4	600mg /25ml	12	i-Propanol	180	73	4	87	73	9	15		Musolino 2009
						8	100	84	3	9		
Cu/Al2O3	166mg/g GL	4	i-Propanol	320	652	24	14.6	40.5	47.5			Ganarias 2011
				450			39.1	59.4	26.3			
			H2	320			32.9	0.1	90.1			
				450			57	0.8	72.8			
Ni/Al2O3			i-Propanol	320			2	60.3	7.5			
				450			31.8	50.4	32.6			
			H2	320			5.2	7.2	73.7			
				450			69	0.9	61.3			
Cu-Ni/Al2O3			i-Propanol	320			41.2	48.3	41.7			
				450			57.3	62.1	27			

			H2	320			31	84.7	0.9			
				450			70.5	66.9	0.6			
Pt-Hydrotalcite	0.2g/20ml	10	GL SR	250	652	3	98.4	70.2				Pendem 2012
Pt-Hydrotalcite Recycle							93.1	67.6				
Ni-Cu/Al2O3	0.9/135	4	Formic Acid	220	653	16	49.3	75.4				Gandarias 2012
Ni-Cu/Al2O3	0.5/20ml	20	Formic Acid 1.8mmol/h	220	653	10	33.5	85.9	6.7			Gandarias 2012
Pt-yAl2O3	0.1g/g GL	11.4	Methanol	250	35bar	4	70.4	9.5				**EP 2565175 A1**
Pt-SiO2							58.9	36.2				
						8	62.8	27.6				
CuZnAl (Oxalic)	0.35g/g GL					4	88.8	39.2				

Appendix B Supplementary Data

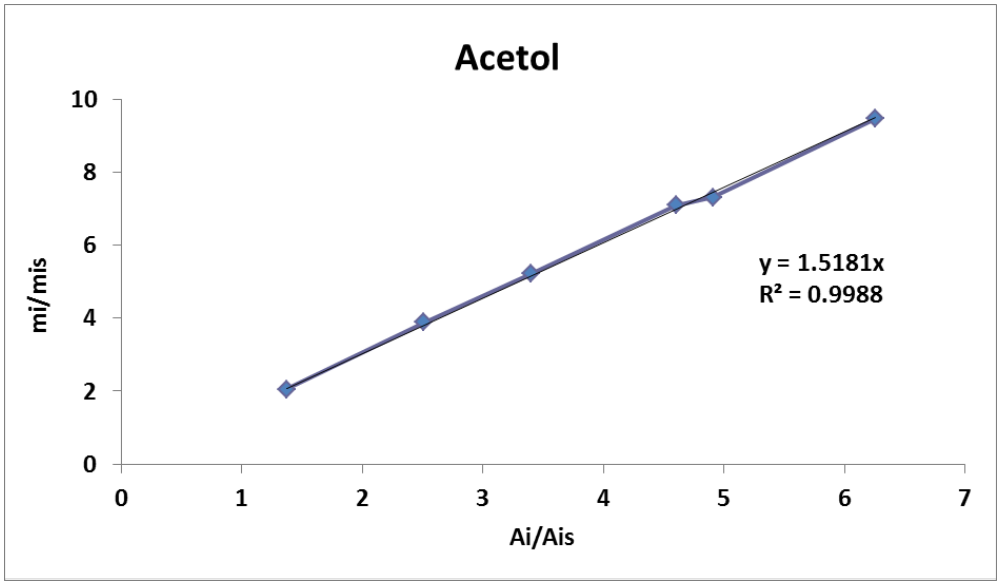

Figure B-1 Calibration Curve for Acetol.

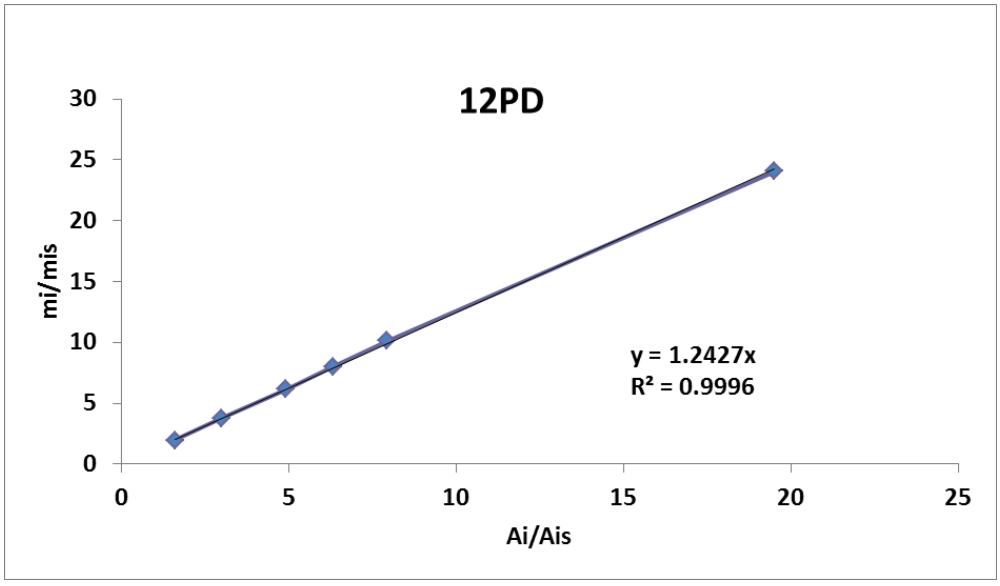

Figure B-2 Calibration Curve for 1,2PD

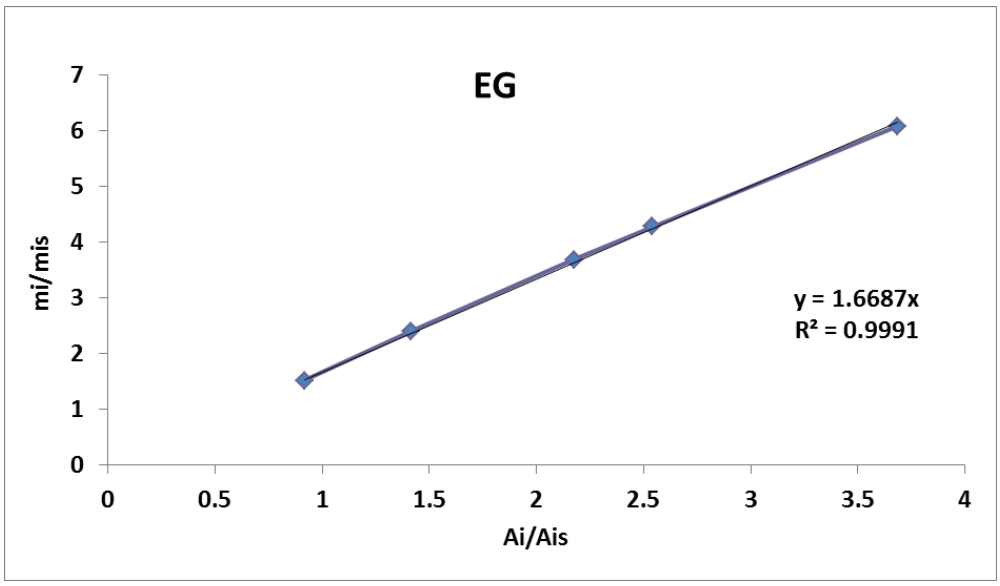

Figure B-3 Calibration Curve for EG.

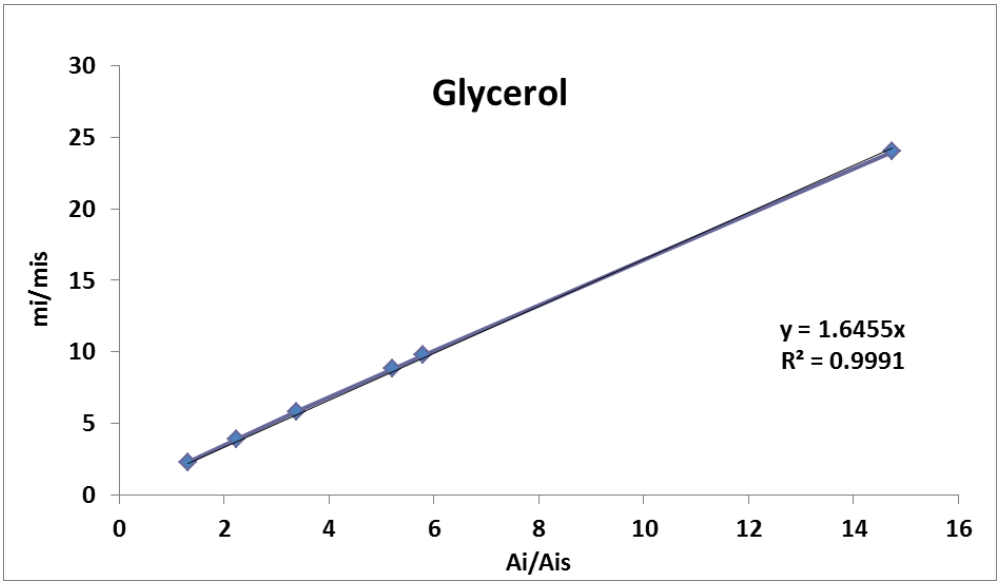

Figure B-4 Calibration Curve for Glycerol.

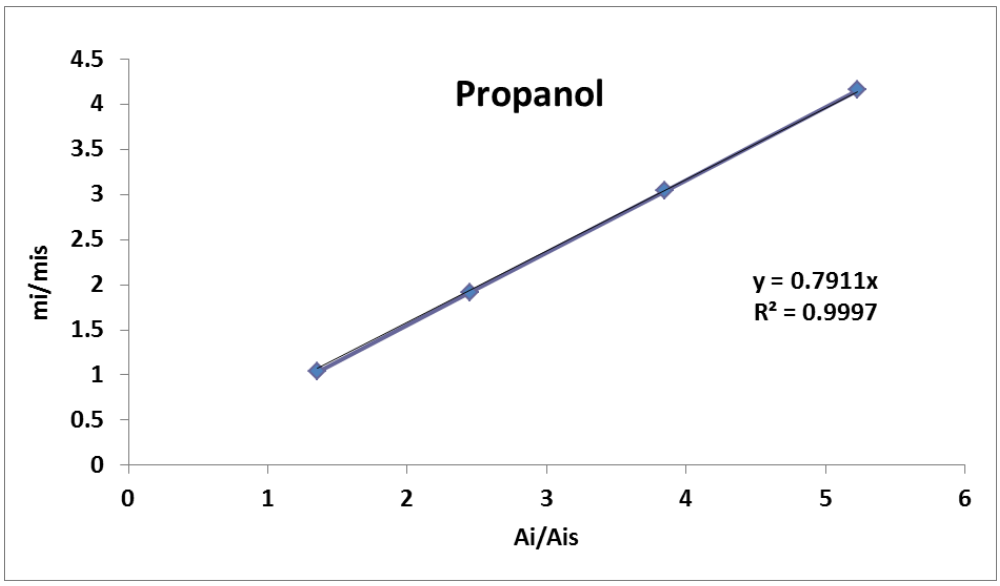

Figure B-5 Calibration Curve for Propanol.

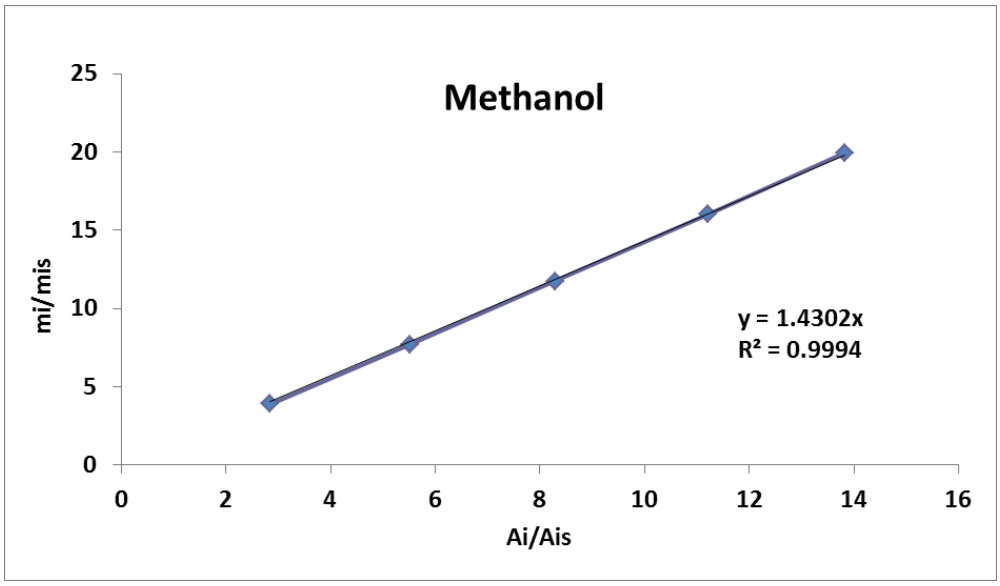

Figure B-6 Calibration for Methanol.

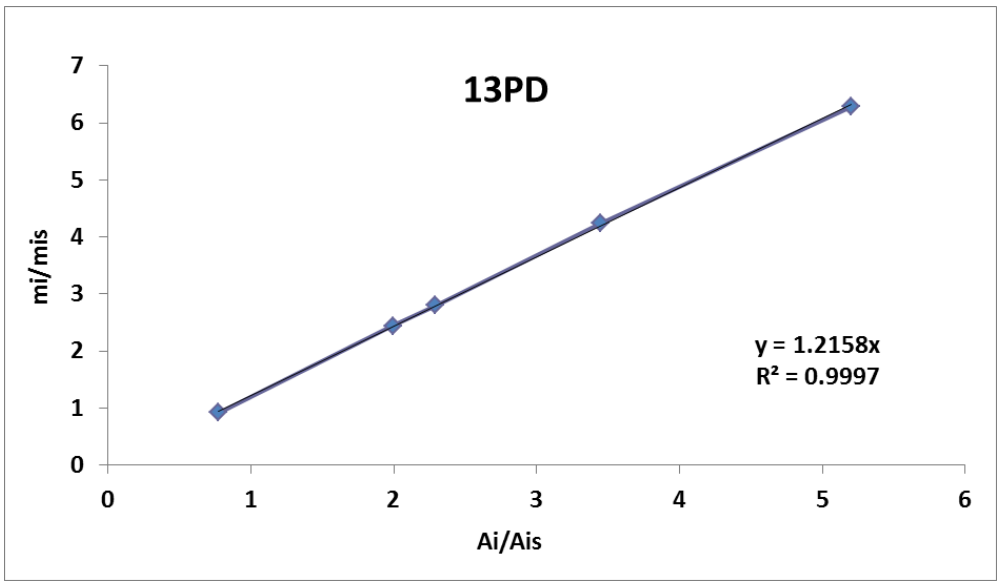

Figure B-7 Calibration Curve for 1,3PD.

Table B-1 Ni/Cu/Zn/Al Composition Study[a].

Glycerol Conversion

Ni\Al	10	30	50
0%	80.2	87.1	85.7
1%		85.52346467	
3%	81.28806309	77.39553329	76.42285
5%		70.02560644	62.86014
10%	61.97284165		

12PD Selectivity

Ni\Al	10	30	50
0%	65.7	70.7	69.9
1%		76.71889496	
3%	79.57717781	82.8013258	80.30146
5%		85.5225695	80.7363
10%	76.2590697		

12PD Yield

Ni\Al	10	30	50
0%	52.7	61.6	59.9
1%		65.6	
3%	64.7	64.1	61.4
5%		59.9	50.8
10%	47.3		

[a] Conditions: 220ºC, 15bar N_2, 20wt% Glycerol, Water/Methanol=1.2, 3wt% catalyst, 500RPM, 8 Hours.

Appendix C Permission to Re-print Copyrighted Material

SPRINGER LICENSE
TERMS AND CONDITIONS

Dec 27, 2013

This is a License Agreement between University of Waterloo ("You") and Springer ("Springer") provided by Copyright Clearance Center ("CCC"). The license consists of your order details, the terms and conditions provided by Springer, and the payment terms and conditions.

All payments must be made in full to CCC. For payment instructions, please see information listed at the bottom of this form.

License Number	3297340823059
License date	Dec 27, 2013
Licensed content publisher	Springer
Licensed content publication	Catalysis Letters
Licensed content title	Direct Hydrogenolysis of Highly Concentrated Glycerol Solutions Over Supported Ru, Pd and Pt Catalyst Systems
Licensed content author	Esti van Ryneveld
Licensed content date	Jan 1, 2011
Volume number	141
Issue number	7
Type of Use	Thesis/Dissertation
Portion	Figures
Author of this Springer article	No
Order reference number	
Title of your thesis / dissertation	Catalytic Conversion of Glycerol into Propylene Glycol
Expected completion date	Feb 2014
Estimated size(pages)	270
Total	0.00 CAD
Terms and Conditions	

Introduction
The publisher for this copyrighted material is Springer Science + Business Media. By clicking "accept" in connection with completing this licensing transaction, you agree that the following terms and conditions apply to this transaction (along with the Billing and Payment terms and conditions established by Copyright Clearance Center, Inc. ("CCC"), at the time that you opened your Rightslink account and that are available at any time at http://myaccount.copyright.com).

Limited License
With reference to your request to reprint in your thesis material on which Springer Science

ROYAL SOCIETY OF CHEMISTRY LICENSE TERMS AND CONDITIONS

Dec 27, 2013

This is a License Agreement between University of Waterloo ("You") and Royal Society of Chemistry ("Royal Society of Chemistry") provided by Copyright Clearance Center ("CCC"). The license consists of your order details, the terms and conditions provided by Royal Society of Chemistry, and the payment terms and conditions.

All payments must be made in full to CCC. For payment instructions, please see information listed at the bottom of this form.

License Number	3297380486844
License date	Dec 27, 2013
Licensed content publisher	Royal Society of Chemistry
Licensed content publication	Chemical Communications (Cambridge)
Licensed content title	Catalytic glycerol conversion into 1,2-propanediol in absence of added hydrogen
Licensed content author	Els D'Hondt,Stijn Van de Vyver,Bert F. Sels,Pierre A. Jacobs
Licensed content date	Oct 14, 2008
Issue number	45
Type of Use	Thesis/Dissertation
Requestor type	academic/educational
Portion	figures/tables/images
Number of figures/tables/images	1
Format	electronic
Distribution quantity	1
Will you be translating?	no
Order reference number	
Title of the thesis/dissertation	Catalytic Conversion of Glycerol into Propylene Glycol
Expected completion date	Feb 2014
Estimated size	270
Total	0.00 USD

Terms and Conditions

This License Agreement is between {Requestor Name} ("You") and The Royal Society of Chemistry ("RSC") provided by the Copyright Clearance Center ("CCC"). The license consists of your order details, the terms and conditions provided by the Royal Society of Chemistry, and the payment terms and conditions.

ELSEVIER LICENSE
TERMS AND CONDITIONS

Dec 27, 2013

This is a License Agreement between University of Waterloo ("You") and Elsevier ("Elsevier") provided by Copyright Clearance Center ("CCC"). The license consists of your order details, the terms and conditions provided by Elsevier, and the payment terms and conditions.

All payments must be made in full to CCC. For payment instructions, please see information listed at the bottom of this form.

Supplier	Elsevier Limited The Boulevard,Langford Lane Kidlington,Oxford,OX5 1GB,UK
Registered Company Number	1982084
Customer name	University of Waterloo
Customer address	200 University Ave. W. Waterloo, ON N2L3G1
License number	3297400107001
License date	Dec 27, 2013
Licensed content publisher	Elsevier
Licensed content publication	Catalysis Today
Licensed content title	Hydrogenolysis through catalytic transfer hydrogenation: Glycerol conversion to 1,2-propanediol
Licensed content author	Inaki Gandarias,Pedro Luis Arias,Sara G. Fernández,Jesús Requies,Mohammed El Doukkali,María Belén Güemez
Licensed content date	15 November 2012
Licensed content volume number	195
Licensed content issue number	1
Number of pages	10
Start Page	22
End Page	31
Type of Use	reuse in a thesis/dissertation
Intended publisher of new work	other
Portion	figures/tables/illustrations
Number of figures/tables/illustrations	1
Format	electronic

Permission Request Form Canada

Safdar, Sheik - Hoboken [ssafdar@wiley.com]

Actions

To:

M

Yuanqing Liu

Inbox

January 6, 2014 4:22 PM

Dear Yuanqing,

Permission is hereby granted for the use requested subject to the usual acknowledgements (author, title, and copyright [year and owner]. And the statement "This material is reproduced with permission of John Wiley & Sons, Inc.").

Any third party material is expressly excluded from this permission. If any of the material you wish to use appears within our work with credit to another source, authorization from that source must be obtained.

This permission does not include the right to grant others permission to photocopy or otherwise reproduce this material except for accessible versions made by non-profit organizations serving the blind, visually impaired and other persons with print disabilities (VIPs).

Sincerely,

Sheik Safdar | Permissions Coordinator | P: 201-748-6512 | F: 201-748-6008

John Wiley & Sons, Inc. | 111 River Street | Hoboken, NJ | 07030 | Mailstop: 4-02

A01_First_Name: Yuanqing
A02_Last_Name: Liu
A03_Company: University of Waterloo
A04_Address: 200 University Ave. W.
A05_City: Waterloo
A06_Province: ON
A07_Zip: N2L3G1
A08_Country: Canada
A09_Phone: 5198884567
A10_Fax:
A11_Email: y289liu@uwaterloo.ca
A12_Reference_Number:

A13_Requestor_Name:
A14_Requestor_Phone: 5198884567ext31601
A15_Requestor_Fax:
A16_Product_Title: Applied statistics and probability for engineers 3rd edition
A17_ISBN: 0-471-20454-4
A18_Author_Name: Douglas C. Montgomery & George C. Runger
A19_Page_Number: 14/560/Table 14-29
A20_Number_of_Copies: 1
A21_Semesters: 15
A22_Professor_Name: Flora Ng, Garry Rempel
A23_Course_Name: PhD Thesis
A24_Organization_Name: University of Waterloo
A25_Purpose_Reproduction: Thesis/Dissertation
A26_Title_Your_Work: Catalytic Conversion of Glycerol into Propylene Glycol
A26A_Resale: No
A27_Print_Run:
A28_Publication_Date:
A29_World_Rights:
A30_Medium:
A31_Password:
32_Users:
A33_Duration_Posted_Web:
A34_CD_Print_Run: ,

References

[1] A. Baig and F. T. T. Ng, "A Single-Step Solid Acid-Catalyzed Process for the Production of Biodiesel from High Free Fatty Acid Feedstocks†," *Energy & Fuels*, vol. 24, pp. 4712-4720, 2010/09/16 2010.

[2] M. G. Kulkarni and A. K. Dalai, "Waste Cooking OilAn Economical Source for Biodiesel: A Review," *Industrial & Engineering Chemistry Research*, vol. 45, pp. 2901-2913, 2006/04/01 2006.

[3] J. M. Marchetti and A. F. Errazu, "Comparison of different heterogeneous catalysts and different alcohols for the esterification reaction of oleic acid," *Fuel*, vol. 87, pp. 3477-3480, 2008.

[4] Canadian Renewable Fuel Association. (2013, November 12, 2013). *Biodiesel: Canadian Production List as at September 25, 2013*. Available: http://www.greenfuels.org/en/industry-information/plants.aspx

[5] Canadian National Energy Board, "Canada's Energy Future: Energy Supply and Demand Projections to 2035," Canadian National Energy Board, Ottawa2011.

[6] Y. Zhang, M. A. Dubé, D. D. McLean, and M. Kates, "Biodiesel production from waste cooking oil: 2. Economic assessment and sensitivity analysis," *Bioresource Technology*, vol. 90, pp. 229-240, 2003.

[7] H. Safaei Mohamadabadi, G. Tichkowsky, and A. Kumar, "Development of a multi-criteria assessment model for ranking of renewable and non-renewable transportation fuel vehicles," *Energy*, vol. 34, pp. 112-125, 2009.

[8] M. Canakci and H. Sanli, "Biodiesel production from various feedstocks and their effects on the fuel properties," *Journal of Industrial Microbiology & Biotechnology*, vol. 35, pp. 431-441, 2008/05/01 2008.

[9] M. G. Kulkarni, R. Gopinath, L. C. Meher, and A. K. Dalai, "Solid acid catalyzed biodiesel production by simultaneous esterification and transesterification," *Green Chemistry*, vol. 8, pp. 1056-1062, 2006.

[10] A. Kumar Tiwari, A. Kumar, and H. Raheman, "Biodiesel production from jatropha oil (Jatropha curcas) with high free fatty acids: An optimized process," *Biomass and Bioenergy*, vol. 31, pp. 569-575, 2007.

[11] H. J. Berchmans and S. Hirata, "Biodiesel production from crude Jatropha curcas L. seed oil with a high content of free fatty acids," *Bioresource Technology*, vol. 99, pp. 1716-1721, 2008.

[12] S. Shah, S. Sharma, and M. N. Gupta, "Biodiesel Preparation by Lipase-Catalyzed Transesterification of Jatropha Oil," *Energy & Fuels*, vol. 18, pp. 154-159, 2004/01/01 2004.

[13] N. Pasupulety, K. Gunda, Y. Liu, G. L. Rempel, and F. T. T. Ng, "Production of biodiesel from soybean oil on CaO/Al2O3 solid base catalysts," *Applied Catalysis A: General*, vol. 452, pp. 189-202, 2013.

[14] B. Sims. (2011, August 03, 2011) BIOX lands funding to install glycerin refining equipment. *Biodiesel Magazine*. Available: http://www.biodieselmagazine.com/articles/7954/biox-lands-funding-to-install-glycerin-refining-equipment

[15] B. Sims. (2011, Benchmark Energy supplies UND glycerin for coal-fired operations. *Biodiesel Magazine*. Available: http://www.biodieselmagazine.com/articles/8214/benchmark-energy-supplies-und-glycerin-for-coal-fired-operations

[16] G. P. da Silva, M. Mack, and J. Contiero, "Glycerol: A promising and abundant carbon source for industrial microbiology," *Biotechnology Advances*, vol. 27, pp. 30-39, 2009.

[17] M. A. Dasari, "Catalytic Conversion of Glycerol and Sugar Alcohols to Value-added Products," Doctor of Philosophy, Department of Chemical Engineering, University of Missouri-Columbia, Columbia, 2006.

[18] B. Sims. (2011, Clearing the Way for Byproduct Quality *Biodiesel Magazine*. Available: http://biodieselmagazine.com/articles/8137/clearing-the-way-for-byproduct-quality

[19] M. Pagliaro and M. Rossi, *The Future of Glycerol: New Usages for a Versatile Raw Material*. Cambridge: RSC Publishing, 2008.

[20] A. Corma, S. Iborra, and A. Velty, "Chemical Routes for the Transformation of Biomass into Chemicals," *Chemical Reviews*, vol. 107, pp. 2411-2502, 2007.

[21] D. T. Johnson and K. A. Taconi, "The glycerin glut: Options for the value-added conversion of crude glycerol resulting from biodiesel production," *Environmental Progress*, vol. 26, pp. 338-348, 2007.

[22] A. Behr, J. Eilting, K. Irawadi, J. Leschinski, and F. Lindner, "Improved utilisation of renewable resources: New important derivatives of glycerol," *Green Chemistry*, vol. 10, pp. 13-30, 2007.

[23] C.-H. Zhou, J. N. Beltramini, Y.-X. Fan, and G. Q. Lu, "Chemoselective catalytic conversion of glycerol as a biorenewable source to valuable commodity chemicals," *Chemical Society Reviews*, vol. 37, pp. 527-549, 2008.

[24] K. Wang, M. C. Hawley, and S. J. DeAthos, "Conversion of Glycerol to 1,3-Propanediol via Selective Dehydroxylation," *Industrial & Engineering Chemistry Research*, vol. 42, pp. 2913-2923, 2003/06/01 2003.

[25] V. E. T. Maervoet, M. De Mey, J. Beauprez, S. De Maeseneire, and W. K. Soetaert, "Enhancing the Microbial Conversion of Glycerol to 1,3-Propanediol Using Metabolic Engineering," *Organic Process Research & Development*, vol. 15, pp. 189-202, 2011/01/21 2010.

[26] W.-D. Deckwer, "Microbial conversion of glycerol to 1,3-propanediol," *FEMS Microbiology Reviews*, vol. 16, pp. 143-149, 1995.

[27] Y. Nakagawa and K. Tomishige, "Heterogeneous catalysis of the glycerol hydrogenolysis," *Catalysis Science & Technology*, vol. 1, pp. 179-190, 2011.

[28] M. A. Dasari, P.-P. Kiatsimkul, W. R. Sutterlin, and G. J. Suppes, "Low-pressure hydrogenolysis of glycerol to propylene glycol," *Applied Catalysis A: General*, vol. 281, pp. 225-231, 2005.

[29] L. Bowei. (2012, March 19 2012). *OUTLOOK '12: Asian MPG market uncertain in Q1 on macroeconomic woes*. Available: http://www.icis.com/Articles/2012/01/03/9519597/outlook-12-asian-mpg-market-uncertain-in-q1-on-macroeconomic-woes.html

[30] J. Lorenz, "Environmental Credits Ltd - FORM 8-K/A," U. S. S. A. E. COMMISSION, Ed., ed. Washington D.C., 2011.

[31] DOTCHEM. (March 19). *5000t/a 1,3-Propanediol Production Technology Development*. Available: http://www.jldot.com/tech10.htm

[32] C. M. Romero, M. S. Páez, and D. Pérez, "A comparative study of the volumetric properties of dilute aqueous solutions of 1-propanol, 1,2-propanediol, 1,3-propanediol, and 1,2,3-propanetriol at various temperatures," *The Journal of Chemical Thermodynamics*, vol. 40, pp. 1645-1653, 2008.

[33] J. Graetz, "New approaches to hydrogen storage," *Chemical Society Reviews*, vol. 38, pp. 73-82, 2009.

[34] P. Jena, "Materials for Hydrogen Storage: Past, Present, and Future," *The Journal of Physical Chemistry Letters*, vol. 2, pp. 206-211, 2011/02/03 2011.

[35] F. Alonso, P. Riente, F. Rodríguez-Reinoso, J. Ruiz-Martínez, A. Sepúlveda-Escribano, and M. Yus, "Platinum nanoparticles supported on titania as an efficient hydrogen-transfer catalyst," *Journal of Catalysis*, vol. 260, pp. 113-118, 2008.

[36] M. Gliński, "Catalytic hydrogen transfer over magnesia: Vapour and liquid phase reduction of various aralkyl ketones," *Applied Catalysis A: General*, vol. 349, pp. 133-139, 2008.

[37] F.-D. Kopinke, K. Mackenzie, R. Koehler, and A. Georgi, "Alternative sources of hydrogen for hydrodechlorination of chlorinated organic compounds in water on Pd catalysts," *Applied Catalysis A: General*, vol. 271, pp. 119-128, 2004.

[38] S. U. Sonavane, M. B. Gawande, S. S. Deshpande, A. Venkataraman, and R. V. Jayaram, "Chemoselective transfer hydrogenation reactions over nanosized γ-Fe2O3 catalyst prepared by novel combustion route," *Catalysis Communications*, vol. 8, pp. 1803-1806, 2007.

[39] L. Zhou, H. Gu, and X. Yan, "A Novel Transfer Hydrogenation with High Hydrogen Utilization for the Hydrogenation of Halogenated Nitrobenzene without Hydrodehalogenation," *Catalysis Letters*, vol. 132, pp. 16-21, 2009/09/01 2009.

[40] D. R. Palo, R. A. Dagle, and J. D. Holladay, "Methanol Steam Reforming for Hydrogen Production," *Chemical Reviews*, vol. 107, pp. 3992-4021, 2007.

[41] E. D'Hondt, S. V. d. Vyver, B. F. Sels, and P. A. Jacobs, "Catalytic glycerol conversion into 1,2-propanediol in absence of added hydrogen," *Chemical Communications*, pp. 6011-6012, 2008.

[42] E. D'Hondt, S. V. d. Vyver, P. A. Jacobs, and B. F. Sels, "Catalytic Glycerol Conversion into 1,2-Propanediol in Absence of Added Hydrogen: Bifunctional catalysis with Pt/NaY," in *21st. NACS Meeting*, San Francisco Pacific, 2009.

[43] A. Yamaguchi, N. Hiyoshi, O. Sato, C. V. Rode, and M. Shirai, "Enhancement of Glycerol Conversion to Acetol in High-temperature Liquid Water by High-pressure Carbon Dioxide," *Chemistry Letters*, vol. 37, pp. 926-927, 2008.

[44] L. C. Meher, D. Vidya Sagar, and S. N. Naik, "Technical aspects of biodiesel production by transesterification--a review," *Renewable and Sustainable Energy Reviews*, vol. 10, pp. 248-268, 2006.

[45] S. K. Tanielyan, N. Marin, G. Alvez, R. Bhagat, B. Miryala, R. L. Augustine, and S. R. Schmidt, "An Efficient, Selective Process for the Conversion of Glycerol to Propylene Glycol Using Fixed Bed Raney Copper Catalysts," *Organic Process Research & Development*, 2013.

[46] C.-W. Chiu, A. Tekeei, J. M. Ronco, M.-L. Banks, and G. J. Suppes, "Reducing Byproduct Formation during Conversion of Glycerol to Propylene Glycol," *Industrial & Engineering Chemistry Research*, vol. 47, pp. 6878-6884, 2008.

[47] L. C. Meher, R. Gopinath, S. N. Naik, and A. K. Dalai, "Catalytic Hydrogenolysis of Glycerol to Propylene Glycol over Mixed Oxides Derived from a Hydrotalcite-Type Precursor," *Industrial & Engineering Chemistry Research*, vol. 48, pp. 1840-1846, 2009/02/18 2009.

[48] Z. Zhou, X. Li, T. Zeng, W. Hong, Z. Cheng, and W. Yuan, "Kinetics of Hydrogenolysis of Glycerol to Propylene Glycol over Cu-ZnO-Al2O3 Catalysts," *Chinese Journal of Chemical Engineering*, vol. 18, pp. 384-390, 2010.

[49] A. Wolosiak-Hnat, E. Milchert, and B. Grzmil, "Influence of Parameters on Glycerol Hydrogenolysis over a Cu/Al2O3 Catalyst," *Chemical Engineering & Technology*, vol. 36, pp. 411-418, 2013.

[50] E. S. Vasiliadou and A. A. Lemonidou, "Kinetic study of liquid-phase glycerol hydrogenolysis over Cu/SiO2 catalyst," *Chemical Engineering Journal*, vol. 231, pp. 103-112, 2013.

[51] Z. Xiao, C. Li, J. Xiu, X. Wang, C. T. Williams, and C. Liang, "Insights into the reaction pathways of glycerol hydrogenolysis over Cu–Cr catalysts," *Journal of Molecular Catalysis A: Chemical*, vol. 365, pp. 24-31, 2012.

[52] B. C. Miranda, R. J. Chimentão, J. B. O. Santos, F. Gispert-Guirado, J. Llorca, F. Medina, F. L. Bonillo, and J. E. Sueiras, "Conversion of glycerol over 10%Ni/γ-Al2O3 catalyst," *Applied Catalysis B: Environmental*, 2013.

[53] J. Hu, X. Liu, Y. Fan, S. Xie, Y. Pei, M. Qiao, K. Fan, X. Zhang, and B. Zong, "Physically mixed ZnO and skeletal NiMo for one-pot reforming-hydrogenolysis of glycerol to 1,2-propanediol," *Chinese Journal of Catalysis*, vol. 34, pp. 1020-1026, 2013.

[54] I. Gandarias, J. Requies, P. L. Arias, U. Armbruster, and A. Martin, "Liquid-phase glycerol hydrogenolysis by formic acid over Ni–Cu/Al2O3 catalysts," *Journal of Catalysis*, vol. 290, pp. 79-89, 2012.

[55] J. Huang and J. Chen, "Comparison of Ni2P/SiO2 and Ni/SiO2 for Hydrogenolysis of Glycerol: A Consideration of Factors Influencing Catalyst Activity and Product Selectivity," *Chinese Journal of Catalysis*, vol. 33, pp. 790-796, 2012.

[56] E. Gallegos-Suarez, M. Pérez-Cadenas, A. Guerrero-Ruiz, I. Rodriguez-Ramos, and A. Arcoya, "Effect of the functional groups of carbon on the surface and catalytic properties of Ru/C catalysts for hydrogenolysis of glycerol," *Applied Surface Science*, 2013.

[57] N. Hamzah, N. M. Nordin, A. H. A. Nadzri, Y. A. Nik, M. B. Kassim, and M. A. Yarmo, "Enhanced activity of Ru/TiO2 catalyst using bisupport, bentonite-TiO2 for hydrogenolysis of glycerol in aqueous media," *Applied Catalysis A: General*, vol. 419–420, pp. 133-141, 2012.

[58] H. Liu, S. Liang, T. Jiang, B. Han, and Y. Zhou, "Hydrogenolysis of Glycerol to 1,2-Propanediol over Ru–Cu Bimetals Supported on Different Supports," *CLEAN – Soil, Air, Water*, vol. 40, pp. 318-324, 2012.

[59] C. Pendem, P. Gupta, N. Chaudhary, S. Singh, J. Kumar, T. Sasaki, A. Datta, and R. Bal, "Aqueous phase reforming of glycerol to 1,2-propanediol over Pt-nanoparticles supported on hydrotalcite in the absence of hydrogen," *Green Chemistry*, vol. 14, pp. 3107-3113, 2012.

[60] M. Checa, F. Auneau, J. Hidalgo-Carrillo, A. Marinas, J. M. Marinas, C. Pinel, and F. J. Urbano, "Catalytic transformation of glycerol on several metal systems supported on ZnO," *Catalysis Today*, vol. 196, pp. 91-100, 2012.

[61] R. Rodrigues, N. Isoda, M. Gonçalves, F. C. A. Figueiredo, D. Mandelli, and W. A. Carvalho, "Effect of niobia and alumina as support for Pt catalysts in the hydrogenolysis of glycerol," *Chemical Engineering Journal*, vol. 198–199, pp. 457-467, 2012.

[62] M. Balaraju, K. Jagadeeswaraiah, P. S. S. Prasad, and N. Lingaiah, "Catalytic hydrogenolysis of biodiesel derived glycerol to 1,2-propanediol over Cu-MgO catalysts," *Catalysis Science & Technology*, vol. 2, pp. 1967-1976, 2012.

[63] S. Xia, L. Zheng, L. Wang, P. Chen, and Z. Hou, "Hydrogen-free synthesis of 1,2-propanediol from glycerol over Cu-Mg-Al catalysts," *RSC Advances*, vol. 3, pp. 16569-16576, 2013.

[64] S. Xia, R. Nie, X. Lu, L. Wang, P. Chen, and Z. Hou, "Hydrogenolysis of glycerol over Cu0.4/Zn5.6−xMgxAl2O8.6 catalysts: The role of basicity and hydrogen spillover," *Journal of Catalysis*, vol. 296, pp. 1-11, 2012.

[65] S. Wang, K. Yin, Y. Zhang, and H. Liu, "Glycerol Hydrogenolysis to Propylene Glycol and Ethylene Glycol on Zirconia Supported Noble Metal Catalysts," *ACS Catalysis*, vol. 3, pp. 2112-2121, 2013/09/06 2013.

[66] J. Ge, Z. Zeng, F. Liao, W. Zheng, X. Hong, and S. C. E. Tsang, "Palladium on iron oxide nanoparticles: the morphological effect of the support in glycerol hydrogenolysis," *Green Chemistry*, vol. 15, pp. 2064-2069, 2013.

[67] S. Wang and H. Liu, "Selective hydrogenolysis of glycerol to propylene glycol on Cu–ZnO catalysts," *Catalysis Letters,* vol. 117, pp. 62-67, 2007/08/01 2007.

[68] A. Bienholz, F. Schwab, and P. Claus, "Hydrogenolysis of glycerol over a highly active CuO/ZnO catalyst prepared by an oxalate gel method: influence of solvent and reaction temperature on catalyst deactivation," *Green Chemistry,* vol. 12, pp. 290-295, 2010.

[69] H. L. Hoşgün, M. Yıldız, and H. F. Gerçel, "Hydrogenolysis of Aqueous Glycerol over Raney Nickel Catalyst: Comparison of Pure and Biodiesel By-Product," *Industrial & Engineering Chemistry Research,* vol. 51, pp. 3863-3869, 2012/03/14 2012.

[70] M. Balaraju, V. Rekha, P. Sai Prasad, R. Prasad, and N. Lingaiah, "Selective Hydrogenolysis of Glycerol to 1, 2 Propanediol Over Cu–ZnO Catalysts," *Catalysis Letters,* vol. 126, pp. 119-124, 2008.

[71] Z. Huang, F. Cui, H. Kang, J. Chen, and C. Xia, "Characterization and catalytic properties of the CuO/SiO2 catalysts prepared by precipitation-gel method in the hydrogenolysis of glycerol to 1,2-propanediol: Effect of residual sodium," *Applied Catalysis A: General,* vol. 366, pp. 288-298, 2009.

[72] C. Liang, Z. Ma, L. Ding, and J. Qiu, "Template Preparation of Highly Active and Selective Cu–Cr Catalysts with High Surface Area for Glycerol Hydrogenolysis," *Catalysis Letters,* vol. 130, pp. 169-176, 2009.

[73] N. Kim, S. Oh, J. Joo, K. Jung, and J. Yi, "The Promotion Effect of Cr on Copper Catalyst in Hydrogenolysis of Glycerol to Propylene Glycol," *Topics in Catalysis,* vol. 53, pp. 517-522, 2010/06/01 2010.

[74] R. B. Mane, A. A. Ghalwadkar, A. M. Hengne, Y. R. Suryawanshi, and C. V. Rode, "Role of promoters in copper chromite catalysts for hydrogenolysis of glycerol," *Catalysis Today,* vol. 164, pp. 447-450, 2011.

[75] Z. Xiao, J. Xiu, X. Wang, B. Zhang, C. T. Williams, D. Su, and C. Liang, "Controlled preparation and characterization of supported CuCr2O4 catalysts for hydrogenolysis of highly concentrated glycerol," *Catalysis Science & Technology,* vol. 3, pp. 1108-1115, 2013.

[76] S. Wang, Y. Zhang, and H. Liu, "Selective Hydrogenolysis of Glycerol to Propylene Glycol on Cu–ZnO Composite Catalysts: Structural Requirements and Reaction Mechanism," *Chemistry – An Asian Journal,* vol. 5, pp. 1100-1111, 2010.

[77] L. Huang, Y. L. Zhu, H. Y. Zheng, Y. W. Li, and Z. Y. Zeng, "Continuous production of 1,2-propanediol by the selective hydrogenolysis of solvent-free glycerol under mild conditions," *Journal of Chemical Technology & Biotechnology,* vol. 83, pp. 1670-1675, 2008.

[78] D. Jingfa, S. Qi, Z. Yulong, C. Songying, and W. Dong, "A novel process for preparation of a Cu/ZnO/Al2O3 ultrafine catalyst for methanol synthesis from CO2 + H2: comparison of various preparation methods," *Applied Catalysis A: General,* vol. 139, pp. 75-85, 1996.

[79] Q. Sun, Y.-L. Zhang, H.-Y. Chen, J.-F. Deng, D. Wu, and S.-Y. Chen, "A Novel Process for the Preparation of Cu/ZnO and Cu/ZnO/Al2O3Ultrafine Catalyst: Structure, Surface Properties, and Activity for Methanol Synthesis from CO2+H2," *Journal of Catalysis,* vol. 167, pp. 92-105, 1997.

[80] A. Bienholz, R. Blume, A. Knop-Gericke, F. Girgsdies, M. Behrens, and P. Claus, "Prevention of Catalyst Deactivation in the Hydrogenolysis of Glycerol by Ga2O3-Modified Copper/Zinc Oxide Catalysts†," *The Journal of Physical Chemistry C,* vol. 115, pp. 999-1005, 2011/02/03 2010.

[81] Z. Yuan, L. Wang, J. Wang, S. Xia, P. Chen, Z. Hou, and X. Zheng, "Hydrogenolysis of glycerol over homogenously dispersed copper on solid base catalysts," *Applied Catalysis B: Environmental,* vol. 101, pp. 431-440, 2011.

[82] S. Xia, Z. Yuan, L. Wang, P. Chen, and Z. Hou, "Hydrogenolysis of glycerol on bimetallic Pd-Cu/solid-base catalysts prepared via layered double hydroxides precursors," *Applied Catalysis A: General*, vol. 403, pp. 173-182, 2011.

[83] S. Xia, Z. Yuan, L. Wang, P. Chen, and Z. Hou, "Catalytic production of 1,2-propanediol from glycerol in bio-ethanol solvent," *Bioresource Technology*, vol. 104, pp. 814-817, 2012.

[84] F. Vila, M. López Granados, M. Ojeda, J. L. G. Fierro, and R. Mariscal, "Glycerol hydrogenolysis to 1,2-propanediol with Cu/γ-Al2O3: Effect of the activation process," *Catalysis Today*, vol. 187, pp. 122-128, 2012.

[85] J. Zhou, L. Guo, X. Guo, J. Mao, and S. Zhang, "Selective hydrogenolysis of glycerol to propanediols on supported Cu-containing bimetallic catalysts," *Green Chemistry*, vol. 12, pp. 1835-1843, 2010.

[86] A. Wołosiak-Hnat, E. Milchert, and G. Lewandowski, "Optimization of Hydrogenolysis of Glycerol to 1,2-Propanediol," *Organic Process Research & Development*, vol. 17, pp. 701-713, 2013/04/19 2013.

[87] E. S. Vasiliadou, T. M. Eggenhuisen, P. Munnik, P. E. de Jongh, K. P. de Jong, and A. A. Lemonidou, "Synthesis and performance of highly dispersed Cu/SiO2 catalysts for the hydrogenolysis of glycerol," *Applied Catalysis B: Environmental*, 2013.

[88] Z. Huang, F. Cui, H. Kang, J. Chen, X. Zhang, and C. Xia, "Highly Dispersed Silica-Supported Copper Nanoparticles Prepared by Precipitation−Gel Method: A Simple but Efficient and Stable Catalyst for Glycerol Hydrogenolysis," *Chemistry of Materials*, vol. 20, pp. 5090-5099, 2008.

[89] E. S. Vasiliadou and A. A. Lemonidou, "Investigating the performance and deactivation behaviour of silica-supported copper catalysts in glycerol hydrogenolysis," *Applied Catalysis A: General*, vol. 396, pp. 177-185, 2011.

[90] D. Durán-Martín, M. Ojeda, M. L. Granados, J. L. G. Fierro, and R. Mariscal, "Stability and regeneration of Cu–ZrO2 catalysts used in glycerol hydrogenolysis to 1,2-propanediol," *Catalysis Today*, vol. 210, pp. 98-105, 2013.

[91] T. Mizugaki, R. Arundhathi, T. Mitsudome, K. Jitsukawa, and K. Kaneda, "Selective Hydrogenolysis of Glycerol to 1,2-Propanediol Using Heterogeneous Copper Nanoparticle Catalyst Derived from Cu–Al Hydrotalcite," *Chemistry Letters*, vol. 42, pp. 729-731, 2013.

[92] Z. Wu, Y. Mao, X. Wang, and M. Zhang, "Preparation of a Cu-Ru/carbon nanotube catalyst for hydrogenolysis of glycerol to 1,2-propanediol via hydrogen spillover," *Green Chemistry*, vol. 13, pp. 1311-1316, 2011.

[93] C. W. Chiu, M. A. Dasari, G. J. Suppes, and W. R. Sutterlin, "Dehydration of glycerol to acetol via catalytic reactive distillation," *AIChE Journal*, vol. 52, pp. 3543-3548, 2006.

[94] T. Miyazawa, Y. Kusunoki, K. Kunimori, and K. Tomishige, "Glycerol conversion in the aqueous solution under hydrogen over Ru/C + an ion-exchange resin and its reaction mechanism," *Journal of Catalysis*, vol. 240, pp. 213-221, 2006.

[95] T. Miyazawa, S. Koso, K. Kunimori, and K. Tomishige, "Development of a Ru/C catalyst for glycerol hydrogenolysis in combination with an ion-exchange resin," *Applied Catalysis A: General*, vol. 318, pp. 244-251, 2007.

[96] M. Balaraju, V. Rekha, P. S. S. Prasad, B. L. A. P. Devi, R. B. N. Prasad, and N. Lingaiah, "Influence of solid acids as co-catalysts on glycerol hydrogenolysis to propylene glycol over Ru/C catalysts," *Applied Catalysis A: General*, vol. 354, pp. 82-87, 2009.

[97] J. Wang, S. Shen, B. Li, H. Lin, and Y. Yuan, "Ruthenium Nanoparticles Supported on Carbon Nanotubes for Selective Hydrogenolysis of Glycerol to Glycols," *Chemistry Letters*, vol. 38, pp. 572-573, 2009.

[98] A. Alhanash, E. Kozhevnikova, and I. Kozhevnikov, "Hydrogenolysis of Glycerol to Propanediol Over Ru: Polyoxometalate Bifunctional Catalyst," *Catalysis Letters*, vol. 120, pp. 307-311, 2008.

[99] E. Ryneveld, A. Mahomed, P. Heerden, and H. Friedrich, "Direct Hydrogenolysis of Highly Concentrated Glycerol Solutions Over Supported Ru, Pd and Pt Catalyst Systems," *Catalysis Letters*, vol. 141, pp. 958-967, 2011/07/01 2011.

[100] T. Jiang, Y. Zhou, S. Liang, H. Liu, and B. Han, "Hydrogenolysis of glycerol catalyzed by Ru-Cu bimetallic catalysts supported on clay with the aid of ionic liquids," *Green Chemistry*, vol. 11, pp. 1000-1006, 2009.

[101] E. S. Vasiliadou and A. A. Lemonidou, "Parameters Affecting the Formation of 1,2-Propanediol from Glycerol over Ru/SiO2 Catalyst," *Organic Process Research & Development*, vol. 15, pp. 925-931, 2011/07/15 2011.

[102] S.-H. Lee and D. J. Moon, "Studies on the conversion of glycerol to 1,2-propanediol over Ru-based catalyst under mild conditions," *Catalysis Today*, vol. 174, pp. 10-16, 2011.

[103] L. Ma, D. He, and Z. Li, "Promoting effect of rhenium on catalytic performance of Ru catalysts in hydrogenolysis of glycerol to propanediol," *Catalysis Communications*, vol. 9, pp. 2489-2495, 2008.

[104] L. Ma and D. He, "Hydrogenolysis of Glycerol to Propanediols Over Highly Active Ru–Re Bimetallic Catalysts," *Topics in Catalysis*, vol. 52, pp. 834-844, 2009.

[105] L. Ma and D. He, "Influence of catalyst pretreatment on catalytic properties and performances of Ru-Re/SiO2 in glycerol hydrogenolysis to propanediols," *Catalysis Today*, vol. 149, pp. 148-156, 2010.

[106] N. D. Kim, J. R. Park, D. S. Park, B. K. Kwak, and J. Yi, "Promoter effect of Pd in CuCr2O4 catalysts on the hydrogenolysis of glycerol to 1,2-propanediol," *Green Chemistry*, vol. 14, pp. 2638-2646, 2012.

[107] M. L. Barbelli, G. F. Santori, and N. N. Nichio, "Aqueous phase hydrogenolysis of glycerol to bio-propylene glycol over Pt–Sn catalysts," *Bioresource Technology*.

[108] R. L. Maglinao and B. B. He, "Catalytic Thermochemical Conversion of Glycerol to Simple and Polyhydric Alcohols Using Raney Nickel Catalyst," *Industrial & Engineering Chemistry Research*, vol. 50, pp. 6028-6033, 2011/05/18 2011.

[109] M. G. Musolino, L. A. Scarpino, F. Mauriello, and R. Pietropaolo, "Selective transfer hydrogenolysis of glycerol promoted by palladium catalysts in absence of hydrogen," *Green Chemistry*, vol. 11, pp. 1511-1513, 2009.

[110] I. Gandarias, P. L. Arias, J. Requies, M. El Doukkali, and M. B. Güemez, "Liquid-phase glycerol hydrogenolysis to 1,2-propanediol under nitrogen pressure using 2-propanol as hydrogen source," *Journal of Catalysis*, vol. 282, pp. 237-247, 2011.

[111] I. Gandarias, P. L. Arias, S. G. Fernández, J. Requies, M. El Doukkali, and M. B. Güemez, "Hydrogenolysis through catalytic transfer hydrogenation: Glycerol conversion to 1,2-propanediol," *Catalysis Today*, vol. 195, pp. 22-31, 2012.

[112] I. Gandarias, S. Fernández, M. El Doukkali, J. Requies, and P. Arias, "Physicochemical Study of Glycerol Hydrogenolysis Over a Ni–Cu/Al2O3 Catalyst Using Formic Acid as the Hydrogen Source," *Topics in Catalysis*, vol. 56, pp. 995-1007, 2013/08/01 2013.

[113] A. Martin, U. Armbruster, I. Gandarias, and P. L. Arias, "Glycerol hydrogenolysis into propanediols using in situ generated hydrogen – A critical review," *European Journal of Lipid Science and Technology*, vol. 115, pp. 9-27, 2013.

[114] Y. Nakagawa, Y. Shinmi, S. Koso, and K. Tomishige, "Direct hydrogenolysis of glycerol into 1,3-propanediol over rhenium-modified iridium catalyst," *Journal of Catalysis*, vol. 272, pp. 191-194, 2010.

[115] Y. Amada, Y. Shinmi, S. Koso, T. Kubota, Y. Nakagawa, and K. Tomishige, "Reaction mechanism of the glycerol hydrogenolysis to 1,3-propanediol over Ir–ReOx/SiO2 catalyst," *Applied Catalysis B: Environmental,* vol. 105, pp. 117-127, 2011.

[116] J. Oh, S. Dash, and H. Lee, "Selective conversion of glycerol to 1,3-propanediol using Pt-sulfated zirconia," *Green Chemistry,* vol. 13, pp. 2004-2007, 2011.

[117] L. Gong, Y. Lu, Y. Ding, R. Lin, J. Li, W. Dong, T. Wang, and W. Chen, "Selective hydrogenolysis of glycerol to 1,3-propanediol over a Pt/WO3/TiO2/SiO2 catalyst in aqueous media," *Applied Catalysis A: General,* vol. 390, pp. 119-126, 2010.

[118] S. Zhu, Y. Zhu, S. Hao, L. Chen, B. Zhang, and Y. Li, "Aqueous-Phase Hydrogenolysis of Glycerol to 1,3-propanediol Over Pt-H₄SiW₁₂O₄₀/SiO₂," *Catalysis Letters,* vol. 142, pp. 267-274, 2012.

[119] K. Ouyang, Y. Huang, H. Chen, T. Li, F. Cao, and D. Fang, "Thermodynamic analysis of liquid phase in situ hydrogenation of glycerol for 1,3-propanediol synthesis," *Frontiers of Chemical Science and Engineering,* vol. 5, pp. 67-73, 2011.

[120] Y. Ma, Q. Sun, D. Wu, W.-H. Fan, and J.-F. Deng, "A gel-oxalate co-precipitation process for preparation of Cu/ZnO/Al2O3 ultrafine catalyst for methanol synthesis from CO2+H2: (II) effect of various calcination conditions," *Applied Catalysis A: General,* vol. 177, pp. 177-184, 1999.

[121] W. O'Keefe, F. Ng, and G. Rempel, "Kinetics of the Syntheses of Mesityl Oxide (MO) and Methyl Isobutyl Ketone (MIBK) in a Fixed-Bed Flow Reactor (FBR)," *Topics in Catalysis,* vol. 53, pp. 1104-1109, 2010.

[122] Y. Zhang, Q. Sun, J. Deng, D. Wu, and S. Chen, "A high activity Cu/ZnO/Al2O3 catalyst for methanol synthesis: Preparation and catalytic properties," *Applied Catalysis A: General,* vol. 158, pp. 105-120, 1997.

[123] M. Balaraju, V. Rekha, P. S. Sai Prasad, R. B. N. Prasad, and N. Lingaiah, "Selective Hydrogenolysis of Glycerol to 1, 2 Propanediol Over Cu–ZnO Catalysts," *Catalysis Letters,* vol. 126, pp. 119-124, 2008/11/01 2008.

[124] J. Słoczyński, R. Grabowski, P. Olszewski, A. Kozłowska, J. Stoch, M. Lachowska, and J. Skrzypek, "Effect of metal oxide additives on the activity and stability of Cu/ZnO/ZrO2 catalysts in the synthesis of methanol from CO2 and H2," *Applied Catalysis A: General,* vol. 310, pp. 127-137, 2006.

[125] C.-W. CHIU, "CATALYTIC CONVERSION OF GLYCEROL TO PROPYLENE GLYCOL: SYNTHESIS AND TECHNOLOGY ASSESSMENT," Ph.D, University of Missouri, Columbia, 2006.

[126] F. Ma and M. A. Hanna, "Biodiesel production: a review," *Bioresource Technology,* vol. 70, pp. 1-15, 1999.

[127] A. E. Atabani, A. S. Silitonga, I. A. Badruddin, T. M. I. Mahlia, H. H. Masjuki, and S. Mekhilef, "A comprehensive review on biodiesel as an alternative energy resource and its characteristics," *Renewable and Sustainable Energy Reviews,* vol. 16, pp. 2070-2093, 2012.

[128] M. E. Borges and L. Díaz, "Recent developments on heterogeneous catalysts for biodiesel production by oil esterification and transesterification reactions: A review," *Renewable and Sustainable Energy Reviews,* vol. 16, pp. 2839-2849, 2012.

[129] T. Valliyappan, D. Ferdous, N. N. Bakhshi, and A. K. Dalai, "Production of Hydrogen and Syngas via Steam Gasification of Glycerol in a Fixed-Bed Reactor," *Topics in Catalysis,* vol. 49, pp. 59-67, 2008/07/01 2008.

[130] C. Descamps, C. Coquelet, C. Bouallou, and D. Richon, "Solubility of hydrogen in methanol at temperatures from 248.41 to 308.20K," *Thermochimica Acta,* vol. 430, pp. 1-7, 2005.

[131] Liu, F. Takemura, and A. Yabe, "Solubility of Hydrogen in Liquid Methanol and Methyl Formate at 20 °C to 140 °C," *Journal of Chemical & Engineering Data*, vol. 41, pp. 1141-1143, 1996/01/01 1996.

[132] Purwanto, R. M. Deshpande, R. V. Chaudhari, and H. Delmas, "Solubility of Hydrogen, Carbon Monoxide, and 1-Octene in Various Solvents and Solvent Mixtures," *Journal of Chemical & Engineering Data*, vol. 41, pp. 1414-1417, 1996/01/01 1996.

[133] K. Radhakrishnan, P. A. Ramachandran, P. H. Brahme, and R. V. Chaudhari, "Solubility of hydrogen in methanol, nitrobenzene, and their mixtures experimental data and correlation," *Journal of Chemical & Engineering Data*, vol. 28, pp. 1-4, 1983/01/01 1983.

[134] M. Saito, T. Fujitani, M. Takeuchi, and T. Watanabe, "Development of copper/zinc oxide-based multicomponent catalysts for methanol synthesis from carbon dioxide and hydrogen," *Applied Catalysis A: General*, vol. 138, pp. 311-318, 1996.

[135] M. V. Twigg and M. S. Spencer, "Deactivation of supported copper metal catalysts for hydrogenation reactions," *Applied Catalysis A: General*, vol. 212, pp. 161-174, 2001.

[136] C. Li, Y. Chen, S. Zhang, S. Xu, J. Zhou, F. Wang, M. Wei, D. G. Evans, and X. Duan, "Ni–In Intermetallic Nanocrystals as Efficient Catalysts toward Unsaturated Aldehydes Hydrogenation," *Chemistry of Materials*, vol. 25, pp. 3888-3896, 2013/10/08 2013.

[137] F. Nerozzi, "Heterogeneous Catalytic Hydrogenation-Platinum Group Metals as Hydrogenation Catalysts in a Two-day Course," *Platinum Metals Review*, vol. 56, pp. 236-241, 2012.

[138] J.-P. Shen and C. Song, "Influence of preparation method on performance of Cu/Zn-based catalysts for low-temperature steam reforming and oxidative steam reforming of methanol for H2 production for fuel cells," *Catalysis Today*, vol. 77, pp. 89-98, 2002.

[139] T. Shishido, Y. Yamamoto, H. Morioka, and K. Takehira, "Production of hydrogen from methanol over Cu/ZnO and Cu/ZnO/Al2O3 catalysts prepared by homogeneous precipitation: Steam reforming and oxidative steam reforming," *Journal of Molecular Catalysis A: Chemical*, vol. 268, pp. 185-194, 2007.

[140] S. Kuhl, M. Friedrich, M. Armbruster, and M. Behrens, "Cu,Zn,Al layered double hydroxides as precursors for copper catalysts in methanol steam reforming - pH-controlled synthesis by microemulsion technique," *Journal of Materials Chemistry*, vol. 22, pp. 9632-9638, 2012.

[141] J. P. Breen and J. R. H. Ross, "Methanol reforming for fuel-cell applications: development of zirconia-containing Cu–Zn–Al catalysts," *Catalysis Today*, vol. 51, pp. 521-533, 1999.

[142] S. Patel and K. K. Pant, "Activity and stability enhancement of copper–alumina catalysts using cerium and zinc promoters for the selective production of hydrogen via steam reforming of methanol," *Journal of Power Sources*, vol. 159, pp. 139-143, 2006.

[143] S. Sato, M. Akiyama, R. Takahashi, T. Hara, K. Inui, and M. Yokota, "Vapor-phase reaction of polyols over copper catalysts," *Applied Catalysis A: General*, vol. 347, pp. 186-191, 2008.

[144] J. Agrell, K. Hasselbo, K. Jansson, S. G. Järås, and M. Boutonnet, "Production of hydrogen by partial oxidation of methanol over Cu/ZnO catalysts prepared by microemulsion technique," *Applied Catalysis A: General*, vol. 211, pp. 239-250, 2001.

[145] C.-Z. Yao, L.-C. Wang, Y.-M. Liu, G.-S. Wu, Y. Cao, W.-L. Dai, H.-Y. He, and K.-N. Fan, "Effect of preparation method on the hydrogen production from methanol steam reforming over binary Cu/ZrO2 catalysts," *Applied Catalysis A: General*, vol. 297, pp. 151-158, 2006.

[146] X.-R. Zhang, L.-C. Wang, C.-Z. Yao, Y. Cao, W.-L. Dai, H.-Y. He, and K.-N. Fan, "A highly efficient Cu/ZnO/Al₂O₃ catalyst via gel-coprecipitation of oxalate precursors for low-temperature steam reforming of methanol," *Catalysis Letters*, vol. 102, pp. 183-190, 2005.

[147] J. Agrell, M. Boutonnet, I. Melián-Cabrera, and J. L. G. Fierro, "Production of hydrogen from methanol over binary Cu/ZnO catalysts: Part I. Catalyst preparation and characterisation," *Applied Catalysis A: General*, vol. 253, pp. 201-211, 2003.

[148] H. Sharifi Pajaie and M. Taghizadeh, "Investigation of Promoted Cu/ZnO/Al2O3 Methanol Steam Reforming Nanocatalysts by Full Factorial Design," *Chemical Engineering & Technology*, vol. 35, pp. 1857-1864, 2012.

[149] Z. Huang, F. Cui, J. Xue, J. Zuo, J. Chen, and C. Xia, "Cu/SiO2 catalysts prepared by hom- and heterogeneous deposition–precipitation methods: Texture, structure, and catalytic performance in the hydrogenolysis of glycerol to 1,2-propanediol," *Catalysis Today*, vol. 183, pp. 42-51, 2012.

[150] M. S. Spencer, "The role of zinc oxide in Cu/ZnO catalysts for methanol synthesis and the water–gas shift reaction," *Topics in Catalysis*, vol. 8, pp. 259-266, 1999.

[151] W. Yu, J. Xu, H. Ma, C. Chen, J. Zhao, H. Miao, and Q. Song, "A remarkable enhancement of catalytic activity for KBH4 treating the carbothermal reduced Ni/AC catalyst in glycerol hydrogenolysis," *Catalysis Communications*, vol. 11, pp. 493-497, 2010.

[152] W. Yu, J. Zhao, H. Ma, H. Miao, Q. Song, and J. Xu, "Aqueous hydrogenolysis of glycerol over Ni–Ce/AC catalyst: Promoting effect of Ce on catalytic performance," *Applied Catalysis A: General*, vol. 383, pp. 73-78, 2010.

[153] I. Jiménez-Morales, F. Vila, R. Mariscal, and A. Jiménez-López, "Hydrogenolysis of glycerol to obtain 1,2-propanediol on Ce-promoted Ni/SBA-15 catalysts," *Applied Catalysis B: Environmental*, vol. 117–118, pp. 253-259, 2012.

[154] J. Zhao, W. Yu, C. Chen, H. Miao, H. Ma, and J. Xu, "Ni/NaX: A Bifunctional Efficient Catalyst for Selective Hydrogenolysis of Glycerol," *Catalysis Letters*, vol. 134, pp. 184-189, 2010.

[155] N. Iwasa, S. Masuda, and N. Takezawa, "Steam reforming of methanol over Ni, Co, Pd and Pt supported on ZnO," *Reaction Kinetics and Catalysis Letters*, vol. 55, pp. 349-353, 1995.

[156] R. Pérez-Hernández, G. Mondragón Galicia, D. Mendoza Anaya, J. Palacios, C. Angeles-Chavez, and J. Arenas-Alatorre, "Synthesis and characterization of bimetallic Cu–Ni/ZrO2 nanocatalysts: H2 production by oxidative steam reforming of methanol," *International Journal of Hydrogen Energy*, vol. 33, pp. 4569-4576, 2008.

[157] R. Pérez-Hernández, A. Gutiérrez-Martínez, J. Palacios, M. Vega-Hernández, and V. Rodríguez-Lugo, "Hydrogen production by oxidative steam reforming of methanol over Ni/CeO2–ZrO2 catalysts," *International Journal of Hydrogen Energy*, vol. 36, pp. 6601-6608, 2011.

[158] M. Khzouz, J. Wood, K. Kendall, and W. Bujalski, "Characterization of Ni–Cu-based catalysts for multi-fuel steam reformer," *International Journal of Low-Carbon Technologies*, vol. 7, pp. 55-59, March 1, 2012 2012.

[159] C. Qi, J. Amphlett, and B. Peppley, "Methanol Steam Reforming Over NiAl and Ni (M) Al Layered Double Hydroxides (M = Au, Rh, Ir) Derived Catalysts," *Catalysis Letters*, vol. 104, pp. 57-62, 2005.

[160] I. N. Buffoni, F. Pompeo, G. F. Santori, and N. N. Nichio, "Nickel catalysts applied in steam reforming of glycerol for hydrogen production," *Catalysis Communications*, vol. 10, pp. 1656-1660, 2009.

[161] M. L. Dieuzeide, V. Iannibelli, M. Jobbagy, and N. Amadeo, "Steam reforming of glycerol over Ni/Mg/γ-Al2O3 catalysts. Effect of calcination temperatures," *International Journal of Hydrogen Energy*, vol. 37, pp. 14926-14930, 2012.

[162] L. F. Bobadilla, A. Álvarez, M. I. Domínguez, F. Romero-Sarria, M. A. Centeno, M. Montes, and J. A. Odriozola, "Influence of the shape of Ni catalysts in the glycerol steam reforming," *Applied Catalysis B: Environmental*, vol. 123–124, pp. 379-390, 2012.

[163] N. Barrabés, A. Frare, K. Föttinger, A. Urakawa, J. Llorca, G. Rupprechter, and D. Tichit, "Pt-Cu bimetallic catalysts obtained from layered double hydroxides by an anion-exchange route," *Applied Clay Science*, vol. 69, pp. 1-10, 2012.

[164] J. J. Bravo-Suárez, B. Subramaniam, and R. V. Chaudhari, "Ultraviolet–Visible Spectroscopy and Temperature-Programmed Techniques as Tools for Structural Characterization of Cu in CuMgAlOx Mixed Metal Oxides," *The Journal of Physical Chemistry C*, vol. 116, pp. 18207-18221, 2012/08/30 2012.

[165] S. Patel and K. Pant, "Influence of preparation method on performance of Cu(Zn)(Zr)-alumina catalysts for the hydrogen production via steam reforming of methanol," *Journal of Porous Materials*, vol. 13, pp. 373-378, 2006.

[166] P. Gao, F. Li, F. Xiao, N. Zhao, N. Sun, W. Wei, L. Zhong, and Y. Sun, "Preparation and activity of Cu/Zn/Al/Zr catalysts via hydrotalcite-containing precursors for methanol synthesis from CO2 hydrogenation," *Catalysis Science & Technology*, vol. 2, pp. 1447-1454, 2012.

[167] Z. Yuan, J. Wang, L. Wang, W. Xie, P. Chen, Z. Hou, and X. Zheng, "Biodiesel derived glycerol hydrogenolysis to 1,2-propanediol on Cu/MgO catalysts," *Bioresource Technology*, vol. 101, pp. 7088-7092, 2010.

[168] D. G. Lahr and B. H. Shanks, "Kinetic Analysis of the Hydrogenolysis of Lower Polyhydric Alcohols: Glycerol to Glycols," *Industrial & Engineering Chemistry Research*, vol. 42, pp. 5467-5472, 2003.

[169] C. Qi, J. C. Amphlett, and B. A. Peppley, "K (Na)-promoted Ni, Al layered double hydroxide catalysts for the steam reforming of methanol," *Journal of Power Sources*, vol. 171, pp. 842-849, 2007.

[170] A. Barau, V. Budarin, A. Caragheorgheopol, R. Luque, D. Macquarrie, A. Prelle, V. Teodorescu, and M. Zaharescu, "A Simple and Efficient Route to Active and Dispersed Silica Supported Palladium Nanoparticles," *Catalysis Letters*, vol. 124, pp. 204-214, 2008.

[171] Z. Kiraly, B. Veisz, I. Dekany, A. Mastalir, and Z. Razga, "Preparation of an organophilic palladium montmorillonite catalyst in a micellar system," *Chemical Communications*, pp. 1925-1926, 1999.

[172] P. D. Burton, T. J. Boyle, and A. K. Datye, "Facile, surfactant-free synthesis of Pd nanoparticles for heterogeneous catalysts," *Journal of Catalysis*, vol. 280, pp. 145-149, 2011.

[173] R. Gopinath, N. Lingaiah, N. Seshu Babu, I. Suryanarayana, P. S. Sai Prasad, and A. Obuchi, "A highly active low Pd content catalyst synthesized by deposition–precipitation method for hydrodechlorination of chlorobenzene," *Journal of Molecular Catalysis A: Chemical*, vol. 223, pp. 289-293, 2004.

[174] Y.-g. Chen, K. Tomishige, K. Yokoyama, and K. Fujimoto, "Promoting effect of Pt, Pd and Rh noble metals to the Ni0.03Mg0.97O solid solution catalysts for the reforming of CH4 with CO2," *Applied Catalysis A: General*, vol. 165, pp. 335-347, 1997.

[175] M. Nurunnabi, K.-i. Fujimoto, K. Suzuki, B. Li, S. Kado, K. Kunimori, and K. Tomishige, "Promoting effect of noble metals addition on activity and resistance to carbon deposition in oxidative steam reforming of methane over NiO–MgO solid solution," *Catalysis Communications*, vol. 7, pp. 73-78, 2006.

[176] K. M. K. Yu, W. Tong, A. West, K. Cheung, T. Li, G. Smith, Y. Guo, and S. C. E. Tsang, "Non-syngas direct steam reforming of methanol to hydrogen and carbon dioxide at low temperature," *Nat Commun*, vol. 3, p. 1230, 2012.

[177] C. D. Montgomery and C. G. Runger, *Applied Statistics and Probability for Engineers*, Third ed. New York: John Wiley & Sons, 2003.

[178] G. Yang, N. Tsubaki, J. Shamoto, Y. Yoneyama, and Y. Zhang, "Confinement Effect and Synergistic Function of H-ZSM-5/Cu-ZnO-Al2O3 Capsule Catalyst for One-Step Controlled Synthesis," *Journal of the American Chemical Society*, vol. 132, pp. 8129-8136, 2010/06/16 2010.

[179] P. Berteau, S. Ceckiewicz, and B. Delmon, "Role of the acid-base properties of aluminas, modified γ-alumina, and silica-alumina in 1-butanol dehydration," *Applied Catalysis*, vol. 31, pp. 361-383, 1987.

[180] L. Karakonstantis, H. Matralis, C. Kordulis, and A. Lycourghiotis, "Tungsten–Oxo-Species Deposited on Alumina. II. Characterization and Catalytic Activity of Unpromoted W(vi)/γ-Al2O3Catalysts Prepared by Equilibrium Deposition Filtration (EDF) at Various pH's and Non-Dry Impregnation (NDI)," *Journal of Catalysis*, vol. 162, pp. 306-319, 1996.

[181] Y. Feng, H. Yin, L. Shen, A. Wang, Y. Shen, and T. Jiang, "Gas-Phase Hydrogenolysis of Glycerol Catalyzed by Cu/MOx Catalysts," *Chemical Engineering & Technology*, vol. 36, pp. 73-82, 2013.

[182] W. K. O'Keefe, "Application of Niobium Compounds Towards the One-Step Synthesis of Methyl Isobutyl Ketone (MIBK) via Catalytic Distillation," Doctor of Philosophy, Chemical Engineering, University of Waterloo, Waterloo, 2008.

[183] S. Damyanova, A. Spojakina, and K. Jiratova, "Effect of mixed titania-alumina supports on the phase composition of NiMo/TiO2Al2O3 catalysts," *Applied Catalysis A: General*, vol. 125, pp. 257-269, 1995.

[184] G. Fierro, M. Lo Jacono, M. Inversi, P. Porta, F. Cioci, and R. Lavecchia, "Study of the reducibility of copper in CuO catalysts by temperature-programmed reduction," *Applied Catalysis A: General*, vol. 137, pp. 327-348, 1996.

[185] S. Panyad, S. Jongpatiwut, T. Sreethawong, T. Rirksomboon, and S. Osuwan, "Catalytic dehydroxylation of glycerol to propylene glycol over Cu–ZnO/Al2O3 catalysts: Effects of catalyst preparation and deactivation," *Catalysis Today*, vol. 174, pp. 59-64, 2011.

[186] J. W. Niemantsverdriet, *Spectroscopy in Catalysis: An Introduction* Third, Completely Revised and Enlarged Edition ed. Weinheim: Wiley-VCH, 2007.

[187] Y. Sun, Y. Guo, Q. Lu, X. Meng, W. Xiaohua, Y. Guo, Y. Wang, X. Liu, and Z. Zhang, "Highly selective asymmetry transfer hydrogenation of prochiral acetophenone catalyzed by palladium–chitosan on silica," *Catalysis Letters*, vol. 100, pp. 213-217, 2005.

[188] L. H. Zhang, F. Li, D. G. Evans, and X. Duan, "Evolution of structure and performance of Cu-based layered double hydroxides," *Journal of Materials Science*, vol. 45, pp. 3741-3751, 2010/07/01 2010.

[189] W. K. L. S.K. Ryu, S.J. Park, "Thermal Decomposition of Hydrated Copper Nitrate [Cu(NO3)2•3H2O] on Activated Carbon Fibers " *Carbon Science* vol. 5, pp. 180-185, 2004.

[190] A. Bienholz, H. Hofmann, and P. Claus, "Selective hydrogenolysis of glycerol over copper catalysts both in liquid and vapour phase: Correlation between the copper surface area and the catalyst's activity," *Applied Catalysis A: General*, vol. 391, pp. 153-157, 2011.

[191] Y. Feng, H. Yin, A. Wang, L. Shen, L. Yu, and T. Jiang, "Gas phase hydrogenolysis of glycerol catalyzed by Cu/ZnO/MOx (MOx = Al2O3, TiO2, and ZrO2) catalysts," *Chemical Engineering Journal*, vol. 168, pp. 403-412, 2011.

[192] C. W. Chiu, A. Tekeei, W. R. Sutterlin, J. M. Ronco, and G. J. Suppes, "Low-pressure packed-bed gas phase conversion of glycerol to acetol," *AIChE Journal*, vol. 54, pp. 2456-2463, 2008.

[193] J. Zheng, W. Zhu, C. Ma, Y. Hou, W. Zhang, and Z. Wang, "Hydrogenolysis of glycerol to 1,2-propanediol on the high dispersed SBA-15 supported copper catalyst prepared by the ion-exchange method," *Reaction Kinetics, Mechanisms and Catalysis*, vol. 99, pp. 455-462, 2010.

[194] G. Busca, U. Costantino, F. Marmottini, T. Montanari, P. Patrono, F. Pinzari, and G. Ramis, "Methanol steam reforming over ex-hydrotalcite Cu–Zn–Al catalysts," *Applied Catalysis A: General*, vol. 310, pp. 70-78, 2006.